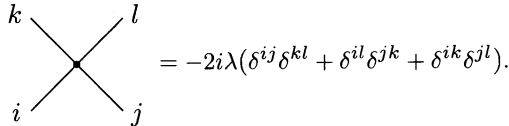


- (a) Analyze the linear sigma model for $m^2 > 0$ by noticing that, for $\lambda = 0$, the Hamiltonian given above is exactly N copies of the Klein-Gordon Hamiltonian. We can then calculate scattering amplitudes as perturbation series in the parameter λ . Show that the propagator is

$$\boxed{\Phi^i(x) \Phi^j(y)} = \delta^{ij} D_F(x - y),$$

where D_F is the standard Klein-Gordon propagator for mass m , and that there is one type of vertex given by



(That is, the vertex between two Φ^1 's and two Φ^2 's has the value $(-2i\lambda)$; that between four Φ^1 's has the value $(-6i\lambda)$.) Compute, to leading order in λ , the differential cross sections $d\sigma/d\Omega$, in the center-of-mass frame, for the scattering processes

$$\Phi^1\Phi^2 \rightarrow \Phi^1\Phi^2, \quad \Phi^1\Phi^1 \rightarrow \Phi^2\Phi^2, \quad \text{and} \quad \Phi^1\Phi^1 \rightarrow \Phi^1\Phi^1$$

as functions of the center-of-mass energy.

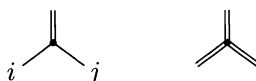
- (b) Now consider the case $m^2 < 0$: $m^2 = -\mu^2$. In this case, V has a local maximum, rather than a minimum, at $\Phi^i = 0$. Since V is a potential energy, this implies that the ground state of the theory is not near $\Phi^i = 0$ but rather is obtained by shifting Φ^i toward the minimum of V . By rotational invariance, we can consider this shift to be in the N th direction. Write, then,

$$\Phi^i(x) = \pi^i(x), \quad i = 1, \dots, N-1,$$

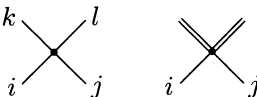
$$\Phi^N(x) = v + \sigma(x),$$

where v is a constant chosen to minimize V . (The notation π^i suggests a pion field and should not be confused with a canonical momentum.) Show that, in these new coordinates (and substituting for v its expression in terms of λ and μ), we have a theory of a massive σ field and $N-1$ *massless* pion fields, interacting through cubic and quartic potential energy terms which all become small as $\lambda \rightarrow 0$. Construct the Feynman rules by assigning values to the propagators and vertices:

$$\boxed{\sigma} = \overrightarrow{\text{---}}$$



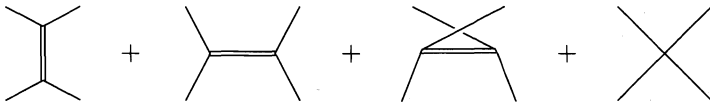
$$\boxed{\pi^i \pi^j} = i \longrightarrow j$$



- (c) Compute the scattering amplitude for the process

$$\pi^i(p_1) \pi^j(p_2) \rightarrow \pi^k(p_3) \pi^l(p_4)$$

to leading order in λ . There are now four Feynman diagrams that contribute:



Show that, at threshold ($\mathbf{p}_i = 0$), these diagrams sum to zero. (Hint: It may be easiest to first consider the specific process $\pi^1\pi^1 \rightarrow \pi^2\pi^2$, for which only the first and fourth diagrams are nonzero, before tackling the general case.) Show that, in the special case $N = 2$ (1 species of pion), the term of $\mathcal{O}(p^2)$ also cancels.

- (d) Add to V a symmetry-breaking term,

$$\Delta V = -a\Phi^N,$$

where a is a (small) constant. (In QCD, a term of this form is produced if the u and d quarks have the same nonvanishing mass.) Find the new value of v that minimizes V , and work out the content of the theory about that point. Show that the pion acquires a mass such that $m_\pi^2 \sim a$, and show that the pion scattering amplitude at threshold is now nonvanishing and also proportional to a .

4.4 Rutherford scattering. The cross section for scattering of an electron by the Coulomb field of a nucleus can be computed, to lowest order, without quantizing the electromagnetic field. Instead, treat the field as a given, classical potential $A_\mu(x)$. The interaction Hamiltonian is

$$H_I = \int d^3x e\bar{\psi}\gamma^\mu\psi A_\mu,$$

where $\psi(x)$ is the usual quantized Dirac field.

- (a) Show that the T -matrix element for electron scattering off a localized classical potential is, to lowest order,

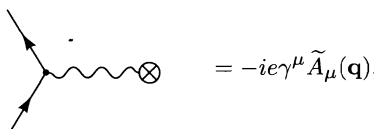
$$\langle p' | iT | p \rangle = -ie\bar{u}(p')\gamma^\mu u(p) \cdot \tilde{A}_\mu(p' - p),$$

where $\tilde{A}_\mu(q)$ is the four-dimensional Fourier transform of $A_\mu(x)$.

- (b) If $A_\mu(x)$ is time independent, its Fourier transform contains a delta function of energy. It is then natural to define

$$\langle p' | iT | p \rangle \equiv i\mathcal{M} \cdot (2\pi)\delta(E_f - E_i),$$

where E_i and E_f are the initial and final energies of the particle, and to adopt a new Feynman rule for computing \mathcal{M} :



where $\tilde{A}_\mu(\mathbf{q})$ is the three-dimensional Fourier transform of $A_\mu(x)$. Given this definition of \mathcal{M} , show that the cross section for scattering off a time-independent,

localized potential is

$$d\sigma = \frac{1}{v_i} \frac{1}{2E_i} \frac{d^3 p_f}{(2\pi)^3} \frac{1}{2E_f} |\mathcal{M}(p_i \rightarrow p_f)|^2 (2\pi) \delta(E_f - E_i),$$

where v_i is the particle's initial velocity. This formula is a natural modification of (4.79). Integrate over $|p_f|$ to find a simple expression for $d\sigma/d\Omega$.

- (c) Specialize to the case of electron scattering from a Coulomb potential ($A^0 = Ze/4\pi r$). Working in the nonrelativistic limit, derive the Rutherford formula,

$$\frac{d\sigma}{d\Omega} = \frac{\alpha^2 Z^2}{4m^2 v^4 \sin^4(\theta/2)}.$$

(With a few calculational tricks from Section 5.1, you will have no difficulty evaluating the general cross section in the relativistic case; see Problem 5.1.)

Chapter 5

Elementary Processes of Quantum Electrodynamics

Finally, after three long chapters of formalism, we are ready to perform some real relativistic calculations, to begin working out the predictions of Quantum Electrodynamics. First we will return to the process considered in Chapter 1, the annihilation of an electron-positron pair into a pair of heavier fermions. We will study this paradigm process in extreme detail in the next three sections, then do a few more simple QED calculations in Sections 5.4 and 5.5. The problems at the end of the chapter treat several additional QED processes. More complete surveys of QED can be found in the books of Jauch and Rohrlich (1976) and of Berestetskii, Lifshitz, and Pitaevskii (1982).

5.1 $e^+e^- \rightarrow \mu^+\mu^-$: Introduction

The reaction $e^+e^- \rightarrow \mu^+\mu^-$ is the simplest of all QED processes, but also one of the most important in high-energy physics. It is fundamental to the understanding of all reactions in e^+e^- colliders, and is in fact used to calibrate such machines. The related process $e^+e^- \rightarrow q\bar{q}$ (a quark-antiquark pair) is extraordinarily useful in determining the properties of elementary particles.

In this section we will compute the *unpolarized* cross section for $e^+e^- \rightarrow \mu^+\mu^-$, to lowest order. In Chapter 1 we used elementary arguments to guess the answer (Eq. (1.8)) in the limit where all the fermions are massless. We now relax that restriction and retain the muon mass in the calculation. Retaining the electron mass as well would be easy but pointless, since the ratio $m_e/m_\mu \approx 1/200$ is much smaller than the fractional error introduced by neglecting higher-order terms in the perturbation series.

Using the Feynman rules from Section 4.8, we can at once draw the diagram and write down the amplitude for our process:

$$= \bar{v}^{s'}(p')(-ie\gamma^\mu)u^s(p) \left(\frac{-ig_{\mu\nu}}{q^2} \right) \bar{u}^r(k)(-ie\gamma^\nu)v^{r'}(k').$$

Rearranging this slightly and leaving the spin superscripts implicit, we have

$$i\mathcal{M}(e^-(p)e^+(p') \rightarrow \mu^-(k)\mu^+(k')) = \frac{ie^2}{q^2} (\bar{v}(p')\gamma^\mu u(p)) (\bar{u}(k)\gamma_\mu v(k')). \quad (5.1)$$

This answer for the amplitude \mathcal{M} is simple, but not yet very illuminating.

To compute the differential cross section, we need an expression for $|\mathcal{M}|^2$, so we must find the complex conjugate of \mathcal{M} . A bi-spinor product such as $\bar{v}\gamma^\mu u$ can be complex-conjugated as follows:

$$(\bar{v}\gamma^\mu u)^* = u^\dagger(\gamma^\mu)^\dagger(\gamma^0)^\dagger v = u^\dagger(\gamma^\mu)^\dagger\gamma^0 v = u^\dagger\gamma^0\gamma^\mu v = \bar{u}\gamma^\mu v.$$

(This is another advantage of the ‘bar’ notation.) Thus the squared matrix element is

$$|\mathcal{M}|^2 = \frac{e^4}{q^4} (\bar{v}(p')\gamma^\mu u(p)\bar{u}(p)\gamma^\nu v(p')) (\bar{u}(k)\gamma_\mu v(k')\bar{v}(k')\gamma_\nu u(k)). \quad (5.2)$$

At this point we are still free to specify any particular spinors $u^s(p)$, $\bar{v}^{s'}(p')$, and so on, corresponding to any desired spin states of the fermions. In actual experiments, however, it is difficult (though not impossible) to retain control over spin states; one would have to prepare the initial state from polarized materials and/or analyze the final state using spin-dependent multiple scattering. In most experiments the electron and positron beams are unpolarized, so the measured cross section is an *average* over the electron and positron spins s and s' . Muon detectors are normally blind to polarization, so the measured cross section is a *sum* over the muon spins r and r' .

The expression for $|\mathcal{M}|^2$ simplifies considerably when we throw away the spin information. We want to compute

$$\frac{1}{2} \sum_s \frac{1}{2} \sum_{s'} \sum_r \sum_{r'} |\mathcal{M}(s, s' \rightarrow r, r')|^2.$$

The spin sums can be performed using the completeness relations from Section 3.3:

$$\sum_s u^s(p)\bar{u}^s(p) = \not{p} + m; \quad \sum_s v^s(p)\bar{v}^s(p) = \not{p} - m. \quad (5.3)$$

Working with the first half of (5.2), and writing in spinor indices so we can freely move the v next to the \bar{v} , we have

$$\begin{aligned} \sum_{s,s'} \bar{v}_a^{s'}(p')\gamma_{ab}^\mu u_b^s(p)\bar{u}_c^s(p)\gamma_{cd}^\nu v_d^{s'}(p') &= (\not{p}' - m)_{da} \gamma_{ab}^\mu (\not{p} + m)_{bc} \gamma_{cd}^\nu \\ &= \text{trace}[(\not{p}' - m)\gamma^\mu(\not{p} + m)\gamma^\nu]. \end{aligned}$$

Evaluating the second half of (5.2) in the same way, we arrive at the desired simplification:

$$\frac{1}{4} \sum_{\text{spins}} |\mathcal{M}|^2 = \frac{e^4}{4q^4} \text{tr}[(\not{p}' - m_e)\gamma^\mu(\not{p} + m_e)\gamma^\nu] \text{tr}[(\not{k} + m_\mu)\gamma_\mu(\not{k}' - m_\mu)\gamma_\nu]. \quad (5.4)$$

The spinors u and v have disappeared, leaving us with a much cleaner expression in terms of γ matrices. This trick is very general: Any QED amplitude involving external fermions, when squared and summed or averaged over spins, can be converted in this way to traces of products of Dirac matrices.

Trace Technology

This last step would hardly be an improvement if the traces had to be laboriously computed by brute force. But Feynman found that they could be worked out easily by appealing to the algebraic properties of the γ matrices. Since the evaluation of such traces occurs so often in QED calculations, it is worthwhile to pause and attack the problem systematically, once and for all.

We would like to evaluate traces of products of n gamma matrices, where $n = 0, 1, 2, \dots$. (For the present problem we need $n = 2, 3, 4$.) The $n = 0$ case is fairly easy: $\text{tr } \mathbf{1} = 4$. The trace of one γ matrix is also easy. From the explicit form of the matrices in the chiral representation, we have

$$\text{tr } \gamma^\mu = \text{tr} \begin{pmatrix} 0 & \sigma^\mu \\ \bar{\sigma}^\mu & 0 \end{pmatrix} = 0.$$

It is useful to prove this result in a more abstract way, which generalizes to an arbitrary odd number of γ matrices:

$$\begin{aligned} \text{tr } \gamma^\mu &= \text{tr } \gamma^5 \gamma^5 \gamma^\mu && \text{since } (\gamma^5)^2 = 1 \\ &= -\text{tr } \gamma^5 \gamma^\mu \gamma^5 && \text{since } \{\gamma^\mu, \gamma^5\} = 0 \\ &= -\text{tr } \gamma^5 \gamma^5 \gamma^\mu && \text{using cyclic property of trace} \\ &= -\text{tr } \gamma^\mu. \end{aligned}$$

Since the trace of γ^μ is equal to minus itself, it must vanish. For n γ -matrices we would get n minus signs in the second step (as we move the second γ^5 all the way to the right), so the trace must vanish if n is odd.

To evaluate the trace of two γ matrices, we again use the anticommutation properties and the cyclic property of the trace:

$$\begin{aligned} \text{tr } \gamma^\mu \gamma^\nu &= \text{tr} (2g^{\mu\nu} \cdot \mathbf{1} - \gamma^\nu \gamma^\mu) && \text{(anticommutation)} \\ &= 8g^{\mu\nu} - \text{tr } \gamma^\mu \gamma^\nu && \text{(cyclicity)} \end{aligned}$$

Thus $\text{tr } \gamma^\mu \gamma^\nu = 4g^{\mu\nu}$. The trace of any even number of γ matrices can be evaluated in the same way: Anticomute the first γ matrix all the way to the right, then cycle it back to the left. Thus for the trace of four γ matrices, we have

$$\begin{aligned} \text{tr}(\gamma^\mu \gamma^\nu \gamma^\rho \gamma^\sigma) &= \text{tr}(2g^{\mu\nu} \gamma^\rho \gamma^\sigma - \gamma^\nu \gamma^\mu \gamma^\rho \gamma^\sigma) \\ &= \text{tr}(2g^{\mu\nu} \gamma^\rho \gamma^\sigma - \gamma^\nu 2g^{\mu\rho} \gamma^\sigma + \gamma^\nu \gamma^\rho 2g^{\mu\sigma} - \gamma^\nu \gamma^\rho \gamma^\sigma \gamma^\mu). \end{aligned}$$

Using the cyclic property on the last term and bringing it to the left-hand side, we find

$$\begin{aligned}\text{tr}(\gamma^\mu \gamma^\nu \gamma^\rho \gamma^\sigma) &= g^{\mu\nu} \text{tr} \gamma^\rho \gamma^\sigma - g^{\mu\rho} \text{tr} \gamma^\nu \gamma^\sigma + g^{\mu\sigma} \text{tr} \gamma^\nu \gamma^\rho \\ &= 4(g^{\mu\nu} g^{\rho\sigma} - g^{\mu\rho} g^{\nu\sigma} + g^{\mu\sigma} g^{\nu\rho}).\end{aligned}$$

In this manner one can always reduce a trace of n γ -matrices to a sum of traces of $(n - 2)$ γ -matrices. The case $n = 6$ is easy to work out, but has fifteen terms (the number of ways of grouping the six indices in pairs to make terms of the form $g^{\mu\nu} g^{\rho\sigma} g^{\alpha\beta}$). Fortunately, we will not need it in this book. (If you ever do need to evaluate such complicated traces, it may be easier to learn to use one of the several computer programs that can perform symbolic manipulations on Dirac matrices.)

Starting in Section 5.2, we will often need to evaluate traces involving γ^5 . Since $\gamma^5 = i\gamma^0\gamma^1\gamma^2\gamma^3$, the trace of γ^5 times any odd number of other γ matrices is zero. It is also easy to show that the trace of γ^5 itself is zero:

$$\text{tr} \gamma^5 = \text{tr}(\gamma^0 \gamma^0 \gamma^5) = -\text{tr}(\gamma^0 \gamma^5 \gamma^0) = -\text{tr}(\gamma^0 \gamma^0 \gamma^5) = -\text{tr} \gamma^5.$$

The same trick works for $\text{tr}(\gamma^\mu \gamma^\nu \gamma^5)$, if we insert two factors of γ^α for some α different from both μ and ν . The first nonvanishing trace involving γ^5 contains four other γ matrices. In this case the trick still works unless every γ matrix appears, so $\text{tr}(\gamma^\mu \gamma^\nu \gamma^\rho \gamma^\sigma \gamma^5) = 0$ unless $(\mu\nu\rho\sigma)$ is some permutation of (0123) . From the anticommutation rules it also follows that interchanging any two of the indices simply changes the sign of the trace, so $\text{tr}(\gamma^\mu \gamma^\nu \gamma^\rho \gamma^\sigma \gamma^5)$ must be proportional to $\epsilon^{\mu\nu\rho\sigma}$. The overall constant turns out to be $-4i$, as you can easily check by plugging in $(\mu\nu\rho\sigma) = (0123)$.

Here is a summary of the trace theorems, for convenient reference:

$$\begin{aligned}\text{tr}(\mathbf{1}) &= 4 \\ \text{tr}(\text{any odd } \# \text{ of } \gamma\text{'s}) &= 0 \\ \text{tr}(\gamma^\mu \gamma^\nu) &= 4g^{\mu\nu} \\ \text{tr}(\gamma^\mu \gamma^\nu \gamma^\rho \gamma^\sigma) &= 4(g^{\mu\nu} g^{\rho\sigma} - g^{\mu\rho} g^{\nu\sigma} + g^{\mu\sigma} g^{\nu\rho}) \\ \text{tr}(\gamma^5) &= 0 \\ \text{tr}(\gamma^\mu \gamma^\nu \gamma^5) &= 0 \\ \text{tr}(\gamma^\mu \gamma^\nu \gamma^\rho \gamma^\sigma \gamma^5) &= -4i\epsilon^{\mu\nu\rho\sigma}\end{aligned}\tag{5.5}$$

Expressions resulting from use of the last formula can be simplified by means of the identities

$$\begin{aligned}\epsilon^{\alpha\beta\gamma\delta} \epsilon_{\alpha\beta\gamma\delta} &= -24 \\ \epsilon^{\alpha\beta\gamma\mu} \epsilon_{\alpha\beta\gamma\nu} &= -6\delta_\nu^\mu \\ \epsilon^{\alpha\beta\mu\nu} \epsilon_{\alpha\beta\rho\sigma} &= -2(\delta_\rho^\mu \delta_\sigma^\nu - \delta_\sigma^\mu \delta_\rho^\nu)\end{aligned}\tag{5.6}$$

All of these can be derived by first appealing to symmetry arguments, then evaluating one special case to determine the overall constant.

Another useful identity allows one to reverse the order of all the γ matrices inside a trace:

$$\text{tr}(\gamma^\mu\gamma^\nu\gamma^\rho\gamma^\sigma\cdots) = \text{tr}(\cdots\gamma^\sigma\gamma^\rho\gamma^\nu\gamma^\mu). \quad (5.7)$$

To prove this relation, consider the matrix $C \equiv \gamma^0\gamma^2$ (essentially the charge-conjugation operator). This matrix satisfies $C^2 = 1$ and $C\gamma^\mu C = -(\gamma^\mu)^T$. Thus if there are n γ -matrices inside the trace,

$$\begin{aligned} \text{tr}(\gamma^\mu\gamma^\nu\cdots) &= \text{tr}(C\gamma^\mu C C\gamma^\nu C\cdots) \\ &= (-1)^n \text{tr}[(\gamma^\mu)^T(\gamma^\nu)^T\cdots] \\ &= \text{tr}(\cdots\gamma^\nu\gamma^\mu), \end{aligned}$$

since the trace vanishes unless n is even. It is easy to show that the reversal identity (5.7) is also valid when the trace contains one or more factors of γ^5 .

When two γ matrices inside a trace are dotted together, it is easiest to eliminate them before evaluating the trace. For example,

$$\gamma^\mu\gamma_\mu = g_{\mu\nu}\gamma^\mu\gamma^\nu = \frac{1}{2}g_{\mu\nu}\{\gamma^\mu,\gamma^\nu\} = g_{\mu\nu}g^{\mu\nu} = 4. \quad (5.8)$$

The following *contraction identities*, all easy to prove using the anticommutation relations, can be used when other γ matrices lie in between:

$$\begin{aligned} \gamma^\mu\gamma^\nu\gamma_\mu &= -2\gamma^\nu \\ \gamma^\mu\gamma^\nu\gamma^\rho\gamma_\mu &= 4g^{\nu\rho} \\ \gamma^\mu\gamma^\nu\gamma^\rho\gamma^\sigma\gamma_\mu &= -2\gamma^\sigma\gamma^\rho\gamma^\nu \end{aligned} \quad (5.9)$$

Note the reversal of order in the last identity.

All of the γ matrix identities proved in this section are collected for reference in the Appendix.

Unpolarized Cross Section

We now return to the evaluation of the squared matrix element, Eq. (5.4). The electron trace is

$$\text{tr}[(\not{p}' - m_e)\gamma^\mu(\not{p} + m_e)\gamma^\nu] = 4[p'^\mu p^\nu + p'^\nu p^\mu - g^{\mu\nu}(p \cdot p' + m_e^2)].$$

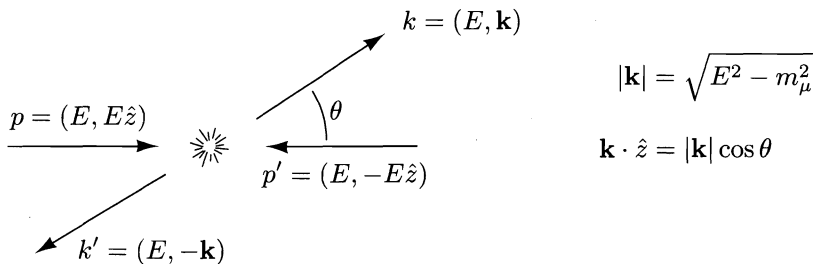
The terms with only one factor of m vanish, since they contain an odd number of γ matrices. Similarly, the muon trace is

$$\text{tr}[(\not{k} + m_\mu)\gamma_\mu(\not{k}' - m_\mu)\gamma_\nu] = 4[k_\mu k'_\nu + k_\nu k'_\mu - g_{\mu\nu}(k \cdot k' + m_\mu^2)].$$

From now on we will set $m_e = 0$, as discussed at the beginning of this section. Dotting these expressions together and collecting terms, we get the simple result

$$\frac{1}{4} \sum_{\text{spins}} |\mathcal{M}|^2 = \frac{8e^4}{q^4} \left[(p \cdot k)(p' \cdot k') + (p \cdot k')(p' \cdot k) + m_\mu^2(p \cdot p') \right]. \quad (5.10)$$

To obtain a more explicit formula we must specialize to a particular frame of reference and express the vectors p , p' , k , k' , and q in terms of the basic kinematic variables—energies and angles—in that frame. In practice, the choice of frame will be dictated by the experimental conditions. In this book, we will usually make the simplest choice of evaluating cross sections in the center-of-mass frame. For this choice, the initial and final 4-momenta for $e^+ e^- \rightarrow \mu^+ \mu^-$ can be written as follows:



To compute the squared matrix element we need

$$\begin{aligned} q^2 &= (p + p')^2 = 4E^2; & p \cdot p' &= 2E^2; \\ p \cdot k &= p' \cdot k' = E^2 - E|\mathbf{k}| \cos \theta; & p \cdot k' &= p' \cdot k = E^2 + E|\mathbf{k}| \cos \theta. \end{aligned}$$

We can now rewrite Eq. (5.10) in terms of E and θ :

$$\begin{aligned} \frac{1}{4} \sum_{\text{spins}} |\mathcal{M}|^2 &= \frac{8e^4}{16E^4} \left[E^2(E - |\mathbf{k}| \cos \theta)^2 + E^2(E + |\mathbf{k}| \cos \theta)^2 + 2m_\mu^2 E^2 \right] \\ &= e^4 \left[\left(1 + \frac{m_\mu^2}{E^2} \right) + \left(1 - \frac{m_\mu^2}{E^2} \right) \cos^2 \theta \right]. \end{aligned} \quad (5.11)$$

All that remains is to plug this expression into the cross-section formula derived in Section 4.5. Since there are only two particles in the final state and we are working in the center-of-mass frame, we can use the simplified formula (4.84). For our problem $|v_A - v_B| = 2$ and $E_A = E_B = E_{\text{cm}}/2$, so we have

$$\begin{aligned} \frac{d\sigma}{d\Omega} &= \frac{1}{2E_{\text{cm}}^2} \frac{|\mathbf{k}|}{16\pi^2 E_{\text{cm}}} \cdot \frac{1}{4} \sum_{\text{spins}} |\mathcal{M}|^2 \\ &= \frac{\alpha^2}{4E_{\text{cm}}^2} \sqrt{1 - \frac{m_\mu^2}{E^2}} \left[\left(1 + \frac{m_\mu^2}{E^2} \right) + \left(1 - \frac{m_\mu^2}{E^2} \right) \cos^2 \theta \right]. \end{aligned} \quad (5.12)$$

Integrating over $d\Omega$, we find the total cross section:

$$\sigma_{\text{total}} = \frac{4\pi\alpha^2}{3E_{\text{cm}}^2} \sqrt{1 - \frac{m_\mu^2}{E^2}} \left(1 + \frac{1}{2} \frac{m_\mu^2}{E^2} \right). \quad (5.13)$$

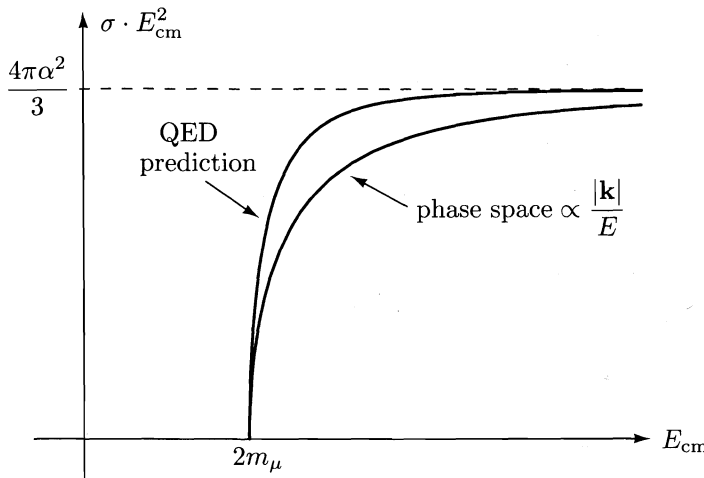


Figure 5.1. Energy dependence of the total cross section for $e^+e^- \rightarrow \mu^+\mu^-$, compared to “phase space” energy dependence.

In the high-energy limit where $E \gg m_\mu$, these formulae reduce to those given in Chapter 1:

$$\begin{aligned} \frac{d\sigma}{d\Omega} &\xrightarrow{E \gg m_\mu} \frac{\alpha^2}{4E_{\text{cm}}^2} (1 + \cos^2 \theta); \\ \sigma_{\text{total}} &\xrightarrow{E \gg m_\mu} \frac{4\pi\alpha^2}{3E_{\text{cm}}^2} \left(1 - \frac{3}{8} \left(\frac{m_\mu}{E} \right)^4 - \dots \right). \end{aligned} \quad (5.14)$$

Note that these expressions have the correct dimensions of cross sections. In the high-energy limit, E_{cm} is the only dimensionful quantity in the problem, so dimensional analysis dictates that $\sigma_{\text{total}} \propto E_{\text{cm}}^{-2}$. Since we knew from the beginning that $\sigma_{\text{total}} \propto \alpha^2$, we only had to work to get the factor of $4\pi/3$.

The energy dependence of the total cross-section formula (5.13) near threshold is shown in Fig. 5.1. Of course the cross section is zero for $E_{\text{cm}} < 2m_\mu$. It is interesting to compare the shape of the actual curve to the shape one would obtain if $|\mathcal{M}|^2$ did not depend on energy, that is, if all the energy dependence came from the phase-space factor $|k|/E$. To test Quantum Electrodynamics, an experiment must be able to resolve deviations from the naive phase-space prediction. Experimental results from pair production of both μ and τ leptons confirm that these particles behave as QED predicts. Figure 5.2 compares formula (5.13) to experimental measurements of the $\tau^+\tau^-$ threshold.

Before discussing our result further, let us pause to summarize how we obtained it. The method extends in a straightforward way to the calculation of unpolarized cross sections for other QED processes. The general procedure is as follows:

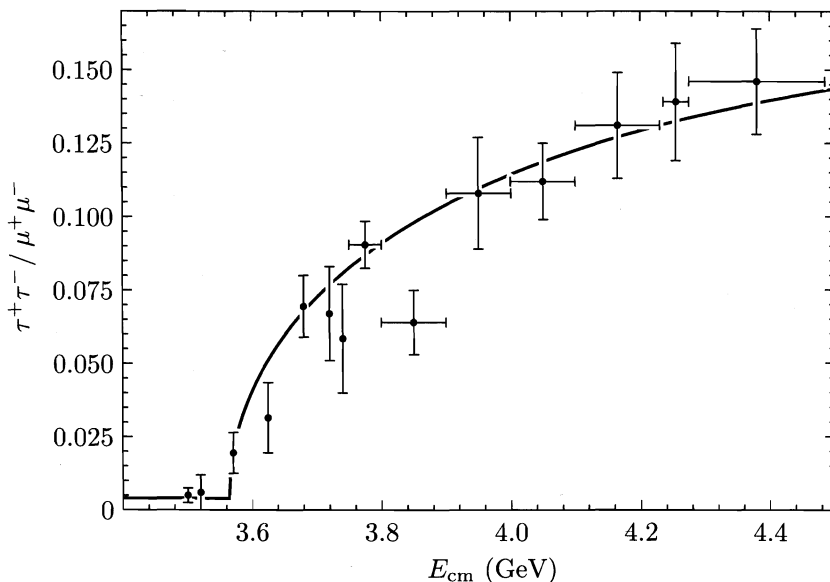


Figure 5.2. The ratio $\sigma(e^+e^- \rightarrow \tau^+\tau^-)/\sigma(e^+e^- \rightarrow \mu^+\mu^-)$ of measured cross sections near the threshold for $\tau^+\tau^-$ pair-production, as measured by the DELCO collaboration, W. Bacino, et. al., *Phys. Rev. Lett.* **41**, 13 (1978). Only a fraction of τ decays are included, hence the small overall scale. The curve shows a fit to the theoretical formula (5.13), with a small energy-independent background added. The fit yields $m_\tau = 1782^{+2}_{-7}$ MeV.

1. Draw the diagram(s) for the desired process.
2. Use the Feynman rules to write down the amplitude \mathcal{M} .
3. Square the amplitude and average or sum over spins, using the completeness relations (5.3). (For processes involving photons in the final state there is an analogous completeness relation, derived in Section 5.5.)
4. Evaluate traces using the trace theorems (5.5); collect terms and simplify the answer as much as possible.
5. Specialize to a particular frame of reference, and draw a picture of the kinematic variables in that frame. Express all 4-momentum vectors in terms of a suitably chosen set of variables such as E and θ .
6. Plug the resulting expression for $|\mathcal{M}|^2$ into the cross-section formula (4.79), and integrate over phase-space variables that are not measured to obtain a differential cross section in the desired form. (In our case these integrations were over the constrained momenta \mathbf{k}' and $|\mathbf{k}|$, and were performed in the derivation of Eq. (4.84).)

While other calculations (especially those involving loop diagrams) often require additional tricks, nearly every QED calculation will involve the basic procedures outlined here.

Production of Quark-Antiquark Pairs

The asymptotic energy dependence of the $e^+e^- \rightarrow \mu^+\mu^-$ cross-section formula sets the scale for all e^+e^- annihilation cross sections. A particularly important example is the cross section for

$$e^+e^- \rightarrow \text{hadrons},$$

that is, the total cross section for production of any number of strongly interacting particles.

In our current understanding of the strong interactions, given by the theory called Quantum Chromodynamics (QCD), all hadrons are composed of Dirac fermions called *quarks*. Quarks appear in a variety of types, called *flavors*, each with its own mass and electric charge. A quark also carries an additional quantum number, *color*, which takes one of three values. Color serves as the “charge” of QCD, as we will discuss in Chapter 17.

According to QCD, the simplest e^+e^- process that ends in hadrons is

$$e^+e^- \rightarrow q\bar{q},$$

the annihilation of an electron and a positron, through a virtual photon, into a quark-antiquark pair. After they are created, the quarks interact with one another through their strong forces, producing more quark pairs. Eventually the quarks and antiquarks combine to form some number of mesons and baryons.

To adapt our results for muon production to handle the case of quarks, we must make three modifications:

1. Replace the muon charge e with the quark charge $Q|e|$.
2. Count each quark three times, one for each color.
3. Include the effects of the strong interactions of the produced quark and antiquark.

The first two changes are easy to make. For the first, it is simply necessary to know the masses and charges of each flavor of quark. For u , c , and t quarks we have $Q = 2/3$, while for d , s , and b quarks we have $Q = -1/3$. The cross-section formulae are proportional to the square of the charge of the final-state particle, so we can simply insert a factor of Q^2 into any of these formulae to obtain the cross section for production of any particular variety of quark. Counting colors is necessary because experiments measure only the total cross section for production of all three colors. (The hadrons that are actually detected are colorless.) In any case, this counting is easy: Just multiply the answer by 3.

If you know a little about the strong interaction, however, you might think this is all a big joke. Surely the third modification is extremely difficult to make, and will drastically alter the predictions of QED. The amazing truth is that in the high-energy limit, the effect of the strong interaction on the quark production process can be completely neglected. As we will discuss in Part III, the only effect of the strong interaction (in this limit) is to dress

up the final-state quarks into bunches of hadrons. This simplification is due to a phenomenon called *asymptotic freedom*; it played a crucial role in the identification of Quantum Chromodynamics as the correct theory of the strong force.

Thus in the high-energy limit, we expect the cross section for the reaction $e^+e^- \rightarrow q\bar{q}$ to approach $3 \cdot Q^2 \cdot 4\pi\alpha^2/3E_{\text{cm}}^2$. It is conventional to define

$$1 \text{ unit of } R \equiv \frac{4\pi\alpha^2}{3E_{\text{cm}}^2} = \frac{86.8 \text{ nbarns}}{(E_{\text{cm}} \text{ in GeV})^2}. \quad (5.15)$$

The value of a cross section in units of R is therefore its ratio to the asymptotic value of the $e^+e^- \rightarrow \mu^+\mu^-$ cross section predicted by Eq. (5.14). Experimentally, the easiest quantity to measure is the total rate for production of all hadrons. Asymptotically, we expect

$$\sigma(e^+e^- \rightarrow \text{hadrons}) \xrightarrow{E_{\text{cm}} \rightarrow \infty} 3 \cdot \left(\sum_i Q_i^2 \right) R, \quad (5.16)$$

where the sum runs over all quarks whose masses are smaller than $E_{\text{cm}}/2$. When $E_{\text{cm}}/2$ is in the vicinity of one of the quark masses, the strong interactions cause large deviations from this formula. The most dramatic such effect is the appearance of *bound states* just below $E_{\text{cm}} = 2m_q$, manifested as very sharp spikes in the cross section.

Experimental measurements of the cross section for e^+e^- annihilation to hadrons between 2.5 and 40 GeV are shown in Fig. 5.3. The data shows three distinct regions: a low-energy region in which u , d , and s quark pairs are produced; a region above the threshold for production of c quark pairs; and a region also above the threshold for b quark pairs. The prediction (5.16) is shown as a set of solid lines; it agrees quite well with the data in each region, as long as the energy is well away from the thresholds where the high-energy approximation breaks down. The dotted curves show an improved theoretical prediction, including higher-order corrections from QCD, which we will discuss in Section 17.2. This explanation of the e^+e^- annihilation cross section is a remarkable success of QCD. In particular, experimental verification of the factor of 3 in (5.16) is one piece of evidence for the existence of color.

The angular dependence of the differential cross section is also observed experimentally.* At high energy the hadrons appear in *jets*, clusters of several hadrons all moving in approximately the same direction. In most cases there are two jets, with back-to-back momenta, and these indeed have the angular dependence $(1 + \cos^2 \theta)$.

*The basic features of hadron production in high-energy e^+e^- annihilation are reviewed by P. Duinker, *Rev. Mod. Phys.* **54**, 325 (1982).

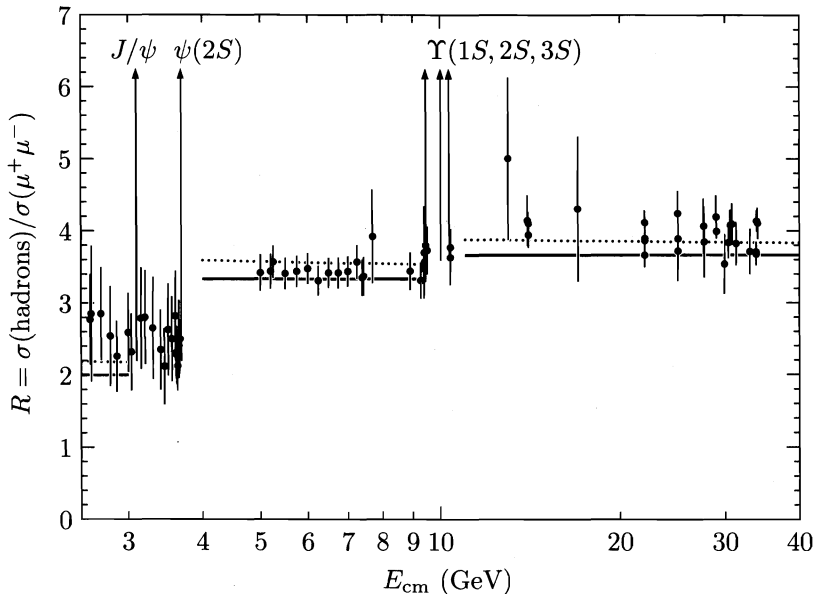


Figure 5.3. Experimental measurements of the total cross section for the reaction $e^+e^- \rightarrow$ hadrons, from the data compilation of M. Swartz, *Phys. Rev. D* 53, 5268 (1996). Complete references to the various experiments are given there. The measurements are compared to theoretical predictions from Quantum Chromodynamics, as explained in the text. The solid line is the simple prediction (5.16).

5.2 $e^+e^- \rightarrow \mu^+\mu^-$: Helicity Structure

The unpolarized cross section for a reaction is generally easy to calculate (and to measure) but hard to understand. Where does the $(1 + \cos^2 \theta)$ angular dependence come from? We can answer this question by computing the $e^+e^- \rightarrow \mu^+\mu^-$ cross section for each set of spin orientations separately.

First we must choose a basis of polarization states. To get a simple answer in the high-energy limit, the best choice is to quantize each spin along the direction of the particle's motion, that is, to use states of definite helicity. Recall that in the massless limit, the left- and right-handed helicity states of a Dirac particle live in different representations of the Lorentz group. We might therefore expect them to behave independently, and in fact they do.

In this section we will compute the polarized $e^+e^- \rightarrow \mu^+\mu^-$ cross sections, using the helicity basis, in two different ways: first, by using trace technology but with the addition of helicity projection operators to project out the desired left- or right-handed spinors; and second, by plugging explicit expressions for these spinors directly into our formula for the amplitude \mathcal{M} . Throughout this section we work in the high-energy limit where all fermions are effectively

massless. (The calculation can be done for lower energy, but it is much more difficult and no more instructive.)[†]

Our starting point for both methods of calculating the polarized cross section is the amplitude

$$i\mathcal{M}(e^-(p)e^+(p') \rightarrow \mu^-(k)\mu^+(k')) = \frac{ie^2}{q^2} (\bar{v}(p')\gamma^\mu u(p)) (\bar{u}(k)\gamma_\mu v(k')). \quad (5.1)$$

We would like to use the spin sum identities to write the squared amplitude in terms of traces as before, even though we now want to consider only one set of polarizations at a time. To do this, we note that for massless fermions, the matrices

$$\frac{1+\gamma^5}{2} = \begin{pmatrix} 0 & 0 \\ 0 & 1 \end{pmatrix}, \quad \frac{1-\gamma^5}{2} = \begin{pmatrix} 1 & 0 \\ 0 & 0 \end{pmatrix} \quad (5.17)$$

are *projection operators* onto right- and left-handed spinors, respectively. Thus if in (5.1) we make the replacement

$$\bar{v}(p')\gamma^\mu u(p) \longrightarrow \bar{v}(p')\gamma^\mu \left(\frac{1+\gamma^5}{2}\right) u(p),$$

the amplitude for a right-handed electron is unchanged while that for a left-handed electron becomes zero. Note that since

$$\bar{v}(p')\gamma^\mu \left(\frac{1+\gamma^5}{2}\right) u(p) = v^\dagger(p') \left(\frac{1+\gamma^5}{2}\right) \gamma^0 \gamma^\mu u(p), \quad (5.18)$$

this same replacement imposes the requirement that $v(p')$ also be a right-handed spinor. Recall from Section 3.5, however, that the right-handed spinor $v(p')$ corresponds to a *left*-handed positron. Thus we see that the annihilation amplitude vanishes when both the electron and the positron are right-handed. In general, the amplitude vanishes (in the massless limit) unless the electron and positron have opposite helicity, or equivalently, unless their spinors have the same helicity.

Having inserted this projection operator, we are now free to sum over the electron and positron spins in the squared amplitude; of the four terms in the sum, only one (the one we want) is nonzero. The electron half of $|\mathcal{M}|^2$, for a right-handed electron and a left-handed positron, is then

$$\begin{aligned} \sum_{\text{spins}} \left| \bar{v}(p')\gamma^\mu \left(\frac{1+\gamma^5}{2}\right) u(p) \right|^2 &= \sum_{\text{spins}} \bar{v}(p')\gamma^\mu \left(\frac{1+\gamma^5}{2}\right) u(p) \bar{u}(p)\gamma^\nu \left(\frac{1+\gamma^5}{2}\right) v(p') \\ &= \text{tr} \left[\not{p}' \gamma^\mu \left(\frac{1+\gamma^5}{2}\right) \not{p} \gamma^\nu \left(\frac{1+\gamma^5}{2}\right) \right] \\ &= \text{tr} \left[\not{p}' \gamma^\mu \not{p} \gamma^\nu \left(\frac{1+\gamma^5}{2}\right) \right] \end{aligned}$$

[†]The general formalism for *S*-matrix elements between states of definite helicity is presented in a beautiful paper of M. Jacob and G. C. Wick, *Ann. Phys.* **7**, 404 (1959).

$$= 2(p'^\mu p^\nu + p'^\nu p^\mu - g^{\mu\nu} p \cdot p' - i\epsilon^{\alpha\mu\beta\nu} p'_\alpha p_\beta). \quad (5.19)$$

The indices in this expression are to be dotted into those of the muon half of the squared amplitude. For a right-handed μ^- and a left-handed μ^+ , an identical calculation yields

$$\sum_{\text{spins}} \left| \bar{u}(k) \gamma_\mu \left(\frac{1+\gamma^5}{2} \right) v(k') \right|^2 = 2(k_\mu k'_\nu + k_\nu k'_\mu - g_{\mu\nu} k \cdot k' - i\epsilon_{\rho\mu\sigma\nu} k^\rho k'^\sigma). \quad (5.20)$$

Dotting (5.19) into (5.20), we find that the squared matrix element for $e_R^- e_L^+ \rightarrow \mu_R^- \mu_L^+$ in the center-of-mass frame is

$$\begin{aligned} |\mathcal{M}|^2 &= \frac{4e^4}{q^4} \left[2(p \cdot k)(p' \cdot k') + 2(p \cdot k')(p' \cdot k) - \epsilon^{\alpha\mu\beta\nu} \epsilon_{\rho\mu\sigma\nu} p'_\alpha p_\beta k^\rho k'^\sigma \right] \\ &= \frac{8e^4}{q^4} \left[(p \cdot k)(p' \cdot k') + (p \cdot k')(p' \cdot k) - (p \cdot k)(p' \cdot k') + (p \cdot k')(p' \cdot k) \right] \\ &= \frac{16e^4}{q^4} (p \cdot k')(p' \cdot k) \\ &= e^4 (1 + \cos \theta)^2. \end{aligned} \quad (5.21)$$

Plugging this result into (4.85) gives the differential cross section,

$$\frac{d\sigma}{d\Omega} (e_R^- e_L^+ \rightarrow \mu_R^- \mu_L^+) = \frac{\alpha^2}{4E_{\text{cm}}^2} (1 + \cos \theta)^2. \quad (5.22)$$

There is no need to repeat the entire calculation to obtain the other three nonvanishing helicity amplitudes. For example, the squared amplitude for $e_R^- e_L^+ \rightarrow \mu_L^- \mu_R^+$ is identical to (5.20) but with γ^5 replaced by $-\gamma^5$ on the left-hand side, and thus $\epsilon_{\rho\mu\sigma\nu}$ replaced by $-\epsilon_{\rho\mu\sigma\nu}$ on the right-hand side. Propagating this sign through (5.21), we easily see that

$$\frac{d\sigma}{d\Omega} (e_R^- e_L^+ \rightarrow \mu_L^- \mu_R^+) = \frac{\alpha^2}{4E_{\text{cm}}^2} (1 - \cos \theta)^2. \quad (5.23)$$

Similarly,

$$\begin{aligned} \frac{d\sigma}{d\Omega} (e_L^- e_R^+ \rightarrow \mu_R^- \mu_L^+) &= \frac{\alpha^2}{4E_{\text{cm}}^2} (1 - \cos \theta)^2; \\ \frac{d\sigma}{d\Omega} (e_L^- e_R^+ \rightarrow \mu_L^- \mu_R^+) &= \frac{\alpha^2}{4E_{\text{cm}}^2} (1 + \cos \theta)^2. \end{aligned} \quad (5.24)$$

(These two results actually follow from the previous two by parity invariance.) The other twelve helicity cross sections (for instance, $e_L^- e_R^+ \rightarrow \mu_L^- \mu_L^+$) are zero, as we saw from Eq. (5.18). Adding up all sixteen contributions, and dividing by 4 to average over the electron and positron spins, we recover the unpolarized cross section in the massless limit, Eq. (5.14).

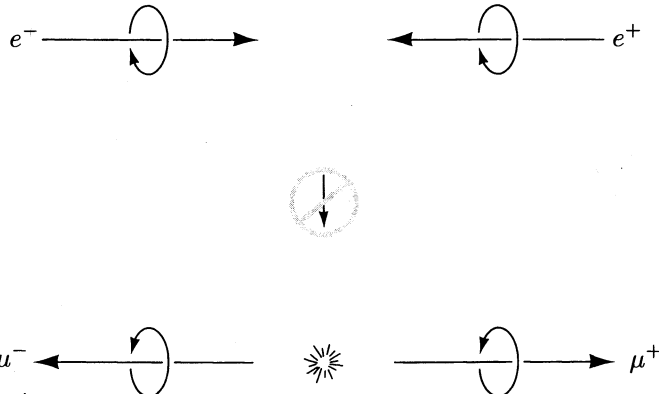


Figure 5.4. Conservation of angular momentum requires that if the z -component of angular momentum is measured, it must have the same value as initially.

Note that the cross section (5.22) for $e_R^- e_L^+ \rightarrow \mu_R^- \mu_L^+$ vanishes at $\theta = 180^\circ$. This is just what we would expect, since for $\theta = 180^\circ$, the total angular momentum of the final state is opposite to that of the initial state (see Figure 5.4).

This completes our first calculation of the polarized $e^+ e^- \rightarrow \mu^+ \mu^-$ cross sections. We will now redo the calculation in a manner that is more straightforward, more enlightening, and no more difficult. We will calculate the amplitude \mathcal{M} (rather than the squared amplitude) directly, using explicit values for the spinors and γ matrices. This method does have its drawbacks: It forces us to specialize to a particular frame of reference much sooner, so manifest Lorentz invariance is lost. More pragmatically, it is very cumbersome except in the nonrelativistic and ultra-relativistic limits.

Consider again the amplitude

$$\mathcal{M} = \frac{e^2}{q^2} (\bar{v}(p') \gamma^\mu u(p)) (\bar{u}(k) \gamma_\mu v(k')). \quad (5.25)$$

In the high-energy limit, our general expressions for Dirac spinors become

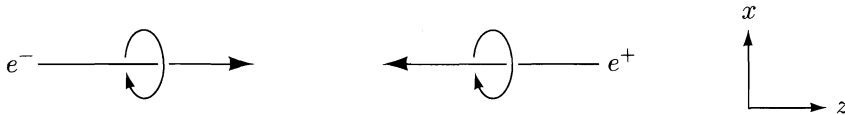
$$\begin{aligned} u(p) &= \begin{pmatrix} \sqrt{p \cdot \sigma} \xi \\ \sqrt{p \cdot \bar{\sigma}} \xi \end{pmatrix} \xrightarrow{E \rightarrow \infty} \sqrt{2E} \begin{pmatrix} \frac{1}{2}(1 - \hat{p} \cdot \sigma) \xi \\ \frac{1}{2}(1 + \hat{p} \cdot \sigma) \xi \end{pmatrix}; \\ v(p) &= \begin{pmatrix} \sqrt{p \cdot \sigma} \xi \\ -\sqrt{p \cdot \bar{\sigma}} \xi \end{pmatrix} \xrightarrow{E \rightarrow \infty} \sqrt{2E} \begin{pmatrix} \frac{1}{2}(1 - \hat{p} \cdot \sigma) \xi \\ -\frac{1}{2}(1 + \hat{p} \cdot \sigma) \xi \end{pmatrix}. \end{aligned} \quad (5.26)$$

A right-handed spinor satisfies $(\hat{p} \cdot \sigma)\xi = +\xi$, while a left-handed spinor has $(\hat{p} \cdot \sigma)\xi = -\xi$. (Remember once again that for antiparticles, the handedness of the spinor is the opposite of the handedness of the particle.) We must evaluate expressions of the form $\bar{v}\gamma^\mu u$, so we need

$$\gamma^0 \gamma^\mu = \begin{pmatrix} 0 & 1 \\ 1 & 0 \end{pmatrix} \begin{pmatrix} 0 & \sigma^\mu \\ \bar{\sigma}^\mu & 0 \end{pmatrix} = \begin{pmatrix} \bar{\sigma}^\mu & 0 \\ 0 & \sigma^\mu \end{pmatrix}. \quad (5.27)$$

Thus we see explicitly that the amplitude is zero when one of the spinors is left-handed and the other is right-handed. In the language of Chapter 1, the Clebsch-Gordan coefficients that couple the vector photon to the product of such spinors are zero; those coefficients are just the off-block-diagonal elements of the matrix $\gamma^0\gamma^\mu$ (in the chiral representation).

Let us choose p and p' to be in the $\pm z$ -directions, and first consider the case where the electron is right-handed and the positron is left-handed:



Thus for the electron we have $\xi = \begin{pmatrix} 1 \\ 0 \end{pmatrix}$, corresponding to spin up in the z -direction, while for the positron we have $\xi = \begin{pmatrix} 0 \\ 1 \end{pmatrix}$, also corresponding to (physical) spin up in the z -direction. Both particles have $(\hat{p} \cdot \sigma)\xi = +\xi$, so the spinors are

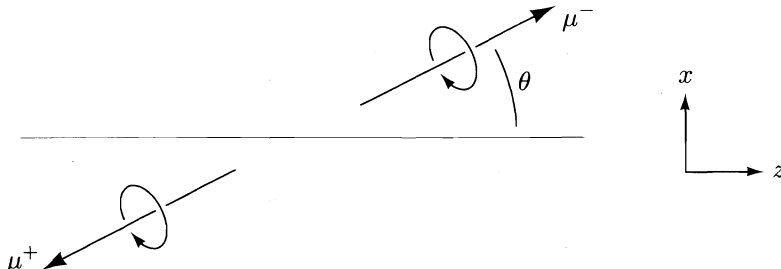
$$u(p) = \sqrt{2E} \begin{pmatrix} 0 \\ 0 \\ 1 \\ 0 \end{pmatrix}; \quad v(p') = \sqrt{2E} \begin{pmatrix} 0 \\ 0 \\ 0 \\ -1 \end{pmatrix}. \quad (5.28)$$

The electron half of the matrix element is therefore

$$\bar{v}(p')\gamma^\mu u(p) = 2E (0, -1)\sigma^\mu \begin{pmatrix} 1 \\ 0 \end{pmatrix} = -2E (0, 1, i, 0). \quad (5.29)$$

We can interpret this expression by saying that the virtual photon has circular polarization in the $+z$ -direction; its polarization vector is $\epsilon_+ = (1/\sqrt{2})(\hat{x} + i\hat{y})$.

Next we must calculate the muon half of the matrix element. Let the μ^- be emitted at an angle θ to the z -axis, and consider first the case where it is right-handed (and the μ^+ is therefore left-handed):



To calculate $\bar{u}(k)\gamma^\mu v(k')$ we could go back to expressions (5.26), but then it would be necessary to find the correct spinors ξ corresponding to polarization along the muon momentum. It is much easier to use a trick: Since any expression of the form $\bar{\psi}\gamma^\mu\psi$ transforms like a 4-vector, we can just rotate the result

(5.29). Rotating that vector by an angle θ in the xz -plane, we find

$$\begin{aligned}\bar{u}(k)\gamma^\mu v(k') &= [\bar{v}(k')\gamma^\mu u(k)]^* \\ &= [-2E(0, \cos\theta, i, -\sin\theta)]^* \\ &= -2E(0, \cos\theta, -i, -\sin\theta).\end{aligned}\quad (5.30)$$

This vector can also be interpreted as the polarization of the virtual photon; when it has a nonzero overlap with (5.29), we get a nonzero amplitude. Plugging (5.29) and (5.30) into (5.25), we see that the amplitude is

$$\mathcal{M}(e_R^- e_L^+ \rightarrow \mu_R^- \mu_L^+) = \frac{e^2}{q^2} (2E)^2 (-\cos\theta - 1) = -e^2(1 + \cos\theta), \quad (5.31)$$

in agreement with (1.6), and also with (5.21). The differential cross section for this set of helicities can now be obtained in the same way as above, yielding (5.22).

We can calculate the other three nonvanishing helicity amplitudes in an analogous manner. For a left-handed electron and a right-handed positron, we easily find

$$\bar{v}(p')\gamma^\mu u(p) = -2E(0, 1, -i, 0) \equiv -2E \cdot \sqrt{2} \epsilon_-^\mu.$$

Perform a rotation to get the vector corresponding to a left-handed μ^- and a right-handed μ^+ :

$$\bar{u}(k)\gamma^\mu v(k') = -2E(0, \cos\theta, i, -\sin\theta).$$

Putting the pieces together in various ways yields the remaining amplitudes,

$$\begin{aligned}\mathcal{M}(e_L^- e_R^+ \rightarrow \mu_L^- \mu_R^+) &= -e^2(1 + \cos\theta); \\ \mathcal{M}(e_R^- e_L^+ \rightarrow \mu_L^- \mu_R^+) &= \mathcal{M}(e_L^- e_R^+ \rightarrow \mu_R^- \mu_L^+) = -e^2(1 - \cos\theta).\end{aligned}\quad (5.32)$$

5.3 $e^+ e^- \rightarrow \mu^+ \mu^-$: Nonrelativistic Limit

Now let us go to the other end of the energy spectrum, and discuss the reaction $e^+ e^- \rightarrow \mu^+ \mu^-$ in the extreme nonrelativistic limit. When E is barely larger than m_μ , our previous result (5.12) for the unpolarized differential cross section becomes

$$\frac{d\sigma}{d\Omega} \xrightarrow[|\mathbf{k}| \rightarrow 0]{} \frac{\alpha^2}{2E_{\text{cm}}^2} \sqrt{1 - \frac{m_\mu^2}{E^2}} = \frac{\alpha^2}{2E_{\text{cm}}^2} \frac{|\mathbf{k}|}{E}. \quad (5.33)$$

We can recover this result, and also learn something about the spin dependence of the reaction, by evaluating the amplitude with explicit spinors. Once again we begin with the matrix element

$$\mathcal{M} = \frac{e^2}{q^2} (\bar{v}(p')\gamma^\mu u(p)) (\bar{u}(k)\gamma_\mu v(k')).$$

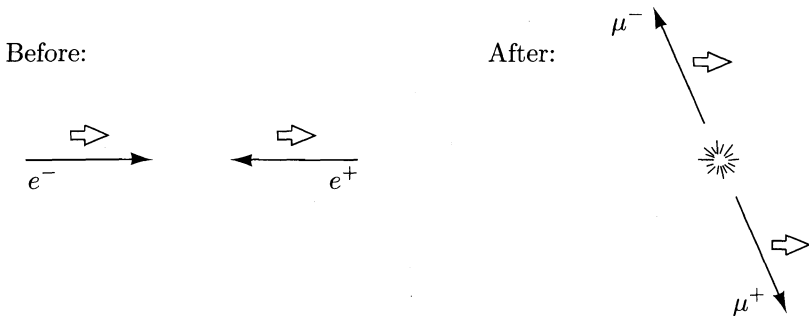


Figure 5.5. In the nonrelativistic limit the total spin of the system is conserved, and thus the muons are produced with both spins up along the z -axis.

The electron and positron are still very relativistic, so this expression will be simplest if we choose them to have definite helicity. Let the electron be right-handed, moving in the $+z$ -direction, and the positron be left-handed, moving in the $-z$ -direction. Then from Eq. (5.29) we have

$$\bar{v}(p')\gamma^\mu u(p) = -2E(0, 1, i, 0). \quad (5.34)$$

In the other half of the matrix element we should use the nonrelativistic expressions

$$u(k) = \sqrt{m} \begin{pmatrix} \xi \\ \xi \end{pmatrix}, \quad v(k') = \sqrt{m} \begin{pmatrix} \xi' \\ -\xi' \end{pmatrix}. \quad (5.35)$$

Keep in mind, in the discussion of this section, that the spinor ξ' gives the flipped spin of the antiparticle. Leaving the muon spinors ξ and ξ' undetermined for now, we can easily compute

$$\begin{aligned} \bar{u}(k)\gamma^\mu v(k') &= m(\xi^\dagger, \xi^\dagger) \begin{pmatrix} \bar{\sigma}^\mu & 0 \\ 0 & \sigma^\mu \end{pmatrix} \begin{pmatrix} \xi' \\ -\xi' \end{pmatrix} \\ &= \begin{cases} 0 & \text{for } \mu = 0, \\ -2m\xi^\dagger \sigma^i \xi' & \text{for } \mu = i. \end{cases} \end{aligned} \quad (5.36)$$

To evaluate \mathcal{M} , we simply dot (5.34) into (5.36) and multiply by $e^2/q^2 = e^2/4m^2$. The result is

$$\mathcal{M}(e_R^- e_L^+ \rightarrow \mu^+ \mu^-) = -2e^2 \xi^\dagger \begin{pmatrix} 0 & 1 \\ 0 & 0 \end{pmatrix} \xi'. \quad (5.37)$$

Since there is no angular dependence in this expression, the muons are equally likely to come out in any direction. More precisely, they are emitted in an s -wave; their orbital angular momentum is zero. Angular momentum conservation therefore requires that the total spin of the final state equal 1, and indeed the matrix product gives zero unless both the muon and the antimuon have spin up along the z -axis (see Fig. 5.5).

To find the total rate for this process, we sum over muon spins to obtain $\mathcal{M}^2 = 4e^4$, which yields the cross section

$$\frac{d\sigma}{d\Omega}(e_R^- e_L^+ \rightarrow \mu^+ \mu^-) = \frac{\alpha^2}{E_{cm}^2} \frac{|\mathbf{k}|}{E}. \quad (5.38)$$

The same expression holds for a left-handed electron and a right-handed positron. Thus the spin-averaged cross section is just $2 \cdot (1/4)$ times this expression, in agreement with (5.33).

Bound States

Until now we have considered the initial and final states of scattering processes to be states of isolated single particles. Very close to threshold, however, the Coulomb attraction of the muons should become an important effect. Just below threshold, we can still form $\mu^+ \mu^-$ pairs in electromagnetic bound states.

The treatment of bound states in quantum field theory is a rich and complex subject, but one that lies mainly beyond the scope of this book.[‡] Fortunately, many of the familiar bound systems in Nature can be treated (at least to a good first approximation) as nonrelativistic systems, in which the internal motions are slow. The process of creating the constituent particles out of the vacuum is still a relativistic effect, requiring quantum field theory for its proper description. In this section we will develop a formalism for computing the amplitudes for creation and annihilation of two-particle, nonrelativistic bound states. We begin with a computation of the cross section for producing a $\mu^+ \mu^-$ bound state in $e^+ e^-$ annihilation.

Consider first the case where the spins of the electron and positron both point up along the z -axis. From the preceding discussion we know that the resulting muons both have spin up, so the only type of bound state we can produce will have total spin 1, also pointing up. The amplitude for producing free muons in this configuration is

$$\mathcal{M}(\uparrow\uparrow \rightarrow \mathbf{k}_1 \uparrow, \mathbf{k}_2 \uparrow) = -2e^2, \quad (5.39)$$

independent of the momenta (which we now call \mathbf{k}_1 and \mathbf{k}_2) of the muons.

Next we need to know how to write a bound state in terms of free-particle states. For a general two-body system with equal constituent masses, the center-of-mass and relative coordinates are

$$\mathbf{R} = \frac{1}{2}(\mathbf{r}_1 + \mathbf{r}_2), \quad \mathbf{r} = \mathbf{r}_1 - \mathbf{r}_2. \quad (5.40)$$

These have conjugate momenta

$$\mathbf{K} = \mathbf{k}_1 + \mathbf{k}_2, \quad \mathbf{k} = \frac{1}{2}(\mathbf{k}_1 - \mathbf{k}_2). \quad (5.41)$$

The total momentum \mathbf{K} is zero in the center-of-mass frame. If we know the force between the particles (for $\mu^+ \mu^-$, it is just the Coulomb force), we can

[‡]Reviews of this subject can be found in Bodwin, Yennie, and Gregorio, Rev. Mod. Phys. **57**, 723 (1985), and in Sapirstein and Yennie, in Kinoshita (1990).

solve the nonrelativistic Schrödinger equation to find the Schrödinger wavefunction, $\psi(\mathbf{r})$. The bound state is just a linear superposition of free states of definite \mathbf{r} or \mathbf{k} , weighted by this wavefunction. For our purposes it is more convenient to build this superposition in momentum space, using the Fourier transform of $\psi(\mathbf{r})$:

$$\tilde{\psi}(\mathbf{k}) = \int d^3x e^{i\mathbf{k}\cdot\mathbf{r}} \psi(\mathbf{r}); \quad \int \frac{d^3k}{(2\pi)^3} |\tilde{\psi}(\mathbf{k})|^2 = 1. \quad (5.42)$$

If $\psi(\mathbf{r})$ is normalized conventionally, $\tilde{\psi}(\mathbf{k})$ gives the amplitude for finding a particular value of \mathbf{k} . An explicit expression for a bound state with mass $M \approx 2m$, momentum $\mathbf{K} = 0$, and spin 1 oriented up is then

$$|B\rangle = \sqrt{2M} \int \frac{d^3k}{(2\pi)^3} \tilde{\psi}(\mathbf{k}) \frac{1}{\sqrt{2m}} \frac{1}{\sqrt{2m}} |\mathbf{k} \uparrow, -\mathbf{k} \uparrow\rangle. \quad (5.43)$$

The factors of $(1/\sqrt{2m})$ convert our relativistically normalized free-particle states so that their integral with $\tilde{\psi}(\mathbf{k})$ is a state of norm 1. (The factors should involve $\sqrt{2E_{\pm\mathbf{k}}}$, but for a nonrelativistic bound state, $|\mathbf{k}| \ll m$.) The outside factor of $\sqrt{2M}$ converts back to the relativistic normalization assumed by our formula for cross sections. These normalization factors could easily be modified to describe a bound state with nonzero total momentum \mathbf{K} .

Given this expression for the bound state, we can immediately write down the amplitude for its production:

$$\mathcal{M}(\uparrow\uparrow \rightarrow B) = \sqrt{2M} \int \frac{d^3k}{(2\pi)^3} \tilde{\psi}^*(\mathbf{k}) \frac{1}{\sqrt{2m}} \frac{1}{\sqrt{2m}} \mathcal{M}(\uparrow\uparrow \rightarrow \mathbf{k} \uparrow, -\mathbf{k} \uparrow). \quad (5.44)$$

Since the free-state amplitude from (5.39) is independent of the momenta of the muons, the integral over \mathbf{k} gives $\psi^*(0)$, the position-space wavefunction evaluated at the origin. It is quite natural that the amplitude for creation of a two-particle state from a pointlike virtual photon should be proportional to the value of the wavefunction at zero separation. Assembling the pieces, we find that the amplitude is simply

$$\mathcal{M}(\uparrow\uparrow \rightarrow B) = \sqrt{\frac{2}{M}} (-2e^2) \psi^*(0). \quad (5.45)$$

In a moment we will compute the cross section from this amplitude. First, however, let us generalize this discussion to treat bound states with more general spin configurations. The analysis leading up to (5.37) will cast any S -matrix element for the production of nonrelativistic fermions with momenta \mathbf{k} and $-\mathbf{k}$ into the form of a spin matrix element

$$i\mathcal{M}(\text{something} \rightarrow \mathbf{k}, \mathbf{k}') = \xi^\dagger [\Gamma(\mathbf{k})] \xi', \quad (5.46)$$

where $\Gamma(\mathbf{k})$ is some 2×2 matrix. We now must replace the spinors with a normalized spin wavefunction for the bound state. In the example just completed,

we replaced

$$\xi' \xi^\dagger \rightarrow \begin{pmatrix} 0 \\ 1 \end{pmatrix} (1 \quad 0) = \begin{pmatrix} 0 & 0 \\ 1 & 0 \end{pmatrix}. \quad (5.47)$$

More generally, a spin-1 state is obtained by the replacement

$$\xi' \xi^\dagger \rightarrow \frac{1}{\sqrt{2}} \mathbf{n}^* \cdot \boldsymbol{\sigma}, \quad (5.48)$$

where \mathbf{n} is a unit vector. Choosing $\mathbf{n} = (\hat{x} + i\hat{y})/\sqrt{2}$ gives back (5.47), while the choices $\mathbf{n} = (\hat{x} - i\hat{y})/\sqrt{2}$ and $\mathbf{n} = \hat{z}$ give the other two spin-1 states $\downarrow\downarrow$ and $(\uparrow\downarrow + \downarrow\uparrow)/\sqrt{2}$. (The relative minus sign in (5.48) for this last case comes from the rule (3.135) for the flipped spin.) Similarly, the spin-zero state $(\uparrow\downarrow - \downarrow\uparrow)/\sqrt{2}$ is given by the replacement

$$\xi' \xi^\dagger \rightarrow \frac{1}{\sqrt{2}} \mathbf{1}, \quad (5.49)$$

involving the 2×2 unit matrix. With these rules, we can convert an S -matrix element of the form (5.46) quite generally into an S -matrix element for production of a bound state at rest:

$$i\mathcal{M}(\text{something} \rightarrow B) = \sqrt{\frac{2}{M}} \int \frac{d^3 k}{(2\pi)^3} \tilde{\psi}^*(\mathbf{k}) \text{tr}\left(\frac{\mathbf{n}^* \cdot \boldsymbol{\sigma}}{\sqrt{2}} \Gamma(\mathbf{k})\right), \quad (5.50)$$

where the trace is taken over 2-component spinor indices. For a spin-0 bound state, replace $\mathbf{n} \cdot \boldsymbol{\sigma}$ by the unit matrix.

Vector Meson Production and Decay

Equation (5.45) can be straightforwardly converted into a cross section for production of $\mu^+ \mu^-$ bound states in $e^+ e^-$ annihilation. To make it easier to extract all the physics in this equation, let us introduce polarization vectors for the initial and final spin configurations: $\epsilon_+ = (\hat{x} + i\hat{y})/\sqrt{2}$, from Eq. (5.29), and \mathbf{n} , from Eq. (5.48). Then (5.45) can be rewritten in a more invariant form as

$$\mathcal{M}(e_R^- e_L^+ \rightarrow B) = \sqrt{\frac{2}{M}} (-2e^2) (\mathbf{n}^* \cdot \boldsymbol{\epsilon}_+) \psi^*(0). \quad (5.51)$$

The bound state spin polarization \mathbf{n} is projected parallel to $\boldsymbol{\epsilon}_+$. Note that if the electrons are initially unpolarized, the cross section for production of B will involve the polarization average

$$\frac{1}{4} (|\mathbf{n}^* \cdot \boldsymbol{\epsilon}_+|^2 + |\mathbf{n}^* \cdot \boldsymbol{\epsilon}_-|^2) = \frac{1}{4} (|n^x|^2 + |n^y|^2). \quad (5.52)$$

Thus, the bound states produced will still be preferentially polarized along the $e^+ e^-$ collision axis.

Assuming an unpolarized electron beam, and summing (5.52) over the three possible directions of \mathbf{n} , we find the following expression for the total cross section for production of the bound state:

$$\sigma(e^+e^- \rightarrow B) = \frac{1}{2} \frac{1}{2m} \frac{1}{2m} \int \frac{d^3 K}{(2\pi)^3} \frac{1}{2E_K} (2\pi)^4 \delta^{(4)}(p+p'-K) \cdot \frac{2}{M} (4e^4) \frac{1}{2} |\psi(0)|^2. \quad (5.53)$$

Notice that the 1-body phase space integral can remove only three of the four delta functions. It is conventional to rewrite the last delta function using $\delta(P^0 - K^0) = 2K^0 \delta(P^2 - K^2)$. Then

$$\sigma(e^+e^- \rightarrow B) = 64\pi^3 \alpha^2 \frac{|\psi(0)|^2}{M^3} \delta(E_{cm}^2 - M^2). \quad (5.54)$$

The last delta function enforces the constraint that the total center-of-mass energy must equal the bound-state mass; thus, the bound state is produced as a resonance in e^+e^- annihilation. If the bound state has a finite lifetime, this delta function will be broadened into a resonance peak. In practice, the intrinsic spread of the e^+e^- beam energy is often a more important broadening mechanism. In either case, (5.54) correctly predicts the area under the resonance peak.

If the bound state B can be produced from e^+e^- , it can also annihilate back to e^+e^- , or to any other sufficiently light lepton pair. According to (4.86), the total width for this decay mode is given by

$$\Gamma(B \rightarrow e^+e^-) = \frac{1}{2M} \int d\Pi_2 |\mathcal{M}|^2, \quad (5.55)$$

where \mathcal{M} is just the complex conjugate of the matrix element (5.51) we used to compute B production. Thus

$$\Gamma = \frac{1}{2M} \int \left(\frac{1}{8\pi} \frac{d\cos\theta}{2} \right) \frac{8e^4}{M} |\psi(0)|^2 (|\mathbf{n} \cdot \boldsymbol{\epsilon}|^2 + |\mathbf{n} \cdot \boldsymbol{\epsilon}^*|^2). \quad (5.56)$$

This formula is summed over the possible final electron polarization states. It is easiest to evaluate by averaging over the three possible values of \mathbf{n} . We thus obtain

$$\Gamma(B \rightarrow e^+e^-) = \frac{16\pi\alpha^2}{3} \frac{|\psi(0)|^2}{M^2}. \quad (5.57)$$

The formula for the decay width of B is very similar to that for the production cross section, and this is no surprise: Both calculations involve the square of the same matrix element, summed over initial and final polarizations. The two calculations differed only in how we formed the polarization averages, and in the phase-space factors. By this logic, the relation we have found between the two quantities,

$$\sigma(e^+e^- \rightarrow B) = 4\pi^2 \cdot \frac{3\Gamma(B \rightarrow e^+e^-)}{M} \cdot \delta(E_{cm}^2 - M^2), \quad (5.58)$$

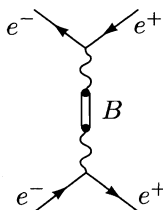
is very general and completely independent of the details of the matrix element computation. The factor 3 in (5.58) came from the orientation average for \mathbf{n} ; for a spin- J bound state, this factor would be $(2J+1)$.

The most famous application of this formalism is to bound states not of muons but of quarks: *quarkonium*. We saw the experimental evidence for $q\bar{q}$ bound states (the J/ψ and Υ , for example) in Fig. 5.3. (The resonance peaks are much too high and too narrow to show in the figure, but their sizes have been carefully measured.) Equations (5.54) and (5.57) must be multiplied by a color factor of 3 to give the production cross section and decay width for a spin-1 $q\bar{q}$ bound state. The value $\psi(0)$ of the $q\bar{q}$ wavefunction at the origin cannot be computed from first principles, but can be estimated from a nonrelativistic model of the $q\bar{q}$ spectrum with a phenomenologically chosen potential. Alternatively, we can use the formula

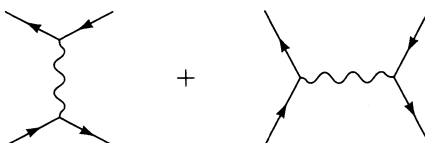
$$\Gamma(B(q\bar{q}) \rightarrow e^+e^-) = 16\pi\alpha^2 Q^2 \frac{|\psi(0)|^2}{M^2} \quad (5.59)$$

to measure $\psi(0)$ for a $q\bar{q}$ bound state. For example, the $1S$ spin-1 state of $s\bar{s}$, the ϕ meson, has an e^+e^- partial width of 1.4 keV and a mass of 1.02 GeV. From this we can infer $|\psi(0)|^2 = (1.2 \text{ fm})^{-3}$. This result is physically reasonable, since hadronic dimensions are typically $\sim 1 \text{ fm}$.

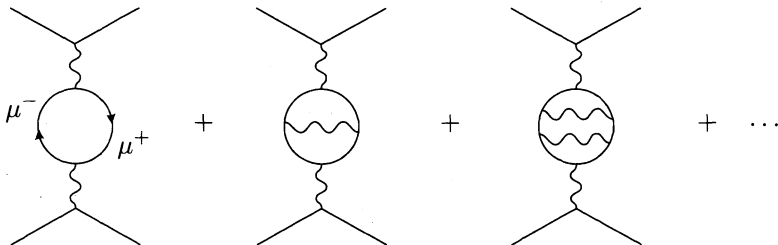
Our viewpoint in this section has been quite different from that of earlier sections: Instead of computing everything from first principles, we have pieced together an approximate formula using a bit of quantum field theory and a bit of nonrelativistic quantum mechanics. In principle, however, we could treat bound states entirely in the relativistic formalism. Consider the annihilation of an e^+e^- pair to form a $\mu^+\mu^-$ bound state, which subsequently decays back into e^+e^- . In our present formalism we might represent this process by the diagram



The net process is simply $e^+e^- \rightarrow e^+e^-$ (Bhabha scattering). What would happen if we tried to compute the Bhabha scattering cross section directly in QED perturbation theory? Obviously there is no $\mu^+\mu^-$ contribution in the tree-level diagrams:



As we go to higher orders in the perturbation series, however, we find (among others) the following set of diagrams:



At most values of E_{cm} , these diagrams give only a small correction to the tree-level expression. But when E_{cm} is near the $\mu^+\mu^-$ threshold, the diagrams involving the exchange of photons within the muon loop contain the Coulomb interaction between the muons, and therefore become quite large. One must sum over all such diagrams, and it can be shown that this summation is equivalent to solving the nonrelativistic Schrödinger equation.* The final prediction is that the cross section contains a resonance peak, whose area is given by (5.54) and whose width is given by (5.57).

5.4 Crossing Symmetry

Electron-Muon Scattering

Now that we have completed our discussion of the process $e^+e^- \rightarrow \mu^+\mu^-$, let us consider a different but closely related QED process: electron-muon scattering, or $e^-\mu^- \rightarrow e^-\mu^-$. The lowest-order Feynman diagram is just the previous one turned on its side:

$$\frac{ie^2}{q^2} \bar{u}(p'_1)\gamma^\mu u(p_1) \bar{u}(p'_2)\gamma_\mu u(p_2).$$

The relation between the processes $e^+e^- \rightarrow \mu^+\mu^-$ and $e^-\mu^- \rightarrow e^-\mu^-$ becomes clear when we compute the squared amplitude, averaged and summed over spins:

$$\frac{1}{4} \sum_{\text{spins}} |\mathcal{M}|^2 = \frac{e^4}{4q^4} \text{tr}[(\not{p}'_1 + m_e)\gamma^\mu(\not{p}_1 + m_e)\gamma^\nu] \text{tr}[(\not{p}'_2 + m_\mu)\gamma_\mu(\not{p}_2 + m_\mu)\gamma_\nu].$$

This is exactly the same as our result (5.4) for $e^+e^- \rightarrow \mu^+\mu^-$, with the replacements

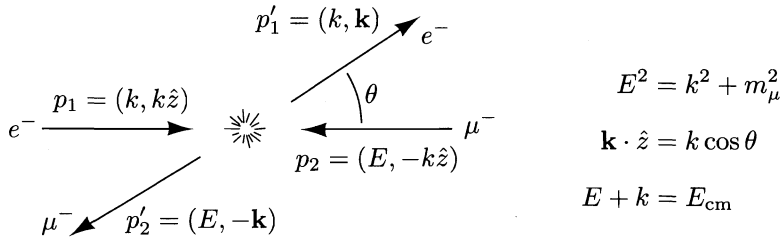
$$p \rightarrow p_1, \quad p' \rightarrow -p'_1, \quad k \rightarrow p'_2, \quad k' \rightarrow -p_2. \quad (5.60)$$

*This analysis is carried out in Berestetskii, Lifshitz, and Pitaevskii (1982).

So instead of evaluating the traces from scratch, we can just make the same replacements in our previous result, Eq. (5.10). Setting $m_e = 0$, we find

$$\frac{1}{4} \sum_{\text{spins}} |\mathcal{M}|^2 = \frac{8e^4}{q^4} \left[(p_1 \cdot p'_2)(p'_1 \cdot p_2) + (p_1 \cdot p_2)(p'_1 \cdot p'_2) - m_\mu^2(p_1 \cdot p'_1) \right]. \quad (5.61)$$

To evaluate this expression, we must work out the kinematics, which will be completely different. Working in the center-of-mass frame, we make the following assignments:



The combinations we need are

$$\begin{aligned} p_1 \cdot p_2 &= p'_1 \cdot p'_2 = k(E + k); & p'_1 \cdot p_2 &= p_1 \cdot p'_2 = k(E + k \cos \theta); \\ p_1 \cdot p'_1 &= k^2(1 - \cos \theta); & q^2 &= -2p_1 \cdot p'_1 = -2k^2(1 - \cos \theta). \end{aligned}$$

Our expression for the squared matrix element now becomes

$$\frac{1}{4} \sum_{\text{spins}} |\mathcal{M}|^2 = \frac{2e^4}{k^2(1 - \cos \theta)^2} \left((E+k)^2 + (E+k \cos \theta)^2 - m_\mu^2(1 - \cos \theta) \right). \quad (5.62)$$

To find the cross section from this expression, we use Eq. (4.84), which in the case where one particle is massless takes the simple form

$$\left(\frac{d\sigma}{d\Omega} \right)_{\text{CM}} = \frac{|\mathcal{M}|^2}{64\pi^2(E+k)^2}. \quad (5.63)$$

Thus we have our result for unpolarized electron-muon scattering in the center-of-mass frame:

$$\frac{d\sigma}{d\Omega} = \frac{\alpha^2}{2k^2(E+k)^2(1 - \cos \theta)^2} \left((E+k)^2 + (E+k \cos \theta)^2 - m_\mu^2(1 - \cos \theta) \right), \quad (5.64)$$

where $k = \sqrt{E^2 - m_\mu^2}$. In the high-energy limit where we can set $m_\mu = 0$, the differential cross section becomes

$$\frac{d\sigma}{d\Omega} = \frac{\alpha^2}{2E_{\text{cm}}^2(1 - \cos \theta)^2} \left(4 + (1 + \cos \theta)^2 \right). \quad (5.65)$$

Note the singular behavior

$$\frac{d\sigma}{d\Omega} \propto \frac{1}{\theta^4} \quad \text{as } \theta \rightarrow 0 \quad (5.66)$$

of formulae (5.64) and (5.65). This singularity is the same as in the Rutherford formula (Problem 4.4). Such behavior is always present in Coulomb scattering; it arises from the nearly on-shell (that is, $q^2 \approx 0$) virtual photon.

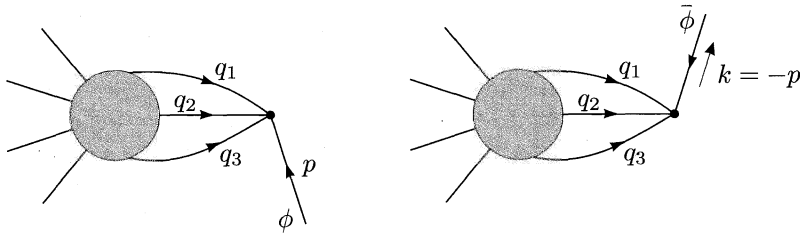
Crossing Symmetry

The trick we made use of here, namely the relation between the two processes $e^+e^- \rightarrow \mu^+\mu^-$ and $e^-\mu^- \rightarrow e^-\mu^-$, is our first example of a type of relation known as *crossing symmetry*. In general, the S -matrix for any process involving a particle with momentum p in the initial state is equal to the S -matrix for an otherwise identical process but with an antiparticle of momentum $k = -p$ in the final state. That is,

$$\mathcal{M}(\phi(p) + \dots \rightarrow \dots) = \mathcal{M}(\dots \rightarrow \dots + \bar{\phi}(k)), \quad (5.67)$$

where $\bar{\phi}$ is the antiparticle of ϕ and $k = -p$. (Note that there is no value of p for which p and k are both physically allowed, since the particle must have $p^0 > 0$ and the antiparticle must have $k^0 > 0$. So technically, we should say that either amplitude can be obtained from the other by analytic continuation.)

Relation (5.67) follows directly from the Feynman rules. The diagrams that contribute to the two amplitudes fall into a natural one-to-one correspondence, where corresponding diagrams differ only by changing the incoming ϕ into the outgoing $\bar{\phi}$. A typical pair of diagrams looks like this:



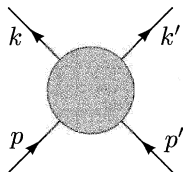
In the first diagram, the momenta q_i coming into the vertex from the rest of the diagram must add up to $-p$, while in the second diagram they must add up to k . Thus the two diagrams are equal, except for any possible difference in the external leg factors, if $p = -k$. If ϕ is a spin-zero boson, there is no external leg factor, so the identity is proved. If ϕ is a fermion, the analysis becomes more subtle, since the relation depends on the relative phase convention for the external spinors u and v . If we simply replace p by $-k$ in the fermion polarization sum, we find

$$\sum u(p)\bar{u}(p) = \not{p} + m = -(\not{k} - m) = -\sum v(k)\bar{v}(k). \quad (5.68)$$

The minus sign can be compensated by changing our phase convention for $v(k)$. In practice, it is easiest to cancel by hand one minus sign for each crossed fermion. With appropriate conventions for the spinors $u(p)$ and $v(k)$, it is possible to prove the identity (5.67) without spin-averaging.

Mandelstam Variables

It is often useful to express scattering amplitudes in terms of variables that make it easy to apply crossing relations. For 2-body \rightarrow 2-body processes, this can be done as follows. Label the four external momenta as



We now define three new quantities, the *Mandelstam variables*:

$$\begin{aligned} s &= (p + p')^2 = (k + k')^2; \\ t &= (k - p)^2 = (k' - p')^2; \\ u &= (k' - p)^2 = (k - p')^2. \end{aligned} \quad (5.69)$$

The definitions of t and u appear to be interchangeable (by renaming $k \rightarrow k'$); it is conventional to define t as the squared difference of the initial and final momenta of the most similar particles. For any process, s is the square of the total initial 4-momentum. Note that if we had defined all four momenta to be ingoing, all signs in these definitions would be +.

To illustrate the use of the Mandelstam variables, let us first consider the squared amplitude for $e^+e^- \rightarrow \mu^+\mu^-$, working in the massless limit for simplicity. In this limit we have $t = -2p \cdot k = -2p' \cdot k'$ and $u = -2p \cdot k' = -2p' \cdot k$, while of course $s = (p + p')^2 = q^2$. Referring to our previous result (5.10), we find

$$\frac{1}{4} \sum_{\text{spins}} |\mathcal{M}|^2 = \frac{8e^4}{s^2} \left[\left(\frac{t}{2} \right)^2 + \left(\frac{u}{2} \right)^2 \right]. \quad (5.70)$$

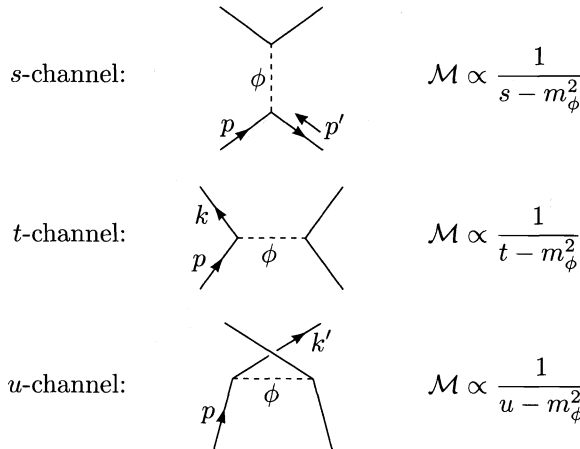
To convert to the process $e^-\mu^- \rightarrow e^-\mu^-$, we turn the diagram on its side and make use of the crossing relations, which become quite simple in terms of Mandelstam variables. For example, the crossing relations tell us to change the sign of p' , the positron momentum, and reinterpret it as the momentum of the outgoing electron. Therefore $s = (p + p')^2$ becomes what we would now call t , the difference of the outgoing and incoming electron momenta. Similarly, t becomes s , while u remains unchanged. Thus for $e^-\mu^- \rightarrow e^-\mu^-$,

we can immediately write down

$$\frac{1}{4} \sum_{\text{spins}} |\mathcal{M}|^2 = \frac{8e^4}{t^2} \left[\left(\frac{s}{2} \right)^2 + \left(\frac{u}{2} \right)^2 \right]. \quad (5.71)$$

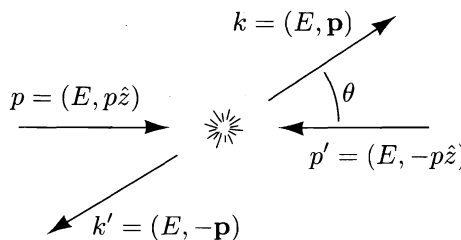
You can easily check that this agrees with (5.61) in the massless limit. Note that while (5.70) and (5.71) look quite similar, they are physically very different: The denominator of the first is just $s^2 = E_{\text{cm}}^4$, but that of the second involves t , which depends on angles and goes to zero as $\theta \rightarrow 0$.

When a 2-body \rightarrow 2-body diagram contains only one virtual particle, it is conventional to describe that particle as being in a certain “channel”. The channel can be read from the form of the Feynman diagram, and each channel leads to a characteristic angular dependence of the cross section:



In many cases, a single process will receive contributions from more than one channel; these must be added coherently. For example, the amplitude for *Bhabha scattering*, $e^+e^- \rightarrow e^+e^-$, is the sum of *s*- and *t*-channel diagrams; *Møller scattering*, $e^-e^- \rightarrow e^-e^-$, involves *t*- and *u*-channel diagrams.

To get a better feel for *s*, *t*, and *u*, let us evaluate them explicitly in the center-of-mass frame for particles all of mass m . The kinematics is as usual:



Thus the Mandelstam variables are

$$\begin{aligned}s &= (p + p')^2 = (2E)^2 = E_{\text{cm}}^2; \\ t &= (k - p)^2 = -p^2 \sin^2 \theta - p^2(\cos \theta - 1)^2 = -2p^2(1 - \cos \theta); \\ u &= (k' - p)^2 = -p^2 \sin^2 \theta - p^2(\cos \theta + 1)^2 = -2p^2(1 + \cos \theta).\end{aligned}\quad (5.72)$$

Thus we see that $t \rightarrow 0$ as $\theta \rightarrow 0$, while $u \rightarrow 0$ as $\theta \rightarrow \pi$. (When the masses are not all equal, the limiting values of t and u will shift slightly.)

Note from (5.72) that when all four particles have mass m , the sum of the Mandelstam variables is $s + t + u = 4E^2 - 4p^2 = 4m^2$. This is a special case of a more general relation, which is often quite useful:

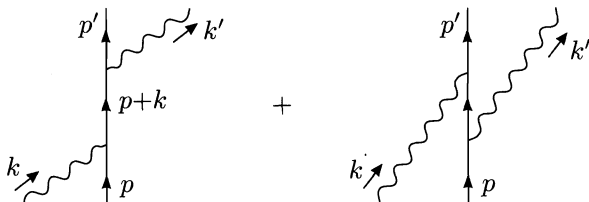
$$s + t + u = \sum_{i=1}^4 m_i^2, \quad (5.73)$$

where the sum runs over the four external particles. This identity is easy to prove by adding up the terms on the right-hand side of Eqs. (5.69), and applying momentum conservation in the form $(p + p' - k - k')^2 = 0$.

5.5 Compton Scattering

We now move on to consider a somewhat different QED process: *Compton scattering*, or $e^- \gamma \rightarrow e^- \gamma$. We will calculate the unpolarized cross section for this reaction, to lowest order in α . The calculation will employ all the machinery we have developed so far, including the Mandelstam variables of the previous section. We will also develop some new technology for dealing with external photons.

This is our first example of a calculation involving two diagrams:



As usual, the Feynman rules tell us exactly how to write down an expression for \mathcal{M} . Note that since the fermion portions of the two diagrams are identical, there is no relative minus sign between the two terms. Using $\epsilon_\nu(k)$ and $\epsilon_\mu^*(k')$ to denote the polarization vectors of the initial and final photons, we have

$$\begin{aligned}i\mathcal{M} &= \bar{u}(p')(-ie\gamma^\mu)\epsilon_\mu^*(k')\frac{i(\not{p} + \not{k} + m)}{(p + k)^2 - m^2}(-ie\gamma^\nu)\epsilon_\nu(k)u(p) \\ &\quad + \bar{u}(p')(-ie\gamma^\nu)\epsilon_\nu(k)\frac{i(\not{p} - \not{k}' + m)}{(p - k')^2 - m^2}(-ie\gamma^\mu)\epsilon_\mu^*(k')u(p)\end{aligned}$$

$$= -ie^2 \epsilon_\mu^*(k') \epsilon_\nu(k) \bar{u}(p') \left[\frac{\gamma^\mu (\not{p} + \not{k} + m) \gamma^\nu}{(p+k)^2 - m^2} + \frac{\gamma^\nu (\not{p} - \not{k}' + m) \gamma^\mu}{(p-k')^2 - m^2} \right] u(p).$$

We can make a few simplifications before squaring this expression. Since $p^2 = m^2$ and $k^2 = 0$, the denominators of the propagators are

$$(p+k)^2 - m^2 = 2p \cdot k \quad \text{and} \quad (p-k')^2 - m^2 = -2p \cdot k'.$$

To simplify the numerators, we use a bit of Dirac algebra:

$$\begin{aligned} (\not{p} + m) \gamma^\nu u(p) &= (2p^\nu - \gamma^\nu \not{p} + \gamma^\nu m) u(p) \\ &= 2p^\nu u(p) - \gamma^\nu (\not{p} - m) u(p) \\ &= 2p^\nu u(p). \end{aligned}$$

Using this trick on the numerator of each propagator, we obtain

$$i\mathcal{M} = -ie^2 \epsilon_\mu^*(k') \epsilon_\nu(k) \bar{u}(p') \left[\frac{\gamma^\mu \not{k} \gamma^\nu + 2\gamma^\mu p^\nu}{2p \cdot k} + \frac{-\gamma^\nu \not{k}' \gamma^\mu + 2\gamma^\nu p^\mu}{-2p \cdot k'} \right] u(p). \quad (5.74)$$

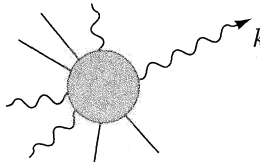
Photon Polarization Sums

The next step in the calculation will be to square this expression for \mathcal{M} and sum (or average) over electron and photon polarization states. The sum over electron polarizations can be performed as before, using the identity $\Sigma u(p) \bar{u}(p) = \not{p} + m$. Fortunately, there is a similar trick for summing over photon polarization vectors. The correct prescription is to make the replacement

$$\sum_{\text{polarizations}} \epsilon_\mu^* \epsilon_\nu \longrightarrow -g_{\mu\nu}. \quad (5.75)$$

The arrow indicates that this is not an actual equality. Nevertheless, the replacement is valid as long as both sides are dotted into the rest of the expression for a QED amplitude \mathcal{M} .

To derive this formula, let us consider an arbitrary QED process involving an external photon with momentum k :



$$= i\mathcal{M}(k) \equiv i\mathcal{M}^\mu(k) \epsilon_\mu^*(k). \quad (5.76)$$

Since the amplitude always contains $\epsilon_\mu^*(k)$, we have extracted this factor and defined $\mathcal{M}^\mu(k)$ to be the rest of the amplitude \mathcal{M} . The cross section will be proportional to

$$\sum_{\epsilon} |\epsilon_\mu^*(k) \mathcal{M}^\mu(k)|^2 = \sum_{\epsilon} \epsilon_\mu^* \epsilon_\nu \mathcal{M}^\mu(k) \mathcal{M}^{\nu*}(k).$$

For simplicity, we orient k in the 3-direction: $k^\mu = (k, 0, 0, k)$. Then the two transverse polarization vectors, over which we are summing, can be chosen to be

$$\epsilon_1^\mu = (0, 1, 0, 0); \quad \epsilon_2^\mu = (0, 0, 1, 0).$$

With these conventions, we have

$$\sum_{\epsilon} |\epsilon_\mu^*(k) \mathcal{M}^\mu(k)|^2 = |\mathcal{M}^1(k)|^2 + |\mathcal{M}^2(k)|^2. \quad (5.77)$$

Now recall from Chapter 4 that external photons are created by the interaction term $\int d^4x e j^\mu A_\mu$, where $j^\mu = \bar{\psi} \gamma^\mu \psi$ is the Dirac vector current. Therefore we expect $\mathcal{M}^\mu(k)$ to be given by a matrix element of the Heisenberg field j^μ :

$$\mathcal{M}^\mu(k) = \int d^4x e^{ik \cdot x} \langle f | j^\mu(x) | i \rangle, \quad (5.78)$$

where the initial and final states include all particles except the photon in question.

From the classical equations of motion, we know that the current j^μ is conserved: $\partial_\mu j^\mu(x) = 0$. Provided that this property still holds in the quantum theory, we can dot k_μ into (5.78) to obtain

$$k_\mu \mathcal{M}^\mu(k) = 0. \quad (5.79)$$

The amplitude \mathcal{M} vanishes when the polarization vector $\epsilon_\mu(k)$ is replaced by k_μ . This famous relation is known as the *Ward identity*. It is essentially a statement of current conservation, which is a consequence of the gauge symmetry (4.6) of QED. We will give a formal proof of the Ward identity in Section 7.4, and discuss a number of subtle points skimmed over in this quick “derivation”.

It is useful to check explicitly that the Compton amplitude given in (5.74) obeys the Ward identity. To do this, replace $\epsilon_\nu(k)$ by k_ν or $\epsilon_\mu^*(k')$ by k'_μ , and manipulate the Dirac matrix products. In either case (after a bit of algebra) the terms from the two diagrams cancel each other to give zero.

Returning to our derivation of the polarization sum formula (5.75), we note that for $k^\mu = (k, 0, 0, k)$, the Ward identity takes the form

$$k \mathcal{M}^0(k) - k \mathcal{M}^3(k) = 0. \quad (5.80)$$

Thus $\mathcal{M}^0 = \mathcal{M}^3$, and we have

$$\begin{aligned} \sum_{\epsilon} \epsilon_\mu^* \epsilon_\nu \mathcal{M}^\mu(k) \mathcal{M}^{\nu*}(k) &= |\mathcal{M}^1|^2 + |\mathcal{M}^2|^2 \\ &= |\mathcal{M}^1|^2 + |\mathcal{M}^2|^2 + |\mathcal{M}^3|^2 - |\mathcal{M}^0|^2 \\ &= -g_{\mu\nu} \mathcal{M}^\mu(k) \mathcal{M}^{\nu*}(k). \end{aligned}$$

That is, we may sum over external photon polarizations by replacing $\sum \epsilon_\mu^* \epsilon_\nu$ with $-g_{\mu\nu}$.

Note that this proves (pending our general proof of the Ward identity) that the unphysical timelike and longitudinal photons can be consistently omitted from QED calculations, since in any event the squared amplitudes for producing these states cancel to give zero total probability. The negative norm of the timelike photon state, a property that troubled us in the discussion after Eq. (4.132), plays an essential role in this cancellation.

The Klein-Nishina Formula

The rest of the computation of the Compton scattering cross section is straightforward, although it helps to be somewhat organized. We want to average the squared amplitude over the initial electron and photon polarizations, and sum over the final electron and photon polarizations. Starting with expression (5.74) for \mathcal{M} , we find

$$\begin{aligned} \frac{1}{4} \sum_{\text{spins}} |\mathcal{M}|^2 &= \frac{e^4}{4} g_{\mu\rho} g_{\nu\sigma} \cdot \text{tr} \left\{ (\not{p}' + m) \left[\frac{\gamma^\mu \not{k} \gamma^\nu + 2\gamma^\mu p^\nu}{2p \cdot k} + \frac{\gamma^\nu \not{k}' \gamma^\mu - 2\gamma^\nu p^\mu}{2p \cdot k'} \right] \right. \\ &\quad \left. \cdot (\not{p} + m) \left[\frac{\gamma^\sigma \not{k} \gamma^\rho + 2\gamma^\rho p^\sigma}{2p \cdot k} + \frac{\gamma^\rho \not{k}' \gamma^\sigma - 2\gamma^\sigma p^\rho}{2p \cdot k'} \right] \right\} \\ &\equiv \frac{e^4}{4} \left[\frac{\mathbf{I}}{(2p \cdot k)^2} + \frac{\mathbf{II}}{(2p \cdot k)(2p \cdot k')} + \frac{\mathbf{III}}{(2p \cdot k')(2p \cdot k)} + \frac{\mathbf{IV}}{(2p \cdot k')^2} \right], \end{aligned} \quad (5.81)$$

where **I**, **II**, **III**, and **IV** are complicated traces. Note that **IV** is the same as **I** if we replace k with $-k'$. Also, since we can reverse the order of the γ matrices inside a trace (Eq. (5.7)), we see that **II** = **III**. Thus we must work only to compute **I** and **II**.

The first of the traces is

$$\mathbf{I} = \text{tr} [(\not{p}' + m)(\gamma^\mu \not{k} \gamma^\nu + 2\gamma^\mu p^\nu)(\not{p} + m)(\gamma_\nu \not{k} \gamma_\mu + 2\gamma_\mu p_\nu)].$$

There are 16 terms inside the trace, but half contain an odd number of γ matrices and therefore vanish. We must now evaluate the other eight terms, one at a time. For example,

$$\begin{aligned} \text{tr} [\not{p}' \gamma^\mu \not{k} \gamma^\nu \not{p} \gamma_\nu \not{k} \gamma_\mu] &= \text{tr} [(-2\not{p}') \not{k} (-2\not{p}) \not{k}] \\ &= \text{tr} [4\not{p}' \not{k} (2p \cdot k - \not{k} \not{p})] \\ &= 8p \cdot k \text{ tr} [\not{p}' \not{k}] \\ &= 32(p \cdot k)(p' \cdot k). \end{aligned}$$

By similar use of the contraction identities (5.8) and (5.9), and other Dirac algebra such as $\not{p}\not{p}' = p^2 = m^2$, each term in **I** can be reduced to a trace of no more than two γ matrices. When the smoke clears, we find

$$\mathbf{I} = 16(4m^4 - 2m^2 p \cdot p' + 4m^2 p \cdot k - 2m^2 p' \cdot k + 2(p \cdot k)(p' \cdot k)). \quad (5.82)$$

Although it is not obvious, this expression can be simplified further. To see how, introduce the Mandelstam variables:

$$\begin{aligned}s &= (p+k)^2 = 2p \cdot k + m^2 = 2p' \cdot k' + m^2; \\ t &= (p'-p)^2 = -2p \cdot p' + 2m^2 = -2k \cdot k'; \\ u &= (k'-p)^2 = -2k' \cdot p + m^2 = -2k \cdot p' + m^2.\end{aligned}\quad (5.83)$$

Recall from (5.73) that momentum conservation implies $s+t+u = 2m^2$. Writing everything in terms of s , t , and u , and using this identity, we eventually obtain

$$\mathbf{I} = 16(2m^4 + m^2(s-m^2) - \frac{1}{2}(s-m^2)(u-m^2)). \quad (5.84)$$

Sending $k \leftrightarrow -k'$, we can immediately write

$$\mathbf{IV} = 16(2m^4 + m^2(u-m^2) - \frac{1}{2}(s-m^2)(u-m^2)). \quad (5.85)$$

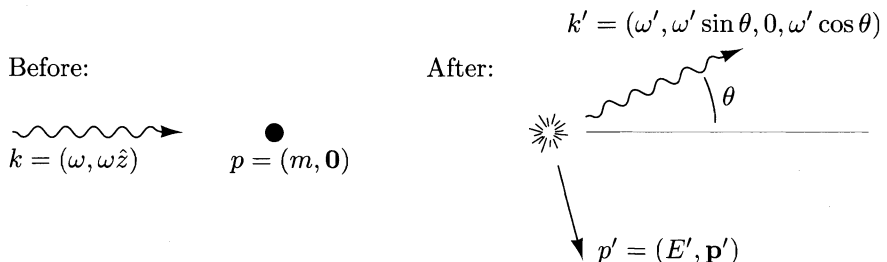
Evaluating the traces in the numerators **II** and **III** requires about the same amount of work as we have just done. The answer is

$$\mathbf{II} = \mathbf{III} = -8(4m^4 + m^2(s-m^2) + m^2(u-m^2)). \quad (5.86)$$

Putting together the pieces of the squared matrix element (5.81), and rewriting s and u in terms of $p \cdot k$ and $p \cdot k'$, we finally obtain

$$\frac{1}{4} \sum_{\text{spins}} |\mathcal{M}|^2 = 2e^4 \left[\frac{p \cdot k'}{p \cdot k} + \frac{p \cdot k}{p \cdot k'} + 2m^2 \left(\frac{1}{p \cdot k} - \frac{1}{p \cdot k'} \right) + m^4 \left(\frac{1}{p \cdot k} - \frac{1}{p \cdot k'} \right)^2 \right]. \quad (5.87)$$

To turn this expression into a cross section we must decide on a frame of reference and draw a picture of the kinematics. Compton scattering is most often analyzed in the “lab” frame, in which the electron is initially at rest:



We will express the cross section in terms of ω and θ . We can find ω' , the energy of the final photon, using the following trick:

$$\begin{aligned}m^2 &= (p')^2 = (p+k-k')^2 = p^2 + 2p \cdot (k-k') - 2k \cdot k' \\ &= m^2 + 2m(\omega - \omega') - 2\omega\omega'(1 - \cos\theta),\end{aligned}$$

hence, $\frac{1}{\omega'} - \frac{1}{\omega} = \frac{1}{m}(1 - \cos\theta).$ (5.88)

The last line is Compton's formula for the shift in the photon wavelength. For our purposes, however, it is more useful to solve for ω' :

$$\omega' = \frac{\omega}{1 + \frac{\omega}{m}(1 - \cos \theta)}. \quad (5.89)$$

The phase space integral in this frame is

$$\begin{aligned} \int d\Pi_2 &= \int \frac{d^3 k'}{(2\pi)^3} \frac{1}{2\omega'} \frac{d^3 p'}{(2\pi)^3} \frac{1}{2E'} (2\pi)^4 \delta^{(4)}(k' + p' - k - p) \\ &= \int \frac{(\omega')^2 d\omega' d\Omega}{(2\pi)^3} \frac{1}{4\omega' E'} \\ &\quad \times 2\pi \delta(\omega' + \sqrt{m^2 + \omega^2 + (\omega')^2 - 2\omega\omega' \cos \theta} - \omega - m) \\ &= \int \frac{d \cos \theta}{2\pi} \frac{\omega'}{4E'} \frac{1}{\left| 1 + \frac{\omega' - \omega \cos \theta}{E'} \right|} \\ &= \frac{1}{8\pi} \int d \cos \theta \frac{\omega'}{m + \omega(1 - \cos \theta)} \\ &= \frac{1}{8\pi} \int d \cos \theta \frac{(\omega')^2}{\omega m}. \end{aligned} \quad (5.90)$$

Plugging everything into our general cross-section formula (4.79) and setting $|v_A - v_B| = 1$, we find

$$\frac{d\sigma}{d \cos \theta} = \frac{1}{2\omega} \frac{1}{2m} \cdot \frac{1}{8\pi} \frac{(\omega')^2}{\omega m} \cdot \left(\frac{1}{4} \sum_{\text{spins}} |\mathcal{M}|^2 \right).$$

To evaluate $|\mathcal{M}|^2$, we replace $p \cdot k = m\omega$ and $p \cdot k' = m\omega'$ in (5.87). The shortest way to write the final result is

$$\frac{d\sigma}{d \cos \theta} = \frac{\pi \alpha^2}{m^2} \left(\frac{\omega'}{\omega} \right)^2 \left[\frac{\omega'}{\omega} + \frac{\omega}{\omega'} - \sin^2 \theta \right], \quad (5.91)$$

where ω'/ω is given by (5.89). This is the (spin-averaged) *Klein-Nishina formula*, first derived in 1929.[†]

In the limit $\omega \rightarrow 0$ we see from (5.89) that $\omega'/\omega \rightarrow 1$, so the cross section becomes

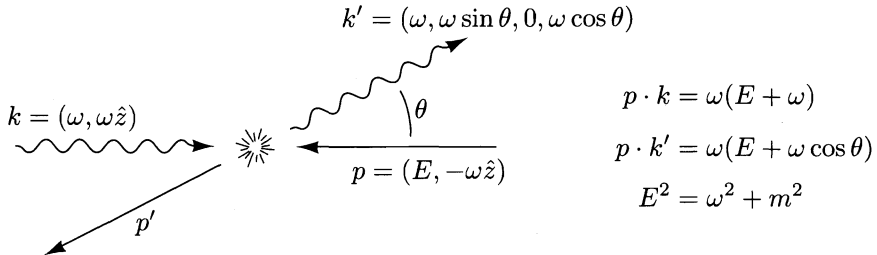
$$\frac{d\sigma}{d \cos \theta} = \frac{\pi \alpha^2}{m^2} (1 + \cos^2 \theta); \quad \sigma_{\text{total}} = \frac{8\pi \alpha^2}{3m^2}. \quad (5.92)$$

This is the familiar Thomson cross section for scattering of classical electromagnetic radiation by a free electron.

[†]O. Klein and Y. Nishina, *Z. Physik*, **52**, 853 (1929).

High-Energy Behavior

To analyze the high-energy behavior of the Compton scattering cross section, it is easiest to work in the center-of-mass frame. We can easily construct the differential cross section in this frame from the invariant expression (5.87). The kinematics of the reaction now looks like this:



Plugging these values into (5.87), we see that for $\theta \approx \pi$, the term $p \cdot k / p \cdot k'$ becomes very large, while the other terms are all of $\mathcal{O}(1)$ or smaller. Thus for $E \gg m$ and $\theta \approx \pi$, we have

$$\frac{1}{4} \sum_{\text{spins}} |\mathcal{M}|^2 \approx 2e^4 \cdot \frac{p \cdot k}{p \cdot k'} = 2e^4 \cdot \frac{E + \omega}{E + \omega \cos \theta}. \quad (5.93)$$

The cross section in the CM frame is given by (4.84):

$$\begin{aligned} \frac{d\sigma}{d \cos \theta} &= \frac{1}{2} \cdot \frac{1}{2E} \cdot \frac{1}{2\omega} \cdot \frac{\omega}{(2\pi)4(E + \omega)} \cdot \frac{2e^4(E + \omega)}{E + \omega \cos \theta} \\ &\approx \frac{2\pi\alpha^2}{2m^2 + s(1 + \cos \theta)}. \end{aligned} \quad (5.94)$$

Notice that, since $s \gg m^2$, the denominator of (5.94) almost vanishes when the photon is emitted in the backward direction ($\theta \approx \pi$). In fact, the electron mass m could be neglected completely in this formula if it were not necessary to cut off this singularity. To integrate over $\cos \theta$, we can drop the electron mass term if we supply an equivalent cutoff near $\theta = \pi$. In this way, we can approximate the total Compton scattering cross section by

$$\int_{-1}^1 d(\cos \theta) \frac{d\sigma}{d \cos \theta} \approx \frac{2\pi\alpha^2}{s} \int_{-1+2m^2/s}^1 d(\cos \theta) \frac{1}{(1 + \cos \theta)}. \quad (5.95)$$

Thus, we find that the total cross section behaves at high energy as

$$\sigma_{\text{total}} = \frac{2\pi\alpha^2}{s} \log\left(\frac{s}{m^2}\right). \quad (5.96)$$

The main dependence α^2/s follows from dimensional analysis. But the singularity associated with backward scattering of photons leads to an enhancement by an extra logarithm of the energy.

Let us try to understand the physics of this singularity. The singular term comes from the square of the u -channel diagram,

$$= -ie^2 \epsilon_\mu(k) \epsilon_\nu^*(k') \bar{u}(p') \gamma^\mu \frac{\not{p} - \not{k}' + m}{(p - k')^2 - m^2} \gamma^\nu u(p). \quad (5.97)$$

The amplitude is large at $\theta \approx \pi$ because the denominator of the propagator is then small ($\sim m^2$) compared to s . To be more precise, define $\chi \equiv \pi - \theta$. We will be interested in values of χ that are somewhat larger than m/ω , but still small enough that we can approximate $1 - \cos \chi \approx \chi^2/2$. For χ in this range, the denominator is

$$(p - k')^2 - m^2 = -2p \cdot k' \approx -2\omega^2 \left(\frac{m^2}{2\omega^2} + 1 - \cos \chi \right) \approx -(\omega^2 \chi^2 + m^2). \quad (5.98)$$

This is small compared to s over a wide range of values for χ , hence the enhancement in the total cross section.

Looking back at (5.93), we see that for χ such that $m/\omega \ll \chi \ll 1$, the squared amplitude is proportional to $1/\chi^2$, and hence we expect $\mathcal{M} \propto 1/\chi$. But we have just seen that the denominator of \mathcal{M} is proportional to χ^2 , so there must be a compensating factor of χ in the numerator. We can understand the physical origin of that factor by looking at the amplitude for a particular set of electron and photon polarizations.

Suppose that the initial electron is right-handed. The dominant term of (5.97) comes from the term that involves $(\not{p} - \not{k}')$ in the numerator of the propagator. Since this term contains three γ -matrices in (5.97) between the \bar{u} and the u , the final electron must also be right-handed. The amplitude is therefore

$$i\mathcal{M} = -ie^2 \epsilon_\mu(k) \epsilon_\nu^*(k') u_R^\dagger(p') \sigma^\mu \frac{\bar{\sigma} \cdot (p - k')}{-(\omega^2 \chi^2 + m^2)} \sigma^\nu u_R(p), \quad (5.99)$$

where

$$u_R(p) = \sqrt{2E} \begin{pmatrix} 0 \\ 1 \end{pmatrix} \quad \text{and} \quad u_R(p') = \sqrt{2E} \begin{pmatrix} 1 \\ 0 \end{pmatrix}. \quad (5.100)$$

If the initial photon is left-handed, with $\epsilon^\mu = (1/\sqrt{2})(0, 1, -i, 0)^\mu$, then

$$\sigma^\mu \epsilon_\mu(k) = \begin{pmatrix} 0 & 0 \\ -\sqrt{2} & 0 \end{pmatrix},$$

and the combination $u_R^\dagger(p') \sigma^\mu \epsilon_\mu(k)$ vanishes. The initial photon must therefore be right-handed. Similarly, the amplitude vanishes unless the final photon is right-handed. The kinematic situation for this set of polarizations is shown

Before:



After:

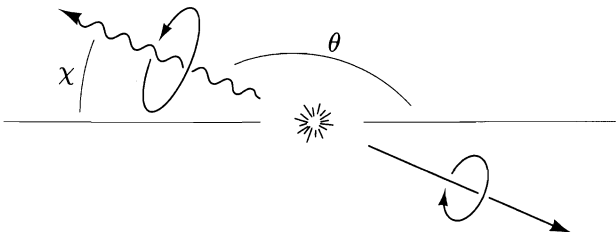


Figure 5.6. In the high-energy limit, the final photon is most likely to be emitted at backward angles. Since helicity is conserved, a unit of spin angular momentum is converted to orbital angular momentum.

in Fig. 5.6. Note that the total spin angular momentum of the final state is one unit less than that of the initial state.

Continuing with our calculation, let us consider the numerator of the propagator in (5.99). For χ in the range of interest, the dominant term is

$$-\sigma^1(p - k')^1 = \sigma^1 \cdot \omega \chi.$$

This is the factor of χ anticipated above. It indicates that the final state is a p -wave, as required by angular momentum conservation. Assembling all the pieces, we obtain

$$\mathcal{M}(e_R^- \gamma_R \rightarrow e_R^- \gamma_R) \approx e^2 \sqrt{2E} \sqrt{2} \frac{\omega \chi}{(\omega^2 \chi^2 + m^2)} \sqrt{2E} \sqrt{2} \approx \frac{4e^2 \chi}{\chi^2 + m^2/\omega^2}. \quad (5.101)$$

We would find the same result in the case where all initial and final particles are left-handed.

Notice that for directly backward scattering, $\chi = 0$, the matrix element (5.101) vanishes due to the angular momentum zero in the numerator. Thus, at angles very close to backward, we should also take into account the mass term in the numerator of the propagator in (5.97). This term contains only two gamma matrices and so converts a right-handed electron into a left-handed electron. By an analysis similar to the one that led to Eq. (5.101), we can see that this amplitude is nonvanishing only when the initial photon is left-handed and the final photon is right-handed. Following this analysis in more detail, we find

$$\mathcal{M}(e_R^- \gamma_L \rightarrow e_L^- \gamma_R) \approx \frac{4e^2 m/\omega}{\chi^2 + m^2/\omega^2}. \quad (5.102)$$

The reaction with all four helicities reversed gives the same matrix element.

To compare this result to our previous calculations, we should add the contributions to the cross section from (5.101) and (5.102) and equal contributions for the reactions involving initial left-handed electrons, and divide by 4 to average over initial spins. The unpolarized differential cross section should then be

$$\begin{aligned} \frac{d\sigma}{d \cos \theta} &= \frac{1}{2} \frac{1}{2E} \frac{1}{2\omega} \frac{\omega}{(2\pi) 4(E+\omega)} \left[\frac{8e^4 \chi^2}{(\chi^2 + m^2/\omega^2)^2} + \frac{8e^4 m^2/\omega^2}{(\chi^2 + m^2/\omega^2)^2} \right] \\ &= \frac{4\pi\alpha^2}{s(\chi^2 + 4m^2/s)}, \end{aligned} \quad (5.103)$$

which agrees precisely with Eq. (5.94).

The importance of the helicity-flip process (5.102) just at the kinematic endpoint has an interesting experimental consequence. Consider the process of *inverse* Compton scattering, a high-energy electron beam colliding with a low-energy photon beam (for example, a laser beam) to produce a high-energy photon beam. Let the electrons have energy E and the laser photons have energy ϖ , let the energy of the scattered photon be $E' = yE$, and assume for simplicity that $s = 4E\varpi \gg m^2$. Then the computation we have just done applies to this situation, with the highest energy photons resulting from scattering that is precisely backward in the center-of-mass frame. By computing $2k \cdot k'$ in the center-of-mass frame and in the lab frame, it is easy to show that the final photon energy is related to the center-of-mass scattering angle through

$$y \approx \frac{1}{2}(1 - \cos \theta) \approx 1 - \frac{\chi^2}{4}.$$

Then Eq. (5.103) can be rewritten as a formula for the energy distribution of backscattered photons near the endpoint:

$$\frac{d\sigma}{dy} = \frac{2\pi\alpha^2}{s((1-y) + m^2/s)^2} \left[(1-y) + \frac{m^2}{s} \right], \quad (5.104)$$

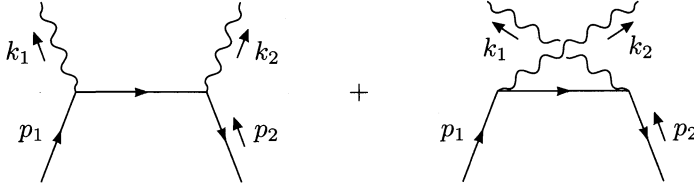
where the first term in brackets corresponds to the helicity-conserving process and the second term to the helicity-flip process. Thus, for example, if a right-handed polarized laser beam is scattered from an unpolarized high-energy electron beam, most of the backscattered photons will be right-handed but the highest-energy photons will be left-handed. This effect can be used experimentally to measure the polarization of an electron beam or to create high-energy photon sources with adjustable energy distribution and polarization.

Pair Annihilation into Photons

We can still obtain one more result from the Compton-scattering amplitude. Consider the annihilation process

$$e^+ e^- \rightarrow 2\gamma,$$

given to lowest order by the diagrams



This process is related to Compton scattering by crossing symmetry; we can obtain the correct amplitude from the Compton amplitude by making the replacements

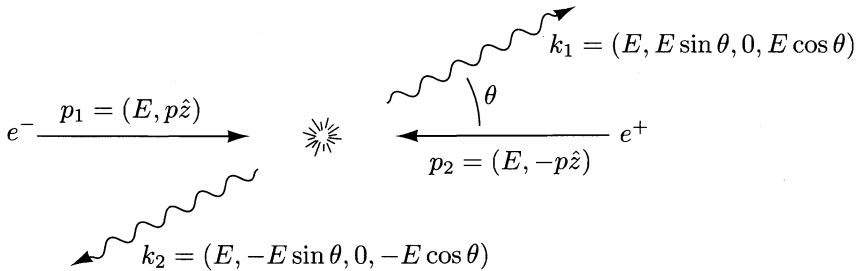
$$p \rightarrow p_1 \quad p' \rightarrow -p_2 \quad k \rightarrow -k_1 \quad k' \rightarrow k_2.$$

Making these substitutions in (5.87), we find

$$\frac{1}{4} \sum_{\text{spins}} |\mathcal{M}|^2 = -2e^4 \left[\frac{p_1 \cdot k_2}{p_1 \cdot k_1} + \frac{p_1 \cdot k_1}{p_1 \cdot k_2} + 2m^2 \left(\frac{1}{p_1 \cdot k_1} + \frac{1}{p_1 \cdot k_2} \right) - m^4 \left(\frac{1}{p_1 \cdot k_1} + \frac{1}{p_1 \cdot k_2} \right)^2 \right]. \quad (5.105)$$

The overall minus sign is the result of the crossing relation (5.68) and should be removed.

Now specialize to the center-of-mass frame. The kinematics is



A routine calculation yields the differential cross section,

$$\frac{d\sigma}{d \cos \theta} = \frac{2\pi\alpha^2}{s} \left(\frac{E}{p} \right) \left[\frac{E^2 + p^2 \cos^2 \theta}{m^2 + p^2 \sin^2 \theta} + \frac{2m^2}{m^2 + p^2 \sin^2 \theta} - \frac{2m^4}{(m^2 + p^2 \sin^2 \theta)^2} \right]. \quad (5.106)$$

In the high-energy limit, this becomes

$$\frac{d\sigma}{d \cos \theta} \xrightarrow{E \gg m} \frac{2\pi\alpha^2}{s} \left(\frac{1 + \cos^2 \theta}{\sin^2 \theta} \right), \quad (5.107)$$

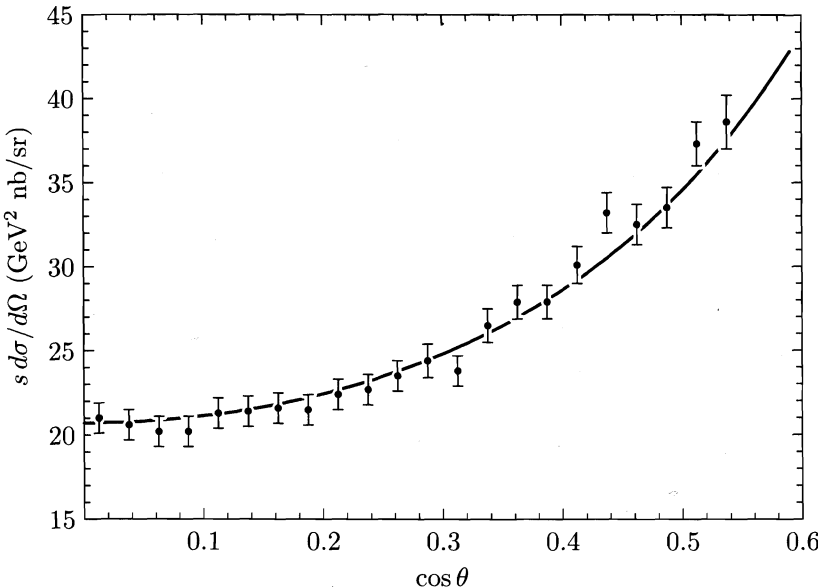


Figure 5.7. Angular dependence of the cross section for $e^+e^- \rightarrow 2\gamma$ at $E_{cm} = 29$ GeV, as measured by the HRS collaboration, M. Derrick, et. al., *Phys. Rev. D* **34**, 3286 (1986). The solid line is the lowest-order theoretical prediction, Eq. (5.107).

except when $\sin \theta$ is of order m/p or smaller. Note that since the two photons are identical, we count all possible final states by integrating only over $0 \leq \theta \leq \pi/2$. Thus the total cross section is computed as

$$\sigma_{\text{total}} = \int_0^1 d(\cos \theta) \frac{d\sigma}{d \cos \theta}. \quad (5.108)$$

Figure 5.7 compares the asymptotic formula (5.107) for the differential cross section to measurements of e^+e^- annihilation into two photons at very high energy.

Problems

5.1 Coulomb scattering. Repeat the computation of Problem 4.4, part (c), this time using the full relativistic expression for the matrix element. You should find, for the spin-averaged cross section,

$$\frac{d\sigma}{d\Omega} = \frac{\alpha^2}{4|\mathbf{p}|^2 \beta^2 \sin^4(\theta/2)} \left(1 - \beta^2 \sin^2 \frac{\theta}{2} \right),$$

where \mathbf{p} is the electron's 3-momentum and β is its velocity. This is the *Mott formula* for Coulomb scattering of relativistic electrons. Now derive it in a second way, by working

out the cross section for electron-muon scattering, in the muon rest frame, retaining the electron mass but sending $m_\mu \rightarrow \infty$.

5.2 Bhabha scattering. Compute the differential cross section $d\sigma/d\cos\theta$ for Bhabha scattering, $e^+e^- \rightarrow e^+e^-$. You may work in the limit $E_{\text{cm}} \gg m_e$, in which it is permissible to ignore the electron mass. There are two Feynman diagrams; these must be added in the invariant matrix element before squaring. Be sure that you have the correct relative sign between these diagrams. The intermediate steps are complicated, but the final result is quite simple. In particular, you may find it useful to introduce the Mandelstam variables s , t , and u . Note that, if we ignore the electron mass, $s + t + u = 0$. You should be able to cast the differential cross section into the form

$$\frac{d\sigma}{d\cos\theta} = \frac{\pi\alpha^2}{s} \left[u^2 \left(\frac{1}{s} + \frac{1}{t} \right)^2 + \left(\frac{t}{s} \right)^2 + \left(\frac{s}{t} \right)^2 \right].$$

Rewrite this formula in terms of $\cos\theta$ and graph it. What feature of the diagrams causes the differential cross section to diverge as $\theta \rightarrow 0$?

5.3 The *spinor product* formalism introduced in Problem 3.3 provides an efficient way to compute tree diagrams involving massless particles. Recall that in Problem 3.3 we defined spinor products as follows: Let u_{L0} , u_{R0} be the left- and right-handed spinors at some fixed lightlike momentum k_0 . These satisfy

$$u_{L0}\bar{u}_{L0} = \left(\frac{1-\gamma^5}{2} \right) \not{k}_0, \quad u_{R0}\bar{u}_{R0} = \left(\frac{1+\gamma^5}{2} \right) \not{k}_0. \quad (1)$$

(These relations are just the projections onto definite helicity of the more standard formula $\sum u_0\bar{u}_0 = \not{k}_0$.) Then define spinors for any other lightlike momentum p by

$$u_L(p) = \frac{1}{\sqrt{2p \cdot k_0}} \not{p} u_{R0}, \quad u_R(p) = \frac{1}{\sqrt{2p \cdot k_0}} \not{p} u_{L0}. \quad (2)$$

We showed that these spinors satisfy $\not{p}u(p) = 0$; because there is no m around, they can be used as spinors for either fermions or antifermions. We defined

$$s(p_1, p_2) = \bar{u}_R(p_1)u_L(p_2), \quad t(p_1, p_2) = \bar{u}_L(p_1)u_R(p_2),$$

and, in a special frame, we proved the properties

$$t(p_1, p_2) = (s(p_2, p_1))^*, \quad s(p_1, p_2) = -s(p_2, p_1), \quad |s(p_1, p_2)|^2 = 2p_1 \cdot p_2. \quad (3)$$

Now let us apply these results.

- (a) To warm up, give another proof of the last relation in Eq. (3) by using (1) to rewrite $|s(p_1, p_2)|^2$ as a trace of Dirac matrices, and then applying the trace calculus.
- (b) Show that, for any string of Dirac matrices,

$$\text{tr}[\gamma^\mu \gamma^\nu \gamma^\rho \dots] = \text{tr}[\dots \gamma^\rho \gamma^\nu \gamma^\mu]$$

where $\mu, \nu, \rho, \dots = 0, 1, 2, 3$, or 5. Use this identity to show that

$$\bar{u}_L(p_1)\gamma^\mu u_L(p_2) = \bar{u}_R(p_2)\gamma^\mu u_R(p_1).$$

- (c) Prove the Fierz identity

$$\bar{u}_L(p_1)\gamma^\mu u_L(p_2) [\gamma_\mu]_{ab} = 2 [u_L(p_2)\bar{u}_L(p_1) + u_R(p_1)\bar{u}_R(p_2)]_{ab},$$

where $a, b = 1, 2, 3, 4$ are Dirac indices. This can be done by justifying the following statements: The right-hand side of this equation is a Dirac matrix; thus, it can be written as a linear combination of the 16 Γ matrices discussed in Section 3.4. It satisfies

$$\gamma^5[M] = -[M]\gamma^5,$$

thus, it must have the form

$$[M] = \left(\frac{1-\gamma^5}{2}\right)\gamma_\mu V^\mu + \left(\frac{1+\gamma^5}{2}\right)\gamma_\mu W^\mu$$

where V^μ and W^μ are 4-vectors. These 4-vectors can be computed by trace technology; for example,

$$V^\nu = \frac{1}{2} \text{tr}[\gamma^\nu \left(\frac{1-\gamma^5}{2}\right) M].$$

- (d) Consider the process $e^+e^- \rightarrow \mu^+\mu^-$, to the leading order in α , ignoring the masses of both the electron and the muon. Consider first the case in which the electron and the final muon are both right-handed and the positron and the final antimuon are both left-handed. (Use the spinor v_R for the antimuon and \bar{u}_R for the positron.) Apply the Fierz identity to show that the amplitude can be evaluated directly in terms of spinor products. Square the amplitude and reproduce the result for

$$\frac{d\sigma}{d\cos\theta}(e_R^- e_L^+ \rightarrow \mu_R^- \mu_L^+)$$

given in Eq. (5.22). Compute the other helicity cross sections for this process and show that they also reproduce the results found in Section 5.2.

- (e) Compute the differential cross section for Bhabha scattering of massless electrons, helicity state by helicity state, using the spinor product formalism. The average over initial helicities, summed over final helicities, should reproduce the result of Problem 5.2. In the process, you should see how this result arises as the sum of definite-helicity contributions.

5.4 Positronium lifetimes.

- (a) Compute the amplitude \mathcal{M} for e^+e^- annihilation into 2 photons in the extreme nonrelativistic limit (i.e., keep only the term proportional to zero powers of the electron and positron 3-momentum). Use this result, together with our formalism for fermion-antifermion bound states, to compute the rate of annihilation of the $1S$ states of positronium into 2 photons. You should find that the spin-1 states of positronium do not annihilate into 2 photons, confirming the symmetry argument of Problem 3.8. For the spin-0 state of positronium, you should find a result proportional to the square of the $1S$ wavefunction at the origin. Inserting the value of this wavefunction from nonrelativistic quantum mechanics, you should find

$$\frac{1}{\tau} = \Gamma = \frac{\alpha^5 m_e}{2} \approx 8.03 \times 10^9 \text{ sec}^{-1}.$$

A recent measurement[†] gives $\Gamma = 7.994 \pm .011 \text{ nsec}^{-1}$; the 0.5% discrepancy is accounted for by radiative corrections.

- (b) Computing the decay rates of higher- l positronium states is somewhat more difficult; in the rest of this problem, we will consider the case $l = 1$. First, work out the terms in the $e^+e^- \rightarrow 2\gamma$ amplitude proportional to one power of the 3-momentum. (For simplicity, work in the center-of-mass frame.) Since

$$\int \frac{d^3 p}{(2\pi)^3} p^i \psi(\mathbf{p}) = i \frac{\partial}{\partial x^i} \psi(\mathbf{x}) \Big|_{\mathbf{x}=0},$$

this piece of the amplitude has overlap with P -wave bound states. Show that the $S = 1$, but not the $S = 0$ states, can decay to 2 photons. Again, this is a consequence of C .

- (c) To compute the decay rates of these P -wave states, we need properly normalized state vectors. Denote the three P -state wavefunctions by

$$\psi_i = x^i f(|\mathbf{x}|), \quad \text{normalized to } \int d^3 x \psi_i^*(\mathbf{x}) \psi_j(\mathbf{x}) = \delta_{ij},$$

and their Fourier transforms by $\psi_i(\mathbf{p})$. Show that

$$|B(\mathbf{k})\rangle = \sqrt{2M} \int \frac{d^3 p}{(2\pi)^3} \psi_i(\mathbf{p}) a_{\mathbf{p}+\mathbf{k}/2}^\dagger \Sigma^i b_{-\mathbf{p}+\mathbf{k}/2}^\dagger |0\rangle$$

is a properly normalized bound-state vector if Σ^i denotes a set of three 2×2 matrices normalized to

$$\sum_i \text{tr}(\Sigma^{i\dagger} \Sigma^i) = 1.$$

To build $S = 1$ states, we should take each Σ^i to contain a Pauli sigma matrix. In general, spin-orbit coupling will split the multiplet of $S = 1$, $L = 1$ states according to the total angular momentum J . The states of definite J are given by

$$\begin{aligned} J = 0 : \quad \Sigma^i &= \frac{1}{\sqrt{6}} \sigma^i, \\ J = 1 : \quad \Sigma^i &= \frac{1}{2} \epsilon^{ijk} n^j \sigma^k, \\ J = 2 : \quad \Sigma^i &= \frac{1}{\sqrt{3}} h^{ij} \sigma^j, \end{aligned}$$

where \mathbf{n} is a polarization vector satisfying $|\mathbf{n}|^2 = 1$ and h^{ij} is a traceless tensor, for which a typical value might be $h^{12} = 1$ and all other components zero.

- (d) Using the expanded form for the $e^+e^- \rightarrow 2\gamma$ amplitude derived in part (b) and the explicit form of the $S = 1$, $L = 1$, definite- J positronium states found in part (c), compute, for each J , the decay rate of the state into two photons.

[†]D. W. Gidley et. al., *Phys. Rev. Lett.* **49**, 525 (1982).

5.5 Physics of a massive vector boson. Add to QED a massive photon field B_μ of mass M , which couples to electrons via

$$\Delta H = \int d^3x (g\bar{\psi}\gamma^\mu\psi B_\mu).$$

A massive photon in the initial or final state has three possible physical polarizations, corresponding to the three spacelike unit vectors in the boson's rest frame. These can be characterized invariantly, in terms of the boson's 4-momentum k^μ , as the three vectors $\epsilon_\mu^{(i)}$ satisfying

$$\epsilon^{(i)} \cdot \epsilon^{(j)} = -\delta^{ij}, \quad k \cdot \epsilon^{(i)} = 0.$$

The four vectors $(k_\mu/M, \epsilon_\mu^{(i)})$ form a complete orthonormal basis. Because B_μ couples to the conserved current $\bar{\psi}\gamma^\mu\psi$, the Ward identity implies that k_μ dotted into the amplitude for B production gives zero; thus we can replace:

$$\sum_i \epsilon_\mu^{(i)} \epsilon_\nu^{(i)*} \rightarrow -g_{\mu\nu}.$$

This gives a generalization to massive bosons of the Feynman trick for photon polarization vectors and simplifies the calculation of B production cross sections. (Warning: This trick does not work (so simply) for “non-Abelian gauge fields”.) Let's do a few of these computations, using always the approximation of ignoring the mass of the electron.

- (a) Compute the cross section for the process $e^+e^- \rightarrow B$. Compute the lifetime of the B , assuming that it decays only to electrons. Verify the relation

$$\sigma(e^+e^- \rightarrow B) = \frac{12\pi^2}{M} \Gamma(B \rightarrow e^+e^-) \delta(M^2 - s)$$

discussed in Section 5.3.

- (b) Compute the differential cross section, in the center-of-mass system, for the process $e^+e^- \rightarrow \gamma + B$. (This calculation goes over almost unchanged to the realistic process $e^+e^- \rightarrow \gamma + Z^0$; this allows one to measure the number of decays of the Z^0 into unobserved final states, which is in turn proportional to the number of neutrino species.)
- (c) Notice that the cross section of part (b) diverges as $\theta \rightarrow 0$ or π . Let us analyze the region near $\theta = 0$. In this region, the dominant contribution comes from the t -channel diagram and corresponds intuitively to the emission of a photon from the electron line before e^+e^- annihilation into a B . Let us rearrange the formula in such a way as to support this interpretation. First, note that the divergence as $\theta \rightarrow 0$ is cut off by the electron mass: Let the electron momentum be $p^\mu = (E, 0, 0, k)$, with $k = (E^2 - m_e^2)^{1/2}$, and let the photon momentum be $k^\mu = (xE, xE \sin \theta, 0, xE \cos \theta)$. Show that the denominator of the propagator then never becomes smaller than $\mathcal{O}(m_e^2/s)$. Now integrate the cross section of part (b) over forward angles, cutting off the θ integral at $\theta^2 \sim (m_e^2/s)$ and keeping only the leading logarithmic term, proportional to $\log(s/m_e^2)$. Show that, in this approximation, the cross section for forward photon emission can be written

$$\sigma(e^+e^- \rightarrow \gamma + B) \approx \int dx f(x) \cdot \sigma(e^+e^- \rightarrow B \text{ at } E_{cm}^2 = (1-x)s),$$

where the annihilation cross section is evaluated for the collision of a positron of energy E and an electron of energy $(1 - x)E$, and the function $f(x)$, the *Weizsäcker-Williams distribution function*, is given by

$$f(x) = \frac{\alpha}{2\pi} \frac{1 + (1 - x)^2}{x} \cdot \log\left(\frac{s}{m_e^2}\right).$$

This function arises universally in processes in which a photon is emitted collinearly from an electron line, independent of the subsequent dynamics. We will meet it again, in another context, in Problem 6.2.

- 5.6** This problem extends the spinor product technology of Problem 5.3 to external photons.

- (a) Let k be the momentum of a photon, and let p be another lightlike vector, chosen so that $p \cdot k \neq 0$. Let $u_R(p)$, $u_L(p)$ be spinors of definite helicity for fermions with the lightlike momentum p , defined according to the conventions of Problem 5.3. Define photon polarization vectors as follows:

$$\epsilon_+^\mu(k) = \frac{1}{\sqrt{4p \cdot k}} \bar{u}_R(k) \gamma^\mu u_R(p), \quad \epsilon_-^\mu(k) = \frac{1}{\sqrt{4p \cdot k}} \bar{u}_L(k) \gamma^\mu u_L(p).$$

Use the identity

$$u_L(p) \bar{u}_L(p) + u_R(p) \bar{u}_R(p) = \not{1}$$

to compute the polarization sum

$$\epsilon_+^\mu \epsilon_+^{\nu*} + \epsilon_-^\mu \epsilon_-^{\nu*} = -g^{\mu\nu} + \frac{k^\mu p^\nu + k^\nu p^\mu}{p \cdot k}.$$

The second term on the right gives zero when dotted with any photon emission amplitude \mathcal{M}^μ , so we have

$$|\epsilon_+ \cdot \mathcal{M}|^2 + |\epsilon_- \cdot \mathcal{M}|^2 = \mathcal{M}^\mu \mathcal{M}^{\nu*} (-g_{\mu\nu});$$

thus, we can use the vectors ϵ_+ , ϵ_- to compute photon polarization sums.

- (b) Using the polarization vectors just defined, and the spinor products and the Fierz identity from Problem 5.3, compute the differential cross section for a massless electron and positron to annihilate into 2 photons. Show that the result agrees with the massless limit derived in (5.107):

$$\frac{d\sigma}{d\cos\theta} = \frac{2\pi\alpha^2}{s} \left(\frac{1 + \cos^2\theta}{\sin^2\theta} \right)$$

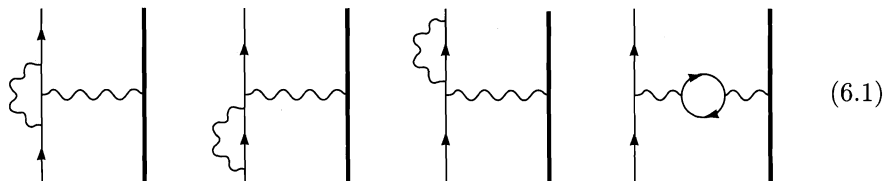
in the center-of-mass frame. It follows from the result of part (a) that this answer is independent of the particular vector p used to define the polarization vectors; however, the calculation is greatly simplified by taking this vector to be the initial electron 4-vector.

Chapter 6

Radiative Corrections: Introduction

Now that we have acquired some experience at performing QED calculations, let us move on to some more complicated problems. Chapter 5 dealt only with *tree-level* processes, that is, with diagrams that contain no loops. But all such processes receive higher-order contributions, known as *radiative corrections*, from diagrams that do contain loops. Another source of radiative corrections in QED is *bremsstrahlung*, the emission of extra final-state photons during a reaction. In this chapter we will investigate both types of radiative corrections, and find that it is inconsistent to include one without also including the other.

Throughout this chapter, in order to illustrate these ideas in the simplest possible context, we will consider the process of electron scattering from another, very heavy, particle. We analyzed this process at tree level in Section 5.4 and Problem 5.1. At the next order in perturbation theory, we encounter the following four diagrams:



The order- α correction to the cross section comes from the interference term between these diagrams and the tree-level diagram. There are six additional one-loop diagrams involving the heavy particle in the loop, but they can be neglected in the limit where that particle is much heavier than the electron, since the mass appears in the denominator of the propagator. (Physically, the heavy particle accelerates less, and therefore radiates less, during the collision.)

Of the four diagrams in (6.1), the first (known as the *vertex correction*) is the most intricate and gives the largest variety of new effects. For example, it gives rise to an anomalous magnetic moment for the electron, which we will compute in Section 6.3.

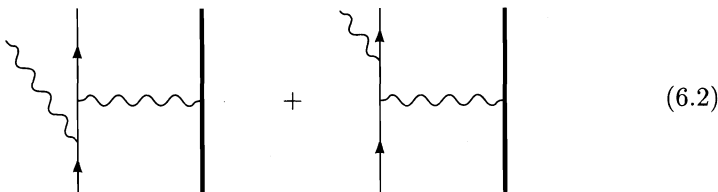
The next two diagrams of (6.1) are *external leg corrections*. We will neglect them in this chapter because they are not amputated, as required by our formula (4.90) for S -matrix elements. We will discuss these diagrams in more

detail when we prove that formula in Section 7.2.

The final diagram of (6.1) is called the *vacuum polarization*. Since it requires more computational machinery than the others, we will not evaluate this diagram until Section 7.5.

Our study of these corrections will be complicated by the fact that they are ill-defined. Each diagram of (6.1) involves an integration over the undetermined loop momentum, and in each case the integral is divergent in the $k \rightarrow \infty$ or *ultraviolet* region. Fortunately, the infinite parts of these integrals will always cancel out of expressions for observable quantities such as cross sections.

The first three diagrams of (6.1) also contain *infrared divergences*: infinities coming from the $k \rightarrow 0$ end of the loop-momentum integrals. We will see in Section 6.4 that these divergences are canceled when we also include the following *bremsstrahlung* diagrams:



These diagrams are divergent in the limit where the energy of the radiated photon tends to zero. In this limit, the photon cannot be observed by any physical detector, so it makes sense to add the cross section for producing these low-energy photons to the cross section for scattering without radiation. The bremsstrahlung diagrams are thus an essential part of the radiative correction, in this and any other QED process.

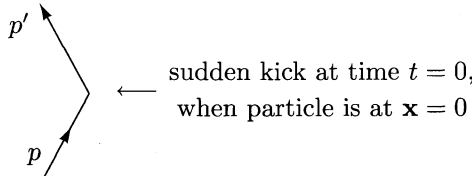
Our main goals in the present chapter are to understand bremsstrahlung of low-energy photons, the vertex correction diagram, and the cancellation of infrared divergences between these two types of radiative corrections.

6.1 Soft Bremsstrahlung

Let us begin our study of radiative corrections by analyzing the bremsstrahlung process. In this section we will first do a classical computation of the intensity of the low-frequency bremsstrahlung radiation when an electron undergoes a sudden acceleration. We will then compute a closely related quantity in quantum field theory: the cross section for emission of one very soft photon, given by diagrams (6.2). We would like to understand how the classical result arises as a limiting case of the quantum result.

Classical Computation

Suppose that a classical electron receives a sudden kick at time $t = 0$ and position $\mathbf{x} = 0$, causing its 4-momentum to change from p to p' . (An infinitely sudden change of momentum is of course an unrealistic idealization. The precise form of the trajectory during the acceleration does not affect the low-frequency radiation, however. Our calculation will be valid for radiation with a frequency less than the reciprocal of the scattering time.)



We can find the radiation field by writing down the current of this electron, and considering that current as a source for Maxwell's equations.

What is the current density of such a particle? For a charged particle at rest at $\mathbf{x} = 0$, the current would be

$$\begin{aligned} j^\mu(x) &= (1, \mathbf{0})^\mu \cdot e \delta^{(3)}(\mathbf{x}) \\ &= \int dt (1, \mathbf{0})^\mu \cdot e \delta^{(4)}(x - y(t)), \quad \text{with } y^\mu(t) = (t, \mathbf{0})^\mu. \end{aligned}$$

From this we can guess the current for an arbitrary trajectory $y^\mu(\tau)$:

$$j^\mu(x) = e \int d\tau \frac{dy^\mu(\tau)}{d\tau} \delta^{(4)}(x - y(\tau)). \quad (6.3)$$

Note that this expression is independent of the precise way in which the curve $y^\mu(\tau)$ is parametrized: Changing variables from τ to $\sigma(\tau)$ gives a factor of $d\tau/d\sigma$ in the integration measure, which combines with $dy^\mu/d\tau$ via the chain rule to give $dy^\mu/d\sigma$. We can also prove from (6.3) that the current is automatically conserved: For any “test function” $f(x)$ that falls off at infinity, we have

$$\begin{aligned} \int d^4x f(x) \partial_\mu j^\mu(x) &= \int d^4x f(x) e \int d\tau \frac{dy^\mu(\tau)}{d\tau} \partial_\mu \delta^{(4)}(x - y(\tau)) \\ &= -e \int d\tau \frac{dy^\mu(\tau)}{d\tau} \frac{\partial}{\partial x^\mu} f(x) \Big|_{x=y(\tau)} \\ &= -e \int d\tau \frac{d}{d\tau} f(y(\tau)) \\ &= -e f(y(\tau)) \Big|_{-\infty}^{\infty} = 0. \end{aligned}$$

For our process the trajectory is

$$y^\mu(\tau) = \begin{cases} (p^\mu/m)\tau & \text{for } \tau < 0; \\ (p'^\mu/m)\tau & \text{for } \tau > 0. \end{cases}$$

Thus the current can be written

$$j^\mu(x) = e \int_0^\infty d\tau \frac{p'^\mu}{m} \delta^{(4)}\left(x - \frac{p'}{m}\tau\right) + e \int_{-\infty}^0 d\tau \frac{p^\mu}{m} \delta^{(4)}\left(x - \frac{p}{m}\tau\right).$$

In a moment we will need to know the Fourier transform of this function. Inserting factors of $e^{-\epsilon\tau}$ and $e^{\epsilon\tau}$ to make the integrals converge, we have

$$\begin{aligned} \tilde{j}^\mu(k) &= \int d^4x e^{ik \cdot x} j^\mu(x) \\ &= e \int_0^\infty d\tau \frac{p'^\mu}{m} e^{i(k \cdot p'/m + i\epsilon)\tau} + e \int_{-\infty}^0 d\tau \frac{p^\mu}{m} e^{i(k \cdot p/m - i\epsilon)\tau} \\ &= ie \left(\frac{p'^\mu}{k \cdot p' + i\epsilon} - \frac{p^\mu}{k \cdot p - i\epsilon} \right). \end{aligned} \quad (6.4)$$

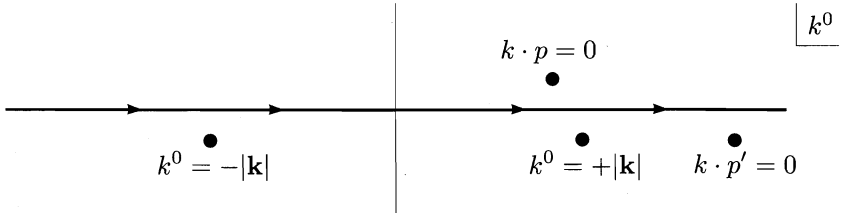
We are now ready to solve Maxwell's equations. In Lorentz gauge ($\partial^\mu A_\mu = 0$) we must solve $\partial^2 A^\mu = j^\mu$, or in Fourier space,

$$\tilde{A}^\mu(k) = -\frac{1}{k^2} \tilde{j}^\mu(k).$$

Plugging in (6.4), we obtain a formula for the vector potential:

$$A^\mu(x) = \int \frac{d^4k}{(2\pi)^4} e^{-ik \cdot x} \frac{-ie}{k^2} \left(\frac{p'^\mu}{k \cdot p' + i\epsilon} - \frac{p^\mu}{k \cdot p - i\epsilon} \right). \quad (6.5)$$

The k^0 integral can be performed as a contour integral in the complex plane. The locations of the poles are as follows:



We place the poles at $k^0 = \pm|\mathbf{k}|$ below the real axis so that (as we shall soon confirm) the radiation field will satisfy retarded boundary conditions.

For $t < 0$ we close the contour upward, picking up the pole at $k \cdot p = 0$, that is, $k^0 = \mathbf{k} \cdot \mathbf{p}/p^0$. The result is

$$A^\mu(x) = \int \frac{d^3k}{(2\pi)^3} e^{i\mathbf{k} \cdot \mathbf{x}} e^{-i(\mathbf{k} \cdot \mathbf{p}/p^0)t} \frac{(2\pi i)(+ie)}{(2\pi)k^2} \frac{p^\mu}{p^0}.$$

In the reference frame where the particle is initially at rest, its momentum vector is $p^\mu = (p^0, \mathbf{0})^\mu$ and the vector potential reduces to

$$A^\mu(x) = \int \frac{d^3k}{(2\pi)^3} e^{i\mathbf{k}\cdot\mathbf{x}} \frac{e}{|\mathbf{k}|^2} \cdot (1, \mathbf{0})^\mu.$$

This is just the Coulomb potential of an unaccelerated charge. As we would expect, there is no radiation field before the particle is scattered.

After scattering ($t > 0$), we close the contour downward, picking up the three poles below the real axis. The pole at $k^0 = \mathbf{k} \cdot \mathbf{p}'/p'^0$ gives the Coulomb potential of the outgoing particle. Thus the other two poles are completely responsible for the radiation field. Their contribution gives

$$\begin{aligned} A_{\text{rad}}^\mu(x) &= \int \frac{d^3k}{(2\pi)^3} \frac{-e}{2|\mathbf{k}|} \left\{ e^{-ik\cdot x} \left(\frac{p'^\mu}{k \cdot p'} - \frac{p^\mu}{k \cdot p} \right) + \text{c.c.} \right\} \Big|_{k^0=|\mathbf{k}|} \\ &= \text{Re} \int \frac{d^3k}{(2\pi)^3} \mathcal{A}^\mu(\mathbf{k}) e^{-ik\cdot x}, \end{aligned} \quad (6.6)$$

where the momentum-space amplitude $\mathcal{A}(\mathbf{k})$ is given by

$$\mathcal{A}^\mu(\mathbf{k}) = \frac{-e}{|\mathbf{k}|} \left(\frac{p'^\mu}{k \cdot p'} - \frac{p^\mu}{k \cdot p} \right). \quad (6.7)$$

(The condition $k^0 = |\mathbf{k}|$ is implicit here and in the rest of this calculation.)

To calculate the energy radiated, we must find the electric and magnetic fields. It is easiest to write \mathbf{E} and \mathbf{B} as the real parts of complex Fourier integrals, just as we did for A^μ :

$$\begin{aligned} \mathbf{E}(x) &= \text{Re} \int \frac{d^3k}{(2\pi)^3} \mathcal{E}(\mathbf{k}) e^{-ik\cdot x}; \\ \mathbf{B}(x) &= \text{Re} \int \frac{d^3k}{(2\pi)^3} \mathcal{B}(\mathbf{k}) e^{-ik\cdot x}. \end{aligned} \quad (6.8)$$

The momentum-space amplitudes $\mathcal{E}(\mathbf{k})$ and $\mathcal{B}(\mathbf{k})$ of the radiation fields are then simply

$$\begin{aligned} \mathcal{E}(\mathbf{k}) &= -i\mathbf{k}\mathcal{A}^0(\mathbf{k}) + ik^0\mathcal{A}(\mathbf{k}); \\ \mathcal{B}(\mathbf{k}) &= i\mathbf{k} \times \mathcal{A}(\mathbf{k}) = \hat{\mathbf{k}} \times \mathcal{E}(\mathbf{k}). \end{aligned} \quad (6.9)$$

Using the explicit form (6.7) of $\mathcal{A}^\mu(\mathbf{k})$, you can easily check that the electric field is transverse: $\mathbf{k} \cdot \mathcal{E}(\mathbf{k}) = 0$.

Having expressed the fields in this way, we can compute the energy radiated:

$$\text{Energy} = \frac{1}{2} \int d^3x (|\mathbf{E}(x)|^2 + |\mathbf{B}(x)|^2). \quad (6.10)$$

The first term is

$$\begin{aligned} & \frac{1}{8} \int d^3x \int \frac{d^3k}{(2\pi)^3} \int \frac{d^3k'}{(2\pi)^3} (\mathcal{E}(\mathbf{k})e^{-ikx} + \mathcal{E}^*(\mathbf{k})e^{ikx}) \cdot (\mathcal{E}(\mathbf{k}')e^{-ik'x} + \mathcal{E}^*(\mathbf{k}')e^{ik'x}) \\ &= \frac{1}{8} \int \frac{d^3k}{(2\pi)^3} (\mathcal{E}(\mathbf{k}) \cdot \mathcal{E}(-\mathbf{k})e^{-2ik^0t} + 2\mathcal{E}(\mathbf{k}) \cdot \mathcal{E}^*(\mathbf{k}) + \mathcal{E}^*(\mathbf{k}) \cdot \mathcal{E}^*(-\mathbf{k})e^{2ik^0t}). \end{aligned}$$

A similar expression involving $\mathcal{B}(\mathbf{k})$ holds for the second term. Using (6.9) and the fact that $\mathcal{E}(\mathbf{k})$ is transverse, you can show that the time-dependent terms cancel between \mathcal{E} and \mathcal{B} , while the remaining terms add to give

$$\text{Energy} = \frac{1}{2} \int \frac{d^3k}{(2\pi)^3} \mathcal{E}(\mathbf{k}) \cdot \mathcal{E}^*(\mathbf{k}). \quad (6.11)$$

Since $\mathcal{E}(\mathbf{k})$ is transverse, let us introduce two transverse unit polarization vectors $\epsilon_\lambda(\mathbf{k})$, $\lambda = 1, 2$. We can then write the integrand as

$$\mathcal{E}(\mathbf{k}) \cdot \mathcal{E}^*(\mathbf{k}) = \sum_{\lambda=1,2} |\epsilon_\lambda(\mathbf{k}) \cdot \mathcal{E}(\mathbf{k})|^2 = |\mathbf{k}|^2 \sum_{\lambda=1,2} |\epsilon_\lambda(\mathbf{k}) \cdot \mathcal{A}(\mathbf{k})|^2.$$

Using the explicit form of $\mathcal{A}(\mathbf{k})$ (6.7), we finally arrive at an expression for the energy radiated*:

$$\text{Energy} = \int \frac{d^3k}{(2\pi)^3} \sum_{\lambda=1,2} \frac{e^2}{2} \left| \epsilon_\lambda(\mathbf{k}) \cdot \left(\frac{\mathbf{p}'}{k \cdot p'} - \frac{\mathbf{p}}{k \cdot p} \right) \right|^2. \quad (6.12)$$

We can freely change ϵ , \mathbf{p}' , and \mathbf{p} into 4-vectors in this expression. Then, noting that substituting k^μ for ϵ^μ would give zero,

$$k_\mu \left(\frac{p'^\mu}{k \cdot p'} - \frac{p^\mu}{k \cdot p} \right) = 0,$$

we find that we can perform the sum over polarizations using the trick of Section 5.5, replacing $\sum \epsilon_\mu \epsilon_\nu^*$ by $-g_{\mu\nu}$. Our result then becomes

$$\begin{aligned} \text{Energy} &= \int \frac{d^3k}{(2\pi)^3} \frac{e^2}{2} (-g_{\mu\nu}) \left(\frac{p'^\mu}{k \cdot p'} - \frac{p^\mu}{k \cdot p} \right) \left(\frac{p'^\nu}{k \cdot p'} - \frac{p^\nu}{k \cdot p} \right) \\ &= \int \frac{d^3k}{(2\pi)^3} \frac{e^2}{2} \left(\frac{2p \cdot p'}{(k \cdot p')(k \cdot p)} - \frac{m^2}{(k \cdot p')^2} - \frac{m^2}{(k \cdot p)^2} \right). \end{aligned} \quad (6.13)$$

To make this formula more explicit, choose a frame in which $p^0 = p'^0 = E$. Then the momenta are

$$k^\mu = (k, \mathbf{k}), \quad p^\mu = E(1, \mathbf{v}), \quad p'^\mu = E(1, \mathbf{v}').$$

*This result is also derived in Jackson (1975), p. 703.

In such a frame our formula becomes

$$\text{Energy} = \frac{e^2}{(2\pi)^2} \int dk \mathcal{I}(\mathbf{v}, \mathbf{v}'), \quad (6.14)$$

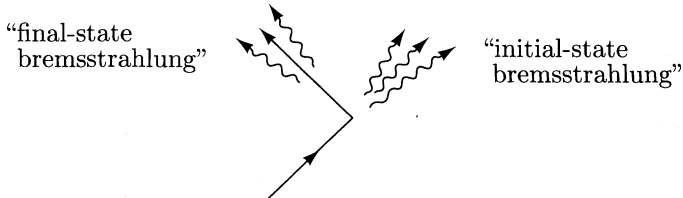
where $\mathcal{I}(\mathbf{v}, \mathbf{v}')$ (which is essentially the differential intensity $d(\text{Energy})/dk$) is given by

$$\mathcal{I}(\mathbf{v}, \mathbf{v}') = \int \frac{d\Omega_{\hat{k}}}{4\pi} \left(\frac{2(1-\mathbf{v} \cdot \mathbf{v}')}{(1-\hat{k} \cdot \mathbf{v})(1-\hat{k} \cdot \mathbf{v}')} - \frac{m^2/E^2}{(1-\hat{k} \cdot \mathbf{v}')^2} - \frac{m^2/E^2}{(1-\hat{k} \cdot \mathbf{v})^2} \right). \quad (6.15)$$

Since $\mathcal{I}(\mathbf{v}, \mathbf{v}')$ does not depend on k , we see that the integral over k in (6.14) is trivial but divergent. This divergence comes from our idealization of an infinitely sudden change in momentum. We expect our formula to be valid only for radiation whose frequency is less than the reciprocal of the scattering time. For a relativistic electron, another possible cutoff would take effect when individual photons carry away a sizable fraction of the electron's energy. In either case our formula is valid in the low-frequency limit, provided that we cut off the integral at some maximum frequency k_{\max} . We then have

$$\text{Energy} = \frac{\alpha}{\pi} \cdot k_{\max} \cdot \mathcal{I}(\mathbf{v}, \mathbf{v}'). \quad (6.16)$$

The integrand of $\mathcal{I}(\mathbf{v}, \mathbf{v}')$ peaks when \hat{k} is parallel to either \mathbf{v} or \mathbf{v}' :



In the extreme relativistic limit, most of the radiated energy comes from the two peaks in the first term of (6.15). Let us evaluate $\mathcal{I}(\mathbf{v}, \mathbf{v}')$ in this limit, by concentrating on the regions around these peaks. Break up the integral into a piece for each peak, and let $\theta = 0$ along the peak in each case. Integrate over a small region around $\theta = 0$, as follows:

$$\begin{aligned} \mathcal{I}(\mathbf{v}, \mathbf{v}') &\approx \int_{\hat{k} \cdot \mathbf{v} = \mathbf{v}' \cdot \mathbf{v}}^{\cos \theta = 1} d\cos \theta \frac{1 - \mathbf{v} \cdot \mathbf{v}'}{(1 - v \cos \theta)(1 - \mathbf{v} \cdot \mathbf{v}')} \\ &+ \int_{\hat{k} \cdot \mathbf{v}' = \mathbf{v}' \cdot \mathbf{v}}^{\cos \theta = 1} d\cos \theta \frac{1 - \mathbf{v} \cdot \mathbf{v}'}{(1 - \mathbf{v} \cdot \mathbf{v}')(1 - v' \cos \theta)}. \end{aligned}$$

(The lower limits on the integrals are not critical; an equally good choice would be $\hat{k} \cdot \mathbf{v} = 1 - x(1 - \mathbf{v} \cdot \mathbf{v}')$, as long as x is neither too close to 0 nor too much bigger than 1. It is then easy to show that the leading term in the

relativistic limit does not depend on x .) The integrals are easy to perform, and we obtain

$$\begin{aligned}\mathcal{I}(\mathbf{v}, \mathbf{v}') &\approx \log\left(\frac{1 - \mathbf{v}' \cdot \mathbf{v}}{1 - |\mathbf{v}|}\right) + \log\left(\frac{1 - \mathbf{v}' \cdot \mathbf{v}}{1 - |\mathbf{v}'|}\right) = \log\left(\frac{(E^2 - \mathbf{p} \cdot \mathbf{p}')^2}{E^2(E - |\mathbf{p}|)^2}\right) \\ &\approx 2 \log\left(\frac{\mathbf{p} \cdot \mathbf{p}'}{(E^2 - |\mathbf{p}|^2)/2}\right) = 2 \log\left(\frac{-q^2}{m^2}\right),\end{aligned}\quad (6.17)$$

where $q^2 = (p' - p)^2$.

In conclusion, we have found that the radiated energy at low frequencies is given by

$$\text{Energy} = \frac{\alpha}{\pi} \int_0^{k_{\max}} dk \mathcal{I}(\mathbf{v}, \mathbf{v}') \xrightarrow{E \gg m} \frac{2\alpha}{\pi} \int_0^{k_{\max}} dk \log\left(\frac{-q^2}{m^2}\right). \quad (6.18)$$

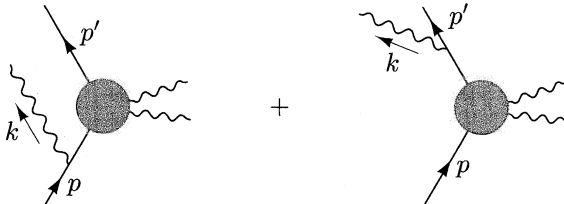
If this energy is made up of photons, each photon contributes energy k . We would then expect

$$\text{Number of photons} = \frac{\alpha}{\pi} \int_0^{k_{\max}} dk \frac{1}{k} \mathcal{I}(\mathbf{v}, \mathbf{v}'). \quad (6.19)$$

We hope that a quantum-mechanical calculation will confirm this result.

Quantum Computation

Consider now the quantum-mechanical process in which one photon is radiated during the scattering of an electron:



Let \mathcal{M}_0 denote the part of the amplitude that comes from the electron's interaction with the external field. Then the amplitude for the whole process is

$$\begin{aligned}i\mathcal{M} &= -ie\bar{u}(p') \left(\mathcal{M}_0(p', p - k) \frac{i(p - k + m)}{(p - k)^2 - m^2} \gamma^\mu \epsilon_\mu^*(k) \right. \\ &\quad \left. + \gamma^\mu \epsilon_\mu^*(k) \frac{i(p' + k + m)}{(p' + k)^2 - m^2} \mathcal{M}_0(p' + k, p) \right) u(p).\end{aligned}\quad (6.20)$$

Since we are interested in connecting with the classical limit, assume that the photon radiated is soft: $|\mathbf{k}| \ll |\mathbf{p}' - \mathbf{p}|$. Then we can approximate

$$\mathcal{M}_0(p', p - k) \approx \mathcal{M}_0(p' + k, p) \approx \mathcal{M}_0(p', p), \quad (6.21)$$

and we can ignore \not{p} in the numerators of the propagators. The numerators can be further simplified with some Dirac algebra. In the first term we have

$$\begin{aligned} (\not{p} + m)\gamma^\mu \epsilon_\mu^* u(p) &= [2p^\mu \epsilon_\mu^* + \gamma^\mu \epsilon_\mu^*(-\not{p} + m)]u(p) \\ &= 2p^\mu \epsilon_\mu^* u(p). \end{aligned}$$

Similarly, in the second term,

$$\bar{u}(p') \gamma^\mu \epsilon_\mu^*(\not{p}' + m) = \bar{u}(p') 2p'^\mu \epsilon_\mu^*.$$

The denominators of the propagators also simplify:

$$(p - k)^2 - m^2 = -2p \cdot k; \quad (p' + k)^2 - m^2 = 2p' \cdot k.$$

So in the soft-photon approximation, the amplitude becomes

$$i\mathcal{M} = \bar{u}(p') [\mathcal{M}_0(p', p)] u(p) \cdot \left[e \left(\frac{\not{p}' \cdot \epsilon^*}{\not{p}' \cdot k} - \frac{\not{p} \cdot \epsilon^*}{\not{p} \cdot k} \right) \right]. \quad (6.22)$$

This is just the amplitude for elastic scattering (without bremsstrahlung), times a factor (in brackets) for the emission of the photon.

The cross section for our process is also easy to express in terms of the elastic cross section; just insert an additional phase-space integration for the photon variable k . Summing over the two photon polarization states, we have

$$d\sigma(p \rightarrow p' + \gamma) = d\sigma(p \rightarrow p') \cdot \int \frac{d^3k}{(2\pi)^3} \frac{1}{2k} \sum_{\lambda=1,2} e^2 \left| \frac{\not{p}' \cdot \epsilon^{(\lambda)}}{\not{p}' \cdot k} - \frac{\not{p} \cdot \epsilon^{(\lambda)}}{\not{p} \cdot k} \right|^2. \quad (6.23)$$

Thus the differential probability of radiating a photon with momentum k , given that the electron scatters from p to p' , is

$$d(\text{prob}) = \frac{d^3k}{(2\pi)^3} \sum_{\lambda} \frac{e^2}{2k} \left| \epsilon_{\lambda} \cdot \left(\frac{\not{p}'}{\not{p}' \cdot k} - \frac{\not{p}}{\not{p} \cdot k} \right) \right|^2. \quad (6.24)$$

This looks very familiar; if we multiply by the photon energy k to compute the expected energy radiated, we recover the classical expression (6.12).

But there is a problem. Equation (6.24) is an expression not for the expected number of photons radiated, but for the probability of radiating a single photon. The problem becomes worse if we integrate over the photon momentum. As in (6.16), we can integrate only up to the energy at which our soft-photon approximations break down; a reasonable estimate for this energy is $|\mathbf{q}| = |\mathbf{p} - \mathbf{p}'|$. The integral is therefore

$$\text{Total probability} \approx \frac{\alpha}{\pi} \int_0^{|\mathbf{q}|} dk \frac{1}{k} \mathcal{I}(\mathbf{v}, \mathbf{v}'). \quad (6.25)$$

Since $\mathcal{I}(\mathbf{v}, \mathbf{v}')$ is independent of k , the integral diverges at its lower limit (where all our approximations are well justified). In other words, the total

probability of radiating a very soft photon is infinite. This is the famous problem of infrared divergences in QED perturbation theory.

We can artificially make the integral in (6.25) well-defined by pretending that the photon has a very small mass μ . This mass would then provide a lower cutoff for the integral, allowing us to write the result of this section as

$$\begin{aligned} d\sigma(p \rightarrow p' + \gamma(k)) &= d\sigma(p \rightarrow p') \cdot \frac{\alpha}{2\pi} \log\left(\frac{-q^2}{\mu^2}\right) \mathcal{I}(\mathbf{v}, \mathbf{v}') \\ &\underset{-q^2 \rightarrow \infty}{\approx} d\sigma(p \rightarrow p') \cdot \frac{\alpha}{\pi} \log\left(\frac{-q^2}{\mu^2}\right) \log\left(\frac{-q^2}{m^2}\right). \end{aligned} \quad (6.26)$$

The q^2 dependence of this result, known as the *Sudakov double logarithm*, is physical and will appear again in Section 6.4. The dependence on μ , however, presents a problem that we must solve. It is not hard to guess that the resolution of this problem will involve reinterpreting (6.24) as the expected number of radiated photons, rather than the probability of radiating a single photon. We will see in Sections 6.4 and 6.5 how this reinterpretation follows from the Feynman diagrams. To prepare for that discussion, however, we need to improve our understanding of the amplitude for scattering without radiation.

6.2 The Electron Vertex Function: Formal Structure

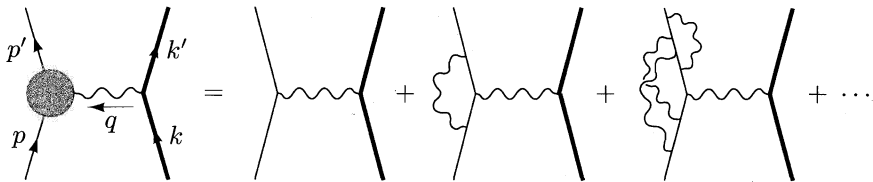
Having briefly discussed QED radiative corrections due to emission of photons (bremsstrahlung), let us now study the correction to electron scattering that comes from the presence of an additional *virtual* photon:



This will be our first experience with a Feynman diagram containing a loop. Such diagrams give rise to significant and profound complications in quantum field theory.

The result of computing this diagram will be rather complicated, so it will be useful to think ahead about what form we expect this correction to take and how to interpret its various possible terms. In this section, we will consider the general properties of vertex correction diagrams. We will see that the basic requirements of Lorentz invariance, the discrete symmetries of QED, and the Ward identity strongly constrain the form of the vertex.

Consider, then, the class of diagrams



where the gray circle indicates the sum of the lowest-order electron-photon vertex and all amputated loop corrections. We will call this sum of vertex diagrams $-ie\Gamma^\mu(p', p)$. Then, according to our master formula (4.103) for S -matrix elements, the amplitude for electron scattering from a heavy target is

$$i\mathcal{M} = ie^2 \left(\bar{u}(p') \Gamma^\mu(p', p) u(p) \right) \frac{1}{q^2} \left(\bar{u}(k') \gamma_\mu u(k) \right). \quad (6.28)$$

More generally, the function $\Gamma^\mu(p', p)$ appears in the S -matrix element for the scattering of an electron from an external electromagnetic field. As in Problem 4.4, add to the Hamiltonian of QED the interaction

$$\Delta H_{\text{int}} = \int d^3x e A_\mu^{\text{cl}} j^\mu, \quad (6.29)$$

where $j^\mu(x) = \bar{\psi}(x)\gamma^\mu\psi(x)$ is the electromagnetic current and A_μ^{cl} is a fixed classical potential. In the leading order of perturbation theory, the S -matrix element for scattering from this field is

$$i\mathcal{M}(2\pi)\delta(p^{0'} - p^0) = -ie\bar{u}(p')\gamma^\mu u(p) \cdot \tilde{A}_\mu^{\text{cl}}(p' - p),$$

where $\tilde{A}_\mu^{\text{cl}}(q)$ is the Fourier transform of $A_\mu^{\text{cl}}(x)$. The vertex corrections modify this expression to

$$i\mathcal{M}(2\pi)\delta(p^{0'} - p^0) = -ie\bar{u}(p')\Gamma^\mu(p', p) u(p) \cdot \tilde{A}_\mu^{\text{cl}}(p' - p). \quad (6.30)$$

In writing (6.28) and (6.30), we have deliberately omitted the contribution of vacuum polarization diagrams, such as the fourth diagram of (6.1). The reason for this omission is that these diagrams should be considered corrections to the electromagnetic field itself, while the diagrams included in Γ^μ represent corrections to the electron's response to a given applied field.[†]

We can use general arguments to restrict the form of $\Gamma^\mu(p', p)$. To lowest order, $\Gamma^\mu = \gamma^\mu$. In general, Γ^μ is some expression that involves p , p' , γ^μ , and constants such as m , e , and pure numbers. This list is exhaustive, since no other objects appear in the Feynman rules for evaluating the diagrams that contribute to Γ^μ . The only other object that could appear in any theory is $\epsilon^{\mu\nu\rho\sigma}$ (or equivalently, γ^5); but this is forbidden in any parity-conserving theory.

[†]To justify this statement, we must give a careful definition of an applied external field in a quantum field theory. We will do this in Chapter 11.

We can narrow down the form of Γ^μ considerably by appealing to Lorentz invariance. Since Γ^μ transforms as a vector (in the same sense that γ^μ does), it must be a linear combination of the vectors from the list above: γ^μ , p^μ , and p'^μ . Using the combinations $p' + p$ and $p' - p$ for convenience, we have

$$\Gamma^\mu = \gamma^\mu \cdot A + (p'^\mu + p^\mu) \cdot B + (p'^\mu - p^\mu) \cdot C. \quad (6.31)$$

The coefficients A , B , and C could involve Dirac matrices dotted into vectors, that is, \not{p} or \not{p}' . But since $\not{p}u(p) = m \cdot u(p)$ and $\bar{u}(p')\not{p}' = \bar{u}(p') \cdot m$, we can write the coefficients in terms of ordinary numbers without loss of generality. The only nontrivial scalar available is $q^2 = -2p' \cdot p + 2m^2$, so A , B , and C must be functions only of q^2 (and of constants such as m).

The list of allowed vectors can be further shortened by applying the Ward identity (5.79): $q_\mu \Gamma^\mu = 0$. (Note that our arguments for this identity in Section 5.5—and the proof in Section 7.4—do not require $q^2 = 0$.) Dotting q_μ into (6.31), we find that the second term vanishes, as does the first when sandwiched between $\bar{u}(p')$ and $u(p)$. The third term does not automatically vanish, so C must be zero.

We can make no further simplifications of (6.31) on general principles. It is conventional, however, to rewrite (6.31) by means of the Gordon identity (see Problem 3.2):

$$\bar{u}(p')\gamma^\mu u(p) = \bar{u}(p') \left[\frac{p'^\mu + p^\mu}{2m} + \frac{i\sigma^{\mu\nu}q_\nu}{2m} \right] u(p). \quad (6.32)$$

This identity allows us to swap the $(p' + p)$ term for one involving $\sigma^{\mu\nu}q_\nu$. We write our final result as

$$\Gamma^\mu(p', p) = \gamma^\mu F_1(q^2) + \frac{i\sigma^{\mu\nu}q_\nu}{2m} F_2(q^2), \quad (6.33)$$

where F_1 and F_2 are unknown functions of q^2 called *form factors*.

To lowest order, $F_1 = 1$ and $F_2 = 0$. In the next section we will compute the one-loop (order- α) corrections to the form factors, due to the vertex correction diagram (6.27). In principle, the form factors can be computed to any order in perturbation theory.

Since F_1 and F_2 contain complete information about the influence of an electromagnetic field on the electron, they should, in particular, contain the electron's gross electric and magnetic couplings. To identify the electric charge of the electron, we can use (6.30) to compute the amplitude for elastic Coulomb scattering of a nonrelativistic electron from a region of nonzero electrostatic potential. Set $A_\mu^{\text{cl}}(x) = (\phi(\mathbf{x}), \mathbf{0})$. Then $\tilde{A}_\mu^{\text{cl}}(q) = ((2\pi)\delta(q^0)\tilde{\phi}(\mathbf{q}), \mathbf{0})$. Inserting this into (6.30), we find

$$i\mathcal{M} = -ie\bar{u}(p') \Gamma^0(p', p) u(p) \cdot \tilde{\phi}(\mathbf{q}).$$

If the electrostatic field is very slowly varying over a large (perhaps macroscopic) region, $\tilde{\phi}(\mathbf{q})$ will be concentrated about $\mathbf{q} = 0$; then we can take the

limit $\mathbf{q} \rightarrow 0$ in the spinor matrix element. Only the form factor F_1 contributes. Using the nonrelativistic limit of the spinors,

$$\bar{u}(p')\gamma^0 u(p) = u^\dagger(p')u(p) \approx 2m\xi'^\dagger\xi,$$

the amplitude for electron scattering from an electric field takes the form

$$i\mathcal{M} = -ieF_1(0)\tilde{\phi}(\mathbf{q}) \cdot 2m\xi'^\dagger\xi. \quad (6.34)$$

This is the Born approximation for scattering from a potential

$$V(\mathbf{x}) = eF_1(0)\phi(\mathbf{x}).$$

Thus $F_1(0)$ is the electric charge of the electron, in units of e . Since $F_1(0) = 1$ already in the leading order of perturbation theory, radiative corrections to $F_1(q^2)$ should vanish at $q^2 = 0$.

By repeating this analysis for an electron scattering from a static vector potential, we can derive a similar connection between the form factors and the electron's magnetic moment.[†] Set $A_\mu^{\text{cl}}(x) = (0, \mathbf{A}^{\text{cl}}(\mathbf{x}))$. Then the amplitude for scattering from this field is

$$i\mathcal{M} = +ie\left[\bar{u}(p')\left(\gamma^i F_1 + \frac{i\sigma^{i\nu} q_\nu}{2m} F_2\right)u(p)\right]\tilde{A}_{\text{cl}}^i(\mathbf{q}). \quad (6.35)$$

The expression in brackets vanishes at $\mathbf{q} = 0$, so we must carefully extract from it a contribution linear in q^i . To do this, insert the nonrelativistic expansion of the spinors $u(p)$, keeping terms through first order in momenta:

$$u(p) = \begin{pmatrix} \sqrt{p \cdot \sigma}\xi \\ \sqrt{p \cdot \bar{\sigma}}\xi \end{pmatrix} \approx \sqrt{m} \begin{pmatrix} (1 - \mathbf{p} \cdot \boldsymbol{\sigma}/2m)\xi \\ (1 + \mathbf{p} \cdot \boldsymbol{\sigma}/2m)\xi \end{pmatrix}. \quad (6.36)$$

Then the F_1 term can be simplified as follows:

$$\bar{u}(p')\gamma^i u(p) = 2m\xi'^\dagger \left(\frac{\mathbf{p}' \cdot \boldsymbol{\sigma}}{2m} \sigma^i + \sigma^i \frac{\mathbf{p} \cdot \boldsymbol{\sigma}}{2m} \right) \xi.$$

Applying the identity $\sigma^i \sigma^j = \delta^{ij} + i\epsilon^{ijk}\sigma^k$, we find a spin-independent term, proportional to $(\mathbf{p}' + \mathbf{p})$, and a spin-dependent term, proportional to $(\mathbf{p}' - \mathbf{p})$. The first of these terms is the contribution of the operator $[\mathbf{p} \cdot \mathbf{A} + \mathbf{A} \cdot \mathbf{p}]$ in the standard kinetic energy term of nonrelativistic quantum mechanics. The second is the magnetic moment interaction we are seeking. Retaining only the latter term, we have

$$\bar{u}(p')\gamma^i u(p) = 2m\xi'^\dagger \left(\frac{-i}{2m} \epsilon^{ijk} q^j \sigma^k \right) \xi.$$

The F_2 term already contains an explicit factor of q , so we can evaluate it using the leading-order term of the expansion of the spinors. This gives

$$\bar{u}(p') \left(\frac{i}{2m} \sigma^{i\nu} q_\nu \right) u(p) = 2m\xi'^\dagger \left(\frac{-i}{2m} \epsilon^{ijk} q^j \sigma^k \right) \xi.$$

[†]The following argument contains numerous factors of (-1) from raising and lowering spacelike indices. Be careful in verifying the algebra.

Thus, the complete term linear in q^j in the electron-photon vertex function is

$$\bar{u}(p') \left(\gamma^i F_1 + \frac{i\sigma^{i\nu} q_\nu}{2m} F_2 \right) u(p) \underset{q \rightarrow 0}{\approx} 2m \xi'^\dagger \left(\frac{-i}{2m} \epsilon^{ijk} q^j \sigma^k [F_1(0) + F_2(0)] \right) \xi.$$

Inserting this expression into (6.35), we find

$$i\mathcal{M} = -i(2m) \cdot e \xi'^\dagger \left(\frac{-1}{2m} \sigma^k [F_1(0) + F_2(0)] \right) \xi \tilde{B}^k(\mathbf{q}),$$

where

$$\tilde{B}^k(\mathbf{q}) = -i\epsilon^{ijk} q^i \tilde{A}_{\text{cl}}^j(\mathbf{q})$$

is the Fourier transform of the magnetic field produced by $\mathbf{A}^{\text{cl}}(\mathbf{x})$.

Again we can interpret \mathcal{M} as the Born approximation to the scattering of the electron from a potential well. The potential is just that of a magnetic moment interaction,

$$V(\mathbf{x}) = -\langle \boldsymbol{\mu} \rangle \cdot \mathbf{B}(\mathbf{x}),$$

where

$$\langle \boldsymbol{\mu} \rangle = \frac{e}{m} [F_1(0) + F_2(0)] \xi'^\dagger \frac{\boldsymbol{\sigma}}{2} \xi.$$

This expression for the magnetic moment of the electron can be rewritten in the standard form

$$\boldsymbol{\mu} = g \left(\frac{e}{2m} \right) \mathbf{S},$$

where \mathbf{S} is the electron spin. The coefficient g , called the *Landé g-factor*, is

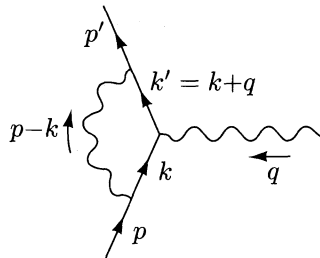
$$g = 2[F_1(0) + F_2(0)] = 2 + 2F_2(0). \quad (6.37)$$

Since the leading order of perturbation theory gives no F_2 term, QED predicts $g = 2 + \mathcal{O}(\alpha)$. The leading term is the standard prediction of the Dirac equation. In higher orders, however, we will find a nonzero F_2 and thus a small difference between the electron's magnetic moment and the Dirac value. We will compute the order- α contribution to this *anomalous magnetic moment* in the next section.

Since our derivation of the structure (6.33) for the vertex function used only general symmetry principles, we expect this formula to apply not only to the electron but to any fermion with electromagnetic interactions. For example, the electromagnetic scattering amplitude of the proton should also be described by two invariant functions of q^2 . Since the proton is not an elementary particle, we should not expect the Dirac equation values $F_1 = 1$ and $F_2 = 0$ to be good approximations to the form factors of the proton. In fact, both proton form factors depend strongly on q^2 . However, the description of the vertex function in term of form factors provides a useful summary of data on scattering at many energies and angles. The precise transcription between form factors and cross sections is worked out in Problem 6.1. In addition, the general constraints at $q^2 = 0$ that we have just derived apply to the proton: $F_1(0) = 1$, and $2F_2(0) = (g_p - 2)$, though the g -factor of the proton differs by 40% from the Dirac value.

6.3 The Electron Vertex Function: Evaluation

Now that we know what form the answer is to take (Eq. (6.33)), we are ready to evaluate the one-loop contribution to the electron vertex function. Assign momenta on the diagram as follows:



Applying the Feynman rules, we find, to order α , that $\Gamma^\mu = \gamma^\mu + \delta\Gamma^\mu$, where

$$\begin{aligned} \bar{u}(p')\delta\Gamma^\mu(p', p)u(p) &= \int \frac{d^4k}{(2\pi)^4} \frac{-ig_{\nu\rho}}{(k-p)^2+i\epsilon} \bar{u}(p')(-ie\gamma^\nu) \frac{i(k'+m)}{k'^2-m^2+i\epsilon} \gamma^\mu \frac{i(k+m)}{k^2-m^2+i\epsilon} (-ie\gamma^\rho)u(p) \\ &= 2ie^2 \int \frac{d^4k}{(2\pi)^4} \frac{\bar{u}(p')[k'\gamma^\mu k' + m^2\gamma^\mu - 2m(k+k')^\mu]u(p)}{((k-p)^2+i\epsilon)(k'^2-m^2+i\epsilon)(k^2-m^2+i\epsilon)}. \end{aligned} \quad (6.38)$$

In the second line we have used the contraction identity $\gamma^\nu\gamma^\mu\gamma_\nu = -2\gamma^\mu$. Note that the $+i\epsilon$ terms in the denominators cannot be dropped; they are necessary for proper evaluation of the loop-momentum integral.

The integral looks impossible, and in fact it will not be easy. The evaluation of such integrals requires another piece of computational technology, known as the method of *Feynman parameters* (although a very similar method was introduced earlier by Schwinger).

Feynman Parameters

The goal of this method is to squeeze the three denominator factors of (6.38) into a single quadratic polynomial in k , raised to the third power. We can then shift k by a constant to complete the square in this polynomial and evaluate the remaining spherically symmetric integral without difficulty. The price will be the introduction of auxiliary parameters to be integrated over.

It is easiest to begin with the simpler case of two factors in the denominator. We would then use the identity

$$\frac{1}{AB} = \int_0^1 dx \frac{1}{[xA + (1-x)B]^2} = \int_0^1 dx dy \delta(x+y-1) \frac{1}{[xA + yB]^2}. \quad (6.39)$$

An example of its use might look like this:

$$\begin{aligned} \frac{1}{(k-p)^2(k^2-m^2)} &= \int_0^1 dx dy \delta(x+y-1) \frac{1}{[x(k-p)^2 + y(k^2-m^2)]^2} \\ &= \int_0^1 dx dy \delta(x+y-1) \frac{1}{[k^2 - 2xk \cdot p + xp^2 - ym^2]^2}. \end{aligned}$$

If we now let $\ell \equiv k - xp$, we see that the denominator depends only on ℓ^2 . Integrating over $d^4 k$ would now be much easier, since $d^4 k = d^4 \ell$ and the integrand is spherically symmetric with respect to ℓ . The variables x and y that make this transformation possible are called *Feynman parameters*.

Our integral (6.38) involves a denominator with three factors, so we need a slightly better identity. By differentiating (6.39) with respect to B , it is easy to prove

$$\frac{1}{AB^n} = \int_0^1 dx dy \delta(x+y-1) \frac{ny^{n-1}}{[xA + yB]^{n+1}}. \quad (6.40)$$

But this still isn't quite good enough. The formula we need is

$$\frac{1}{A_1 A_2 \cdots A_n} = \int_0^1 dx_1 \cdots dx_n \delta(\sum x_i - 1) \frac{(n-1)!}{[x_1 A_1 + x_2 A_2 + \cdots + x_n A_n]^n}. \quad (6.41)$$

The proof of this identity is by induction. The case $n = 2$ is just Eq. (6.39); the induction step is not difficult and involves the use of (6.40).

By repeated differentiation of (6.41), you can derive the even more general identity

$$\frac{1}{A_1^{m_1} A_2^{m_2} \cdots A_n^{m_n}} = \int_0^1 dx_1 \cdots dx_n \delta(\sum x_i - 1) \frac{\prod x_i^{m_i-1}}{[\sum x_i A_i]^{\sum m_i}} \frac{\Gamma(m_1 + \cdots + m_n)}{\Gamma(m_1) \cdots \Gamma(m_n)}. \quad (6.42)$$

This formula is true even when the m_i are not integers; in Section 10.5 we will apply it in such a case.

Evaluation of the Form Factors

Now let us apply formula (6.41) to the denominator of (6.38):

$$\frac{1}{((k-p)^2+i\epsilon)(k'^2-m^2+i\epsilon)(k^2-m^2+i\epsilon)} = \int_0^1 dx dy dz \delta(x+y+z-1) \frac{2}{D^3},$$

where the new denominator D is

$$\begin{aligned} D &= x(k^2 - m^2) + y(k'^2 - m^2) + z(k - p)^2 + (x + y + z)i\epsilon \\ &= k^2 + 2k \cdot (yq - zp) + yq^2 + zp^2 - (x + y)m^2 + i\epsilon. \end{aligned} \quad (6.43)$$

In the second line we have used $x + y + z = 1$ and $k' = k + q$. Now shift k to complete the square:

$$\ell \equiv k + yq - zp.$$

After a bit of algebra we find that D simplifies to

$$D = \ell^2 - \Delta + i\epsilon,$$

where

$$\Delta \equiv -xyq^2 + (1 - z)^2m^2. \quad (6.44)$$

Since $q^2 < 0$ for a scattering process, Δ is positive; we can think of it as an effective mass term.

Next we must express the numerator of (6.38) in terms of ℓ . This task is simplified by noting that since D depends only on the magnitude of ℓ ,

$$\int \frac{d^4\ell}{(2\pi)^4} \frac{\ell^\mu}{D^3} = 0; \quad (6.45)$$

$$\int \frac{d^4\ell}{(2\pi)^4} \frac{\ell^\mu \ell^\nu}{D^3} = \int \frac{d^4\ell}{(2\pi)^4} \frac{\frac{1}{4}g^{\mu\nu}\ell^2}{D^3}. \quad (6.46)$$

The first identity follows from symmetry. To prove the second, note that the integral vanishes by symmetry unless $\mu = \nu$. Lorentz invariance therefore requires that we get something proportional to $g^{\mu\nu}$. To check the coefficient, contract each side with $g_{\mu\nu}$. Using these identities, we have

$$\begin{aligned} \text{Numerator} &= \bar{u}(p') \left[\not{k}\gamma^\mu \not{k}' + m^2\gamma^\mu - 2m(k + k')^\mu \right] u(p) \\ &\rightarrow \bar{u}(p') \left[-\frac{1}{2}\gamma^\mu \ell^2 + (-y\not{q} + z\not{p})\gamma^\mu ((1 - y)\not{q} + z\not{p}) \right. \\ &\quad \left. + m^2\gamma^\mu - 2m((1 - 2y)q^\mu + 2zp^\mu) \right] u(p). \end{aligned}$$

(Remember that $k' = k + q$.)

Putting the numerator into a useful form is now just a matter of some tedious Dirac algebra (about a page or two). This is where our work in the last section pays off, since it tells us what kind of an answer to expect. We eventually want to group everything into two terms, proportional to γ^μ and $i\sigma^{\mu\nu}q_\nu$. The most straightforward way to accomplish this is to aim instead for an expression of the form

$$\gamma^\mu \cdot A + (p'^\mu + p^\mu) \cdot B + q^\mu \cdot C,$$

just as in (6.31). Attaining this form requires only the anticommutation relations (for example, $\not{p}\gamma^\mu = 2p^\mu - \gamma^\mu\not{p}$) and the Dirac equation ($\not{p}u(p) = m u(p)$)

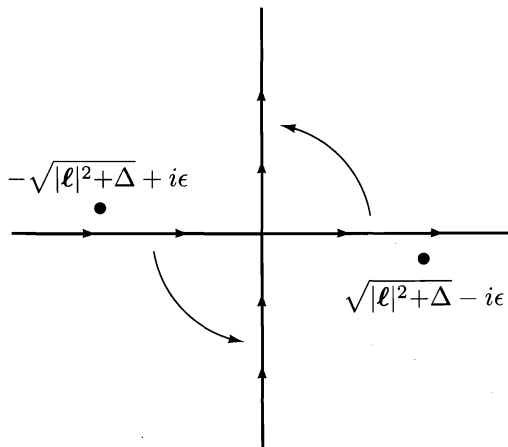


Figure 6.1. The contour of the ℓ^0 integration can be rotated as shown.

and $\bar{u}(p')\not{p}' = \bar{u}(p') m$; note that this implies $\bar{u}(p')\not{q} u(p) = 0$). It is also useful to remember that $x + y + z = 1$. When the smoke clears, we have

$$\begin{aligned} \text{Numerator} = \bar{u}(p') & \left[\gamma^\mu \cdot \left(-\frac{1}{2}\ell^2 + (1-x)(1-y)q^2 + (1-2z-z^2)m^2 \right) \right. \\ & \left. + (p'^\mu + p^\mu) \cdot mz(z-1) + q^\mu \cdot m(z-2)(x-y) \right] u(p). \end{aligned}$$

The coefficient of q^μ must vanish according to the Ward identity, as discussed after Eq. (6.31). To see that it does, note from (6.44) that the denominator is symmetric under $x \leftrightarrow y$. The coefficient of q^μ is odd under $x \leftrightarrow y$ and therefore vanishes when integrated over x and y .

Still following our work in the previous section, we now use the Gordon identity (6.32) to eliminate $(p' + p)$ in favor of $i\sigma^{\mu\nu}q_\nu$. Our entire expression for the $\mathcal{O}(\alpha)$ contribution to the electron vertex then becomes

$$\begin{aligned} \bar{u}(p')\delta\Gamma^\mu(p', p)u(p) &= 2ie^2 \int \frac{d^4\ell}{(2\pi)^4} \int_0^1 dx dy dz \delta(x+y+z-1) \frac{2}{D^3} \\ & \times \bar{u}(p') \left[\gamma^\mu \cdot \left(-\frac{1}{2}\ell^2 + (1-x)(1-y)q^2 + (1-4z+z^2)m^2 \right) \right. \\ & \left. + \frac{i\sigma^{\mu\nu}q_\nu}{2m} (2m^2 z(1-z)) \right] u(p), \end{aligned} \quad (6.47)$$

where as before,

$$D = \ell^2 - \Delta + i\epsilon, \quad \Delta = -xyq^2 + (1-z)^2m^2 > 0.$$

The decomposition into form factors is now manifest.

With most of the work behind us, our main remaining task is to perform the momentum integral. It is not difficult to evaluate the ℓ^0 integral as a

contour integral, then do the spatial integrals in spherical coordinates. We will use an even easier method, making use of a trick called *Wick rotation*. Note that if it were not for the minus signs in the Minkowski metric, we could perform the entire four-dimensional integral in four-dimensional “spherical” coordinates. To remove the minus signs, consider the contour of integration in the ℓ^0 -plane (see Fig. 6.1). The locations of the poles, and the fact that the integrand falls off sufficiently rapidly at large $|\ell^0|$, allow us to rotate the contour counterclockwise by 90° . We then define a *Euclidean* 4-momentum variable ℓ_E :

$$\ell^0 \equiv i\ell_E^0; \quad \ell = \ell_E. \quad (6.48)$$

Our rotated contour goes from $\ell_E^0 = -\infty$ to ∞ . By simply changing variables to ℓ_E , we can now evaluate the integral in four-dimensional spherical coordinates.

Let us first evaluate

$$\begin{aligned} \int \frac{d^4\ell}{(2\pi)^4} \frac{1}{[\ell^2 - \Delta]^m} &= \frac{i}{(-1)^m} \frac{1}{(2\pi)^4} \int d^4\ell_E \frac{1}{[\ell_E^2 + \Delta]^m} \\ &= \frac{i(-1)^m}{(2\pi)^4} \int d\Omega_4 \int_0^\infty d\ell_E \frac{\ell_E^3}{[\ell_E^2 + \Delta]^m}. \end{aligned}$$

(Here we need only the case $m = 3$, but the more general result will be useful for other loop calculations.) The factor $\int d\Omega_4$ is the surface “area” of a four-dimensional unit sphere, which happens to equal $2\pi^2$. (One way to compute this area is to use four-dimensional spherical coordinates,

$$x = (r \sin \omega \sin \theta \cos \phi, r \sin \omega \sin \theta \sin \phi, r \sin \omega \cos \theta, r \cos \omega).$$

The integration measure is then $d^4x = r^3 \sin^2 \omega \sin \theta d\phi d\theta d\omega dr$.) The rest of the integral is straightforward, and we have

$$\int \frac{d^4\ell}{(2\pi)^4} \frac{1}{[\ell^2 - \Delta]^m} = \frac{i(-1)^m}{(4\pi)^2} \frac{1}{(m-1)(m-2)} \frac{1}{\Delta^{m-2}}. \quad (6.49)$$

Similarly,

$$\int \frac{d^4\ell}{(2\pi)^4} \frac{\ell^2}{[\ell^2 - \Delta]^m} = \frac{i(-1)^{m-1}}{(4\pi)^2} \frac{2}{(m-1)(m-2)(m-3)} \frac{1}{\Delta^{m-3}}. \quad (6.50)$$

Note that this second result is valid only when $m > 3$. When $m = 3$, the Wick rotation cannot be justified, and the integral is in any event divergent. But it is just this case that we need for (6.47).

We will eventually explore the physical meaning of this divergence, but for the moment we simply introduce an artificial prescription to make our integral finite. Go back to the original expression for the Feynman integral in

(6.38), and replace in the photon propagator

$$\frac{1}{(k-p)^2 + i\epsilon} \longrightarrow \frac{1}{(k-p)^2 + i\epsilon} - \frac{1}{(k-p)^2 - \Lambda^2 + i\epsilon}, \quad (6.51)$$

where Λ is a very large mass. The integrand is unaffected for small k (since Λ is large), but cuts off smoothly when $k \gtrsim \Lambda$. We can think of the second term as the propagator of a fictitious heavy photon, whose contribution is subtracted from that of the ordinary photon. In terms involving the heavy photon, the numerator algebra is unchanged and the denominator is altered by

$$\Delta \longrightarrow \Delta_\Lambda = -xyq^2 + (1-z)^2m^2 + z\Lambda^2. \quad (6.52)$$

The integral (6.50) is then replaced with a convergent integral, which can be Wick-rotated and evaluated:

$$\begin{aligned} \int \frac{d^4\ell}{(2\pi)^4} \left(\frac{\ell^2}{[\ell^2 - \Delta]^3} - \frac{\ell^2}{[\ell^2 - \Delta_\Lambda]^3} \right) &= \frac{i}{(4\pi)^2} \int_0^\infty d\ell_E^2 \left(\frac{\ell_E^4}{[\ell_E^2 + \Delta]^3} - \frac{\ell_E^4}{[\ell_E^2 + \Delta_\Lambda]^3} \right) \\ &= \frac{i}{(4\pi)^2} \log\left(\frac{\Delta_\Lambda}{\Delta}\right). \end{aligned} \quad (6.53)$$

The convergent terms in (6.47) are modified by terms of order Λ^{-2} , which we ignore.

This prescription for rendering Feynman integrals finite by introducing fictitious heavy particles is known as *Pauli-Villars regularization*. Please note that the fictitious photon has no physical significance, and that this method is only one of many for defining the divergent integrals. (We will discuss other methods in the next chapter; see especially Problem 7.2.) We must hope that the new parameter Λ will not appear in our final results for observable cross sections.

Using formulae (6.49) and (6.53) to evaluate the integrals in (6.47), we obtain an explicit, though complicated, expression for the one-loop vertex correction:

$$\begin{aligned} \text{Diagram} &= \frac{\alpha}{2\pi} \int_0^1 dx dy dz \delta(x+y+z-1) \\ &\times \bar{u}(p') \left(\gamma^\mu \left[\log \frac{z\Lambda^2}{\Delta} + \frac{1}{\Delta} \left((1-x)(1-y)q^2 + (1-4z+z^2)m^2 \right) \right] \right. \\ &\left. + \frac{i\sigma^{\mu\nu}q_\nu}{2m} \left[\frac{1}{\Delta} 2m^2 z(1-z) \right] \right) u(p). \end{aligned} \quad (6.54)$$

The bracketed expressions are our desired corrections to the form factors.

Before we try to interpret this result, let us summarize the calculational methods we used. The techniques are common to all loop calculations:

1. Draw the diagram(s) and write down the amplitude.
2. Introduce Feynman parameters to combine the denominators of the propagators.
3. Complete the square in the new denominator by shifting to a new loop momentum variable, ℓ .
4. Write the numerator in terms of ℓ . Drop odd powers of ℓ , and rewrite even powers using identities like (6.46).
5. Perform the momentum integral by means of a Wick rotation and four-dimensional spherical coordinates.

The momentum integral in the last step will often be divergent. In that case we must define (or *regularize*) the integral using the Pauli-Villars prescription or some other device.

Now that we have parametrized the ultraviolet divergence in (6.54), let us try to interpret it. Notice that the divergence appears in the worst possible place: It corrects $F_1(q^2 = 0)$, which should (according to our discussion at the end of the previous section) be fixed at the value 1. But this is the only effect of the divergent term. We will therefore adopt a simple but completely *ad hoc* fix for this difficulty: Subtract from the above expression a term proportional to the zeroth-order vertex function ($\bar{u}(p')\gamma^\mu u(p)$), in such a way as to maintain the condition $F_1(0) = 1$. In other words, make the substitution

$$\delta F_1(q^2) \rightarrow \delta F_1(q^2) - \delta F_1(0) \quad (6.55)$$

(where δF_1 denotes the first-order correction to F_1). The justification of this procedure involves the minor correction to our S -matrix formula (4.103) mentioned in Section 4.6. In brief, the term we are subtracting corrects for our omission of the external leg correction diagrams of (6.1). We postpone the justification of this statement until Section 7.2.

There is also an infrared divergence in $F_1(q^2)$, coming from the $1/\Delta$ term. For example, at $q^2 = 0$ this term is

$$\begin{aligned} \int_0^1 dx dy dz \delta(x+y+z-1) \frac{1-4z+z^2}{\Delta(q^2=0)} &= \int_0^1 dz \int_0^{1-z} dy \frac{-2 + (1-z)(3-z)}{m^2(1-z)^2} \\ &= \int_0^1 dz \frac{-2}{m^2(1-z)} + \text{finite terms}. \end{aligned}$$

We can cure this disease by pretending that the photon has a small nonzero mass μ . Then in the denominator of the photon propagator, $(k-p)^2$ would become $(k-p)^2 - \mu^2$. This denominator was multiplied by z in (6.43), so the net effect is to add a term $z\mu^2$ to Δ . We will discuss the infrared divergence further in the next two sections.

With both of these provisional modifications, the form factors are

$$F_1(q^2) = 1 + \frac{\alpha}{2\pi} \int_0^1 dx dy dz \delta(x+y+z-1) \times \left[\log\left(\frac{m^2(1-z)^2}{m^2(1-z)^2 - q^2 xy}\right) + \frac{m^2(1-4z+z^2) + q^2(1-x)(1-y)}{m^2(1-z)^2 - q^2 xy + \mu^2 z} - \frac{m^2(1-4z+z^2)}{m^2(1-z)^2 + \mu^2 z} \right] + \mathcal{O}(\alpha^2); \quad (6.56)$$

$$F_2(q^2) = \frac{\alpha}{2\pi} \int_0^1 dx dy dz \delta(x+y+z-1) \left[\frac{2m^2 z(1-z)}{m^2(1-z)^2 - q^2 xy} \right] + \mathcal{O}(\alpha^2). \quad (6.57)$$

Note that neither the ultraviolet nor the infrared divergence affects $F_2(q^2)$. We can therefore evaluate unambiguously

$$\begin{aligned} F_2(q^2 = 0) &= \frac{\alpha}{2\pi} \int_0^1 dx dy dz \delta(x+y+z-1) \frac{2m^2 z(1-z)}{m^2(1-z)^2} \\ &= \frac{\alpha}{\pi} \int_0^1 dz \int_0^{1-z} dy \frac{z}{1-z} = \frac{\alpha}{2\pi}. \end{aligned} \quad (6.58)$$

Thus, we get a correction to the g -factor of the electron:

$$a_e \equiv \frac{g-2}{2} = \frac{\alpha}{2\pi} \approx .0011614. \quad (6.59)$$

This result was first obtained by Schwinger in 1948.* Experiments give $a_e = .0011597$. Apparently, the unambiguous value that we obtained for $F_2(0)$ is also, up to higher orders in α , unambiguously correct.

Precision Tests of QED

Building on the success of the order- α QED prediction for a_e , successive generations of physicists have improved the accuracy of both the theoretical and the experimental determination of this quantity. The coefficients of the QED formula for a_e are now known through order α^4 . The calculation of the order- α^2 and higher coefficients requires a systematic treatment of ultraviolet divergences.

These challenging theoretical calculations have been matched by increasingly imaginative experiments. The most recent measurement of a_e uses a technique, developed by Dehmelt and collaborators, in which individual electrons are trapped in a system of electrostatic and magnetostatic fields and

*J. Schwinger, *Phys. Rev.* **73**, 416L (1948).

excited to a spin resonance.[†] Today, the best theoretical and experimental values of a_e agree to eight significant figures.

High-order QED calculations have also been carried out for several other quantities. These include transition energies in hydrogen and hydrogen-like atoms, the anomalous magnetic moment of the muon, and the decay rates of singlet and triplet positronium. Many of these quantities have also been measured to high precision. The full set of these comparisons gives a detailed test of the validity of QED in a variety of settings. The results of these precision tests are summarized in Table 6.1.

There is some subtlety in reporting the results of precision comparisons between QED theory and experiment, since theoretical predictions require an extremely precise value of α , which can only be obtained from another precision QED experiment. We therefore quote each comparison between theory and experiment as an independent determination of α . Each value of α is assigned an error that is the composite of the expected uncertainties from theory and experiment. QED is confirmed to the extent that the values of α from different sources agree.

The first nine entries in Table 6.1 refer to QED calculations in atomic physics settings. Of these, the hydrogen hyperfine splitting, measured using Ramsey's hydrogen maser, is the most precisely known quantity in physics. Unfortunately, the influence of the internal structure of the proton leads to uncertainties that limit the accuracy with which this quantity can be predicted theoretically. The same difficulty applies to the Lamb shift, the splitting between the $j = 1/2$ $2S$ and $2P$ levels of hydrogen. The most accurate QED tests now come from systems that involve no strongly interacting particles, the electron $g-2$ and the hyperfine splitting in the $e^- \mu^+$ atom, muonium. The last entry in this group gives a new method for determining α , by converting a very accurate measurement of the neutron Compton wavelength, using accurately known mass ratios, to a value of the electron mass. This can be combined with the known value of the Rydberg energy and accurate QED formulae to determine α . The only serious discrepancy among these numbers comes in the triplet positronium decay rate; however, there is some evidence that diagrams of relative order α^2 give a large correction to the value quoted in the table.

The next two entries are determinations of α from higher-order QED reactions at high-energy electron colliders. These high-energy experiments typically achieve only percent-level accuracy, but their results are consistent with the precise information available at lower energies.

Finally, the last two entries in the table give two independent measurements of α from exotic quantum interference phenomena in condensed-matter systems. These two effects provide a standard resistance and a standard frequency, respectively, which are believed to measure the charge of the electron

[†]R. Van Dyck, Jr., P. Schwinberg, and H. Dehmelt, *Phys. Rev. Lett.* **59**, 26 (1987).

Table 6.1. Values of α^{-1} Obtained from Precision QED Experiments

Low-Energy QED:

Electron ($g - 2$)	137.035 992 35 (73)
Muon ($g - 2$)	137.035 5 (1 1)
Muonium hyperfine splitting	137.035 994 (18)
Lamb shift	137.036 8 (7)
Hydrogen hyperfine splitting	137.036 0 (3)
$2^3S_1 - 1^3S_1$ splitting in positronium	137.034 (16)
1S_0 positronium decay rate	137.00 (6)
3S_1 positronium decay rate	136.971 (6)
Neutron compton wavelength	137.036 010 1 (5 4)

High-Energy QED:

$\sigma(e^+e^- \rightarrow e^+e^-e^+e^-)$	136.5 (2.7)
$\sigma(e^+e^- \rightarrow e^+e^-\mu^+\mu^-)$	139.9 (1.2)

Condensed Matter:

Quantum Hall effect	137.035 997 9 (3 2)
AC Josephson effect	137.035 977 0 (7 7)

Each value of α displayed in this table is obtained by fitting an experimental measurement to a theoretical expression that contains α as a parameter. The numbers in parentheses are the standard errors in the last displayed digits, including both theoretical and experimental uncertainties. This table is based on results presented in the survey of precision QED of Kinoshita (1990). That book contains a series of lucid reviews of the remarkable theoretical and experimental technology that has been developed for the detailed analysis of QED processes. The five most accurate values are updated as given by T. Kinoshita in *History of Original Ideas and Basic Discoveries in Particle Physics*, H. Newman and T. Ypsilantis, eds. (Plenum Press, New York, 1995). This latter paper also gives an interesting perspective on the future of precision QED experiments.

with corrections that are strictly zero for macroscopic systems.[‡]

The entire picture fits together well beyond any reasonable expectation. On the evidence presented in this table, QED is the most stringently tested—and the most dramatically successful—of all physical theories.

[‡]For a discussion of these effects, and their exact relation to α , see D. R. Yennie, *Rev. Mod. Phys.* **59**, 781 (1987).

6.4 The Electron Vertex Function: Infrared Divergence

Now let us confront the infrared divergence in our result (6.56) for $F_1(q^2)$. The dominant part, in the $\mu \rightarrow 0$ limit, is

$$F_1(q^2) \approx \frac{\alpha}{2\pi} \int_0^1 dx dy dz \delta(x+y+z-1) \left[\frac{m^2(1-4z+z^2) + q^2(1-x)(1-y)}{m^2(1-z)^2 - q^2xy + \mu^2 z} - \frac{m^2(1-4z+z^2)}{m^2(1-z)^2 + \mu^2 z} \right]. \quad (6.60)$$

To understand this expression we must do some work to simplify it, extracting and evaluating the divergent part of the integral. Throughout this section we will retain only terms that diverge in the limit $\mu \rightarrow 0$.

First note that the divergence occurs in the corner of Feynman-parameter space where $z \approx 1$ (and therefore $x \approx y \approx 0$). In this region we can set $z = 1$ and $x = y = 0$ in the numerators of (6.60). We can also set $z = 1$ in the μ^2 terms in the denominators. Using the delta function to evaluate the x -integral, we then have

$$F_1(q^2) = \frac{\alpha}{2\pi} \int_0^1 dz \int_0^{1-z} dy \left[\frac{-2m^2 + q^2}{m^2(1-z)^2 - q^2y(1-z-y) + \mu^2} - \frac{-2m^2}{m^2(1-z)^2 + \mu^2} \right].$$

(The lower limit on the z -integral is unimportant.) Making the variable changes

$$y = (1-z)\xi, \quad w = (1-z),$$

this expression becomes

$$\begin{aligned} F_1(q^2) &= \frac{\alpha}{2\pi} \int_0^1 d\xi \frac{1}{2} \int_0^1 d(w^2) \left[\frac{-2m^2 + q^2}{[m^2 - q^2\xi(1-\xi)]w^2 + \mu^2} - \frac{-2m^2}{m^2w^2 + \mu^2} \right] \\ &= \frac{\alpha}{4\pi} \int_0^1 d\xi \left[\frac{-2m^2 + q^2}{m^2 - q^2\xi(1-\xi)} \log\left(\frac{m^2 - q^2\xi(1-\xi)}{\mu^2}\right) + 2\log\left(\frac{m^2}{\mu^2}\right) \right]. \end{aligned}$$

In the limit $\mu \rightarrow 0$ we can ignore the details of the numerators inside the logarithms; anything proportional to m^2 or q^2 is effectively the same. We therefore write

$$F_1(q^2) = 1 - \frac{\alpha}{2\pi} f_{\text{IR}}(q^2) \log\left(\frac{-q^2 \text{ or } m^2}{\mu^2}\right) + \mathcal{O}(\alpha^2), \quad (6.61)$$

where the coefficient of the divergent logarithm is

$$f_{\text{IR}}(q^2) = \int_0^1 \left(\frac{m^2 - q^2/2}{m^2 - q^2\xi(1-\xi)} \right) d\xi - 1. \quad (6.62)$$

Since q^2 is negative and $\xi(1-\xi)$ has a maximum value of $1/4$, the first term is greater than 1 and hence $f_{\text{IR}}(q^2)$ is positive.

How does this infinite term affect the cross section for electron scattering off a potential? Since $F_1(q^2)$ is just the quantity that multiplies γ^μ in the matrix element, we can find the new cross section by making the replacement $e \rightarrow e \cdot F_1(q^2)$. The cross section for the process $\mathbf{p} \rightarrow \mathbf{p}'$ is therefore

$$\frac{d\sigma}{d\Omega} \simeq \left(\frac{d\sigma}{d\Omega} \right)_0 \cdot \left[1 - \frac{\alpha}{\pi} f_{\text{IR}}(q^2) \log \left(\frac{-q^2 \text{ or } m^2}{\mu^2} \right) + \mathcal{O}(\alpha^2) \right], \quad (6.63)$$

where the first factor is the tree-level result. Note that the $\mathcal{O}(\alpha)$ correction to the cross section is not only infinite, but negative. Something is terribly wrong.

To gain a better understanding of the divergence, let us evaluate the coefficient of the divergent logarithm, $f_{\text{IR}}(q^2)$, in the limit $-q^2 \rightarrow \infty$. In this limit, we find a second logarithm:

$$\begin{aligned} \int_0^1 d\xi \frac{-q^2/2}{-q^2\xi(1-\xi) + m^2} &\simeq \frac{1}{2} \int_0^1 d\xi \frac{-q^2}{-q^2\xi + m^2} + \left(\begin{array}{c} \text{equal contribution} \\ \text{from } \xi \approx 1 \end{array} \right) \\ &= \log \left(\frac{-q^2}{m^2} \right). \end{aligned} \quad (6.64)$$

The form factor in this limit is therefore

$$F_1(-q^2 \rightarrow \infty) = 1 - \frac{\alpha}{2\pi} \log \left(\frac{-q^2}{m^2} \right) \log \left(\frac{-q^2}{\mu^2} \right) + \mathcal{O}(\alpha^2). \quad (6.65)$$

Note that the numerator in the second logarithm is $-q^2$, not m^2 ; this expression contains not only the correct coefficient of $\log(1/\mu^2)$, but also the correct coefficient of $\log^2(q^2)$.

The same double logarithm of $-q^2$ appeared in the cross section for soft bremsstrahlung, Eq. (6.26). This correspondence points to a resolution of the infrared divergence problem. Comparing (6.65) with (6.26), we find in the limit $-q^2 \rightarrow \infty$

$$\begin{aligned} \frac{d\sigma}{d\Omega}(p \rightarrow p') &= \left(\frac{d\sigma}{d\Omega} \right)_0 \left[1 - \frac{\alpha}{\pi} \log \left(\frac{-q^2}{m^2} \right) \log \left(\frac{-q^2}{\mu^2} \right) + \mathcal{O}(\alpha^2) \right]; \\ \frac{d\sigma}{d\Omega}(p \rightarrow p' + \gamma) &= \left(\frac{d\sigma}{d\Omega} \right)_0 \left[+ \frac{\alpha}{\pi} \log \left(\frac{-q^2}{m^2} \right) \log \left(\frac{-q^2}{\mu^2} \right) + \mathcal{O}(\alpha^2) \right]. \end{aligned} \quad (6.66)$$

The separate cross sections are divergent, but their sum is independent of μ and therefore finite.

In fact, neither the elastic cross section nor the soft bremsstrahlung cross section can be measured individually; only their sum is physically observable. In any real experiment, a photon detector can detect photons only down to

some minimum limiting energy E_ℓ . The probability that a scattering event occurs and this detector does not see a photon is the sum

$$\frac{d\sigma}{d\Omega}(p \rightarrow p') + \frac{d\sigma}{d\Omega}(p \rightarrow p' + \gamma(k < E_\ell)) \equiv \left(\frac{d\sigma}{d\Omega}\right)_{\text{measured}}. \quad (6.67)$$

The divergent part of this “measured” cross section is

$$\begin{aligned} \left(\frac{d\sigma}{d\Omega}\right)_{\text{measured}} &\approx \left(\frac{d\sigma}{d\Omega}\right)_0 \left[1 - \frac{\alpha}{\pi} f_{\text{IR}}(q^2) \log\left(\frac{-q^2 \text{ or } m^2}{\mu^2}\right) \right. \\ &\quad \left. + \frac{\alpha}{2\pi} \mathcal{I}(\mathbf{v}, \mathbf{v}') \log\left(\frac{E_\ell^2}{\mu^2}\right) + \mathcal{O}(\alpha^2) \right]. \end{aligned}$$

We have just seen that $\mathcal{I}(\mathbf{v}, \mathbf{v}') = 2f_{\text{IR}}(q^2)$ when $-q^2 \gg m^2$. If the same relation holds for general q^2 , the measured cross section becomes

$$\left(\frac{d\sigma}{d\Omega}\right)_{\text{measured}} \approx \left(\frac{d\sigma}{d\Omega}\right)_0 \left[1 - \frac{\alpha}{\pi} f_{\text{IR}}(q^2) \log\left(\frac{-q^2 \text{ or } m^2}{E_\ell^2}\right) + \mathcal{O}(\alpha^2) \right], \quad (6.68)$$

which depends on the experimental conditions, but no longer on μ^2 . The infrared divergences from soft bremsstrahlung and from $F_1(q^2)$ cancel each other, yielding a finite cross section for the quantity that can actually be measured.

We must still verify the identity $\mathcal{I}(\mathbf{v}, \mathbf{v}') = 2f_{\text{IR}}(q^2)$ for arbitrary values of q^2 . From (6.13) we have

$$\mathcal{I}(\mathbf{v}, \mathbf{v}') = \int \frac{d\Omega_{\mathbf{k}}}{4\pi} \left(\frac{2p \cdot p'}{(\hat{k} \cdot p')(\hat{k} \cdot p)} - \frac{m^2}{(\hat{k} \cdot p')^2} - \frac{m^2}{(\hat{k} \cdot p)^2} \right). \quad (6.69)$$

The last two terms are easy to evaluate:

$$\int \frac{d\Omega_{\mathbf{k}}}{4\pi} \frac{1}{(\hat{k} \cdot p)^2} = \frac{1}{2} \int_{-1}^1 d\cos\theta \frac{1}{(p^0 - p \cos\theta)^2} = \frac{1}{p^2} = \frac{1}{m^2}.$$

In the first term, we can combine the denominators with a Feynman parameter and perform the integral in the same way:

$$\begin{aligned} \int \frac{d\Omega_{\mathbf{k}}}{4\pi} \frac{1}{(\hat{k} \cdot p')(\hat{k} \cdot p)} &= \int_0^1 d\xi \int \frac{d\Omega_{\mathbf{k}}}{4\pi} \frac{1}{[\xi \hat{k} \cdot p' + (1-\xi) \hat{k} \cdot p]^2} \\ &= \int_0^1 d\xi \frac{1}{[\xi p' + (1-\xi)p]^2} = \int_0^1 d\xi \frac{1}{m^2 - \xi(1-\xi)q^2}. \end{aligned}$$

(In the last step we have used $2p \cdot p' = 2m^2 - q^2$.) Putting all the terms of (6.69) together, we find

$$\mathcal{I}(\mathbf{v}, \mathbf{v}') = \int_0^1 \left(\frac{2m^2 - q^2}{m^2 - \xi(1-\xi)q^2} \right) d\xi - 2 = 2f_{\text{IR}}(q^2), \quad (6.70)$$

just what we need to cancel the infrared divergence.

Although Eq. (6.68) demonstrates the cancellation of the infrared divergence, this result has little practical use. An experimentalist would want to know the precise dependence on q^2 , which we did not evaluate carefully. Recall from (6.65), however, that we were careful to obtain the correct coefficient of $\log^2(-q^2)$ in the limit $-q^2 \gg m^2$. In that limit, therefore, (6.68) becomes

$$\left(\frac{d\sigma}{d\Omega}\right)_{\text{measured}} \approx \left(\frac{d\sigma}{d\Omega}\right)_0 \left[1 - \frac{\alpha}{\pi} \log\left(\frac{-q^2}{m^2}\right) \log\left(\frac{-q^2}{E_\ell^2}\right) + \mathcal{O}(\alpha^2) \right]. \quad (6.71)$$

This result is unambiguous and useful. Note that the $\mathcal{O}(\alpha)$ correction again involves the Sudakov double logarithm.

6.5 Summation and Interpretation of Infrared Divergences

The discussion of infrared divergences in the previous section suffices for removing the infinities from our bremsstrahlung and vertex-correction calculations. There are still, however, three points that we have not addressed:

1. We have not demonstrated the cancellation of infrared divergences beyond the leading order.
2. The correction to the measured cross section that we found after the infrared cancellation (Eqs. (6.68) and (6.71)) can be made arbitrarily negative by making photon detectors with a sufficiently low threshold E_ℓ .
3. We have not yet reproduced the classical result (6.19) for the number of photons radiated during a collision.

The solutions of the second and third problems will follow immediately from that of the first, to which we now turn.

A complete treatment of infrared divergences to all orders is beyond the scope of this book.* We will discuss here only the terms with the largest logarithmic enhancement at each order of perturbation theory. In general, these terms are of order

$$\left[\frac{\alpha}{\pi} \log\left(\frac{-q^2}{\mu^2}\right) \log\left(\frac{-q^2}{m^2}\right) \right]^n \quad (6.72)$$

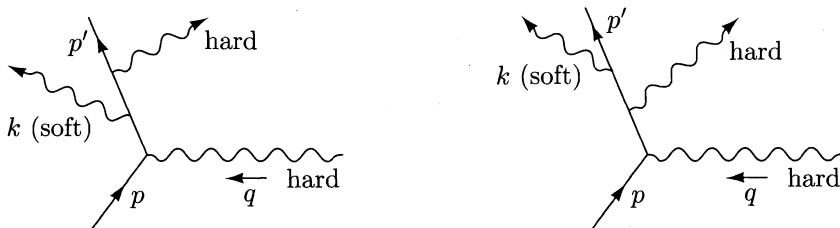
in the n th order of perturbation theory. Our final physical conclusions were first presented by Bloch and Nordsieck in a prescient paper written before the invention of relativistic perturbation theory.[†] We will follow a modern, and simplified, version of the analysis due to Weinberg.[‡]

*The definitive treatment is given in D. Yennie, S. Frautschi, and H. Suura, *Ann. Phys.* **13**, 379 (1961).

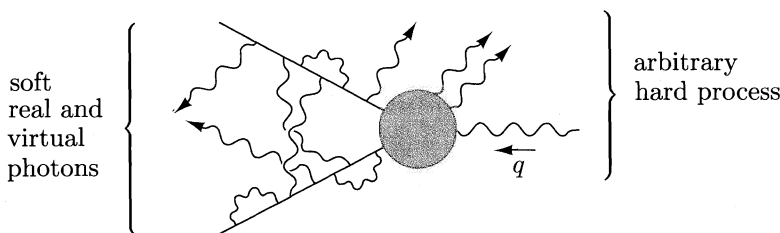
[†]F. Bloch and A. Nordsieck, *Phys. Rev.* **52**, 54 (1937).

[‡]S. Weinberg, *Phys. Rev.* **140**, B516 (1965).

Infrared divergences arise from photons with “soft” momenta: real photons with energy less than some cutoff E_ℓ , and virtual photons with (after Wick rotation) $k^2 < E_\ell^2$. A typical higher-order diagram will involve numerous real and virtual photons. But to find a divergence, we need more than a soft photon; we need a singular denominator in an electron propagator. Consider, for example, the following two diagrams:

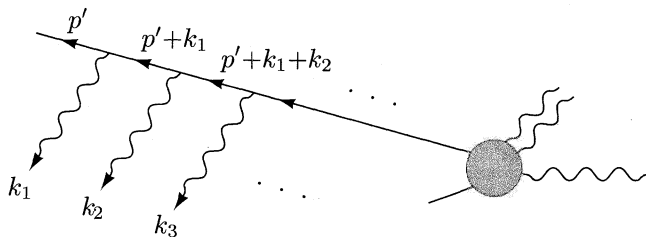


The first diagram, in which the electron emits a soft photon followed by a hard photon, has no infrared divergence, since the momenta in both electron propagators are far from the mass shell. If the soft photon is emitted last, however, the denominator of the adjacent propagator is $(p' + k)^2 - m^2 = 2p' \cdot k$, which vanishes as $k \rightarrow 0$. Thus the second diagram does contain a divergence. We would like, then, to consider diagrams in which an arbitrary hard process, possibly involving emission of hard and soft photons, is modified by the addition of soft real and virtual photons on the electron legs:



Following Weinberg, we will add up the contributions of all such diagrams. The only new difficulty in this calculation will be in the combinatorics of counting all the ways in which the photons can appear.

First consider the outgoing electron line:



We attach n photons to the line, with momenta $k_1 \dots k_n$. For the moment we do not care whether these are external photons, virtual photons connected to each other, or virtual photons connected to vertices on the incoming electron line. The Dirac structure of this diagram is

$$\bar{u}(p')(-ie\gamma^{\mu_1}) \frac{i(\not{p}' + \not{k}_1 + m)}{2p' \cdot k_1} (-ie\gamma^{\mu_2}) \frac{i(\not{p}' + \not{k}_1 + \not{k}_2 + m)}{2p' \cdot (k_1 + k_2) + \mathcal{O}(k^2)} \dots (-ie\gamma^{\mu_n}) \frac{i(\not{p}' + \not{k}_1 + \dots + \not{k}_n + m)}{2p' \cdot (k_1 + \dots + k_n) + \mathcal{O}(k^2)} (i\mathcal{M}_{\text{hard}}) \dots \quad (6.73)$$

We will assume that all the k_i are small, dropping the $\mathcal{O}(k^2)$ terms in the denominators. We will also drop the \not{k}_i terms in the numerators, just as in our treatment of bremsstrahlung in Section 6.1. Also, as we did there, we can push the factors of $(\not{p}' + m)$ to the left and use $\bar{u}(p')(-\not{p}' + m) = 0$:

$$\begin{aligned} \bar{u}(p') \gamma^{\mu_1} (\not{p}' + m) \gamma^{\mu_2} (\not{p}' + m) \dots &= \bar{u}(p') 2p'^{\mu_1} \gamma^{\mu_2} (\not{p}' + m) \dots \\ &= \bar{u}(p') 2p'^{\mu_1} 2p'^{\mu_2} \dots . \end{aligned}$$

This turns expression (6.73) into

$$\bar{u}(p') \left(e \frac{p'^{\mu_1}}{p' \cdot k_1} \right) \left(e \frac{p'^{\mu_2}}{p' \cdot (k_1 + k_2)} \right) \dots \left(e \frac{p'^{\mu_n}}{p' \cdot (k_1 + \dots + k_n)} \right) \dots \quad (6.74)$$

Still working with only the outgoing electron line, we must now sum over all possible orderings of the momenta $k_1 \dots k_n$. (This procedure will overcount when two of the photons are attached together to form a single virtual photon. We will deal with this overcounting later.) There are $n!$ different diagrams to sum, corresponding to the $n!$ permutations of the n photon momenta. Let π denote one such permutation, so that $\pi(i)$ is the number between 1 and n that i is taken to. (For example, if π denotes the permutation that takes $1 \rightarrow 3$, $2 \rightarrow 1$ and $3 \rightarrow 2$, then $\pi(1) = 3$, $\pi(2) = 1$, and $\pi(3) = 2$.)

Armed with this notation, we can perform the sum over permutations by means of the following identity:

$$\begin{aligned} \sum_{\text{all permutations } \pi} \frac{1}{p \cdot k_{\pi(1)}} \frac{1}{p \cdot (k_{\pi(1)} + k_{\pi(2)})} \dots \frac{1}{p \cdot (k_{\pi(1)} + k_{\pi(2)} + \dots + k_{\pi(n)})} \\ = \frac{1}{p \cdot k_1} \frac{1}{p \cdot k_2} \dots \frac{1}{p \cdot k_n}. \end{aligned} \quad (6.75)$$

The proof of this formula proceeds by induction on n . For $n = 2$ we have

$$\begin{aligned} \sum_{\pi} \frac{1}{p \cdot k_{\pi(1)}} \frac{1}{p \cdot (k_{\pi(1)} + k_{\pi(2)})} &= \frac{1}{p \cdot k_1} \frac{1}{p \cdot (k_1 + k_2)} + \frac{1}{p \cdot k_2} \frac{1}{p \cdot (k_2 + k_1)} \\ &= \frac{1}{p \cdot k_1} \frac{1}{p \cdot k_2}. \end{aligned}$$

For the induction step, notice that the last factor on the left-hand side of (6.75) is the same for every permutation π . Pulling this factor outside the sum, the left-hand side becomes

$$\text{LHS} = \frac{1}{p \cdot \sum k} \sum_{\pi} \frac{1}{p \cdot k_{\pi(1)}} \frac{1}{p \cdot (k_{\pi(1)} + k_{\pi(2)})} \cdots \frac{1}{p \cdot (k_{\pi(1)} + \cdots + k_{\pi(n-1)})}.$$

For any given π , the quantity being summed is independent of $k_{\pi(n)}$. Letting $i = \pi(n)$, we can now write

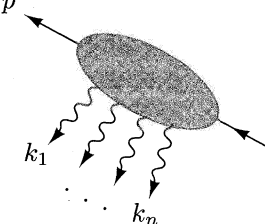
$$\sum_{\pi} = \sum_{i=1}^n \sum_{\pi'(i)},$$

where $\pi'(i)$ is the set of all permutations on the remaining $n - 1$ integers. Assuming by induction that (6.75) is true for $n - 1$, we have

$$\text{LHS} = \frac{1}{p \cdot \sum k} \sum_{i=1}^n \frac{1}{p \cdot k_1} \frac{1}{p \cdot k_2} \cdots \frac{1}{p \cdot k_{i-1}} \frac{1}{p \cdot k_{i+1}} \cdots \frac{1}{p \cdot k_n}.$$

If we now multiply and divide each term in this sum by $p \cdot k_i$, we easily obtain our desired result (6.75).

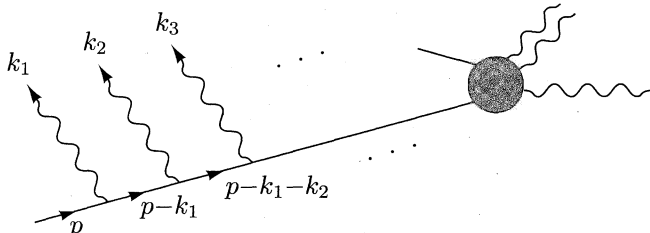
Applying (6.75) to (6.74), we find



$$= \bar{u}(\mathbf{p}') \left(e \frac{p'^{\mu_1}}{p' \cdot k_1} \right) \left(e \frac{p'^{\mu_2}}{p' \cdot k_2} \right) \cdots \left(e \frac{p'^{\mu_n}}{p' \cdot k_n} \right), \quad (6.76)$$

where the blob denotes a sum over all possible orders of inserting the n photon lines.

A similar set of manipulations simplifies the sum over soft photon insertions on the initial electron line. There, however, the propagator momenta are $p - k_1$, $p - k_1 - k_2$, and so on:



We therefore get an extra minus sign in the factor for each photon, since $(p - \sum k)^2 - m^2 \approx -2p \cdot \sum k$.

Now consider diagrams containing a total of n soft photons, connected in any possible order to the initial or final electron lines. The sum over all such diagrams can be written

$$\begin{aligned} & \text{Diagram: } \text{soft} \underbrace{\text{hard}}_{\text{soft}} \text{ hard} = \bar{u}(p') i\mathcal{M}_{\text{hard}} u(p) \\ & \quad \cdot e\left(\frac{p'^{\mu_1}}{p' \cdot k_1} - \frac{p^{\mu_1}}{p \cdot k_1}\right) \cdot e\left(\frac{p'^{\mu_2}}{p' \cdot k_2} - \frac{p^{\mu_2}}{p \cdot k_2}\right) \\ & \quad \cdots e\left(\frac{p'^{\mu_n}}{p' \cdot k_n} - \frac{p^{\mu_n}}{p \cdot k_n}\right). \end{aligned} \quad (6.77)$$

By multiplying out all the factors, you can see that we get the correct term for each possible way of dividing the n photons between the two lines.

Next we must decide which photons are real and which are virtual.

We can make a virtual photon by picking two photon momenta k_i and k_j , setting $k_j = -k_i \equiv k$, multiplying by the photon propagator, and integrating over k . For each virtual photon we then obtain the expression

$$\frac{e^2}{2} \int \frac{d^4 k}{(2\pi)^4} \frac{-i}{k^2 + i\epsilon} \left(\frac{p'}{p' \cdot k} - \frac{p}{p \cdot k} \right) \cdot \left(\frac{p'}{-p' \cdot k} - \frac{p}{-p \cdot k} \right) \equiv \mathbf{X}. \quad (6.78)$$

The factor of $1/2$ is required because our procedure has counted each Feynman diagram twice: interchanging k_i and k_j gives back the same diagram. It is possible to evaluate this expression by careful contour integration, but there is an easier way. Notice that this approximation scheme assigns to the diagram with one loop and no external photons the value

$$\bar{u}(p') (i\mathcal{M}_{\text{hard}}) u(p) \cdot \mathbf{X}.$$

Thus, \mathbf{X} must be precisely the infrared limit of the one-loop correction to the form factor, as displayed in (6.61):

$$\mathbf{X} = -\frac{\alpha}{2\pi} f_{\text{IR}}(q^2) \log\left(\frac{-q^2}{\mu^2}\right). \quad (6.79)$$

A direct derivation of this result from (6.78) is given in Weinberg's paper cited above. Note that result (6.79) followed in our argument of the previous section only after the subtraction at $q^2 = 0$, and so we should worry whether (6.79) is consistent with the corresponding subtraction of the n th-order diagram. In addition, some of the diagrams we are summing contain external-leg corrections, which we have not discussed. Here we simply remark that neither of these subtleties affects the final answer; the proof requires the heavy machinery in the paper of Yennie, Frautschi, and Suura.

If there are m virtual photons we get m factors like (6.79), and also an additional symmetry factor of $1/m!$ since interchanging virtual photons with each other does not change the diagram. We can then sum over m to obtain

the complete correction due to the presence of arbitrarily many soft virtual photons:

$$\text{Feynman diagram: } \text{virtual photon} + \text{hard loop} + \text{sequence of virtual photons} = \text{real photon} \times \sum_{m=0}^{\infty} \frac{\mathbf{X}^m}{m!} = \bar{u}(p') (i\mathcal{M}_{\text{hard}}) u(p) \exp(\mathbf{X}). \quad (6.80)$$

If in addition to the m virtual photons we also emit a real photon, we must multiply by its polarization vector, sum over polarizations, and integrate the squared matrix element over the photon's phase space. This gives an additional factor

$$\int \frac{d^3 k}{(2\pi)^3} \frac{1}{2k} e^2 (-g_{\mu\nu}) \left(\frac{p'^\mu}{p' \cdot k} - \frac{p^\mu}{p \cdot k} \right) \left(\frac{p'^\nu}{p' \cdot k} - \frac{p^\nu}{p \cdot k} \right) \equiv \mathbf{Y} \quad (6.81)$$

in the cross section. Assuming that the energy of the photon is greater than μ and less than E_ℓ (the detector threshold), this expression is simply

$$\mathbf{Y} = \frac{\alpha}{\pi} \mathcal{I}(\mathbf{v}, \mathbf{v}') \log\left(\frac{E_\ell}{\mu}\right) = \frac{\alpha}{\pi} f_{\text{IR}}(q^2) \log\left(\frac{E_\ell^2}{\mu^2}\right). \quad (6.82)$$

If n real photons are emitted we get n such factors, and also a symmetry factor of $1/n!$ since there are n identical bosons in the final state. The cross section for emission of any number of soft photons is therefore

$$\sum_{n=0}^{\infty} \frac{d\sigma}{d\Omega}(\mathbf{p} \rightarrow \mathbf{p}' + n\gamma) = \frac{d\sigma}{d\Omega}(\mathbf{p} \rightarrow \mathbf{p}') \cdot \sum_{n=0}^{\infty} \frac{1}{n!} \mathbf{Y}^n = \frac{d\sigma}{d\Omega}(\mathbf{p} \rightarrow \mathbf{p}') \cdot \exp(\mathbf{Y}). \quad (6.83)$$

Combining our results for virtual and real photons gives our final result for the measured cross section, to all orders in α , for the process $\mathbf{p} \rightarrow \mathbf{p}' +$ (any number of photons with $k < E_\ell$):

$$\begin{aligned} \left(\frac{d\sigma}{d\Omega} \right)_{\text{meas.}} &= \left(\frac{d\sigma}{d\Omega} \right)_0 \times \exp(2\mathbf{X}) \times \exp(\mathbf{Y}) \\ &= \left(\frac{d\sigma}{d\Omega} \right)_0 \times \exp\left[-\frac{\alpha}{\pi} f_{\text{IR}}(q^2) \log\left(\frac{-q^2}{\mu^2}\right)\right] \times \exp\left[\frac{\alpha}{\pi} f_{\text{IR}}(q^2) \log\left(\frac{E_\ell^2}{\mu^2}\right)\right] \\ &= \left(\frac{d\sigma}{d\Omega} \right)_0 \times \exp\left[-\frac{\alpha}{\pi} f_{\text{IR}}(q^2) \log\left(\frac{-q^2}{E_\ell^2}\right)\right]. \end{aligned} \quad (6.84)$$

The correction factor depends on the detector sensitivity E_ℓ , but is independent of the infrared cutoff μ . Note that if we expand this result to $\mathcal{O}(\alpha)$, we recover our earlier result (6.68). Now, however, the correction factor is controlled in magnitude—always between 0 and 1.

In the limit $-q^2 \gg m^2$, our result becomes

$$\left(\frac{d\sigma}{d\Omega} \right)_{\text{meas.}} = \left(\frac{d\sigma}{d\Omega} \right)_0 \times \left| \exp\left[-\frac{\alpha}{2\pi} \log\left(\frac{-q^2}{m^2}\right) \log\left(\frac{-q^2}{E_\ell^2}\right)\right] \right|^2. \quad (6.85)$$

In this limit, the probability of scattering without emitting a hard photon decreases faster than any power of q^2 . The exponential correction factor, containing the Sudakov double logarithm, is known as the *Sudakov form factor*.

To conclude this section, let us calculate the probability, in the same approximation, that some hard scattering process is accompanied by the production of n soft photons, all with energies between E_- and E_+ . The phase-space integral for these photons gives $\log(E_+/E_-)$ instead of $\log(E_\ell/\mu)$. If we assign photons with energy greater than E_+ to the “hard” part of the process, we find that the cross section is given by (6.84), times the additional factor

$$\begin{aligned} \text{Prob}(n\gamma \text{ with } E_- < E < E_+) = & \frac{1}{n!} \left[\frac{\alpha}{\pi} f_{\text{IR}}(q^2) \log\left(\frac{E_+^2}{E_-^2}\right) \right]^n \\ & \times \exp\left[-\frac{\alpha}{\pi} f_{\text{IR}}(q^2) \log\left(\frac{E_+^2}{E_-^2}\right)\right]. \end{aligned} \quad (6.86)$$

This expression has the form of a Poisson distribution,

$$P(n) = \frac{1}{n!} \lambda^n e^{-\lambda},$$

with

$$\lambda = \langle n \rangle = \frac{\alpha}{\pi} \log\left(\frac{E_+}{E_-}\right) \mathcal{I}(\mathbf{v}, \mathbf{v}').$$

This is precisely the semiclassical estimate of the number of radiated photons that we made in Eq. (6.19).

Problems

6.1 Rosenbluth formula. As discussed Section 6.2, the exact electromagnetic interaction vertex for a Dirac fermion can be written quite generally in terms of two form factors $F_1(q^2)$ and $F_2(q^2)$:

$$= \bar{u}(p') \left[\gamma^\mu F_1(q^2) + \frac{i\sigma^{\mu\nu} q_\nu}{2m} F_2(q^2) \right] u(p),$$

where $q = p' - p$ and $\sigma^{\mu\nu} = \frac{1}{2}i[\gamma^\mu, \gamma^\nu]$. If the fermion is a strongly interacting particle such as the proton, the form factors reflect the structure that results from the strong interactions and so are not easy to compute from first principles. However, these form factors can be determined experimentally. Consider the scattering of an electron with energy $E \gg m_e$ from a proton initially at rest. Show that the above expression for the vertex leads to the following expression (the Rosenbluth formula) for the elastic scattering cross section, computed to leading order in α but to all orders in the strong interactions:

$$\frac{d\sigma}{d \cos \theta} = \frac{\pi \alpha^2 \left[(F_1^2 - \frac{q^2}{4m^2} F_2^2) \cos^2 \frac{\theta}{2} - \frac{q^2}{2m^2} (F_1 + F_2)^2 \sin^2 \frac{\theta}{2} \right]}{2E^2 \left[1 + \frac{2E}{m} \sin^2 \frac{\theta}{2} \right] \sin^4 \frac{\theta}{2}},$$

where θ is the lab-frame scattering angle and F_1 and F_2 are to be evaluated at the q^2 associated with elastic scattering at this angle. By measuring $(d\sigma/d\cos\theta)$ as a function of angle, it is thus possible to extract F_1 and F_2 . Note that when $F_1 = 1$ and $F_2 = 0$, the Rosenbluth formula reduces to the Mott formula (in the massless limit) for scattering off a point particle (see Problem 5.1).

6.2 Equivalent photon approximation. Consider the process in which electrons of very high energy scatter from a target. In leading order in α , the electron is connected to the target by one photon propagator. If the initial and final energies of the electron are E and E' , the photon will carry momentum q such that $q^2 \approx -2EE'(1 - \cos\theta)$. In the limit of forward scattering, whatever the energy loss, the photon momentum approaches $q^2 = 0$; thus the reaction is highly peaked in the forward direction. It is tempting to guess that, in this limit, the virtual photon becomes a real photon. Let us investigate in what sense that is true.

(a) The matrix element for the scattering process can be written as

$$\mathcal{M} = (-ie)\bar{u}(p')\gamma^\mu u(p) \frac{-ig_{\mu\nu}}{q^2} \hat{\mathcal{M}}^\nu(q),$$

where $\hat{\mathcal{M}}^\nu$ represents the (in general, complicated) coupling of the virtual photon to the target. Let us analyze the structure of the piece $\bar{u}(p')\gamma^\mu u(p)$. Let $q = (q^0, \mathbf{q})$, and define $\tilde{q} = (q^0, -\mathbf{q})$. We can expand the spinor product as:

$$\bar{u}(p')\gamma^\mu u(p) = A \cdot q^\mu + B \cdot \tilde{q}^\mu + C \cdot \epsilon_1^\mu + D \cdot \epsilon_2^\mu,$$

where A, B, C, D are functions of the scattering angle and energy loss and ϵ_i are two unit vectors transverse to \mathbf{q} . By dotting this expression with q_μ , show that the coefficient B is at most of order θ^2 . This will mean that we can ignore it in the rest of the analysis. The coefficient A is large, but it is also irrelevant, since, by the Ward identity, $q^\mu \hat{\mathcal{M}}_\mu = 0$.

(b) Working in the frame where $p = (E, 0, 0, E)$, compute explicitly

$$\bar{u}(p')\gamma \cdot \epsilon_i u(p)$$

using massless electrons, $u(p)$ and $u(p')$ spinors of definite helicity, and ϵ_1, ϵ_2 unit vectors parallel and perpendicular to the plane of scattering. We need this quantity only for scattering near the forward direction, and we need only the term of order θ . Note, however, that for ϵ in the plane of scattering, the small \hat{z} component of ϵ also gives a term of order θ which must be taken into account.

- (c) Now write the expression for the electron scattering cross section, in terms of $|\hat{\mathcal{M}}^\mu|^2$ and the integral over phase space on the target side. This expression must be integrated over the final electron momentum p' . The integral over p'^3 is an integral over the energy loss of the electron. Show that the integral over p'_\perp diverges logarithmically as p'_\perp or $\theta \rightarrow 0$.
- (d) The divergence as $\theta \rightarrow 0$ appears because we have ignored the electron mass in too many places. Show that reintroducing the electron mass in the expression for q^2 ,

$$q^2 = -2(EE' - pp' \cos\theta) + 2m^2,$$

cuts off the divergence and yields a factor of $\log(s/m^2)$ in its place.

- (e) Assembling all the factors, and assuming that the target cross sections are independent of the photon polarization, show that the largest part of the electron-target scattering cross section is given by considering the electron to be the source of a beam of real photons with energy distribution ($x = E_\gamma/E$):

$$N_\gamma(x)dx = \frac{dx}{x} \frac{\alpha}{2\pi} [1 + (1-x)^2] \log\left(\frac{s}{m^2}\right).$$

This is the Weizsäcker-Williams *equivalent photon approximation*. This phenomenon allows us, for example, to study photon-photon scattering using e^+e^- collisions. Notice that the distribution we have found here is the same one that appeared in Problem 5.5 when we considered soft photon emission before electron scattering. It should be clear that a parallel general derivation can be constructed for that case.

6.3 Exotic contributions to $g - 2$. Any particle that couples to the electron can produce a correction to the electron-photon form factors and, in particular, a correction to $g - 2$. Because the electron $g - 2$ agrees with QED to high accuracy, these corrections allow us to constrain the properties of hypothetical new particles.

- (a) The unified theory of weak and electromagnetic interactions contains a scalar particle h called the *Higgs boson*, which couples to the electron according to

$$H_{\text{int}} = \int d^3x \frac{\lambda}{\sqrt{2}} h \bar{\psi} \psi.$$

Compute the contribution of a virtual Higgs boson to the electron ($g - 2$), in terms of λ and the mass m_h of the Higgs boson.

- (b) QED accounts extremely well for the electron's anomalous magnetic moment. If $a = (g - 2)/2$,

$$|a_{\text{expt.}} - a_{\text{QED}}| < 1 \times 10^{-10}.$$

What limits does this place on λ and m_h ? In the simplest version of the electroweak theory, $\lambda = 3 \times 10^{-6}$ and $m_h > 60$ GeV. Show that these values are not excluded. The coupling of the Higgs boson to the muon is larger by a factor (m_μ/m_e): $\lambda = 6 \times 10^{-4}$. Thus, although our experimental knowledge of the muon anomalous magnetic moment is not as precise,

$$|a_{\text{expt.}} - a_{\text{QED}}| < 3 \times 10^{-8},$$

one can still obtain a stronger limit on m_h . Is it strong enough?

- (c) Some more complex versions of this theory contain a pseudoscalar particle called the *axion*, which couples to the electron according to

$$H_{\text{int}} = \int d^3x \frac{i\lambda}{\sqrt{2}} a \bar{\psi} \gamma^5 \psi.$$

The axion may be as light as the electron, or lighter, and may couple more strongly than the Higgs boson. Compute the contribution of a virtual axion to the $g - 2$ of the electron, and work out the excluded values of λ and m_a .

Radiative Corrections: Some Formal Developments

We cheated four times in the last three chapters,* stating (and sometimes motivating) a result but postponing its proof. Those results were:

1. The formula for decay rates in terms of S -matrix elements, Eq. (4.86).
2. The master formula for S -matrix elements in terms of Feynman diagrams, Eq. (4.103).
3. The Ward identity, Eq. (5.79).
4. The *ad hoc* subtraction to remove the ultraviolet divergence in the vertex-correction diagram, Eq. (6.55).

It is time now to return to these issues and give them a proper treatment. In Sections 7.2 through 7.4 we will derive all four of these results. The knowledge we gain along the way will help us interpret the three remaining loop corrections for electron scattering from a heavy target shown in (6.1): the external leg corrections and the vacuum polarization. We will evaluate the former in Section 7.1 and the latter in Section 7.5.

This chapter will be more abstract than the two preceding ones. Its main theme will be the singularities of Feynman diagrams viewed as analytic functions of their external momenta. We will find, however, that this apparently esoteric subject is rich in physical implications, and that it illuminates the relation between Feynman diagrams and the general principles of quantum theory.

7.1 Field-Strength Renormalization

In this section we will investigate the analytic structure of the two-point correlation function,

$$\langle \Omega | T\phi(x)\phi(y) | \Omega \rangle \quad \text{or} \quad \langle \Omega | T\psi(x)\bar{\psi}(y) | \Omega \rangle .$$

In a free field theory, the two-point function $\langle 0 | T\phi(x)\phi(y) | 0 \rangle$ has a simple interpretation: It is the amplitude for a particle to propagate from y to x . To what extent does this interpretation carry over into an interacting theory?

*A fifth cheat, postulating rather than deriving the photon propagator, will be remedied in Chapter 9.

Our analysis of the two-point function will rely only on general principles of relativity and quantum mechanics; it will not depend on the nature of the interactions or on an expansion in perturbation theory. We will, however, restrict our consideration to scalar fields. Similar results can be obtained for correlation functions of fields with spin; we will display the analogous result for Dirac fields at the end of the analysis.

To dissect the two-point function $\langle \Omega | T\phi(x)\phi(y) | \Omega \rangle$ we will insert the identity operator, in the form of a sum over a complete set of states, between $\phi(x)$ and $\phi(y)$. We choose these states to be eigenstates of the full interacting Hamiltonian, H . Since the momentum operator \mathbf{P} commutes with H , we can also choose the states to be eigenstates of \mathbf{P} . But we can also make a stronger use of Lorentz invariance. Let $|\lambda_0\rangle$ be an eigenstate of H with momentum zero: $\mathbf{P}|\lambda_0\rangle = 0$. Then all the boosts of $|\lambda_0\rangle$ are also eigenstates of H , and these have all possible 3-momenta. Conversely, any eigenstate of H with definite momentum can be written as the boost of some zero-momentum eigenstate $|\lambda_0\rangle$. The eigenvalues of the 4-momentum operator $P^\mu = (H, \mathbf{P})$ organize themselves into hyperboloids, as shown in Fig. 7.1.

Recall from Chapter 2 that the completeness relation for the one-particle states is

$$(1)_{\text{1-particle}} = \int \frac{d^3 p}{(2\pi)^3} \frac{1}{2E_p} |\mathbf{p}\rangle \langle \mathbf{p}|. \quad (7.1)$$

We can write an analogous completeness relation for the entire Hilbert space with the aid of a bit of notation. Let $|\lambda_{\mathbf{p}}\rangle$ be the boost of $|\lambda_0\rangle$ with momentum \mathbf{p} , and assume that the states $|\lambda_{\mathbf{p}}\rangle$, like the one-particle states $|\mathbf{p}\rangle$, are relativistically normalized. Let $E_{\mathbf{p}}(\lambda) \equiv \sqrt{|\mathbf{p}|^2 + m_\lambda^2}$, where m_λ is the “mass” of the states $|\lambda_{\mathbf{p}}\rangle$, that is, the energy of the state $|\lambda_0\rangle$. Then the desired completeness relation is

$$\mathbf{1} = |\Omega\rangle \langle \Omega| + \sum_{\lambda} \int \frac{d^3 p}{(2\pi)^3} \frac{1}{2E_{\mathbf{p}}(\lambda)} |\lambda_{\mathbf{p}}\rangle \langle \lambda_{\mathbf{p}}|, \quad (7.2)$$

where the sum runs over all zero-momentum states $|\lambda_0\rangle$.

We now insert this expansion between the operators in the two-point function. Assume for now that $x^0 > y^0$. Let us drop the uninteresting constant term $\langle \Omega | \phi(x) | \Omega \rangle \langle \Omega | \phi(y) | \Omega \rangle$. (This term is usually zero by symmetry; for higher-spin fields, it is zero by Lorentz invariance.) The two-point function is then

$$\langle \Omega | \phi(x)\phi(y) | \Omega \rangle = \sum_{\lambda} \int \frac{d^3 p}{(2\pi)^3} \frac{1}{2E_{\mathbf{p}}(\lambda)} \langle \Omega | \phi(x) | \lambda_{\mathbf{p}} \rangle \langle \lambda_{\mathbf{p}} | \phi(y) | \Omega \rangle. \quad (7.3)$$

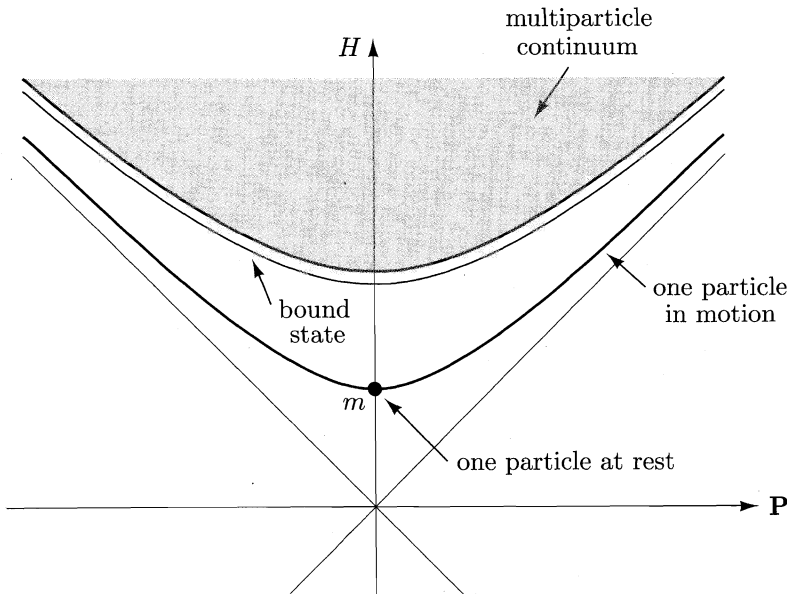


Figure 7.1. The eigenvalues of the 4-momentum operator $P^\mu = (H, \mathbf{P})$ occupy a set of hyperboloids in energy-momentum space. For a typical theory the states consist of one or more particles of mass m . Thus there is a hyperboloid of one-particle states and a continuum of hyperboloids of two-particle states, three-particle states, and so on. There may also be one or more bound-state hyperboloids below the threshold for creation of two free particles.

We can manipulate the matrix elements as follows:

$$\begin{aligned} \langle \Omega | \phi(x) | \lambda_{\mathbf{p}} \rangle &= \langle \Omega | e^{iP \cdot x} \phi(0) e^{-iP \cdot x} | \lambda_{\mathbf{p}} \rangle \\ &= \langle \Omega | \phi(0) | \lambda_{\mathbf{p}} \rangle e^{-ip \cdot x} \Big|_{p^0 = E_{\mathbf{p}}} \\ &= \langle \Omega | \phi(0) | \lambda_0 \rangle e^{-ip \cdot x} \Big|_{p^0 = E_{\mathbf{p}}}. \end{aligned} \quad (7.4)$$

The last equality is a result of the Lorentz invariance of $\langle \Omega |$ and $\phi(0)$: Insert factors of $U^{-1}U$, where U is the unitary operator that implements a Lorentz boost from \mathbf{p} to 0, and use $U\phi(0)U^{-1} = \phi(0)$. (For a field with spin, we would need to keep track of its nontrivial Lorentz transformation.) Introducing an integration over p^0 , our expression for the two-point function (still for $x^0 > y^0$) becomes

$$\langle \Omega | \phi(x) \phi(y) | \Omega \rangle = \sum_{\lambda} \int \frac{d^4 p}{(2\pi)^4} \frac{i}{p^2 - m_{\lambda}^2 + i\epsilon} e^{-ip \cdot (x-y)} |\langle \Omega | \phi(0) | \lambda_0 \rangle|^2. \quad (7.5)$$

Note the appearance of the Feynman propagator, $D_F(x - y)$, but with m replaced by m_{λ} .

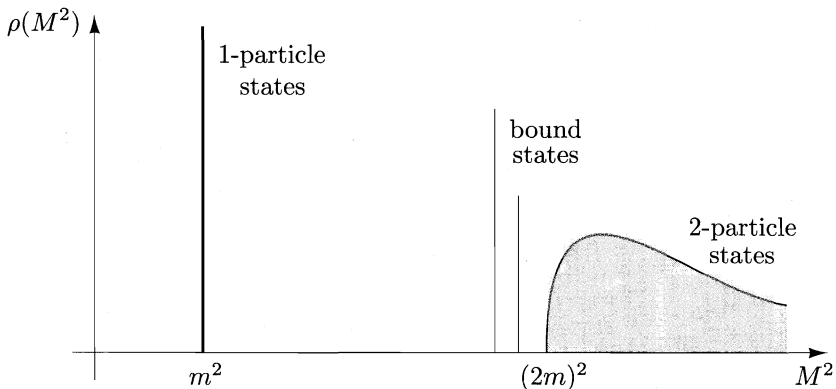


Figure 7.2. The spectral function $\rho(M^2)$ for a typical interacting field theory. The one-particle states contribute a delta function at m^2 (the square of the particle's mass). Multiparticle states have a continuous spectrum beginning at $(2m)^2$. There may also be bound states.

Analogous expressions hold for the case $y^0 > x^0$. Both cases can be summarized in the following general representation of the two-point function (the Källén-Lehmann *spectral representation*):

$$\langle \Omega | T\phi(x)\phi(y) | \Omega \rangle = \int_0^\infty \frac{dM^2}{2\pi} \rho(M^2) D_F(x-y; M^2), \quad (7.6)$$

where $\rho(M^2)$ is a positive *spectral density* function,

$$\rho(M^2) = \sum_\lambda (2\pi) \delta(M^2 - m_\lambda^2) |\langle \Omega | \phi(0) | \lambda_0 \rangle|^2. \quad (7.7)$$

The spectral density $\rho(M^2)$ for a typical theory is plotted in Fig. 7.2. Note that the one-particle states contribute an isolated delta function to the spectral density:

$$\rho(M^2) = 2\pi \delta(M^2 - m^2) \cdot Z + (\text{nothing else until } M^2 \gtrsim (2m)^2), \quad (7.8)$$

where Z is some number given by the squared matrix element in (7.7). We refer to Z as the *field-strength renormalization*. The quantity m is the exact mass of a single particle—the exact energy eigenvalue at rest. This quantity will in general differ from the value of the mass parameter that appears in the Lagrangian. We will refer to the parameter in the Lagrangian as m_0 , the *bare* mass, and refer to m as the *physical* mass of the ϕ boson. Only the physical mass m is directly observable.

The spectral decomposition (7.6) yields the following form for the Fourier

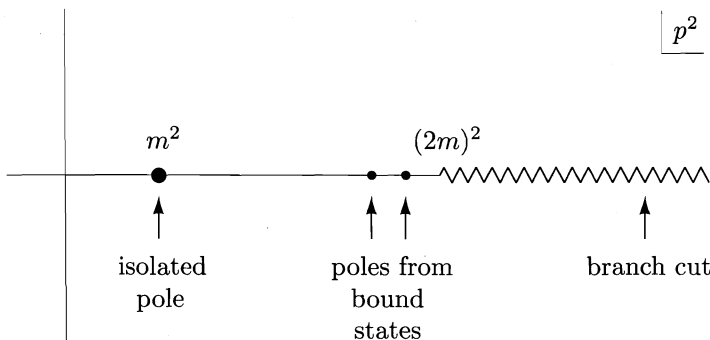


Figure 7.3. Analytic structure in the complex p^2 -plane of the Fourier transform of the two-point function for a typical theory. The one-particle states contribute an isolated pole at the square of the particle mass. States of two or more free particles give a branch cut, while bound states give additional poles.

transform of the two-point function:

$$\begin{aligned} \int d^4x e^{ip \cdot x} \langle \Omega | T\phi(x)\phi(0) | \Omega \rangle &= \int_0^\infty \frac{dM^2}{2\pi} \rho(M^2) \frac{i}{p^2 - M^2 + i\epsilon} \\ &= \frac{iZ}{p^2 - m^2 + i\epsilon} + \int_{\sim 4m^2}^\infty \frac{dM^2}{2\pi} \rho(M^2) \frac{i}{p^2 - M^2 + i\epsilon}. \end{aligned} \quad (7.9)$$

The analytic structure of this function in the complex p^2 -plane is shown in Fig. 7.3. The first term gives an isolated simple pole at $p^2 = m^2$, while the second term contributes a branch cut beginning at $p^2 = (2m)^2$. If there are any two-particle bound states, these will appear as additional delta functions in $\rho(M^2)$ and thus as additional poles below the cut.

In Section 2.4, we found an explicit result for the two-point correlation function in the theory of a free scalar field:

$$\int d^4x e^{ip \cdot x} \langle 0 | T\phi(x)\phi(0) | 0 \rangle = \frac{i}{p^2 - m^2 + i\epsilon}. \quad (7.10)$$

We interpreted this formula, for $x^0 > 0$, as the amplitude for a particle to propagate from 0 to x . Equation (7.9) shows that the two-point function takes a similar form in the most general theory of an interacting scalar field. The general expression is essentially a sum of scalar propagation amplitudes for states created from the vacuum by the field operator $\phi(0)$. There are two differences between (7.9) and (7.10). First, Eq. (7.9) contains the field-strength renormalization factor $Z = |\langle \lambda_0 | \phi(0) | \Omega \rangle|^2$, the probability for $\phi(0)$ to create a given state from the vacuum. In (7.10), this factor is included implicitly, since $\langle p | \phi(0) | 0 \rangle = 1$ in free field theory. Second, Eq. (7.9) contains

contributions from multiparticle intermediate states with a continuous mass spectrum. In free field theory, $\phi(0)$ can create only a single particle from the vacuum. With these two differences, (7.9) is a direct generalization of (7.10).

It will be important in our later analysis that the contributions to (7.9) from one-particle and multiparticle intermediate states can be distinguished by the strength of their analytic singularities. The poles in p^2 come only from one-particle intermediate states, while multiparticle intermediate states give weaker branch cut singularities. We will see in the next section that this rather formal observation generalizes to higher-point correlation functions and plays a crucial role in our derivation of the diagrammatic formula for S -matrix elements.

The analysis of this section generalizes directly to two-point functions of higher-spin fields. The main complication comes in the generalization of the manipulation (7.4), since now the field has a nontrivial transformation law under boosts. In general, several invariant spectral functions are required to represent the multiparticle states. But this complication does not affect the major result that a pole in p^2 can arise only from the contribution of a single-particle state created by the field operator. The two-point function of Dirac fields, for example, has the structure

$$\begin{aligned} \int d^4x e^{ip\cdot x} \langle \Omega | T\psi(x)\bar{\psi}(0) | \Omega \rangle &= \frac{iZ_2 \sum_s u^s(p)\bar{u}^s(p)}{p^2 - m^2 + i\epsilon} + \dots \\ &= \frac{iZ_2(\not{p} + m)}{p^2 - m^2 + i\epsilon} + \dots, \end{aligned} \quad (7.11)$$

where the omitted terms give the multiparticle branch cut. As in the scalar case, the constant Z_2 is the probability for the quantum field to create or annihilate an exact one-particle eigenstate of H :

$$\langle \Omega | \psi(0) | p, s \rangle = \sqrt{Z_2} u^s(p). \quad (7.12)$$

(For an antiparticle, replace u with \bar{v} .) At the pole, the Dirac two-point function is exactly that of a free field with the physical mass, aside from the rescaling factor Z_2 .

An Example: The Electron Self-Energy

This nonperturbative analysis of the two-point correlation function has been very different from our usual direct analysis of Feynman diagrams. But since this derivation was done in complete generality, the singularity structure of the two-point function that it implies ought also to be visible in a Feynman diagram computation. In the rest of this section we will explicitly check our results for the electron two-point function in QED.

The electron two-point function is equal to the sum of diagrams

$$\langle \Omega | T\psi(x)\bar{\psi}(y) | \Omega \rangle = \text{---} \leftarrow_x \text{---} \leftarrow_y + \text{---} \overbrace{\text{---}}^{\text{cloud}} \text{---} \leftarrow_y + \dots \quad (7.13)$$

Each of these diagrams, according to the Feynman rules for correlation functions, contains a factor of $e^{-ip \cdot (x-y)}$ for the two external points and an integration $\int (d^4 p / (2\pi)^4)$ over the momentum p carried by the initial and final propagators. We will consistently omit these factors in this section; in other words, each diagram will denote the corresponding term in the Fourier transform of the two-point function.

The first diagram is just the free-field propagator:

$$\begin{array}{c} \text{---} \\ \text{---} \\ p \end{array} = \frac{i(\not{p} + m_0)}{p^2 - m_0^2 + i\epsilon}. \quad (7.14)$$

Throughout this calculation, we will write m_0 instead of m as the mass in the electron propagator. This makes explicit the fact noted above that the mass appearing in the Lagrangian differs, in general, from the observable rest energy of a particle. However, if a perturbation expansion is applicable, the leading-order expression for the propagator should approximate the exact expression. Indeed, the function (7.14) has a pole, of just the form of (7.11), at $p^2 = m_0^2$. We therefore expect that the complete expression for the two-point function also has a pole of this form, at a slightly shifted location $m^2 = m_0^2 + \mathcal{O}(\alpha)$.

The second diagram in (7.13), called the *electron self-energy*, is somewhat more complicated:

$$\begin{array}{c} \text{---} \\ \text{---} \\ p \\ \swarrow \curvearrowleft \\ k \\ \curvearrowright \text{---} \\ p \end{array} = \frac{i(\not{p} + m_0)}{p^2 - m_0^2} [-i\Sigma_2(p)] \frac{i(\not{p} + m_0)}{p^2 - m_0^2}, \quad (7.15)$$

where

$$-i\Sigma_2(p) = (-ie)^2 \int \frac{d^4 k}{(2\pi)^4} \gamma^\mu \frac{i(\not{k} + m_0)}{k^2 - m_0^2 + i\epsilon} \gamma_\mu \frac{-i}{(p-k)^2 - \mu^2 + i\epsilon}. \quad (7.16)$$

(The notation Σ_2 indicates that this is the second-order (in e) contribution to a quantity Σ that we will define below.) The integral Σ_2 has an infrared divergence, which we have regularized by adding a small photon mass μ . Outside this integral, the diagram seems to have a double pole at $p^2 = m_0^2$. All in all, the form of this correction is quite unpleasant. But let us press on and try to evaluate $\Sigma_2(p)$ using the calculational techniques developed for the vertex correction in the Section 6.3.

First introduce a Feynman parameter to combine the two denominators:

$$\frac{1}{k^2 - m_0^2 + i\epsilon} \frac{1}{(p-k)^2 - \mu^2 + i\epsilon} = \int_0^1 dx \frac{1}{[k^2 - 2xk \cdot p + xp^2 - x\mu^2 - (1-x)m_0^2 + i\epsilon]^2}.$$

Now complete the square and define a shifted momentum $\ell \equiv k - xp$. Dropping the term linear in ℓ from the numerator, we have

$$-i\Sigma_2(p) = -e^2 \int_0^1 dx \int \frac{d^4\ell}{(2\pi)^4} \frac{-2x\cancel{p} + 4m_0}{[\ell^2 - \Delta + i\epsilon]^2}, \quad (7.17)$$

where $\Delta = -x(1-x)p^2 + x\mu^2 + (1-x)m_0^2$. The integral over ℓ is divergent. To evaluate it, we first regulate it using the Pauli-Villars procedure (6.51):

$$\frac{1}{(p-k)^2 - \mu^2 + i\epsilon} \rightarrow \frac{1}{(p-k)^2 - \mu^2 + i\epsilon} - \frac{1}{(p-k)^2 - \Lambda^2 + i\epsilon}.$$

The second term will have the same form as (7.17), but with μ replaced by Λ . As in Section 6.3, we now Wick-rotate and substitute the Euclidean variable $\ell_E^0 = -i\ell^0$. This gives

$$\begin{aligned} \int \frac{d^4\ell}{(2\pi)^4} \frac{1}{[\ell^2 - \Delta]^2} &\rightarrow \frac{i}{(4\pi)^2} \int_0^\infty d\ell_E^2 \left(\frac{\ell_E^2}{[\ell_E^2 + \Delta]^2} - \frac{\ell_E^2}{[\ell_E^2 + \Delta_\Lambda]^2} \right) \\ &= \frac{i}{(4\pi)^2} \log\left(\frac{\Delta_\Lambda}{\Delta}\right), \end{aligned} \quad (7.18)$$

where

$$\Delta_\Lambda = -x(1-x)p^2 + x\Lambda^2 + (1-x)m_0^2 \xrightarrow{\Lambda \rightarrow \infty} x\Lambda^2.$$

The final result is therefore

$$\Sigma_2(p) = \frac{\alpha}{2\pi} \int_0^1 dx (2m_0 - x\cancel{p}) \log\left(\frac{x\Lambda^2}{(1-x)m_0^2 + x\mu^2 - x(1-x)p^2}\right). \quad (7.19)$$

Before discussing the divergences in this expression, let us work out its analytic behavior as a function of p^2 . The logarithm in (7.19) has a branch cut when its argument becomes negative, and for any fixed x this will occur for sufficiently large p^2 . More exactly, the cut begins at the point where

$$(1-x)m_0^2 + x\mu^2 - x(1-x)p^2 = 0.$$

Solving this equation for x , we find

$$\begin{aligned} x &= \frac{1}{2} + \frac{m_0^2}{2p^2} - \frac{\mu^2}{2p^2} \pm \sqrt{\frac{(p^2 + m_0^2 - \mu^2)^2}{4p^4} - \frac{m_0^2}{p^2}} \\ &= \frac{1}{2} + \frac{m_0^2}{2p^2} - \frac{\mu^2}{2p^2} \pm \frac{1}{2p^2} \sqrt{[p^2 - (m_0 + \mu)^2][p^2 - (m_0 - \mu)^2]}. \end{aligned} \quad (7.20)$$

The branch cut of $\Sigma_2(p^2)$ begins at the minimum value of p^2 such that this equation has a real solution for x between 0 and 1. This occurs when $p^2 = (m_0 + \mu)^2$, that is, at the threshold for creation of a two-particle (electron

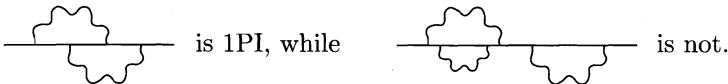
plus photon) state. In fact, it is a simple exercise in relativistic kinematics to show that the square root in (7.20), written in the form

$$k = \frac{1}{2\sqrt{p^2}} \sqrt{[p^2 - (m_0 + \mu)^2][p^2 - (m_0 - \mu)^2]},$$

is precisely the momentum in the center-of-mass frame for two particles of mass m_0 and μ and total energy $\sqrt{p^2}$. It is natural that this momentum becomes real at the two-particle threshold. The location of the branch cut is exactly where we would expect from the Källén-Lehmann spectral representation.[†]

We have now located the two-particle branch cut predicted by the Källén-Lehmann representation, but we have not found the expected simple pole at $p^2 = m^2$. To find it we must actually include an infinite series of Feynman diagrams. Fortunately, this series will be easily summed.

Let us define a *one-particle irreducible* (1PI) diagram to be any diagram that cannot be split in two by removing a single line:



Let $-i\Sigma(p)$ denote the sum of all 1PI diagrams with two external fermion lines:

$$\begin{aligned} -i\Sigma(p) &= \text{---} \xleftarrow{\text{1PI}} \text{---} \\ &= \text{---} \xleftarrow{\text{1PI}} \text{---} + \text{---} \xleftarrow{\text{1PI}} \text{---} + \text{---} \xleftarrow{\text{1PI}} \text{---} + \dots \end{aligned} \quad (7.21)$$

(Although each diagram has two external lines, the Feynman propagators for these lines are not to be included in the expression for $\Sigma(p)$.) To leading order in α we see that $\Sigma = \Sigma_2$.

The Fourier transform of the two-point function can now be written as

$$\begin{aligned} \int d^4x \langle \Omega | T\psi(x)\bar{\psi}(0) | \Omega \rangle e^{ip \cdot x} &= \text{---} \xleftarrow{\text{---}} \text{---} \\ &= \text{---} \text{---} + \text{---} \xleftarrow{\text{1PI}} \text{---} + \text{---} \xleftarrow{\text{1PI}} \text{---} \xleftarrow{\text{1PI}} \text{---} + \dots \\ &= \frac{i(\not{p} + m_0)}{p^2 - m_0^2} + \frac{i(\not{p} + m_0)}{p^2 - m_0^2} (-i\Sigma) \frac{i(\not{p} + m_0)}{p^2 - m_0^2} + \dots \end{aligned} \quad (7.22)$$

[†]In real QED, $\mu = 0$ and the two-particle branch cut merges with the one-particle pole. This subtlety plays a role in the full treatment of the cancellation of infrared divergences, but it is beyond the scope of our present analysis.

The first diagram has a simple pole at $p^2 = m_0^2$. Each diagram in the second class has a double pole at $p^2 = m_0^2$. Each diagram in the third class has a triple pole. The behavior near $p^2 = m_0^2$ gets worse and worse as we include more and more diagrams. But fortunately, the sum of all the diagrams forms a geometric series. Note that $\Sigma(p)$ commutes with \not{p} , since $\Sigma(p)$ is a function only of pure numbers and \not{p} . In fact, we can consider $\Sigma(p)$ to be a function of \not{p} , writing $p^2 = (\not{p})^2$. Then we can rewrite each electron propagator as $i/(\not{p} - m_0)$ and express the above series as

$$\begin{aligned} \int d^4x \langle \Omega | T\psi(x)\bar{\psi}(0) | \Omega \rangle e^{ip \cdot x} \\ = \frac{i}{\not{p} - m_0} + \frac{i}{\not{p} - m_0} \left(\frac{\Sigma(\not{p})}{\not{p} - m_0} \right) + \frac{i}{\not{p} - m_0} \left(\frac{\Sigma(\not{p})}{\not{p} - m_0} \right)^2 + \dots \\ = \frac{i}{\not{p} - m_0 - \Sigma(\not{p})}. \end{aligned} \quad (7.23)$$

The full propagator has a simple pole, which is shifted away from m_0 by $\Sigma(\not{p})$.

The location of this pole, the physical mass m , is the solution of the equation

$$[\not{p} - m_0 - \Sigma(\not{p})] \Big|_{\not{p}=m} = 0. \quad (7.24)$$

Notice that, if $\Sigma(\not{p})$ is defined by the convention (7.21), then a positive contribution to Σ yields a positive shift of the electron mass. Close to the pole, the denominator of (7.23) has the form

$$(\not{p} - m) \cdot \left(1 - \frac{d\Sigma}{d\not{p}} \Big|_{\not{p}=m} \right) + \mathcal{O}((\not{p} - m)^2). \quad (7.25)$$

Thus the full electron propagator has a single-particle pole of just the form (7.11), with m given by (7.24) and

$$Z_2^{-1} = 1 - \frac{d\Sigma}{d\not{p}} \Big|_{\not{p}=m}. \quad (7.26)$$

Our explicit calculation of Σ_2 allows us to compute the first corrections to m and Z_2 . Let us begin with m . To order α , the mass shift is

$$\delta m = m - m_0 = \Sigma_2(\not{p} = m) \approx \Sigma_2(\not{p} = m_0). \quad (7.27)$$

Thus, using (7.19),

$$\delta m = \frac{\alpha}{2\pi} m_0 \int_0^1 dx (2-x) \log \left(\frac{x\Lambda^2}{(1-x)^2 m_0^2 + x\mu^2} \right). \quad (7.28)$$

The mass shift is ultraviolet divergent; the divergent term has the form

$$\delta m \xrightarrow{\Lambda \rightarrow \infty} \frac{3\alpha}{4\pi} m_0 \log \left(\frac{\Lambda^2}{m_0^2} \right). \quad (7.29)$$

Is it a problem that m differs from m_0 by a divergent quantity? This question has two levels, those of concept and practice.

On the conceptual level, we should fully expect the mass of the electron to be modified by its coupling to the electromagnetic field. In classical electrodynamics, the rest energy of any charge is increased by the energy of its electrostatic field, and this energy shift diverges in the case of a point charge:

$$\int d^3r \frac{1}{2} |\mathbf{E}|^2 = \int d^3r \frac{1}{2} \left(\frac{e}{4\pi r^2} \right)^2 = \frac{\alpha}{2} \int \frac{dr}{r^2} \sim \alpha \Lambda. \quad (7.30)$$

In fact, it is puzzling why the divergence in (7.29) is so weak, logarithmic in Λ rather than linear as in (7.30). To understand this feature, suppose that m_0 were set to 0. Then the two helicity components of the electron field ψ_L and ψ_R would not be coupled by any term in the QED Hamiltonian. This would imply that perturbative corrections could never induce a coupling of ψ_L and ψ_R , nor, in particular, an electron mass term. In other words, δm must vanish when $m_0 = 0$. The mass shift must therefore be proportional to m_0 , and so, by dimensional analysis, it can depend only logarithmically on Λ .

On a practical level, the infinite mass shift casts doubt on our perturbative calculations. For example, all of the theoretical results in Chapter 5 should technically involve m_0 rather than m . To compare theory to experiment we must eliminate m_0 in favor of m , using the relation $m_0 = m + \mathcal{O}(\alpha)$. Since the “small” $\mathcal{O}(\alpha)$ correction is infinite, the validity of this procedure is far from obvious. The validity of perturbation theory would be more plausible if we could compute Feynman diagrams using the propagator $i/(\not{p} - m)$, which has the correct pole location, instead of $i/(\not{p} - m_0)$. In Chapter 10 we will see how to rearrange the perturbation series in such a way that m_0 is systematically eliminated in favor of m and the zeroth-order propagator has its pole at the physical mass. In the remainder of this chapter, we will continue to simply replace m_0 by m in expressions for order- α corrections.

Finally, let us examine the perturbative correction to Z_2 . From (7.26), we find that the order- α correction $\delta Z_2 = (Z_2 - 1)$ is

$$\begin{aligned} \delta Z_2 &= \frac{d\Sigma_2}{d\not{p}} \Big|_{\not{p}=m} \\ &= \frac{\alpha}{2\pi} \int_0^1 dx \left[-x \log \frac{x\Lambda^2}{(1-x)^2 m^2 + x\mu^2} + 2(2-x) \frac{x(1-x)m^2}{(1-x)^2 m^2 + x\mu^2} \right]. \end{aligned} \quad (7.31)$$

This expression is also logarithmically ultraviolet divergent. We will discuss the observability of this divergent term at the end of Section 7.2. However, it is interesting to note, even before that discussion, that (7.31) is very similar in form to the value of the *ad hoc* subtraction that we made in our calculation of the electron vertex correction in Section 6.3. From Eq. (6.56), the value of

this subtraction was

$$\begin{aligned}\delta F_1(0) &= \frac{\alpha}{2\pi} \int_0^1 dx dy dz \delta(x+y+z-1) \\ &\quad \times \left[\log\left(\frac{z\Lambda^2}{(1-z)^2 m^2 + z\mu^2}\right) + \frac{(1-4z+z^2)m^2}{(1-z)^2 m^2 + z\mu^2} \right] \\ &= \frac{\alpha}{2\pi} \int_0^1 dz (1-z) \left[\log\left(\frac{z\Lambda^2}{(1-z)^2 m^2 + z\mu^2}\right) + \frac{(1-4z+z^2)m^2}{(1-z)^2 m^2 + z\mu^2} \right]. \quad (7.32)\end{aligned}$$

Using the integration by parts

$$\begin{aligned}\int_0^1 dz (1-2z) \log\left(\frac{\Lambda^2}{(1-z)^2 m^2 + z\mu^2}\right) &= - \int_0^1 dz z(1-z) \frac{2(1-z)m^2 - \mu^2}{(1-z)^2 m^2 + z\mu^2} \\ &= \int_0^1 dz \left[(1-z) - \frac{(1-z)(1-z^2)m^2}{(1-z)^2 m^2 + z\mu^2} \right],\end{aligned}$$

it is not hard to show that $\delta F_1(0) + \delta Z_2 = 0$. This identity will play a crucial role in justifying the *ad hoc* subtraction of Section 6.3.

7.2 The LSZ Reduction Formula

In the last section we saw that the Fourier transform of the two-point correlation function, considered as an analytic function of p^2 , has a simple pole at the mass of the one-particle state:

$$\int d^4x e^{ip \cdot x} \langle \Omega | T\phi(x)\phi(0) | \Omega \rangle \underset{p^2 \rightarrow m^2}{\sim} \frac{iZ}{p^2 - m^2 + i\epsilon}. \quad (7.33)$$

(Here and throughout this section we use the symbol \sim to mean that the poles of both sides are identical; there are additional finite terms, given in this case by Eq. (7.9).) In this section we will generalize this result to higher correlation functions. We will derive a general relation between correlation functions and *S*-matrix elements first obtained by Lehmann, Symanzik, and Zimmermann and known as the *LSZ reduction formula*.[†] This result, combined with our Feynman rules for computing correlation functions, will justify Eq. (4.103), our master formula for *S*-matrix elements in terms of Feynman diagrams. For simplicity, we will carry out the whole analysis for the case of scalar fields.

[†]H. Lehmann, K. Symanzik, and W. Zimmermann, *Nuovo Cimento* **1**, 1425 (1955).

The strategy of the argument will be as follows. To calculate the S -matrix element for a $2\text{-body} \rightarrow n\text{-body}$ scattering process, we begin with the correlation function of $n + 2$ Heisenberg fields. Fourier-transforming with respect to the coordinate of any one of these fields, we will find a pole of the form (7.33) in the Fourier-transform variable p^2 . We will argue that the one-particle states associated with these poles are in fact asymptotic states, that is, states given by the limit of well-separated wavepackets as they become concentrated around definite momenta. Taking the limit in which all $n + 2$ external particles go on-shell, we can then interpret the coefficient of the multiple pole as an S -matrix element.

To begin, let us Fourier-transform the $(n + 2)$ -point correlation function with respect to one argument x . We must then analyze the integral

$$\int d^4x e^{ip \cdot x} \langle \Omega | T\{\phi(x)\phi(z_1)\phi(z_2)\dots\} | \Omega \rangle.$$

We would like to identify poles in the variable p^0 . To do this, divide the integral over x^0 into three regions:

$$\int dx^0 = \int_{T_+}^{\infty} dx^0 + \int_{T_-}^{T_+} dx^0 + \int_{-\infty}^{T_-} dx^0, \quad (7.34)$$

where T_+ is much greater than all the z_i^0 and T_- is much less than all the z_i^0 . Call these three intervals regions I, II, and III. Since region II is bounded and the integrand depends on p^0 through the analytic function $\exp(ip^0 x^0)$, the contribution from this region will be analytic in p^0 . However, regions I and III, which are unbounded, may develop singularities in p^0 .

Consider first region I. Here x^0 is the latest time, so $\phi(x)$ stands first in the time ordering. Insert a complete set of intermediate states in the form of (7.2):

$$\mathbf{1} = \sum_{\lambda} \int \frac{d^3q}{(2\pi)^3} \frac{1}{2E_{\mathbf{q}}(\lambda)} |\lambda_{\mathbf{q}}\rangle \langle \lambda_{\mathbf{q}}|.$$

The integral over region I then becomes

$$\begin{aligned} \int_{T_+}^{\infty} dx^0 \int d^3x e^{ip^0 x^0} e^{-i\mathbf{p} \cdot \mathbf{x}} \sum_{\lambda} \int \frac{d^3q}{(2\pi)^3} \frac{1}{2E_{\mathbf{q}}(\lambda)} \langle \Omega | \phi(x) | \lambda_{\mathbf{q}} \rangle \\ \times \langle \lambda_{\mathbf{q}} | T\{\phi(z_1)\phi(z_2)\dots\} | \Omega \rangle. \end{aligned} \quad (7.35)$$

Using Eq. (7.4),

$$\langle \Omega | \phi(x) | \lambda_{\mathbf{q}} \rangle = \langle \Omega | \phi(0) | \lambda_0 \rangle e^{-iq \cdot x} \Big|_{q^0 = E_{\mathbf{q}}(\lambda)},$$

and including a factor $e^{-\epsilon x^0}$ to insure that the integral is well defined, this integral becomes

$$\begin{aligned} & \sum_{\lambda} \int_{T_+}^{\infty} dx^0 \int \frac{d^3 q}{(2\pi)^3} \frac{1}{2E_{\mathbf{q}}(\lambda)} e^{ip^0 x^0} e^{-iq^0 x^0} e^{-\epsilon x^0} \langle \Omega | \phi(0) | \lambda_0 \rangle (2\pi)^3 \delta^{(3)}(\mathbf{p} - \mathbf{q}) \\ & \quad \times \langle \lambda_{\mathbf{q}} | T\{\phi(z_1) \dots\} | \Omega \rangle \\ &= \sum_{\lambda} \frac{1}{2E_{\mathbf{p}}(\lambda)} \frac{i e^{i(p^0 - E_{\mathbf{p}} + i\epsilon)T_+}}{p^0 - E_{\mathbf{p}}(\lambda) + i\epsilon} \langle \Omega | \phi(0) | \lambda_0 \rangle \langle \lambda_{\mathbf{p}} | T\{\phi(z_1) \dots\} | \Omega \rangle. \end{aligned} \quad (7.36)$$

The denominator is just that of Eq. (7.5): $p^2 - m_{\lambda}^2$. There is an analytic singularity in p^0 ; as in Section 7.1, this singularity will be either a pole or a branch cut depending upon whether or not the rest energy m_{λ} is isolated. The one-particle state corresponds to an isolated energy value $p^0 = E_{\mathbf{p}} = \sqrt{|\mathbf{p}|^2 + m^2}$, and at this point Eq. (7.36) has a pole:

$$\begin{aligned} & \int d^4 x e^{ip \cdot x} \langle \Omega | T\{\phi(x)\phi(z_1) \dots\} | \Omega \rangle \\ & \sim_{p^0 \rightarrow +E_{\mathbf{p}}} \frac{i}{p^2 - m^2 + i\epsilon} \sqrt{Z} \langle \mathbf{p} | T\{\phi(z_1) \dots\} | \Omega \rangle. \end{aligned} \quad (7.37)$$

The factor \sqrt{Z} is the same field strength renormalization factor as in Eq. (7.8), since it replaces the same matrix element as in (7.7).

To evaluate the contribution from region III, we would put $\phi(x)$ last in the operator ordering, then insert a complete set of states between $T\{\phi(z_1) \dots\}$ and $\phi(x)$. Repeating the above argument produces a pole as $p^0 \rightarrow -E_{\mathbf{p}}$:

$$\begin{aligned} & \int d^4 x e^{ip \cdot x} \langle \Omega | T\{\phi(x)\phi(z_1) \dots\} | \Omega \rangle \\ & \sim_{p^0 \rightarrow -E_{\mathbf{p}}} \langle \Omega | T\{\phi(z_1) \dots\} | -\mathbf{p} \rangle \sqrt{Z} \frac{i}{p^2 - m^2 + i\epsilon}. \end{aligned} \quad (7.38)$$

Next we would like to Fourier-transform with respect to the remaining field coordinates. To keep the various external particles from interfering, however, we must isolate them from each other in space. Let us therefore repeat the preceding calculation using a wavepacket rather than a simple Fourier transform. In Eq. (7.35), replace

$$\int d^4 x e^{ip^0 x^0} e^{-i\mathbf{p} \cdot \mathbf{x}} \rightarrow \int \frac{d^3 k}{(2\pi)^3} \int d^4 x e^{ip^0 x^0} e^{-i\mathbf{k} \cdot \mathbf{x}} \varphi(\mathbf{k}), \quad (7.39)$$

where $\varphi(\mathbf{k})$ is a narrow distribution centered on $\mathbf{k} = \mathbf{p}$. This distribution constrains x to lie within a band, whose spatial extent is that of the wavepacket, about the trajectory of a particle with momentum \mathbf{p} . With this modification, the right-hand side of (7.36) has a more complicated singularity structure:

$$\sum_{\lambda} \int \frac{d^3 k}{(2\pi)^3} \varphi(\mathbf{k}) \frac{1}{2E_{\mathbf{k}}(\lambda)} \frac{i}{p^0 - E_{\mathbf{k}}(\lambda) + i\epsilon} \langle \Omega | \phi(0) | \lambda_0 \rangle \langle \lambda_{\mathbf{k}} | T\{\phi(z_1) \dots\} | \Omega \rangle$$

$$\underset{p^0 \rightarrow +E_p}{\sim} \int \frac{d^3 k}{(2\pi)^3} \varphi(\mathbf{k}) \frac{i}{\tilde{p}^2 - m^2 + i\epsilon} \sqrt{Z} \langle \mathbf{k} | T\{\phi(z_1) \cdots\} | \Omega \rangle, \quad (7.40)$$

where, in the second line, $\tilde{p} = (p_0, \mathbf{k})$. The one-particle singularity is now a branch cut, whose length is the width in momentum space of the wavepacket $\varphi(\mathbf{k})$. However, if $\varphi(\mathbf{k})$ defines the momentum narrowly, this branch cut is very short, and (7.40) has a well-defined limit in which $\varphi(\mathbf{k})$ tends to $(2\pi)^3 \delta^{(3)}(\mathbf{k} - \mathbf{p})$ and the singularity of (7.40) sharpens up to the pole of (7.36). The singularity due to single-particle states in the far past, Eq. (7.38), is modified in the same way.

Now consider integrating each of the coordinates in the $(n+2)$ -point correlation function against a wavepacket, to form*

$$\left(\prod_i \int \frac{d^3 k_i}{(2\pi)^3} \int d^4 x_i e^{i\tilde{p}_i \cdot x_i} \varphi_i(\mathbf{k}_i) \right) \langle \Omega | T\{\phi(x_1) \phi(x_2) \cdots\} | \Omega \rangle. \quad (7.41)$$

The wavepackets should be chosen to overlap in a region around $x = 0$ and to separate in the far past and the far future. To analyze this integral, we choose a large positive time T_+ such that all of the wavepackets are well separated for $x_i^0 > T_+$, and we choose a large negative time T_- such that all of the wavepackets are well separated for $x_i^0 < T_-$. Then we can break up each of the integrals over x_i^0 into three regions as in (7.34). The integral of any x_i^0 over the bounded region II leads to an expression analytic in the corresponding energy p_0^i , so we can concentrate on the case in which all of the x_i^0 are placed at large past or future times.

For definiteness, consider the contribution in which only two of the time coordinates, x_1^0 and x_2^0 , are in the future. In this case, the fields $\phi(x_1)$ and $\phi(x_2)$ stand to the left of the other fields in time order. Inserting a complete set of states $|\lambda_{\mathbf{K}}\rangle$, the integrations in (7.41) over the coordinates of these two fields take the form

$$\begin{aligned} \sum_{\lambda} \int \frac{d^3 K}{(2\pi)^3} \frac{1}{2E_{\mathbf{K}}} & \left(\prod_{i=1,2} \int \frac{d^3 k_i}{(2\pi)^3} \int d^4 x_i e^{i\tilde{p}_i \cdot x_i} \varphi_i(\mathbf{k}_i) \right) \\ & \times \langle \Omega | T\{\phi(x_1) \phi(x_2)\} | \lambda_{\mathbf{K}} \rangle \langle \lambda_{\mathbf{K}} | T\{\phi(x_3) \cdots\} | \Omega \rangle. \end{aligned}$$

The state $|\lambda_{\mathbf{K}}\rangle$ is annihilated by two field operators constrained to lie in distant wavepackets. It must therefore consist of two distinct excitations of the vacuum at two distinct locations. If these excitations are well separated,

*As in Section 4.5, the product symbol applies symbolically to the integrations as well as to the other factors within the parentheses; the x_i integrals apply to what lies outside the parentheses as well.

they should be independent of one another, so we can approximate

$$\begin{aligned} & \sum_{\lambda} \int \frac{d^3 K}{(2\pi)^3} \frac{1}{2E_{\mathbf{K}}} \langle \Omega | T\{\phi(x_1)\phi(x_2)\} | \lambda_{\mathbf{K}} \rangle \langle \lambda_{\mathbf{K}} | \\ &= \sum_{\lambda_1, \lambda_2} \int \frac{d^3 q_1}{(2\pi)^3} \frac{1}{2E_{\mathbf{q}_1}} \int \frac{d^3 q_2}{(2\pi)^3} \frac{1}{2E_{\mathbf{q}_2}} \langle \Omega | \phi(x_1) | \lambda_{\mathbf{q}_1} \rangle \langle \Omega | \phi(x_2) | \lambda_{\mathbf{q}_2} \rangle \langle \lambda_{\mathbf{q}_1} \lambda_{\mathbf{q}_2} | . \end{aligned}$$

The sums over λ_1 and λ_2 in this equation run over all zero-momentum states, but only single-particle states will contribute the poles we are looking for. In this case, the integrals over x_1^0 and \mathbf{q}_1 produce a sharp singularity in p_1^0 of the form of (7.40), and the integrals over x_2^0 and \mathbf{q}_2 produce the same singular behavior in p_2^0 . The term in (7.41) with both singularities is

$$\left(\prod_{i=1,2} \int \frac{d^3 k_i}{(2\pi)^3} \varphi_i(\mathbf{k}_i) \frac{i}{\tilde{p}_i^2 - m^2 + i\epsilon} \cdot \sqrt{Z} \right) \langle \mathbf{k}_1 \mathbf{k}_2 | T\{\phi(x_3) \dots\} | \Omega \rangle .$$

In the limit in which the wavepackets tend to delta functions concentrated at definite momenta \mathbf{p}_1 and \mathbf{p}_2 , this expression tends to

$$\left(\prod_{i=1,2} \frac{i}{p_i^2 - m^2 + i\epsilon} \cdot \sqrt{Z} \right)_{\text{out}} \langle \mathbf{p}_1 \mathbf{p}_2 | T\{\phi(x_3) \dots\} | \Omega \rangle .$$

The state $\langle \mathbf{p}_1 \mathbf{p}_2 |$ is precisely an *out* state as defined in Section 4.5, since it is the definite-momentum limit of a state of particles constrained to well-separated wavepackets. Applying the same analysis to the times x_i^0 in the far past gives the result that the coefficient of the maximally singular term in the corresponding p_i^0 is a matrix element with an *in* state. This most singular term in (7.41) thus has the form

$$\left(\prod_{i=1,2} \frac{i}{p_i^2 - m^2 + i\epsilon} \cdot \sqrt{Z} \right) \left(\prod_{i=3,\dots} \frac{i}{p_i^2 - m^2 + i\epsilon} \cdot \sqrt{Z} \right)_{\text{out}} \langle \mathbf{p}_1 \mathbf{p}_2 | -\mathbf{p}_3 \dots \rangle_{\text{in}} .$$

The last factor is just an *S*-matrix element.

We have now shown that we can extract the value of an *S*-matrix element by folding the corresponding vacuum expectation value of fields with wavepackets, extracting the leading singularities in the energies p_i^0 , and then taking the limit as these wavepackets become delta functions of momenta. However, the computation would be made much simpler if we could do these operations in the reverse order—first letting the wavepackets become delta functions, returning us to the simple Fourier transform, and then extracting the singularities. In fact, the result for the leading singularity is not changed by this switch of the order of operations. It is, however, rather subtle to argue this point. Roughly, the explanation is the following: In the language of the analysis just completed, new singularities might arise because, in the Fourier transform, x_1 and x_2 can become close together in the far future. However, in this region, the exponential factor is close to $\exp[i(p_1 + p_2) \cdot x_1]$, and thus the new singularities are single poles in the variable $(p_1^0 + p_2^0)$, rather than

being products of poles in the two separate energy variables. A more careful argument (unfortunately, couched in a rather different language) can be found in the original paper of Lehmann, Symanzik, and Zimmermann cited at the beginning of this section.

Given the ability to make this reversal in the order of operations, we obtain a precise relation between Fourier transforms of correlation functions and S -matrix elements. This is the LSZ reduction formula:

$$\prod_1^n \int d^4 x_i e^{ip_i \cdot x_i} \prod_1^m \int d^4 y_j e^{-ik_j \cdot y_j} \langle \Omega | T\{\phi(x_1) \cdots \phi(x_n) \phi(y_1) \cdots \phi(y_m)\} | \Omega \rangle$$

$$\stackrel{\text{each } p_i^0 \rightarrow +E_{\mathbf{p}_i}}{\sim} \left(\prod_{i=1}^n \frac{\sqrt{Z} i}{p_i^2 - m^2 + i\epsilon} \right) \left(\prod_{j=1}^m \frac{\sqrt{Z} i}{k_j^2 - m^2 + i\epsilon} \right) \langle \mathbf{p}_1 \cdots \mathbf{p}_n | S | \mathbf{k}_1 \cdots \mathbf{k}_m \rangle. \quad (7.42)$$

The quantity Z that appears in this equation is exactly the field-strength renormalization constant, defined in Section 7.1 as the residue of the single-particle pole in the two-point function of fields. Each distinct particle will have a distinct renormalization factor Z , obtained from its own two-point function. For higher-spin fields, each factor of \sqrt{Z} comes with a polarization factor such as $u^s(p)$, as in Eq. (7.12). The polarization s must be summed over in the second line of (7.42).

In words, the LSZ formula says that an S -matrix element can be computed as follows. Compute the appropriate Fourier-transformed correlation function, look at the region of momentum space where the external particles are near the mass shell, and identify the coefficient of the multiparticle pole. For fields with spin, one must also multiply by a polarization spinor (like $u^s(p)$) or vector (like $\epsilon^r(k)$) to project out the desired spin state.

Our next goal is to express this procedure in the language of Feynman diagrams. Let us analyze the relation between the diagrammatic expansion of the scalar field four-point function and the S -matrix element for 2-particle \rightarrow 2-particle scattering. We will consider explicitly the fully connected Feynman diagrams contributing to the correlator. By a similar analysis, it is easy to confirm that disconnected diagrams should be disregarded because they do not have the singularity structure, with a product of four poles, indicated on the right-hand side of (7.42).

The exact four-point function

$$\left(\prod_1^2 \int d^4 x_i e^{ip_i \cdot x_i} \right) \left(\prod_1^2 \int d^4 y_i e^{-ik_i \cdot y_i} \right) \langle \Omega | T\{\phi(x_1) \phi(x_2) \phi(y_1) \phi(y_2)\} | \Omega \rangle$$

has the general form shown in Fig. 7.4. In this figure, we have indicated explicitly the diagrammatic corrections on each leg; the shaded circle in the center represents the sum of all amputated four-point diagrams.

We can sum up the corrections to each external leg just as we did for the electron propagator in the previous section. Let $-iM^2(p^2)$ denote the sum of

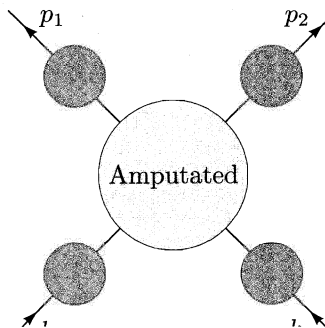


Figure 7.4. Structure of the exact four-point function in scalar field theory.

all one-particle-irreducible (1PI) insertions into the scalar propagator:

$$-iM^2(p^2) = \text{---} + \text{---} + \text{---} + \dots = \text{---} \text{1PI} \text{---}$$

Then the exact propagator can be written as a geometric series and summed as in Eq. (7.23):

$$\begin{aligned} \text{---} \text{---} &= \text{---} + \text{---} \text{1PI} \text{---} + \text{---} \text{1PI} \text{---} \text{1PI} \text{---} + \dots \\ &= \frac{i}{p^2 - m_0^2} + \frac{i}{p^2 - m_0^2} (-iM^2) \frac{i}{p^2 - m_0^2} + \dots \\ &= \frac{i}{p^2 - m_0^2 - M^2(p^2)}. \end{aligned} \quad (7.43)$$

Notice that, as in the case of the electron propagator, our sign convention for the 1PI self-energy $M^2(p^2)$ implies that a positive contribution to $M^2(p^2)$ corresponds to a positive shift of the scalar particle mass. If we expand each resummed propagator about the physical particle pole, we see that each external leg of the four-point amplitude contributes

$$\frac{i}{p^2 - m_0^2 - M^2} \underset{p^0 \rightarrow E_p}{\sim} \frac{iZ}{p^2 - m^2} + (\text{regular}). \quad (7.44)$$

Thus, the sum of diagrams contains a product of four poles:

$$\frac{iZ}{p_1^2 - m^2} \frac{iZ}{p_2^2 - m^2} \frac{iZ}{k_1^2 - m^2} \frac{iZ}{k_2^2 - m^2}.$$

This is exactly the singularity on the second line of (7.42). Comparing the

coefficients of this product of poles, we find the relation

$$\langle \mathbf{p}_1 \mathbf{p}_2 | S | \mathbf{k}_1 \mathbf{k}_2 \rangle = (\sqrt{Z})^4 \quad \text{Amp.} \quad ,$$

where the shaded circle is the sum of amputated four-point diagrams and Z is the field-strength renormalization factor.

An identical analysis can be applied to the Fourier transform of the $(n+2)$ -point correlator in a general field theory. The relation between S -matrix elements and Feynman diagrams then takes the form

$$\langle \mathbf{p}_1 \dots \mathbf{p}_n | S | \mathbf{k}_1 \mathbf{k}_2 \rangle = (\sqrt{Z})^{n+2} \quad \text{Amp.} \quad . \quad (7.45)$$

(If the external particles are of different species, each has its own renormalization factor \sqrt{Z} ; if the particles have nonzero spin, there will be additional polarization factors such as $u^s(k)$ on the right-hand side.) This is almost precisely the diagrammatic formula for the S -matrix that we wrote down in Section 4.6. The only new feature is the appearance of the renormalization factors \sqrt{Z} . The Z factors are irrelevant for calculations at the leading order of perturbation theory, but are important in the calculation of higher-order corrections.

Up to this point, we have performed only one full calculation of a higher-order correction, the computation of the order- α corrections to the electron form factors. We did not take into account the effects of the electron field-strength renormalization. Let us now add in this factor and examine its effects.

Since the expressions (6.28) and (6.30) for electron scattering from a heavy target were derived using our previous, incorrect formula for S -matrix elements, we should correct these formulae by inserting factors of $\sqrt{Z_2}$ for the initial and final electrons. Equation (6.33) for the structure of the exact vertex should then read

$$Z_2 \Gamma^\mu(p', p) = \gamma^\mu F_1(q^2) + \frac{i\sigma^{\mu\nu} q_\nu}{2m} F_2(q^2), \quad (7.46)$$

with $\Gamma^\mu(p', p)$ the sum of amputated electron-photon vertex diagrams.

We can use this equation to reevaluate the form factors to order α . Since $Z_2 = 1 + \mathcal{O}(\alpha)$ and F_2 begins in order α , our previous computation of F_2 is unaffected. To compute F_1 , write the left-hand side of (7.46) as

$$Z_2 \Gamma^\mu = (1 + \delta Z_2)(\gamma^\mu + \delta \Gamma^\mu) = \gamma^\mu + \delta \Gamma^\mu + \gamma^\mu \cdot \delta Z_2,$$

where δZ_2 and $\delta \Gamma^\mu$ denote the order- α corrections to these quantities. Comparing to the right-hand side of (7.46), we see that $F_1(q^2)$ receives a new

contribution equal to δZ_2 . Now let $\delta F_1(q^2)$ denote the (unsubtracted) correction to the form factor that we computed in Section 6.3, and recall from the end of Section 7.1 that $\delta Z_2 = -\delta F_1(0)$. Then

$$F_1(q^2) = 1 + \delta F_1(q^2) + \delta Z_2 = 1 + [\delta F_1(q^2) - \delta F_1(0)].$$

This is exactly the result we claimed, but did not prove, in Section 6.3. The inclusion of field-strength renormalization justifies the subtraction procedure that we applied on an *ad hoc* basis there.

At this level of analysis, it is difficult to see how the cancellation of divergences in F_1 will persist to higher orders. Worse, though we argued in Section 6.3 for the general result $F_1(0) = 1$, our verification of this result in order α seems to depend on a numerical coincidence.

We can state this problem carefully as follows: Define a second rescaling factor Z_1 by the relation

$$\Gamma^\mu(q=0) = Z_1^{-1} \gamma^\mu, \quad (7.47)$$

where Γ^μ is the complete amputated vertex function. To find $F_1(0) = 1$, we must prove the identity $Z_1 = Z_2$, so that the vertex rescaling exactly compensates the electron field-strength renormalization. We will prove this identity to all orders in perturbation theory at the end Section 7.4.

We conclude our discussion of the LSZ reduction formula with one further formal observation. The LSZ formula distinguishes in and out particles only by the sign of the Fourier transform momentum p_i^0 or k_i^0 . This means that, by analytically continuing the residue of the pole in p^2 from positive to negative p^0 , we can convert the S -matrix element with $\phi(\mathbf{p})$ in the final state into the S -matrix element with the antiparticle $\phi^*(-\mathbf{p})$ in the initial state. This is exactly the statement of *crossing symmetry*, which we derived diagrammatically in Section 5.4:

$$\langle \cdots \phi(p) | S | \cdots \rangle|_{p=-k} = \langle \cdots | S | \phi^*(k) \cdots \rangle.$$

Since the proof of the LSZ formula does not depend on perturbation theory, we see that the crossing symmetry of the S -matrix is a general result of quantum theory, not merely a property of Feynman diagrams.

7.3 The Optical Theorem

In Section 7.1 we saw that the two-point correlation function of quantum fields, viewed as an analytic function of the momentum p^2 , has branch cut singularities associated with multiparticle intermediate states. This conclusion should not be surprising to those familiar with nonrelativistic scattering theory, since it is already true there that the scattering amplitude, as a function of energy, has a branch cut on the positive real axis. The imaginary part of the scattering amplitude appears as a discontinuity across this branch cut. By the *optical theorem*, the imaginary part of the forward scattering amplitude is

$$2\text{Im} = \sum_f \int d\Pi_f \left(\begin{array}{c} k_2 \\ k_1 \end{array} \right) \left(\begin{array}{c} f \\ f \end{array} \right)$$

Figure 7.5. The optical theorem: The imaginary part of a forward scattering amplitude arises from a sum of contributions from all possible intermediate-state particles.

proportional to the total cross section. We will now prove the field-theoretic version of the optical theorem and illustrate how it arises in Feynman diagram calculations.

The optical theorem is a straightforward consequence of the unitarity of the S -matrix: $S^\dagger S = 1$. Inserting $S = 1 + iT$ as in (4.72), we have

$$-i(T - T^\dagger) = T^\dagger T. \quad (7.48)$$

Let us take the matrix element of this equation between two-particle states $|\mathbf{p}_1 \mathbf{p}_2\rangle$ and $|\mathbf{k}_1 \mathbf{k}_2\rangle$. To evaluate the right-hand side, insert a complete set of intermediate states:

$$\langle \mathbf{p}_1 \mathbf{p}_2 | T^\dagger T | \mathbf{k}_1 \mathbf{k}_2 \rangle = \sum_n \left(\prod_{i=1}^n \int \frac{d^3 q_i}{(2\pi)^3} \frac{1}{2E_i} \right) \langle \mathbf{p}_1 \mathbf{p}_2 | T^\dagger | \{q_i\} \rangle \langle \{q_i\} | T | \mathbf{k}_1 \mathbf{k}_2 \rangle.$$

Now express the T -matrix elements as invariant matrix elements \mathcal{M} times 4-momentum-conserving delta functions. Identity (7.48) then becomes

$$\begin{aligned} & -i[\mathcal{M}(k_1 k_2 \rightarrow p_1 p_2) - \mathcal{M}^*(p_1 p_2 \rightarrow k_1 k_2)] \\ &= \sum_n \left(\prod_{i=1}^n \int \frac{d^3 q_i}{(2\pi)^3} \frac{1}{2E_i} \right) \mathcal{M}^*(p_1 p_2 \rightarrow \{q_i\}) \mathcal{M}(k_1 k_2 \rightarrow \{q_i\}) \\ & \quad \times (2\pi)^4 \delta^{(4)}(k_1 + k_2 - \sum_i q_i), \end{aligned}$$

times an overall delta function $(2\pi)^4 \delta^{(4)}(k_1 + k_2 - p_1 - p_2)$. Let us abbreviate this identity as

$$-i[\mathcal{M}(a \rightarrow b) - \mathcal{M}^*(b \rightarrow a)] = \sum_f \int d\Pi_f \mathcal{M}^*(b \rightarrow f) \mathcal{M}(a \rightarrow f), \quad (7.49)$$

where the sum runs over all possible sets f of final-state particles. Although we have so far assumed that a and b are two-particle states, they could equally well be one-particle or multiparticle asymptotic states.

For the important special case of forward scattering, we can set $p_i = k_i$ to obtain a simpler identity, shown pictorially in Fig. 7.5. Supplying the kinematic factors required by (4.79) to build a cross section, we obtain the standard form of the optical theorem,

$$\text{Im } \mathcal{M}(k_1, k_2 \rightarrow k_1, k_2) = 2E_{\text{cm}} p_{\text{cm}} \sigma_{\text{tot}}(k_1, k_2 \rightarrow \text{anything}), \quad (7.50)$$

where E_{cm} is the total center-of-mass energy and p_{cm} is the momentum of either particle in the center-of-mass frame. This equation relates the forward scattering amplitude to the total cross section for production of all final states. Since the imaginary part of the forward scattering amplitude gives the attenuation of the forward-going wave as the beam passes through the target, it is natural that this quantity should be proportional to the probability of scattering. Identity (7.50) gives the precise connection.

The Optical Theorem for Feynman Diagrams

Let us now investigate how this identity for the imaginary part of an S -matrix element arises in the Feynman diagram expansion. It is easily checked (in QED, for example) that each diagram contributing to an S -matrix element \mathcal{M} is purely real unless some denominators vanish, so that the $i\epsilon$ prescription for treating the poles becomes relevant. A Feynman diagram thus yields an imaginary part for \mathcal{M} only when the virtual particles in the diagram go on-shell. We will now show how to isolate and compute this imaginary part.

For our present purposes, let us *define* \mathcal{M} by the Feynman rules for perturbation theory. This allows us to consider $\mathcal{M}(s)$ as an analytic function of the complex variable $s = E_{\text{cm}}^2$, even though S -matrix elements are defined only for external particles with real momenta.

We first demonstrate that the appearance of an imaginary part of $\mathcal{M}(s)$ always requires a branch cut singularity. Let s_0 be the threshold energy for production of the lightest multiparticle state. For real s below s_0 the intermediate state cannot go on-shell, so $\mathcal{M}(s)$ is real. Thus, for real $s < s_0$, we have the identity

$$\mathcal{M}(s) = [\mathcal{M}(s^*)]^*. \quad (7.51)$$

Each side of this equation is an analytic function of s , so it can be analytically continued to the entire complex s plane. In particular, near the real axis for $s > s_0$, Eq. (7.51) implies

$$\text{Re } \mathcal{M}(s + i\epsilon) = \text{Re } \mathcal{M}(s - i\epsilon);$$

$$\text{Im } \mathcal{M}(s + i\epsilon) = -\text{Im } \mathcal{M}(s - i\epsilon).$$

There is a branch cut across the real axis, starting at the threshold energy s_0 ; the discontinuity across the cut is

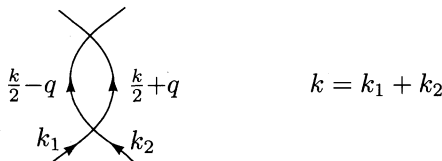
$$\text{Disc } \mathcal{M}(s) = 2i \text{Im } \mathcal{M}(s + i\epsilon).$$

Usually it is easier to compute the discontinuity of a diagram than to compute the imaginary part directly. The $i\epsilon$ prescription in the Feynman propagator indicates that physical scattering amplitudes should be evaluated above the cut, at $s + i\epsilon$.

We already saw in Section 7.1 that the electron self-energy diagram has a branch cut beginning at the physical electron-photon threshold. Let us now study more general one-loop diagrams, and show that their discontinuities

give precisely the imaginary parts required by (7.49). The generalization of this result to multiloop diagrams has been proven by Cutkosky,[†] who showed in the process that the discontinuity of a Feynman diagram across its branch cut is always given by a simple set of *cutting rules*.[‡]

We begin by checking (7.49) in ϕ^4 theory. Since the right-hand side of (7.49) begins in order λ^2 , we expect that $\text{Im } \mathcal{M}$ should also receive its first contribution from higher-order diagrams. Consider, then, the order- λ^2 diagram



with a loop in the s -channel. (It is easy to check that the corresponding t - and u -channel diagrams have no branch cut singularities for s above threshold.) The total momentum is $k = k_1 + k_2$, and for simplicity we have chosen the symmetrical routing of momenta shown above. The value of this Feynman diagram is

$$i\delta\mathcal{M} = \frac{\lambda^2}{2} \int \frac{d^4q}{(2\pi)^4} \frac{1}{(k/2 - q)^2 - m^2 + i\epsilon} \frac{1}{(k/2 + q)^2 - m^2 + i\epsilon}. \quad (7.52)$$

When this integral is evaluated using the methods of Section 6.3, the Wick rotation produces an extra factor of i , so that, below threshold, $\delta\mathcal{M}$ is purely real.

We would like to verify that the integral (7.52) has a discontinuity across the real axis in the physical region $k^0 > 2m$. It is easiest to identify this discontinuity by computing the integral for $k^0 < 2m$, then increasing k^0 by analytic continuation. It is not difficult to compute the integral directly using Feynman parameters (see Problem 7.1). However, it is illuminating to use a less direct approach, as follows.

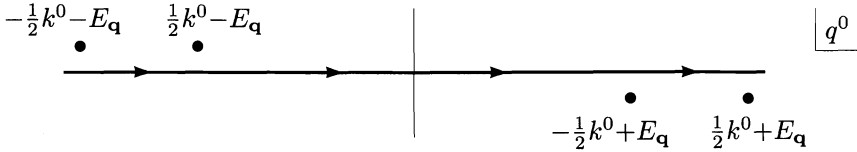
Let us work in the center-of-mass frame, where $k = (k^0, \mathbf{0})$. Then the integrand of (7.52) has four poles in the integration variable q^0 , at the locations

$$q^0 = \frac{1}{2}k^0 \pm (E_{\mathbf{q}} - i\epsilon), \quad q^0 = -\frac{1}{2}k^0 \pm (E_{\mathbf{q}} - i\epsilon).$$

[†]R. E. Cutkosky, *J. Math. Phys.* **1**, 429 (1960).

[‡]These rules are simple only for singularities in the physical region. Away from the physical region, the singularities of three- and higher-point amplitudes can become quite intricate. This subject is reviewed in R. J. Eden, P. V. Landshoff, D. I. Olive, and J. C. Polkinghorne, *The Analytic S-Matrix* (Cambridge University Press, 1966).

Two of these poles lie above the real q^0 axis and two lie below, as shown:



We will close the integration contour downward and pick up the residues of the poles in the lower half-plane. Of these, only the pole at $q^0 = -(1/2)k^0 + E_q$ will contribute to the discontinuity. Note that picking up the residue of this pole is equivalent to replacing

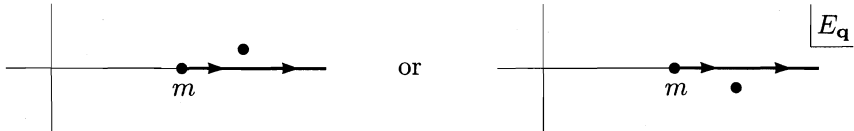
$$\frac{1}{(k/2 + q)^2 - m^2 + i\epsilon} \rightarrow -2\pi i \delta((k/2 + q)^2 - m^2) \quad (7.53)$$

under the dq^0 integral.

The contribution of this pole yields the integral

$$\begin{aligned} i\delta\mathcal{M} &= -2\pi i \frac{\lambda^2}{2} \int \frac{d^3 q}{(2\pi)^4} \frac{1}{2E_q} \frac{1}{(k^0 - E_q)^2 - E_q^2} \\ &= -2\pi i \frac{\lambda^2}{2} \frac{4\pi}{(2\pi)^4} \int_m^\infty dE_q E_q |\mathbf{q}| \frac{1}{2E_q} \frac{1}{k^0(k^0 - 2E_q)}. \end{aligned} \quad (7.54)$$

The integrand in the second line has a pole at $E_q = k^0/2$. When $k^0 < 2m$, this pole does not lie on the integration contour, so $\delta\mathcal{M}$ is manifestly real. When $k^0 > 2m$, however, the pole lies just above or below the contour of integration, depending upon whether k^0 is given a small positive or negative imaginary part:



Thus the integral acquires a discontinuity between $k^2 + i\epsilon$ and $k^2 - i\epsilon$. To compute this discontinuity, apply

$$\frac{1}{k^0 - 2E_q \pm i\epsilon} = P \frac{1}{k^0 - 2E_q} \mp i\pi \delta(k^0 - 2E_q)$$

(where P denotes the principal value). The discontinuity is given by replacing the pole with a delta function. This in turn is equivalent to replacing the original propagator by a delta function:

$$\frac{1}{(k/2 - q)^2 - m^2 + i\epsilon} \rightarrow -2\pi i \delta((k/2 - q)^2 - m^2). \quad (7.55)$$

$$(a) \quad 2\text{Im} \left(\begin{array}{c} \text{Diagram with two wavy lines meeting at a point} \\ | \end{array} \right) = \int d\Pi \left| \begin{array}{c} \text{Diagram with two wavy lines meeting at a point} \\ | \end{array} \right|^2$$

$$(b) \quad 2\text{Im} \left(\begin{array}{c} \text{Diagram with two wavy lines meeting at a circle} \\ | \end{array} \right) = \int d\Pi \left| \begin{array}{c} \text{Diagram with two wavy lines meeting at a circle} \\ | \end{array} \right|^2$$

Figure 7.6. Two contributions to the optical theorem for Bhabha scattering.

Let us now retrace our steps and see what we have proved. Go back to the original integral (7.52), relabel the momenta on the two propagators as p_1, p_2 and substitute

$$\int \frac{d^4 q}{(2\pi)^4} = \int \frac{d^4 p_1}{(2\pi)^4} \int \frac{d^4 p_2}{(2\pi)^4} (2\pi)^4 \delta^{(4)}(p_1 + p_2 - k).$$

We have shown that the discontinuity of the integral is computed by replacing each of the two propagators by a delta function:

$$\frac{1}{p_i^2 - m^2 + i\epsilon} \rightarrow -2\pi i \delta(p_i^2 - m^2). \quad (7.56)$$

The discontinuity of \mathcal{M} comes only from the region of the $d^4 q$ integral in which the two delta functions are simultaneously satisfied. By integrating over the delta functions, we put the momenta p_i on shell and convert the integrals $d^4 p_i$ into integrals over relativistic phase space. What is left over in expression (7.52) is just the factor λ^2 , the square of the leading-order scattering amplitude, and the symmetry factor $(1/2)$, which can be reinterpreted as the symmetry factor for identical bosons in the final state. Thus we have shown that, to order λ^2 on each side of the equation,

$$\begin{aligned} \text{Disc } \mathcal{M}(k) &= 2i \text{Im } \mathcal{M}(k) \\ &= \frac{i}{2} \int \frac{d^3 p_1}{(2\pi)^3} \frac{1}{2E_1} \frac{d^3 p_2}{(2\pi)^3} \frac{1}{2E_2} |\mathcal{M}(k)|^2 (2\pi)^4 \delta^{(4)}(p_1 + p_2 - k). \end{aligned}$$

This explicitly verifies (7.49) to order λ^2 in ϕ^4 theory.

The preceding argument made no essential use of the fact that the two propagators in the diagram had equal masses, or of the fact that these propagators connected to a simple point vertex. Indeed, the analysis can be applied to an arbitrary one-loop diagram. Whenever, in the region of momentum integration of the diagram, two propagators can simultaneously go on-shell, we can follow the argument above to compute a nonzero discontinuity of \mathcal{M} . The value of this discontinuity is given by making the substitution (7.56) for

each of the two propagators. For example, in the order- α^2 Bhabha scattering diagrams shown in Fig. 7.6, we can compute the imaginary parts by cutting through the diagrams as shown and putting the cut propagators on shell using (7.56). The poles of the additional propagators in the diagrams do not contribute to the discontinuities. By integrating over the delta functions as in the previous paragraph, we derive the indicated relations between the imaginary parts of these diagrams and contributions to the total cross section.

Cutkosky proved that this method of computing discontinuities is completely general. The physical discontinuity of any Feynman diagram is given by the following algorithm:

1. Cut through the diagram in all possible ways such that the cut propagators can simultaneously be put on shell.
2. For each cut, replace $1/(p^2 - m^2 + i\epsilon) \rightarrow -2\pi i\delta(p^2 - m^2)$ in each cut propagator, then perform the loop integrals.
3. Sum the contributions of all possible cuts.

Using these *cutting rules*, it is possible to prove the optical theorem (7.49) to all orders in perturbation theory.

Unstable Particles

The cutting rules imply that the generalized optical theorem (7.49) is true not only for S -matrix elements, but for any amplitudes \mathcal{M} that we can define in terms of Feynman diagrams. This fact is extremely useful for dealing with unstable particles, which never appear in asymptotic states.

Recall from Eq. (7.43) that the exact two-point function for a scalar particle has the form

$$\text{---} \circ \text{---} = \frac{i}{p^2 - m_0^2 - M^2(p^2)}.$$

We defined the quantity $-iM^2(p^2)$ as the sum of all 1PI insertions into the boson propagator, but we can equally well think of it as the sum of all amputated diagrams for 1-particle \rightarrow 1-particle “scattering”. The LSZ formula then implies

$$\mathcal{M}(p \rightarrow p) = -ZM^2(p^2). \quad (7.57)$$

We can use this relation and the generalized optical theorem (7.49) to discuss the imaginary part of $M^2(p^2)$.

First consider the familiar case where the scalar boson is stable. In this case, there is no possible final state that can contribute to the right-hand side of (7.49). Thus $M^2(m^2)$ is real. The position of the pole in the propagator is determined by the equation $m^2 - m_0^2 - M^2(m^2) = 0$, which has a real-valued solution m . The pole therefore lies on the real p^2 axis, below the multiparticle branch cut.

Often, however, a particle can decay into two or more lighter particles. In this case $M^2(p^2)$ will acquire an imaginary part, so we must modify our

definitions slightly. Let us define the particle's mass m by the condition

$$m^2 - m_0^2 - \operatorname{Re} M^2(m^2) = 0. \quad (7.58)$$

Then the pole in the propagator is displaced from the real axis:

A Feynman diagram showing a horizontal line with a circular vertex on the left. A vertical line extends downwards from the vertex. A horizontal line extends to the right from the vertex. A small circle is placed on the horizontal line to the right of the vertex.

$$\sim \frac{iZ}{p^2 - m^2 - iZ \operatorname{Im} M^2(p^2)}.$$

If this propagator appears in the s channel of a Feynman diagram, the cross section one computes, in the vicinity of the pole, will have the form

$$\sigma \propto \left| \frac{1}{s - m^2 - iZ \operatorname{Im} M^2(s)} \right|^2. \quad (7.59)$$

This expression closely resembles the relativistic Breit-Wigner formula (4.64) for the cross section in the region of a resonance:

$$\sigma \propto \left| \frac{1}{p^2 - m^2 + i\Gamma} \right|^2. \quad (7.60)$$

The mass m defined by (7.58) is the position of the resonance. If $\operatorname{Im} M^2(m^2)$ is small, so that the resonance in (7.59) is narrow, we can approximate $\operatorname{Im} M^2(s)$ as $\operatorname{Im} M^2(m^2)$ over the width of the resonance; then (7.59) will have precisely the Breit-Wigner form. In this case, we can identify

$$\Gamma = -\frac{Z}{m} \operatorname{Im} M^2(m^2). \quad (7.61)$$

If the resonance is broad, it will show deviations from the Breit-Wigner shape, generally becoming narrower on the leading edge and broader on the trailing edge.

To compute $\operatorname{Im} M^2$, and hence Γ , we could use the definition of M^2 as the sum of 1PI insertions into the propagator. The imaginary parts of the relevant loop diagrams give the decay rate. But the optical theorem (7.49), generalized to Feynman diagrams by the Cutkosky rules, simplifies this procedure. If we take (7.57) as the definition of the matrix element $\mathcal{M}(p \rightarrow p)$, and similarly define the decay matrix elements $\mathcal{M}(p \rightarrow f)$ through their Feynman diagram expansions, then (7.49) implies

$$Z \operatorname{Im} M^2(p^2) = -\operatorname{Im} \mathcal{M}(p \rightarrow p) = -\frac{1}{2} \sum_f \int d\Pi_f |\mathcal{M}(p \rightarrow f)|^2, \quad (7.62)$$

where the sum runs over all possible final states f . The decay rate is therefore

$$\Gamma = \frac{1}{2m} \sum_f \int d\Pi_f |\mathcal{M}(p \rightarrow f)|^2, \quad (7.63)$$

as quoted in Eq. (4.86).

We stress once again that our derivation of this equation applies only to the case of a long-lived unstable particle, so that $\Gamma \ll m$. For a broad resonance, the full energy dependence of $M^2(p^2)$ must be taken into account.

7.4 The Ward-Takahashi Identity

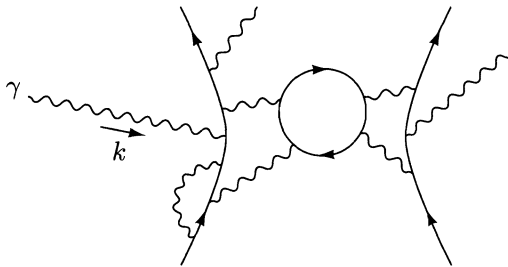
Of the loose ends listed at the beginning of this chapter, only one remains, the proof of the Ward identity. Recall from Section 5.5 that this identity states the following: If $\mathcal{M}(k) = \epsilon_\mu(k)\mathcal{M}^\mu(k)$ is the amplitude for some QED process involving an external photon with momentum k , then this amplitude vanishes if we replace ϵ_μ with k_μ :

$$k_\mu \mathcal{M}^\mu(k) = 0. \quad (7.64)$$

To prove this assertion, it is useful to prove a more general identity for QED correlation functions, called the *Ward-Takahashi identity*. To discuss this more general case we will let \mathcal{M} denote a Fourier-transformed correlation function, in which the external momenta are not necessarily on-shell. The right-hand side of (7.64) will contain nonzero terms in this case; but when we apply the LSZ formula to extract an S -matrix element, those terms will not contribute.

We will prove the Ward-Takahashi identity order by order in α , by looking directly at the Feynman diagrams that contribute to $\mathcal{M}(k)$. The identity is generally not true for individual Feynman diagrams; we must sum over the diagrams for $\mathcal{M}(k)$ at any given order.

Consider a typical diagram for a typical amplitude $\mathcal{M}(k)$:

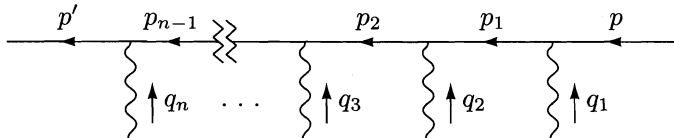


If we remove the photon $\gamma(k)$, we obtain a simpler diagram which is part of a simpler amplitude \mathcal{M}_0 . If we reinsert the photon somewhere else inside the simpler diagram, we again obtain a contribution to $\mathcal{M}(k)$. The crucial observation is that by summing over all the diagrams that contribute to \mathcal{M}_0 , then summing over all possible points of insertion in each of these diagrams, we obtain $\mathcal{M}(k)$. The Ward-Takahashi identity is true individually for each diagram contributing to \mathcal{M}_0 , once we sum over insertion points; this is what we will prove.

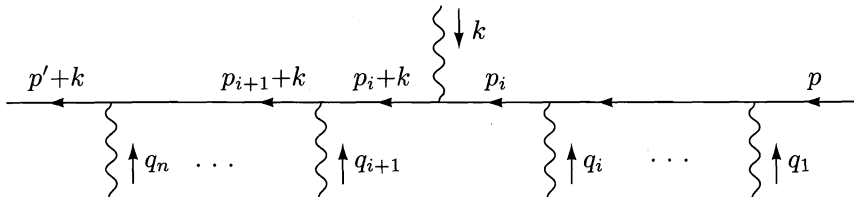
When we insert our photon into one of the diagrams of \mathcal{M}_0 , it must attach either to an electron line that runs out of the diagram to two external points, or to an internal electron loop. Let us consider each of these cases in turn.

First suppose that the electron line runs between external points. Before

we insert our photon $\gamma(k)$, the line looks like this:



The electron propagators have momenta p , $p_1 = p + q_1$, $p_2 = p_1 + q_2$, and so on up to $p' = p_{n-1} + q_n$. If there are n vertices, we can insert our photon in $n+1$ different places. Suppose we insert it after the i th vertex:



The electron propagators to the left of the new photon then have their momenta increased by k .

Let us now look at the values of these diagrams, with the polarization vector $\epsilon_\mu(k)$ replaced by k_μ . The product of k_μ with the new vertex is conveniently written:

$$-ie k_\mu \gamma^\mu = -ie [(\not{p}_i + \not{k} - m) - (\not{p}_i - m)].$$

Multiplying by the adjacent electron propagators, we obtain

$$\frac{i}{\not{p}_i + \not{k} - m} (-ie \not{k}) \frac{i}{\not{p}_i - m} = e \left(\frac{i}{\not{p}_i - m} - \frac{i}{\not{p}_i + \not{k} - m} \right). \quad (7.65)$$

The diagram with the photon inserted at position i therefore has the structure

$$\dots \xrightarrow{\qquad \qquad \qquad \qquad \qquad} \begin{matrix} \not{k} \\ \uparrow q_{i+1} \quad \uparrow q_i \end{matrix} \dots = \dots \left(\frac{i}{\not{p}_{i+1} + \not{k} - m} \right) \gamma^{\lambda_{i+1}} \left(\frac{i}{\not{p}_i - m} - \frac{i}{\not{p}_i + \not{k} - m} \right) \gamma^{\lambda_i} \times \left(\frac{i}{\not{p}_{i-1} - m} \right) \gamma^{\lambda_{i-1}} \dots$$

Similarly, the diagram with the photon inserted at position $i-1$ has the structure

$$\dots \xrightarrow{\qquad \qquad \qquad \qquad \qquad} \begin{matrix} \not{k} \\ \uparrow q_{i+1} \quad \uparrow q_i \end{matrix} \dots = \dots \left(\frac{i}{\not{p}_{i+1} + \not{k} - m} \right) \gamma^{\lambda_{i+1}} \left(\frac{i}{\not{p}_i - m} \right) \gamma^{\lambda_i} \times \left(\frac{i}{\not{p}_{i-1} - m} - \frac{i}{\not{p}_{i-1} + \not{k} - m} \right) \gamma^{\lambda_{i-1}} \dots$$

Note that the first term of this expression cancels the second term of the previous expression. A similar cancellation occurs between any other pair of

diagrams with adjacent insertions. When we sum over all possible insertion points along the line, everything cancels except the unpaired terms at the ends. The unpaired term coming from insertion after the last vertex (on the far left) is just e times the value of the original diagram; the other unpaired term, from insertion before the first vertex, is identical except for a minus sign and the replacement of p by $p + k$ everywhere. Diagrammatically, our result is

$$\sum_{\text{insertion points}} k_\mu \cdot \left(\begin{array}{c} \mu \text{ wavy line} \\ \text{--- wavy line} \\ \vdots \\ p \end{array} \right) = e \left(\begin{array}{c} q-k \text{ wavy line} \\ \text{--- wavy line} \\ \vdots \\ p \end{array} \right) - \left(\begin{array}{c} q \text{ wavy line} \\ \text{--- wavy line} \\ \vdots \\ p+k \end{array} \right), \quad (7.66)$$

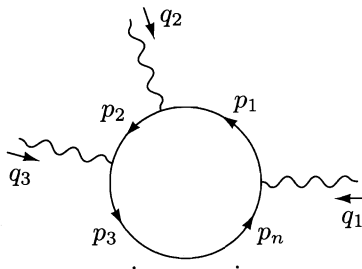
where we have renamed $p' + k \rightarrow q$ for the sake of symmetry.

In each diagram on the left-hand side of (7.66), the momentum entering the electron line is p and the momentum exiting is q . According to the LSZ formula, we can extract from each diagram a contribution to an S -matrix element by taking the coefficient of the product of poles

$$\left(\frac{i}{q-m} \right) \left(\frac{i}{p-m} \right).$$

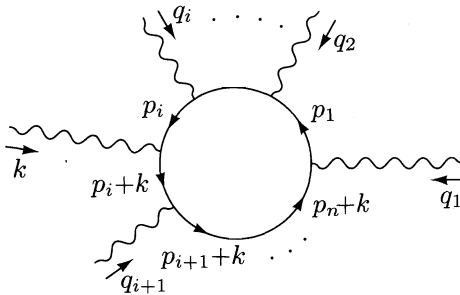
The terms on the right-hand side of (7.66) each contain one of these poles, but neither contains both poles. Thus the right-hand side of (7.66) contributes nothing to the S -matrix.*

To complete the proof of the Ward-Takahashi identity, we must consider the case in which our photon attaches to an internal electron loop. Before the insertion of the photon, a typical loop looks like this:



*This step of the argument is straightforward only if we have arranged the perturbation series so that the propagator contains m rather than m_0 . We will do this in Chapter 10.

The electron propagators have momenta $p_1, p_1 + q_2 = p_2$, and so on up to p_n . Suppose now that we insert the photon $\gamma(k)$ between vertices i and $i+1$:



We now have an additional momentum k running around the loop from the new vertex; by convention, this momentum exits at vertex 1.

To evaluate the sum over all such insertions into the loop, apply identity (7.65) to each diagram. For the diagram in which the photon is inserted between vertices 1 and 2, we obtain

$$\begin{aligned} -e \int \frac{d^4 p_1}{(2\pi)^4} \text{tr} & \left[\left(\frac{i}{\not{p}_n + \not{k} - m} \right) \gamma^{\lambda_n} \dots \left(\frac{i}{\not{p}_2 + \not{k} - m} \right) \gamma^{\lambda_2} \right. \\ & \times \left. \left(\frac{i}{\not{p}_1 - m} - \frac{i}{\not{p}_1 + \not{k} - m} \right) \gamma^{\lambda_1} \right]. \end{aligned}$$

The first term will be canceled by one of the terms from the diagram with the photon inserted between vertices 2 and 3. Similar cancellations take place between terms from other pairs of adjacent insertions. When we sum over all n insertion points we are left with

$$\begin{aligned} -e \int \frac{d^4 p_1}{(2\pi)^4} \text{tr} & \left[\left(\frac{i}{\not{p}_n - m} \right) \gamma^{\lambda_n} \left(\frac{i}{\not{p}_{n-1} - m} \right) \gamma^{\lambda_{n-1}} \dots \left(\frac{i}{\not{p}_1 - m} \right) \gamma^{\lambda_1} \right. \\ & \left. - \left(\frac{i}{\not{p}_n + \not{k} - m} \right) \gamma^{\lambda_n} \left(\frac{i}{\not{p}_{n-1} + \not{k} - m} \right) \gamma^{\lambda_{n-1}} \dots \left(\frac{i}{\not{p}_1 + \not{k} - m} \right) \gamma^{\lambda_1} \right]. \end{aligned} \quad (7.67)$$

Shifting the integration variable from p_1 to $p_1 + k$ in the second term, we see that the two remaining terms cancel. Thus the diagrams in which the photon is inserted along a closed loop add up to zero.

We are now ready to assemble the pieces of the proof. Suppose that the amplitude \mathcal{M} has $2n$ external electron lines, n incoming and n outgoing. Label

the incoming momenta p_i and the outgoing momenta q_i :

$$\mathcal{M}(k; p_1 \dots p_n; q_1 \dots q_n) = \text{Diagram with shaded circle} \quad k \quad q_1 \dots q_n$$

(The amplitude can also involve an arbitrary number of additional external photons.) The amplitude \mathcal{M}_0 lacks the photon $\gamma(k)$ but is otherwise identical. To form $k_\mu \mathcal{M}^\mu$ from \mathcal{M}_0 we must sum over all diagrams that contribute to \mathcal{M}_0 , and for each diagram, sum over all points at which the photon could be inserted. Summing over insertion points along an internal loop in any diagram gives zero. Summing over insertion points along a through-going line in any diagram gives a contribution of the form (7.66). Summing over *all* insertion points for any particular diagram, we obtain

$$\sum_{\text{insertion points}} k_\mu \cdot \left(\text{Diagram with shaded circle} \right) = e \sum_i \left(\text{Diagram with shaded circle} - \text{Diagram with shaded circle} \right),$$

where the shaded circle represents any particular diagram that contributes to \mathcal{M}_0 . Summing over all such diagrams, we finally obtain

$$k_\mu \mathcal{M}^\mu(k; p_1 \dots p_n; q_1 \dots q_n) = e \sum_i \left[\mathcal{M}_0(p_1 \dots p_n; q_1 \dots (q_i - k) \dots) - \mathcal{M}_0(p_1 \dots (p_i + k) \dots; q_1 \dots q_n) \right]. \quad (7.68)$$

This is the Ward-Takahashi identity for correlation functions in QED. We saw below (7.66) that the right-hand side does not contribute to the S -matrix; thus in the special case where \mathcal{M} is an S -matrix element, Eq. (7.68) reduces to the Ward identity (7.64).

Before discussing this identity further, we should mention a potential flaw in the above proof. In order to find the necessary cancellation in Eq. (7.67), we had to shift the integration variable by a constant. If the integral diverges, however, this shift is not permissible. Similarly, there may be divergent loop-momentum integrals in the expressions leading to Eq. (7.66). Here there is no explicit shift in the proof, but in practice one does generally perform a shift while evaluating the integrals. In either case, ultraviolet divergences can potentially invalidate the Ward-Takahashi identity. We will see an example of this problem, as well as a general solution to it, in the next section.

The simplest example of the Ward-Takahashi identity involves, on the left-hand side, the three-point function with one entering and one exiting electron and one external photon:

$$k_\mu \cdot \left(\mu \sim \begin{array}{c} \text{---} \\ \text{---} \\ k \end{array} \right) = e \left(\begin{array}{c} \text{---} \\ \text{---} \\ p \end{array} - \begin{array}{c} \text{---} \\ \text{---} \\ p+k \end{array} \right)$$

The quantities on the right-hand side are exact electron propagators, evaluated at p and $(p + k)$ respectively. Label these quantities $S(p)$ and $S(p + k)$; from Eq. (7.23),

$$S(p) = \frac{i}{\not{p} - m - \Sigma(p)}.$$

The full three-point amplitude on the left-hand side can be rewritten, just as in Eq. (7.44), as a product of full propagators for the entering and exiting electrons, times an amputated scattering diagram. In this case, the amputated function is just the vertex $\Gamma^\mu(p + k, p)$. Then the Ward-Takahashi identity reads:

$$S(p + k) [-ie k_\mu \Gamma^\mu(p + k, p)] S(p) = e(S(p) - S(p + k)).$$

To simplify this equation, multiply, on the left and right respectively, by the Dirac matrices $S^{-1}(p + k)$ and $S^{-1}(p)$. This gives

$$-ie k_\mu \Gamma^\mu(p + k, p) = S^{-1}(p + k) - S^{-1}(p). \quad (7.69)$$

Often the term *Ward-Takahashi identity* is used to mean only this special case.

We can use identity (7.69) to obtain the general relation between the renormalization factors Z_1 and Z_2 . We defined Z_1 in (7.47) by the relation

$$\Gamma^\mu(p + k, p) \rightarrow Z_1^{-1} \gamma^\mu \quad \text{as } k \rightarrow 0.$$

We defined Z_2 as the residue of the pole in $S(p)$:

$$S(p) \sim \frac{iZ_2}{\not{p} - m}.$$

Setting p near mass shell and expanding (7.69) about $k = 0$, we find for the first-order terms on the left and right

$$-iZ_1^{-1} \not{k} = -iZ_2^{-1} \not{k},$$

that is,

$$Z_1 = Z_2. \quad (7.70)$$

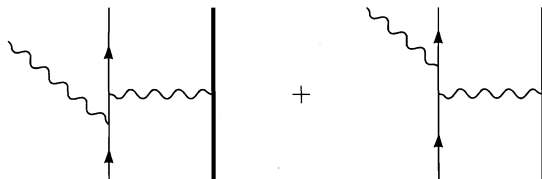
Thus, the Ward-Takahashi identity guarantees the exact cancellation of infinite rescaling factors in the electron scattering amplitude that we found at the end of Section 7.2. When combined with the correct formal expression

(7.46) for the electron form factors, this identity guarantees that $F_1(0) = 1$ to all orders in perturbation theory.

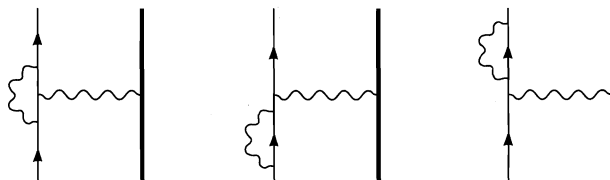
Often, in the literature, the terms *Ward identity*, *current conservation*, and *gauge invariance* are used interchangeably. This is quite natural, since the Ward identity is the diagrammatic expression of the conservation of the electric current, which is in turn a consequence of gauge invariance. In this book, however, we will distinguish these three concepts. By *gauge invariance* we mean the fundamental symmetry of the Lagrangian; by *current conservation* we mean the equation of motion that follows from this symmetry; and by the *Ward identity* we mean the diagrammatic identity that imposes the symmetry on quantum mechanical amplitudes.

7.5 Renormalization of the Electric Charge

At the beginning of Chapter 6 we set out to study the order- α radiative corrections to electron scattering from a heavy target. We evaluated (at least in the classical limit) the bremsstrahlung diagrams,

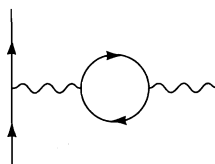


and also the corrections due to virtual photons:



Our discussion of field-strength renormalization in this chapter has finally clarified the role of the last two diagrams. In particular, we have seen that the Ward identity, through the relation $Z_1 = Z_2$, insures that the sum of the virtual photon corrections vanishes as the momentum transfer q goes to zero.

There is one remaining type of radiative correction to this process:



This is the order- α *vacuum polarization* diagram, also known as the *photon self-energy*. It can be viewed as a modification to the photon structure by a

virtual electron-positron pair. This diagram will alter the effective field $A^\mu(x)$ seen by the scattered electron. It can potentially shift the overall strength of this field, and can also change its dependence on x (or in Fourier space, on q). In this section we will compute this diagram, and see that it has both of these effects.

Overview of Charge Renormalization

Before beginning a detailed calculation, let's ask what kind of an answer we expect and what its interpretation will be. The interesting part of the diagram is the electron loop:

$$\begin{array}{c} \text{Diagram of a fermion loop: a circle with a wavy line entering from the left labeled } \mu \text{ and } q, \text{ and a wavy line exiting to the right labeled } \nu \text{ and } k+q. \\ \text{The loop is closed by a curved arrow pointing clockwise.} \end{array} = (-ie)^2(-1) \int \frac{d^4k}{(2\pi)^4} \text{tr} \left[\gamma^\mu \frac{i}{k-m} \gamma^\nu \frac{i}{k+q-m} \right] \equiv i\Pi_2^{\mu\nu}(q). \quad (7.71)$$

(The fermion loop factor of (-1) was derived in Eq. (4.120).) More generally, let us define $i\Pi^{\mu\nu}(q)$ to be the sum of all 1-particle-irreducible insertions into the photon propagator,

$$\text{Diagram of a 1PI insertion: a wavy line entering from the left labeled } \mu \text{ and } q, \text{ passing through a shaded circle labeled "1PI", and exiting to the right labeled } \nu. \equiv i\Pi^{\mu\nu}(q), \quad (7.72)$$

so that $\Pi_2^{\mu\nu}(q)$ is the second-order (in e) contribution to $\Pi^{\mu\nu}(q)$.

The only tensors that can appear in $\Pi^{\mu\nu}(q)$ are $g^{\mu\nu}$ and $q^\mu q^\nu$. The Ward identity, however, tells us that $q_\mu \Pi^{\mu\nu}(q) = 0$. This implies that $\Pi^{\mu\nu}(q)$ is proportional to the projector $(g^{\mu\nu} - q^\mu q^\nu/q^2)$. Furthermore, we expect that $\Pi^{\mu\nu}(q)$ will not have a pole at $q^2 = 0$; the only obvious source of such a pole would be a single-massless-particle intermediate state, which cannot occur in any 1PI diagram.[†] It is therefore convenient to extract the tensor structure from $\Pi^{\mu\nu}$ in the following way:

$$\Pi^{\mu\nu}(q) = (q^2 g^{\mu\nu} - q^\mu q^\nu) \Pi(q^2), \quad (7.73)$$

where $\Pi(q^2)$ is regular at $q^2 = 0$.

Using this notation, the exact photon two-point function is

$$\begin{aligned} \text{Diagram of the exact photon propagator: a wavy line entering from the left labeled } \mu \text{ and } q, \text{ passing through a shaded circle, and exiting to the right labeled } \nu. &= \text{Diagram of the free photon propagator: a wavy line entering from the left labeled } \mu \text{ and } q, \text{ and a wavy line exiting to the right labeled } \nu. + \text{Diagram of a 1PI insertion: a wavy line entering from the left labeled } \mu \text{ and } q, \text{ passing through a shaded circle labeled "1PI", and exiting to the right labeled } \nu. + \dots \\ &= \frac{-ig_{\mu\nu}}{q^2} + \frac{-ig_{\mu\rho}}{q^2} \left[i(q^2 g^{\rho\sigma} - q^\rho q^\sigma) \Pi(q^2) \right] \frac{-ig_{\sigma\nu}}{q^2} + \dots \end{aligned}$$

[†]One can prove that there is no such pole, but the proof is nontrivial. Schwinger has shown that, in two spacetime dimensions, the singularity in Π_2 due to a pair of massless fermions is a pole rather than a cut; this is a famous counterexample to our argument. There is no such problem in four dimensions.

$$= \frac{-ig_{\mu\nu}}{q^2} + \frac{-ig_{\mu\rho}}{q^2} \Delta_\nu^\rho \Pi(q^2) + \frac{-ig_{\mu\rho}}{q^2} \Delta_\sigma^\rho \Delta_\nu^\sigma \Pi^2(q^2) + \dots,$$

where $\Delta_\nu^\rho \equiv \delta_\nu^\rho - q^\rho q_\nu/q^2$. Noting that $\Delta_\sigma^\rho \Delta_\nu^\sigma = \Delta_\nu^\rho$, we can simplify this expression to

$$\begin{aligned} \text{Diagram: } & \mu \sim \text{circle} \sim \nu = \frac{-ig_{\mu\nu}}{q^2} + \frac{-ig_{\mu\rho}}{q^2} \left(\delta_\nu^\rho - \frac{q^\rho q_\nu}{q^2} \right) (\Pi(q^2) + \Pi^2(q^2) + \dots) \\ & = \frac{-i}{q^2(1 - \Pi(q^2))} \left(g_{\mu\nu} - \frac{q_\mu q_\nu}{q^2} \right) + \frac{-i}{q^2} \left(\frac{q_\mu q_\nu}{q^2} \right). \end{aligned} \quad (7.74)$$

In any S -matrix element calculation, at least one end of this exact propagator will connect to a fermion line. When we sum over all places along the line where it could connect, we must find, according to the Ward identity, that terms proportional to q_μ or q_ν vanish. For the purposes of computing S -matrix elements, therefore, we can abbreviate

$$\text{Diagram: } \mu \sim \text{circle} \sim \nu = \frac{-ig_{\mu\nu}}{q^2(1 - \Pi(q^2))}. \quad (7.75)$$

Notice that as long as $\Pi(q^2)$ is regular at $q^2 = 0$, the exact propagator always has a pole at $q^2 = 0$. In other words, the photon remains absolutely massless at all orders in perturbation theory. This claim depends strongly on our use of the Ward identity in (7.73). If, for example, $\Pi^{\mu\nu}(q)$ contained a term $M^2 g^{\mu\nu}$ (with no compensating $q^\mu q^\nu$ term), the photon mass would be shifted to M .

The residue of the $q^2 = 0$ pole is

$$\frac{1}{1 - \Pi(0)} \equiv Z_3.$$

The amplitude for any low- q^2 scattering process will be shifted by this factor, relative to the tree-level approximation:

$$\text{or } \dots \frac{e^2 g_{\mu\nu}}{q^2} \dots \rightarrow \dots \frac{Z_3 e^2 g_{\mu\nu}}{q^2} \dots$$

Since a factor of e lies at each end of the photon propagator, we can conveniently account for this shift by making the replacement $e \rightarrow \sqrt{Z_3} e$. This replacement is called *charge renormalization*; it is in many ways analogous to the mass renormalization introduced in Section 7.1. Note in particular that the “physical” electron charge measured in experiments is $\sqrt{Z_3} e$. We will therefore shift our notation and call this quantity simply e . From now on we

will refer to the “bare” charge (the quantity that multiplies $A_\mu \bar{\psi} \gamma^\mu \psi$ in the Lagrangian) as e_0 . We then have

$$(\text{physical charge}) = e = \sqrt{Z_3} e_0 = \sqrt{Z_3} \cdot (\text{bare charge}). \quad (7.76)$$

To lowest order, $Z_3 = 1$ and $e = e_0$.

In addition to this constant shift in the strength of the electric charge, $\Pi(q^2)$ has another effect. Consider a scattering process with nonzero q^2 , and suppose that we have computed $\Pi(q^2)$ to leading order in α : $\Pi(q^2) \approx \Pi_2(q^2)$. The amplitude for the process will then involve the quantity

$$\frac{-ig_{\mu\nu}}{q^2} \left(\frac{e_0^2}{1 - \Pi(q^2)} \right) \underset{\mathcal{O}(\alpha)}{=} \frac{-ig_{\mu\nu}}{q^2} \left(\frac{e^2}{1 - [\Pi_2(q^2) - \Pi_2(0)]} \right).$$

(Swapping e^2 for e_0^2 does not matter to lowest order.) The quantity in parentheses can be interpreted as a q^2 -dependent electric charge. The full effect of replacing the tree-level photon propagator with the exact photon propagator is therefore to replace

$$\alpha_0 \rightarrow \alpha_{\text{eff}}(q^2) = \frac{e_0^2/4\pi}{1 - \Pi(q^2)} \underset{\mathcal{O}(\alpha)}{=} \frac{\alpha}{1 - [\Pi_2(q^2) - \Pi_2(0)]}. \quad (7.77)$$

(To leading order we could just as well bring the Π -terms into the numerator; but we will see in Chapter 12 that in this form, the expression is true to all orders when Π_2 is replaced by Π .)

Computation of Π_2

Having worked so hard to interpret $\Pi_2(q^2)$, we had better calculate it. Going back to (7.71), we have

$$\begin{aligned} i\Pi_2^{\mu\nu}(q) &= -(-ie)^2 \int \frac{d^4 k}{(2\pi)^4} \text{tr} \left[\gamma^\mu \frac{i(k+m)}{k^2 - m^2} \gamma^\nu \frac{i(k+q+m)}{(k+q)^2 - m^2} \right] \\ &= -4e^2 \int \frac{d^4 k}{(2\pi)^4} \frac{k^\mu (k+q)^\nu + k^\nu (k+q)^\mu - g^{\mu\nu} (k \cdot (k+q) - m^2)}{(k^2 - m^2)((k+q)^2 - m^2)}. \end{aligned} \quad (7.78)$$

We have written e and m instead of e_0 and m_0 for convenience, since the difference would give only an order- α^2 contribution to $\Pi^{\mu\nu}$.

Now introduce a Feynman parameter to combine the denominator factors:

$$\begin{aligned} \frac{1}{(k^2 - m^2)((k+q)^2 - m^2)} &= \int_0^1 dx \frac{1}{(k^2 + 2xk \cdot q + xq^2 - m^2)^2} \\ &= \int_0^1 dx \frac{1}{(\ell^2 + x(1-x)q^2 - m^2)^2}, \end{aligned}$$

where $\ell = k + xq$. In terms of ℓ , the numerator of (7.78) is

$$\begin{aligned} \text{Numerator} &= 2\ell^\mu\ell^\nu - g^{\mu\nu}\ell^2 - 2x(1-x)q^\mu q^\nu + g^{\mu\nu}(m^2 + x(1-x)q^2) \\ &\quad + (\text{terms linear in } \ell). \end{aligned}$$

Performing a Wick rotation and substituting $\ell^0 = i\ell_E^0$, we obtain

$$\begin{aligned} i\Pi_2^{\mu\nu}(q) &= -4ie^2 \int_0^1 dx \int \frac{d^4\ell_E}{(2\pi)^4} \\ &\times \frac{-\frac{1}{2}g^{\mu\nu}\ell_E^2 + g^{\mu\nu}\ell_E^2 - 2x(1-x)q^\mu q^\nu + g^{\mu\nu}(m^2 + x(1-x)q^2)}{(\ell_E^2 + \Delta)^2}, \end{aligned} \tag{7.79}$$

where $\Delta = m^2 - x(1-x)q^2$. This integral is very badly ultraviolet divergent. If we were to cut it off at $\ell_E = \Lambda$, we would find for the leading term,

$$i\Pi_2^{\mu\nu}(q) \propto e^2 \Lambda^2 g^{\mu\nu},$$

with no compensating $q^\mu q^\nu$ term. This result violates the Ward identity; it would give the photon an infinite mass $M \propto e\Lambda$.

Our proof of the Ward identity has failed, in precisely the way anticipated at the end of the previous section: The shift of the integration variable in (7.67) is not permissible when the integral is divergent. In our present calculation, the failure of the Ward identity is catastrophic: It leads to an infinite photon mass,[‡] in conflict with experiment. Fortunately, there is a way to rescue the Ward identity.

In the above analysis we regulated the divergent integral in the most straightforward and most naive way: by cutting it off at a large momentum Λ . But other regulators are possible, and some will in fact preserve the Ward identity. In our computations of the vertex and electron self-energy diagrams, we used a Pauli-Villars regulator. This regulator preserved the relation $Z_1 = Z_2$, a consequence of the Ward identity; a naive cutoff does not (see Problem 7.2). We could fix our present computation by introducing Pauli-Villars fermions. Unfortunately, several sets of fermions are required, making the method rather complicated.* We will use a simpler method, *dimensional regularization*, due to 't Hooft and Veltman.[†] Dimensional regularization preserves the symmetries of QED and also of a wide class of more general theories.

The question of which regulator to use has no *a priori* answer in quantum field theory. Often the choice has no effect on the predictions of the theory.

[‡]We could still make the observed photon mass zero by adding a compensating infinite photon mass term to the Lagrangian. More generally, we could add terms to the Lagrangian to make the Ward identity valid for any n -point correlation function. This procedure would give the same results as the one we are about to follow, but would be much more complicated.

*This method is presented in Bjorken and Drell (1964), p. 154.

[†]G. 't Hooft and M. J. G. Veltman, *Nucl. Phys.* **B44**, 189 (1972).

When two regulators give different answers for observable quantities, it is generally because some symmetry (such as the Ward identity) is being violated by one (or both) of them. In these cases we take the symmetry to be fundamental and demand that it be preserved by the regulator. But the validity of this choice cannot be proven; we are adopting the symmetry as a new axiom.

Dimensional Regularization

The idea of dimensional regularization is very simple to state: Compute the Feynman diagram as an analytic function of the dimensionality of spacetime, d . For sufficiently small d , any loop-momentum integral will converge and therefore the Ward identity can be proved. The final expression for any observable quantity should have a well-defined limit as $d \rightarrow 4$.

Let us do a practice calculation to see how this technique works. We consider spacetime to have one time dimension and $(d-1)$ space dimensions. Then we can Wick-rotate Feynman integrals as before, to give integrals over a d -dimensional Euclidean space. A typical example is

$$\int \frac{d^d \ell_E}{(2\pi)^d} \frac{1}{(\ell_E^2 + \Delta)^2} = \int \frac{d\Omega_d}{(2\pi)^d} \cdot \int_0^\infty d\ell_E \frac{\ell_E^{d-1}}{(\ell_E^2 + \Delta)^2}. \quad (7.80)$$

The first factor in (7.80) contains the area of a unit sphere in d dimensions. To compute it, use the following trick:

$$\begin{aligned} (\sqrt{\pi})^d &= \left(\int dx e^{-x^2} \right)^d = \int d^d x \exp\left(-\sum_{i=1}^d x_i^2\right) \\ &= \int d\Omega_d \int_0^\infty dx x^{d-1} e^{-x^2} = \left(\int d\Omega_d \right) \cdot \frac{1}{2} \int_0^\infty d(x^2) (x^2)^{\frac{d}{2}-1} e^{-(x^2)} \\ &= \left(\int d\Omega_d \right) \cdot \frac{1}{2} \Gamma(d/2). \end{aligned}$$

So the area of a d -dimensional unit sphere is

$$\int d\Omega_d = \frac{2\pi^{d/2}}{\Gamma(d/2)}. \quad (7.81)$$

This formula reproduces the familiar special cases:

d	$\Gamma(d/2)$	$\int d\Omega_d$
1	$\sqrt{\pi}$	2
2	1	2π
3	$\sqrt{\pi}/2$	4π
4	1	$2\pi^2$

The second factor in (7.80) is

$$\begin{aligned} \int_0^\infty d\ell \frac{\ell^{d-1}}{(\ell^2 + \Delta)^2} &= \frac{1}{2} \int_0^\infty d(\ell^2) \frac{(\ell^2)^{\frac{d}{2}-1}}{(\ell^2 + \Delta)^2} \\ &= \frac{1}{2} \left(\frac{1}{\Delta} \right)^{2-\frac{d}{2}} \int_0^1 dx x^{1-\frac{d}{2}} (1-x)^{\frac{d}{2}-1}, \end{aligned}$$

where we have substituted $x = \Delta/(\ell^2 + \Delta)$ in the second line. Using the definition of the beta function,

$$\int_0^1 dx x^{\alpha-1} (1-x)^{\beta-1} = B(\alpha, \beta) = \frac{\Gamma(\alpha)\Gamma(\beta)}{\Gamma(\alpha+\beta)}, \quad (7.82)$$

we can easily evaluate the integral over x . The final result for the d -dimensional integral is

$$\int \frac{d^d \ell_E}{(2\pi)^d} \frac{1}{(\ell_E^2 + \Delta)^2} = \frac{1}{(4\pi)^{d/2}} \frac{\Gamma(2-\frac{d}{2})}{\Gamma(2)} \left(\frac{1}{\Delta} \right)^{2-\frac{d}{2}}.$$

Since $\Gamma(z)$ has isolated poles at $z = 0, -1, -2, \dots$, this integral has isolated poles at $d = 4, 6, 8, \dots$. To find the behavior near $d = 4$, define $\epsilon = 4 - d$, and use the approximation[‡]

$$\Gamma(2-\frac{d}{2}) = \Gamma(\epsilon/2) = \frac{2}{\epsilon} - \gamma + \mathcal{O}(\epsilon), \quad (7.83)$$

where $\gamma \approx .5772$ is the Euler-Mascheroni constant. (This constant will always cancel in observable quantities.) The integral is then

$$\int \frac{d^d \ell_E}{(2\pi)^d} \frac{1}{(\ell_E^2 + \Delta)^2} \xrightarrow{d \rightarrow 4} \frac{1}{(4\pi)^2} \left(\frac{2}{\epsilon} - \log \Delta - \gamma + \log(4\pi) + \mathcal{O}(\epsilon) \right). \quad (7.84)$$

When we defined this integral with a Pauli-Villars regulator in Eq. (7.18), we found

$$\int \frac{d^4 \ell_E}{(2\pi)^4} \frac{1}{(\ell_E^2 + \Delta)^2} \xrightarrow{\Lambda \rightarrow \infty} \frac{1}{(4\pi)^2} \left(\log \frac{x\Lambda^2}{\Delta} + \mathcal{O}(\Lambda^{-1}) \right).$$

Thus the $1/\epsilon$ pole in dimensional regularization corresponds to a logarithmic divergence in the momentum integral. Note the curious fact that (7.84)

[‡]This expansion follows immediately from the infinite product representation

$$\frac{1}{\Gamma(z)} = z e^{\gamma z} \prod_{n=1}^{\infty} \left(1 + \frac{z}{n} \right) e^{-z/n}.$$

involves the logarithm of Δ , a dimensionful quantity. The scale of the logarithm is hidden in the $1/\epsilon$ term, and appears explicitly when the divergence is canceled.

You can easily verify the more general integration formulae,

$$\int \frac{d^d \ell_E}{(2\pi)^d} \frac{1}{(\ell_E^2 + \Delta)^n} = \frac{1}{(4\pi)^{d/2}} \frac{\Gamma(n - \frac{d}{2})}{\Gamma(n)} \left(\frac{1}{\Delta}\right)^{n - \frac{d}{2}}; \quad (7.85)$$

$$\int \frac{d^d \ell_E}{(2\pi)^d} \frac{\ell_E^2}{(\ell_E^2 + \Delta)^n} = \frac{1}{(4\pi)^{d/2}} \frac{d}{2} \frac{\Gamma(n - \frac{d}{2} - 1)}{\Gamma(n)} \left(\frac{1}{\Delta}\right)^{n - \frac{d}{2} - 1}. \quad (7.86)$$

In d dimensions, $g^{\mu\nu}$ obeys $g_{\mu\nu}g^{\mu\nu} = d$. Thus, if the numerator of a symmetric integrand contains $\ell^\mu\ell^\nu$, we should replace

$$\ell^\mu\ell^\nu \rightarrow \frac{1}{d} \ell^2 g^{\mu\nu}, \quad (7.87)$$

in analogy with Eq. (6.46). In QED, the Dirac matrices can be manipulated as a set of d matrices satisfying

$$\{\gamma^\mu, \gamma^\nu\} = 2g^{\mu\nu}, \quad \text{tr}[1] = 4. \quad (7.88)$$

In manipulating Eq. (7.78), these rules give the same result as the purely four-dimensional rules. However, in the evaluation of other diagrams, there are additional contributions of order ϵ . In particular, the contraction identities (5.9) are modified in $d = 4 - \epsilon$ to

$$\begin{aligned} \gamma^\mu\gamma^\nu\gamma_\mu &= -(2 - \epsilon)\gamma^\nu \\ \gamma^\mu\gamma^\nu\gamma^\rho\gamma_\mu &= 4g^{\nu\rho} - \epsilon\gamma^\nu\gamma^\rho \\ \gamma^\mu\gamma^\nu\gamma^\rho\gamma^\sigma\gamma_\mu &= -2\gamma^\sigma\gamma^\rho\gamma^\nu + \epsilon\gamma^\nu\gamma^\rho\gamma^\sigma. \end{aligned} \quad (7.89)$$

These extra terms can contribute to the final value of the Feynman diagram if they multiply a factor ϵ^{-1} from a divergent integral. In QED at one-loop order, such extra terms appear in the vertex and self-energy diagrams but cancel when these diagrams are combined to compute an observable quantity.

Computation of Π_2 , Continued

Now let us apply these dimensional regularization formulae to the momentum integral in (7.79). The unpleasant terms with ℓ^2 in the numerator give

$$\begin{aligned} \int \frac{d^d \ell_E}{(2\pi)^d} \frac{(-\frac{2}{d} + 1)g^{\mu\nu}\ell_E^2}{(\ell_E^2 + \Delta)^2} &= \frac{-1}{(4\pi)^{d/2}} (1 - \frac{d}{2}) \Gamma(1 - \frac{d}{2}) \left(\frac{1}{\Delta}\right)^{1 - \frac{d}{2}} g^{\mu\nu} \\ &= \frac{1}{(4\pi)^{d/2}} \Gamma(2 - \frac{d}{2}) \left(\frac{1}{\Delta}\right)^{2 - \frac{d}{2}} \cdot (-\Delta g^{\mu\nu}). \end{aligned}$$

We would have expected a pole at $d = 2$, since the quadratic divergence in 4 dimensions becomes a logarithmic divergence in 2 dimensions. But the pole cancels. The Ward identity is working.

Evaluating the remaining terms in (7.79) and using $\Delta = m^2 - x(1-x)q^2$, we obtain

$$\begin{aligned} i\Pi_2^{\mu\nu}(q) &= -4ie^2 \int_0^1 dx \frac{1}{(4\pi)^{d/2}} \frac{\Gamma(2-\frac{d}{2})}{\Delta^{2-d/2}} \\ &\quad \times [g^{\mu\nu}(-m^2 + x(1-x)q^2) + g^{\mu\nu}(m^2 + x(1-x)q^2) - 2x(1-x)q^\mu q^\nu] \\ &= (q^2 g^{\mu\nu} - q^\mu q^\nu) \cdot i\Pi_2(q^2), \end{aligned}$$

where

$$\begin{aligned} \Pi_2(q^2) &= \frac{-8e^2}{(4\pi)^{d/2}} \int_0^1 dx x(1-x) \frac{\Gamma(2-\frac{d}{2})}{\Delta^{2-d/2}} \\ &\xrightarrow{d \rightarrow 4} -\frac{2\alpha}{\pi} \int_0^1 dx x(1-x) \left(\frac{2}{\epsilon} - \log \Delta - \gamma + \log(4\pi) \right) \quad (\epsilon = 4 - d). \end{aligned} \quad (7.90)$$

With dimensional regularization, $\Pi_2^{\mu\nu}(q)$ indeed takes the form required by the Ward identity. But it is still logarithmically divergent.

We can now compute the order- α shift in the electric charge:

$$\frac{e^2 - e_0^2}{e_0^2} = \delta Z_3 \underset{\mathcal{O}(\alpha)}{=} \Pi_2(0) \approx -\frac{2\alpha}{3\pi\epsilon}.$$

The bare charge is infinitely larger than the observed charge. But this difference is not observable. What can be observed is the q^2 dependence of the effective electric charge (7.77). This quantity depends on the difference

$$\widehat{\Pi}_2(q^2) \equiv \Pi_2(q^2) - \Pi_2(0) = -\frac{2\alpha}{\pi} \int_0^1 dx x(1-x) \log \left(\frac{m^2}{m^2 - x(1-x)q^2} \right), \quad (7.91)$$

which is independent of ϵ in the limit $\epsilon \rightarrow 0$. For the rest of this section we will investigate what physics this expression contains.

Interpretation of Π_2

First consider the analytic structure of $\widehat{\Pi}_2(q^2)$. For $q^2 < 0$, as is the case when the photon propagator is in the t - or u -channel, $\widehat{\Pi}_2(q^2)$ is manifestly real and analytic. But for an s -channel process, q^2 will be positive. The logarithm function has a branch cut when its argument becomes negative, that is, when

$$m^2 - x(1-x)q^2 < 0.$$

The product $x(1-x)$ is at most $1/4$, so $\widehat{\Pi}_2(q^2)$ has a branch cut beginning at

$$q^2 = 4m^2,$$

at the threshold for creation of a real electron-positron pair.

Let us calculate the imaginary part of $\widehat{\Pi}_2$ for $q^2 > 4m^2$. For any fixed q^2 , the x -values that contribute are between the points $x = \frac{1}{2} \pm \frac{1}{2}\beta$, where $\beta = \sqrt{1 - 4m^2/q^2}$. Since $\text{Im}[\log(-X \pm i\epsilon)] = \pm\pi$, we have

$$\begin{aligned} \text{Im}[\widehat{\Pi}_2(q^2 \pm i\epsilon)] &= -\frac{2\alpha}{\pi} (\pm\pi) \int_{\frac{1}{2}-\frac{1}{2}\beta}^{\frac{1}{2}+\frac{1}{2}\beta} dx x(1-x) \\ &= \mp 2\alpha \int_{-\beta/2}^{\beta/2} dy \left(\frac{1}{4} - y^2\right) \quad (y \equiv x - \frac{1}{2}) \\ &= \mp \frac{\alpha}{3} \sqrt{1 - \frac{4m^2}{q^2}} \left(1 + \frac{2m^2}{q^2}\right). \end{aligned} \quad (7.92)$$

This dependence on q^2 is exactly the same as in Eq. (5.13), the cross section for production of a fermion-antifermion pair. That is just what we would expect from the unitarity relation shown in Fig. 7.6(b); the cut through the diagram for forward Bhabha scattering gives the total cross section for $e^+e^- \rightarrow f\bar{f}$. The parameter β is precisely the velocity of the fermions in the center-of-mass frame.

Next let us examine how $\widehat{\Pi}_2(q^2)$ modifies the electromagnetic interaction, as determined by Eq. (7.77). In the nonrelativistic limit it makes sense to compute the potential $V(r)$. For the interaction between unlike charges, we have, in analogy with Eq. (4.126),

$$V(\mathbf{x}) = \int \frac{d^3q}{(2\pi)^3} e^{i\mathbf{q}\cdot\mathbf{x}} \frac{-e^2}{|\mathbf{q}|^2 [1 - \widehat{\Pi}_2(-|\mathbf{q}|^2)]}. \quad (7.93)$$

Expanding $\widehat{\Pi}_2$ for $|q^2| \ll m^2$, we obtain

$$V(\mathbf{x}) = -\frac{\alpha}{r} - \frac{4\alpha^2}{15m^2} \delta^{(3)}(\mathbf{x}). \quad (7.94)$$

The correction term indicates that the electromagnetic force becomes much stronger at small distances. This effect can be measured in the hydrogen atom, where the energy levels are shifted by

$$\Delta E = \int d^3x |\psi(\mathbf{x})|^2 \cdot \left(-\frac{4\alpha^2}{15m^2} \delta^{(3)}(\mathbf{x})\right) = -\frac{4\alpha^2}{15m^2} |\psi(0)|^2.$$

The wavefunction $\psi(\mathbf{x})$ is nonzero at the origin only for *s*-wave states. For the $2S$ state, the shift is

$$\Delta E = -\frac{4\alpha^2}{15m^2} \cdot \frac{\alpha^3 m^3}{8\pi} = -\frac{\alpha^5 m}{30\pi} = -1.123 \times 10^{-7} \text{ eV}.$$

This is a (small) part of the Lamb shift splitting listed in Table 6.1.

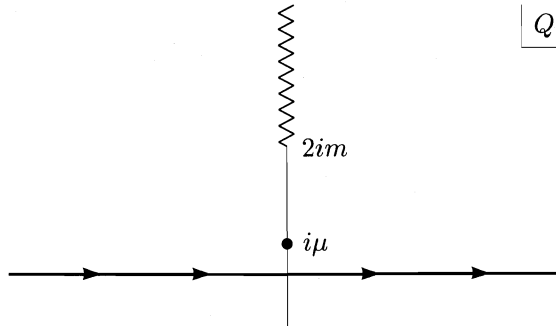


Figure 7.7. Contour for evaluating the effective strength of the electromagnetic interaction in the nonrelativistic limit. The pole at $Q = i\mu$ gives the Coulomb potential. The branch cut gives the order- α correction due to vacuum polarization.

The delta function in Eq. (7.94) is only an approximation; to find the true range of the correction term, we write Eq. (7.93) in the form

$$V(\mathbf{x}) = \frac{ie^2}{(2\pi)^2 r} \int_{-\infty}^{\infty} dQ \frac{Q e^{iQr}}{Q^2 + \mu^2} [1 + \hat{\Pi}_2(-Q^2)] \quad (Q \equiv |\mathbf{q}|),$$

where we have inserted a photon mass μ to regulate the Coulomb potential. To perform this integral we push the contour upward (see Fig. 7.7). The leading contribution comes from the pole at $Q = i\mu$, giving the Coulomb potential, $-\alpha/r$. But there is an additional contribution from the branch cut, which begins at $Q = 2mi$. The real part of the integrand is the same on both sides of the cut, so the only contribution to the integral comes from the imaginary part of $\hat{\Pi}_2$. Defining $q = -iQ$, we find that the contribution from the cut is

$$\begin{aligned} \delta V(r) &= \frac{-e^2}{(2\pi)^2 r} \cdot 2 \int_{2m}^{\infty} dq \frac{e^{-qr}}{q} \text{Im}[\hat{\Pi}_2(q^2 - i\epsilon)] \\ &= -\frac{\alpha}{r} \frac{2}{\pi} \int_{2m}^{\infty} dq \frac{e^{-qr}}{q} \frac{\alpha}{3} \sqrt{1 - \frac{4m^2}{q^2}} \left(1 + \frac{2m^2}{q^2}\right). \end{aligned}$$

When $r \gg 1/m$, this integral is dominated by the region where $q \approx 2m$. Approximating the integrand in this region and substituting $t = q - 2m$, we find

$$\begin{aligned} \delta V(r) &= -\frac{\alpha}{r} \cdot \frac{2}{\pi} \int_0^{\infty} dt \frac{e^{-(t+2m)r}}{2m} \frac{\alpha}{3} \sqrt{\frac{t}{m}} \left(\frac{3}{2}\right) + \mathcal{O}(t) \\ &\approx -\frac{\alpha}{r} \cdot \frac{\alpha}{4\sqrt{\pi}} \frac{e^{-2mr}}{(mr)^{3/2}}, \end{aligned}$$

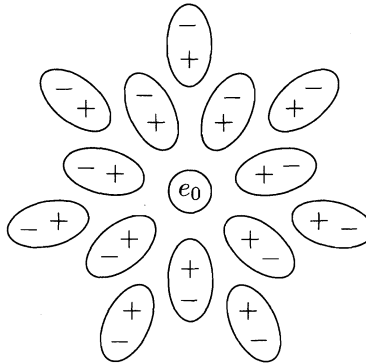


Figure 7.8. Virtual e^+e^- pairs are effectively dipoles of length $\sim 1/m$, which screen the bare charge of the electron.

so that

$$V(r) = -\frac{\alpha}{r} \left(1 + \frac{\alpha}{4\sqrt{\pi}} \frac{e^{-2mr}}{(mr)^{3/2}} + \dots \right). \quad (7.95)$$

Thus the range of the correction term is roughly the electron Compton wavelength, $1/m$. Since hydrogen wavefunctions are nearly constant on this scale, the delta function in Eq. (7.94) was a good approximation. The radiative correction to $V(r)$ is called the *Uehling potential*.

We can interpret the correction as being due to screening. At $r \gtrsim 1/m$, virtual e^+e^- pairs make the vacuum a dielectric medium in which the apparent charge is less than the true charge (see Fig. 7.8). At smaller distances we begin to penetrate the polarization cloud and see the bare charge. This phenomenon is known as *vacuum polarization*.

Now consider the opposite limit: small distance or $-q^2 \gg m^2$. Equation (7.91) then becomes

$$\begin{aligned} \widehat{\Pi}_2(q^2) &\approx \frac{2\alpha}{\pi} \int_0^1 dx x(1-x) \left[\log\left(\frac{-q^2}{m^2}\right) + \log(x(1-x)) + \mathcal{O}\left(\frac{m^2}{q^2}\right) \right] \\ &= \frac{\alpha}{3\pi} \left[\log\left(\frac{-q^2}{m^2}\right) - \frac{5}{3} + \mathcal{O}\left(\frac{m^2}{q^2}\right) \right]. \end{aligned}$$

The effective coupling constant in this limit is therefore

$$\alpha_{\text{eff}}(q^2) = \frac{\alpha}{1 - \frac{\alpha}{3\pi} \log\left(\frac{-q^2}{Am^2}\right)}, \quad (7.96)$$

where $A = \exp(5/3)$. The effective electric charge becomes much larger at small distances, as we penetrate the screening cloud of virtual electron-positron pairs.

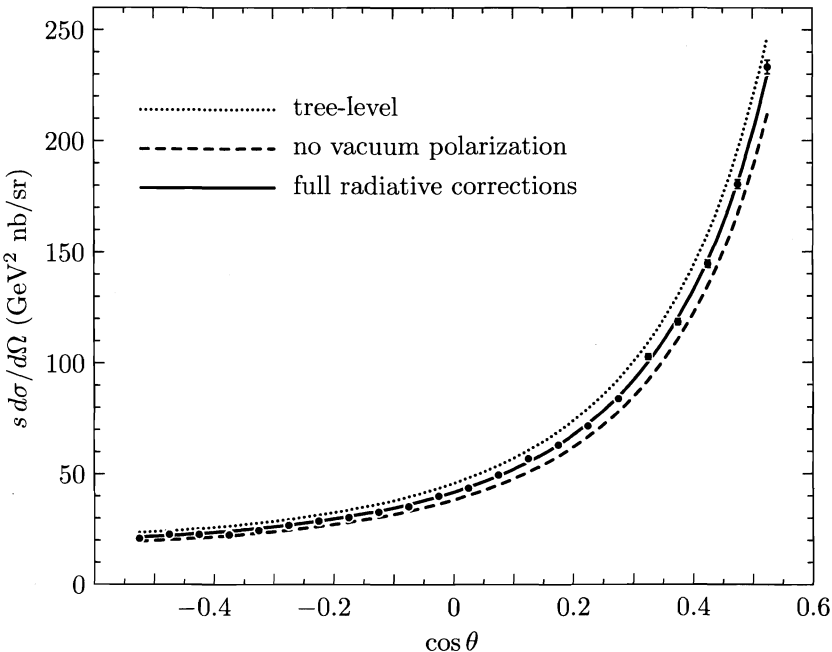


Figure 7.9. Differential cross section for Bhabha scattering, $e^+e^- \rightarrow e^+e^-$, at $E_{\text{cm}} = 29$ GeV, as measured by the HRS collaboration, M. Derrick, et. al., *Phys. Rev. D* **34**, 3286 (1986). The upper curve is the order- α^2 prediction derived in Problem 5.2, plus a very small ($\sim 2\%$) correction due to the weak interaction. The lower curve includes all QED radiative corrections to order α^3 *except* the vacuum polarization contribution; note that these corrections depend on the experimental conditions, as explained in Chapter 6. The middle curve includes the vacuum polarization contribution as well, which increases the effective value of α^2 by about 10% at this energy.

The combined vacuum polarization effect of the electron and of heavier quarks and leptons causes the value of $\alpha_{\text{eff}}(q^2)$ to increase by about 5% from $q = 0$ to $q = 30$ GeV, and this effect is observed in high-energy experiments. Figure 7.9 shows the cross section for Bhabha scattering at $E_{\text{cm}} = 29$ GeV, and a comparison to QED with and without the vacuum polarization diagram.

We can write α_{eff} as a function of r by setting $q = 1/r$. The behavior of $\alpha_{\text{eff}}(r)$ for all r is sketched in Fig. 7.10. The idea of a distance-dependent (or “scale-dependent” or “running”) coupling constant will be a major theme of the rest of this book.

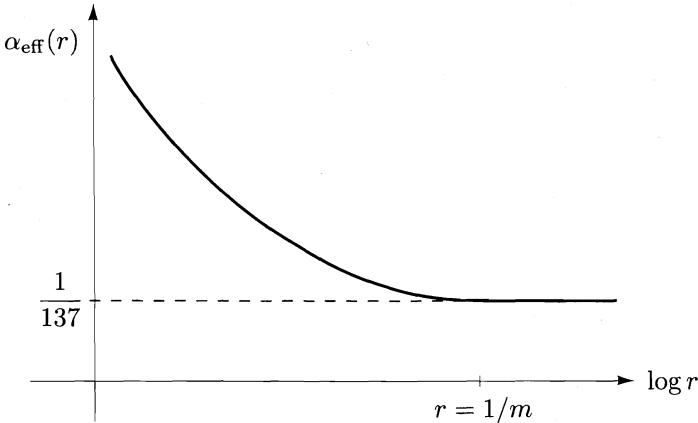


Figure 7.10. A qualitative sketch of the effective electromagnetic coupling constant generated by the one-loop vacuum polarization diagram, as a function of distance. The horizontal scale covers many orders of magnitude.

Problems

7.1 In Section 7.3 we used an indirect method to analyze the one-loop *s*-channel diagram for boson-boson scattering in ϕ^4 theory. To verify our indirect analysis, evaluate all three one-loop diagrams, using the standard method of Feynman parameters. Check the validity of the optical theorem.

7.2 Alternative regulators in QED. In Section 7.5, we saw that the Ward identity can be violated by an improperly chosen regulator. Let us check the validity of the identity $Z_1 = Z_2$, to order α , for several choices of the regulator. We have already verified that the relation holds for Pauli-Villars regularization.

- (a) Recompute δZ_1 and δZ_2 , defining the integrals (6.49) and (6.50) by simply placing an upper limit Λ on the integration over ℓ_E . Show that, with this definition, $\delta Z_1 \neq \delta Z_2$.
- (b) Recompute δZ_1 and δZ_2 , defining the integrals (6.49) and (6.50) by dimensional regularization. You may take the Dirac matrices to be 4×4 as usual, but note that, in *d* dimensions,

$$g_{\mu\nu}\gamma^\mu\gamma^\nu = d.$$

Show that, with this definition, $\delta Z_1 = \delta Z_2$.

7.3 Consider a theory of elementary fermions that couple both to QED and to a Yukawa field ϕ :

$$H_{\text{int}} = \int d^3x \frac{\lambda}{\sqrt{2}} \phi \bar{\psi} \psi + \int d^3x e A_\mu \bar{\psi} \gamma^\mu \psi.$$

- (a) Verify that the contribution to Z_1 from the vertex diagram with a virtual ϕ equals the contribution to Z_2 from the diagram with a virtual ϕ . Use dimensional regularization. Is the Ward identity generally true in this theory?

- (b) Now consider the renormalization of the $\phi\bar{\psi}\psi$ vertex. Show that the rescaling of this vertex at $q^2 = 0$ is *not* canceled by the correction to Z_2 . (It suffices to compute the ultraviolet-divergent parts of the diagrams.) In this theory, the vertex and field-strength rescaling give additional shifts of the observable coupling constant relative to its bare value.

Final Project

Radiation of Gluon Jets

Although we have discussed QED radiative corrections at length in the last two chapters, so far we have made no attempt to compute a full radiatively corrected cross section. The reason is of course that such calculations are quite lengthy. Nevertheless it would be dishonest to pretend that one understands radiative corrections after computing only isolated effects as we have done. This “final project” is an attempt to remedy this situation. The project is the computation of one of the simplest, but most important, radiatively corrected cross sections. You should finish Chapter 6 before starting this project, but you need not have read Chapter 7.

Strongly interacting particles—pions, kaons, and protons—are produced in e^+e^- annihilation when the virtual photon creates a pair of quarks. If one ignores the effects of the strong interactions, it is easy to calculate the total cross section for quark pair production. In this final project, we will analyze the first corrections to this formula due to the strong interactions.

Let us represent the strong interactions by the following simple model: Introduce a new massless vector particle, the *gluon*, which couples universally to quarks:

$$\Delta H = \int d^3x g\bar{\psi}_{fi}\gamma^\mu\psi_{fi}B_\mu.$$

Here f labels the type (“flavor”) of the quark (u , d , s , c , etc.) and $i = 1, 2, 3$ labels the color. The strong coupling constant g is independent of flavor and color. The electromagnetic coupling of quarks depends on the flavor, since the u and c quarks have charge $Q_f = +2/3$ while the d and s quarks have charge $Q_f = -1/3$. By analogy to α , let us define

$$\alpha_g = \frac{g^2}{4\pi}.$$

In this exercise, we will compute the radiative corrections to quark pair production proportional to α_g .

This model of the strong interactions of quarks does not quite agree with the currently accepted theory of the strong interactions, quantum chromodynamics (QCD). However, all of the results that we will derive here are also

correct in QCD with the replacement

$$\alpha_g \rightarrow \frac{4}{3}\alpha_s.$$

We will verify this claim in Chapter 17.

Throughout this exercise, you may ignore the masses of quarks. You may also ignore the mass of the electron, and average over electron and positron polarizations. To control infrared divergences, it will be necessary to assume that the gluons have a small nonzero mass μ , which can be taken to zero only at the end of the calculation. However (as we discussed in Problem 5.5), it is consistent to sum over polarization states of this massive boson by the replacement:

$$\sum \epsilon^\mu \epsilon^{\nu*} \rightarrow -g^{\mu\nu};$$

this also implies that we may use the propagator

$$\overline{B^\mu B^\nu} = \frac{-ig^{\mu\nu}}{k^2 - \mu^2 + i\epsilon}.$$

- (a) Recall from Section 5.1 that, to lowest order in α and neglecting the effects of gluons, the total cross section for production of a pair of quarks of flavor f is

$$\sigma(e^+e^- \rightarrow \bar{q}q) = \frac{4\pi\alpha^2}{3s} \cdot 3Q_f^2.$$

Compute the diagram contributing to $e^+e^- \rightarrow \bar{q}q$ involving one virtual gluon. Reduce this expression to an integral over Feynman parameters, and renormalize it by subtraction at $q^2 = 0$, following the prescription used in Eq. (6.55). Notice that the resulting expression can be considered as a correction to $F_1(q^2)$ for the quark. Argue that, for massless quarks, to all orders in α_g , the total cross section for production of a quark pair unaccompanied by gluons is

$$\sigma(e^+e^- \rightarrow \bar{q}q) = \frac{4\pi\alpha^2}{3s} \cdot 3|F_1(q^2 = s)|^2,$$

with $F_1(q^2 = 0) = Q_f$.

- (b) Before we attempt to evaluate the Feynman parameter integrals in part (a), let us put this contribution aside and study the process $e^+e^- \rightarrow \bar{q}qg$, quark pair production with an additional gluon emitted. Before we compute the cross section, it will be useful to work out some kinematics. Let q be the total 4-momentum of the reaction, let k_1 and k_2 be the 4-momenta of the final quark and antiquark, and let k_3 be the 4-momentum of the gluon. Define

$$x_i = \frac{2k_i \cdot q}{q^2}, \quad i = 1, 2, 3;$$

this is the ratio of the center-of-mass energy of particle i to the maximum available energy. Then show (i) $\sum x_i = 2$, (ii) all other Lorentz scalars involving only the final-state momenta can be computed in terms of the x_i and the particle masses, and (iii) the complete integral over 3-body phase space can be written as

$$\int d\Pi_3 = \prod_i \int \frac{d^3 k_i}{(2\pi)^3} \frac{1}{2E_i} (2\pi)^4 \delta^{(4)}(q - \sum_i k_i) = \frac{q^2}{128\pi^3} \int dx_1 dx_2.$$

Find the region of integration for x_1 and x_2 if the quark and antiquark are massless but the gluon has mass μ .

- (c) Draw the Feynman diagrams for the process $e^+e^- \rightarrow \bar{q}qg$, to leading order in α and α_g , and compute the differential cross section. You may throw away the information concerning the correlation between the initial beam axis and the directions of the final particles. This is conveniently done as follows: The usual trace tricks for evaluating the square of the matrix element give for this process a result of the structure

$$\int d\Pi_3 \frac{1}{4} \sum |\mathcal{M}|^2 = L_{\mu\nu} \int d\Pi_3 H^{\mu\nu},$$

where $L_{\mu\nu}$ represents the electron trace and $H^{\mu\nu}$ represents the quark trace. If we integrate over all parameters of the final state except x_1 and x_2 , which are scalars, the only preferred 4-vector characterizing the final state is q^μ . On the other hand, $H_{\mu\nu}$ satisfies

$$q^\mu H_{\mu\nu} = H_{\mu\nu} q^\nu = 0.$$

Why is this true? (There is an argument based on general principles; however, you might find it a useful check on your calculation to verify this property explicitly.) Since, after integrating over final-state vectors, $\int H^{\mu\nu}$ depends only on q^μ and scalars, it can only have the form

$$\int d\Pi_3 H^{\mu\nu} = \left(g^{\mu\nu} - \frac{q^\mu q^\nu}{q^2} \right) \cdot H,$$

where H is a scalar. With this information, show that

$$L_{\mu\nu} \int d\Pi_3 H^{\mu\nu} = \frac{1}{3} (g^{\mu\nu} L_{\mu\nu}) \cdot \int d\Pi_3 (g^{\rho\sigma} H_{\rho\sigma}).$$

Using this trick, derive the differential cross section

$$\frac{d\sigma}{dx_1 dx_2} (e^+e^- \rightarrow \bar{q}qg) = \frac{4\pi\alpha^2}{3s} \cdot 3Q_f^2 \cdot \frac{\alpha_g}{2\pi} \frac{x_1^2 + x_2^2}{(1-x_1)(1-x_2)}$$

in the limit $\mu \rightarrow 0$. If we assume that each original final-state particle is realized physically as a jet of strongly interacting particles, this formula gives the probability for observing three-jet events in e^+e^- annihilation and the kinematic distribution of these events. The form of the distribution in the x_i is an absolute prediction, and it agrees with experiment. The

normalization of this distribution is a measure of the strong-interaction coupling constant.

- (d) Now replace $\mu \neq 0$ in the formula of part (c) for the differential cross section, and carefully integrate over the region found in part (b). You may assume $\mu^2 \ll q^2$. In this limit, you will find infrared-divergent terms of order $\log(q^2/\mu^2)$ and also $\log^2(q^2/\mu^2)$, finite terms of order 1, and terms explicitly suppressed by powers of (μ^2/q^2) . You may drop terms of the last type throughout this calculation. For the moment, collect and evaluate only the infrared-divergent terms.
- (e) Now analyze the Feynman parameter integral obtained in part (a), again working in the limit $\mu^2 \ll q^2$. Note that this integral has singularities in the region of integration. These should be controlled by evaluating the integral for q spacelike and then analytically continuing into the physical region. That is, write $Q^2 = -q^2$, evaluate the integral for $Q^2 > 0$, and then carefully analytically continue the result to $Q^2 = -q^2 - i\epsilon$. Combine the result with the answer from part (d) to form the total cross section for $e^+e^- \rightarrow$ strongly interacting particles, to order α_g . Show that all infrared-divergent logarithms cancel out of this quantity, so that this total cross section is well-defined in the limit $\mu \rightarrow 0$.
- (f) Finally, collect the terms of order 1 from the integrations of parts (d) and (e) and combine them. To evaluate certain of these terms, you may find the following formula useful:

$$\int_0^1 dx \frac{\log(1-x)}{x} = -\frac{\pi^2}{6}.$$

(It is not hard to prove this.) Show that the total cross section is given, to this order in α_g , by

$$\sigma(e^+e^- \rightarrow \bar{q}q \text{ or } \bar{q}qg) = \frac{4\pi\alpha^2}{3s} \cdot 3Q_f^2 \cdot \left(1 + \frac{3\alpha_g}{4\pi}\right).$$

This formula gives a second way of measuring the strong-interaction coupling constant. The experimental results agree (within the current experimental errors) with the results obtained by the method of part (c). We will discuss the measurement of α_s more fully in Section 17.6.

Part II

Renormalization

Chapter 8

Invitation: Ultraviolet Cutoffs and Critical Fluctuations

The main purpose of Part II of this book is to develop a general theory of renormalization. This theory will explain the origin of ultraviolet divergences in field theory and will indicate when these divergences can be removed systematically. It will also give a way to convert the divergences of Feynman diagrams from a problem into a tool. We will apply this tool to study the asymptotic large- or small-momentum behavior of field theory amplitudes.

When we first encountered an ultraviolet divergence in the calculation of the one-loop vertex correction in Section 6.3, it seemed an aberration that ought to disappear before it caused us too much discomfort. In Chapter 7 we saw further examples of ultraviolet-divergent diagrams, enough to convince us that such divergences occur ubiquitously in Feynman diagram computations. Thus it is necessary for anyone studying field theory to develop a point of view toward these divergences. Most people begin with the belief that any theory that contains divergences must be nonsense. But this viewpoint is overly restrictive, since it excludes not only quantum field theory but even the classical electrodynamics of point particles.

With some experience, one might adopt a more permissive attitude of peaceful coexistence with the divergences: One can accept a theory with divergences, as long as they do not appear in physical predictions. In Chapter 7 we saw that all of the divergences that appear in the one-loop radiative corrections to electron scattering from a heavy target can be eliminated by consistently eliminating the bare values of the mass and charge of the electron in favor of their measured physical values. In Chapter 10, we will argue that all of the ultraviolet divergences of QED, in all orders of perturbation theory, can be eliminated in this way. Thus, as long as one is willing to consider the mass and charge of the electron as measured parameters, the predictions of QED perturbation theory will always be free of divergences. We will also show in Chapter 10 that QED belongs to a well-defined class of field theories in which all ultraviolet divergences are removed after a fixed small number of physical parameters are taken from experiment. These theories, called *renormalizable* quantum field theories, are the only ones in which perturbation theory gives well-defined predictions.

Ideally, though, one should take the further step of trying to understand

physically why the divergences appear and why their effects are more severe in some theories than in others. This direct approach to the divergence problem was pioneered in the 1960s by Kenneth Wilson. The crucial insights needed to solve this problem emerged from a correspondence, discovered by Wilson and others, between quantum field theory and the statistical physics of magnets and fluids. Wilson's approach to renormalization is the subject of Chapter 12. The present chapter gives a brief introduction to the issues in condensed matter physics that have provided insight into the problem of ultraviolet divergences.

Formal and Physical Cutoffs

Ultraviolet divergences signal that quantities calculated in a quantum field theory depend on some very large momentum scale, the ultraviolet cutoff. Equivalently, in position space, divergent quantities depend on some very small distance scale.

The idea of a small-distance cutoff in the continuum description of a system occurs in classical field theories as well. Typically the cutoff is at the scale of atomic distances, where the continuum description no longer applies. However, the size of the cutoff manifests itself in certain parameters of the continuum theory. In fluid dynamics, for instance, parameters such as the viscosity and the speed of sound are of just the size one would expect by combining typical atomic radii and velocities. Similarly, in a magnet, the magnetic susceptibility can be estimated by assuming that the energy cost of flipping an electron spin is on the order of a tenth of an eV, as we would expect from atomic physics. Each of these systems possesses a natural ultraviolet cutoff at the scale of an atom; by understanding the physics at the atomic scale, we can compute the parameters that determine the physics on larger scales.

In quantum field theory, however, we have no precise knowledge of the fundamental physics at very short distance scales. Thus, we can only measure parameters such as the physical charge and mass of the electron, not compute them from first principles. The presence of ultraviolet divergences in the relations between these physical parameters and their bare values is a sign that these parameters are controlled by the unknown short-distance physics.

Whether we know the fundamental physics at small distance scales or not, we need two kinds of information in order to write an effective theory for large-distance phenomena. First, we must know how many parameters from the small distance scale are relevant to large-distance physics. Second, and more importantly, we must know what degrees of freedom from the underlying theory appear at large distances.

In fluid mechanics, it is something of a miracle, from the atomic point of view, that any large-distance degrees of freedom even exist. Nevertheless, the equations that express the transport of energy and mass over large distances do have smooth, coherent solutions. The large-distance degrees of freedom are

the flows that transport these conserved quantities, and sound waves of long wavelength.

In quantum field theory, the large-distance physics involves only those particles that have masses that are very small compared to the fundamental cutoff scale. These particles and their dynamics are the quantum analogues of the large-scale flows in fluid mechanics. The simplest way to naturally arrange for such particles to appear is to make use of particles that naturally have zero mass. So far in this book, we have encountered two types of particles whose mass is precisely zero, the photon and the chiral fermion. (In Chapter 11 we will meet one further naturally massless particle, the *Goldstone boson*.) We might argue that QED exists as a theory on scales much larger than its cutoff because the photon is naturally massless and because the left- and right-handed electrons are very close to being chiral fermions.

There is another way that particles of zero or almost zero mass can arise in quantum field theory: We can simply tune the parameters of a scalar field theory so that the scalar particles have masses small compared to the cut-off. This method of introducing particles with small mass seems arbitrary and unnatural. Nevertheless, it has an analogue in statistical mechanics that is genuinely interesting in that discipline and can teach us some important lessons.

Normally, in a condensed matter system, the thermal fluctuations are correlated only over atomic distances. Under special circumstances, however, they can have much longer range. The clearest example of this phenomenon occurs in a ferromagnet. At high temperature, the electron spins in a magnet are disorganized and fluctuating; but at low temperature, these spins align to a fixed direction.* Let us think about how this alignment builds up as the temperature of the magnet is lowered. As the magnet cools from high temperature, clusters of correlated spins become larger and larger. At a certain point—the temperature of magnetization—the entire sample becomes a single large cluster with a well-defined macroscopic orientation. Just above this temperature, the magnet contains large clusters of spins with a common orientation, which in turn belong to still larger clusters, such that the orientations on the very largest scale are still randomized through the sample. This situation is illustrated in Fig. 8.1. Similar behavior occurs in the vicinity of any other second-order phase transition, for example, the order-disorder transition in binary alloys, the critical point in fluids, or the superfluid transition in Helium-4.

The natural description of these very long wavelength fluctuations is in terms of a fluctuating continuum field. At the lowest intuitive level, we might

*In a real ferromagnet, the long-range magnetic dipole-dipole interaction causes the state of uniform magnetization to break up into an array of magnetic domains. In this book, we will ignore this interaction and think of a magnetic spin as a pure orientation. It is this idealized system that is directly analogous to a quantum field theory.

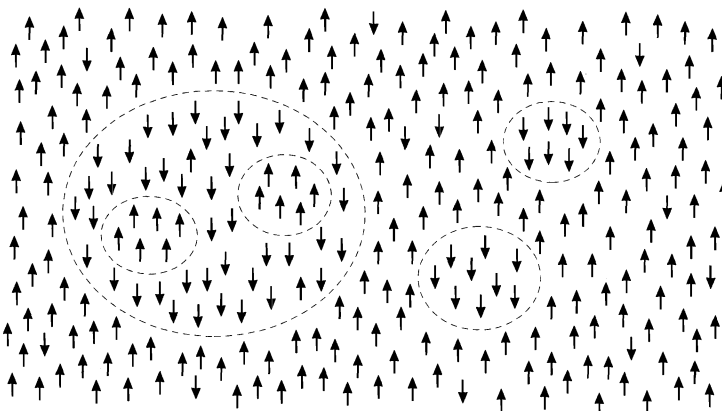


Figure 8.1. Clusters of oriented spins near the critical point of a ferromagnet.

substitute quantum for statistical fluctuations and try to describe this system as a quantum field theory. In Section 9.3 we will derive a somewhat more subtle relation that makes a precise connection between the statistical and the quantum systems. Through this connection, the behavior of any statistical system near a second-order phase transition can be translated into the behavior of a particular quantum field theory. This quantum field theory has a field with a mass that is very small compared to the basic atomic scale and that goes to zero precisely at the phase transition.

But this connection seems to compound the problem of ultraviolet divergences in quantum field theory: If the wealth of phase transitions observed in Nature generates a similar wealth of quantum field theories, how can we possibly define a quantum field theory without detailed reference to its origins in physics at the scale of its ultraviolet cutoff? Saying that a quantum field theory makes predictions independent of the cutoff would be equivalent to saying that the statistical fluctuations in the neighborhood of a critical point are independent of whether the system is a magnet, a fluid, or an alloy. But is this statement so obviously incorrect? By reversing the logic, we would find that quantum field theory makes a remarkably powerful prediction for condensed matter systems, a prediction of *universality* for the statistical fluctuations near a critical point. In fact, this prediction is verified experimentally.

A major theme of Part II of this book will be that these two ideas—cutoff independence in quantum field theory and universality in the theory of critical phenomena—are naturally the same idea, and that understanding either of these ideas gives insight into the other.

Landau Theory of Phase Transitions

To obtain a first notion of what could be universal in the phenomena of phase transitions, let us examine the simplest continuum theory of second-order phase transitions, due to Landau.

First we should review a little thermodynamics and clarify our nomenclature. In thermodynamics, a *first-order phase transition* is a point across which some thermodynamic variable (the density of a fluid, or the magnetization of a ferromagnet) changes discontinuously. At a phase transition point, two quite distinct thermodynamic states (liquid and gas, or magnetization parallel and antiparallel to a given axis) are in equilibrium. The thermodynamic quantity that changes discontinuously across the transition, and that characterizes the difference of the two competing phases, is called the *order parameter*. In most circumstances, it is possible to change a second thermodynamic parameter in such a way that the two competing states move closer together in the thermodynamic space, so that at some value of this parameter, these two states become identical and the discontinuity in the order parameter disappears. This endpoint of the line of first-order transitions is called a *second-order phase transition*, or, more properly, a *critical point*. Viewed from the other direction, a critical point is a point at which a single thermodynamic state bifurcates into two macroscopically distinct states. It is this bifurcation that leads to the long-ranged thermal fluctuations discussed in the previous section.

A concrete example of this behavior is exhibited by a ferromagnet. Let us assume for simplicity that the material we are discussing has a preferred axis of magnetization, so that at low temperature, the system will have its spins ordered either parallel or antiparallel to this axis. The total magnetization along this axis, M , is the order parameter. At low temperature, application of an external magnetic field H will favor one or the other of the two possible states. At $H = 0$, the two states will be in equilibrium; if H is changed from a small negative to a small positive value, the thermodynamic state and the value of M will change discontinuously. Thus, for any fixed (low) temperature, there is a first-order transition at $H = 0$. Now consider the effect of raising the temperature: The fluctuation of the spins increases and the value of $|M|$ decreases. At some temperature T_C the system ceases to be magnetized at $H = 0$. At this point, the first-order phase transition disappears and the two competing thermodynamic states coalesce. The system thus has a critical point at $T = T_C$. The location of these various transitions in the H - T plane is shown in Fig. 8.2.

Landau described this behavior by the use of the Gibbs free energy G ; this is the thermodynamic potential that depends on M and T , such that

$$\left. \frac{\partial G}{\partial M} \right|_T = H. \quad (8.1)$$

He suggested that we concentrate our attention on the region of the critical

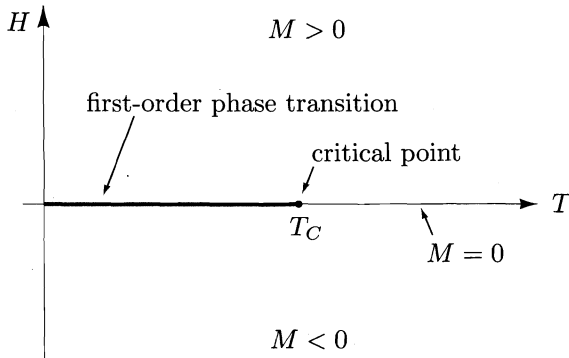


Figure 8.2. Phase diagram in the H - T plane for a uniaxial ferromagnet.

point: $T \approx T_C$, $M \approx 0$. Then it is reasonable to expand $G(M)$ as a Taylor series in M . For $H = 0$, we can write

$$G(M) = A(T) + B(T)M^2 + C(T)M^4 + \dots \quad (8.2)$$

Because the system has a symmetry under $M \rightarrow -M$, $G(M)$ can contain only even powers of M . Since M is small, we will ignore the higher terms in the expansion. Given Eq. (8.2), we can find the possible values of M at $H = 0$ by solving

$$0 = \frac{\partial G}{\partial M} = 2B(T)M + 4C(T)M^3. \quad (8.3)$$

If B and C are positive, the only solution is $M = 0$. However, if $C > 0$ but B is negative below some temperature T_C , we have a nontrivial solution for $T < T_C$, as shown in Fig. 8.3. More concretely, approximate for $T \approx T_C$:

$$B(T) = b(T - T_C), \quad C(T) = c. \quad (8.4)$$

Then the solution to Eq. (8.3) is

$$M = \begin{cases} 0 & \text{for } T > T_C; \\ \pm [(b/2c)(T_C - T)]^{1/2} & \text{for } T < T_C. \end{cases} \quad (8.5)$$

This is just the qualitative behavior that we expect at a critical point.

To find the value of M at nonzero external field, we could solve Eq. (8.1) with the left-hand side given by (8.2). An equivalent procedure is to minimize a new function, related to (8.2). Define

$$G(M, H) = A(T) + B(T)M^2 + C(T)M^4 - HM. \quad (8.6)$$

Then the minimum of $G(M, H)$ with respect to M at fixed H gives the value of M that satisfies Eq. (8.1). The minimum is unique except when $H = 0$ and $T < T_C$, where we find the double minimum in the second line of (8.5). This is consistent with the phase diagram shown in Fig. 8.2.

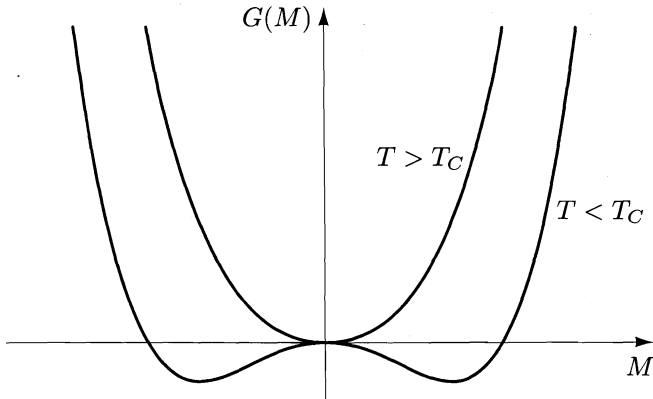


Figure 8.3. Behavior of the Gibbs free energy $G(M)$ in Landau theory, at temperatures above and below the critical temperature.

To study correlations in the vicinity of the phase transition, Landau generalized this description further by considering the magnetization M to be the integral of a local spin density:

$$M = \int d^3x s(\mathbf{x}). \quad (8.7)$$

Then the Gibbs free energy (8.6) becomes the integral of a local function of $s(\mathbf{x})$,

$$G = \int d^3x \left[\frac{1}{2}(\nabla s)^2 + b(T - T_C)s^2 + cs^4 - Hs \right], \quad (8.8)$$

which must be minimized with respect to the field configuration $s(\mathbf{x})$. The first term is the simplest possible way to introduce the tendency of nearby spins to align with one another. We have rescaled $s(\mathbf{x})$ so that the coefficient of this term is set to $1/2$. In writing this free energy integral, we could even consider H to vary as a function of position. In fact, it is useful to do that; we can turn on $H(\mathbf{x})$ near $x = 0$ and see what response we find at another point.

The minimum of the free energy expression (8.8) with respect to $s(\mathbf{x})$ is given by the solution to the variational equation

$$0 = \delta G[s(\mathbf{x})] = -\nabla^2 s + 2b(T - T_C)s + 4cs^3 - H(\mathbf{x}). \quad (8.9)$$

For $T > T_C$, where the macroscopic magnetization vanishes and so $s(\mathbf{x})$ should be small, we can find the qualitative behavior by ignoring the s^3 term. Then $s(\mathbf{x})$ obeys a linear equation,

$$(-\nabla^2 + 2b(T - T_C))s(\mathbf{x}) = H(\mathbf{x}). \quad (8.10)$$

To study correlations of spins, we will set

$$H(\mathbf{x}) = H_0 \delta^{(3)}(\mathbf{x}). \quad (8.11)$$

The resulting configuration $s(\mathbf{x})$ is then the Green's function of the differential operator in Eq. (8.10), so we call it $D(\mathbf{x})$:

$$(-\nabla^2 + 2b(T - T_C))D(\mathbf{x}) = H_0\delta^{(3)}(\mathbf{x}). \quad (8.12)$$

This Green's function tells us the response at \mathbf{x} when the spin at $\mathbf{x} = 0$ is forced into alignment with H . In Sections 9.2 and 9.3 we will see that $D(\mathbf{x})$ is also proportional to the zero-field spin-spin correlation function in the thermal ensemble,

$$D(\mathbf{x}) \propto \langle s(\mathbf{x})s(0) \rangle \equiv \sum_{\text{all } s(\mathbf{x})} s(\mathbf{x})s(0)e^{-\mathbf{H}/kT}, \quad (8.13)$$

where \mathbf{H} is the Hamiltonian of the magnetic system.

The solution to Eq. (8.12) can be found by Fourier transformation:

$$D(\mathbf{x}) = \int \frac{d^3k}{(2\pi)^3} \frac{H_0 e^{i\mathbf{k}\cdot\mathbf{x}}}{|\mathbf{k}|^2 + 2b(T - T_C)}. \quad (8.14)$$

This is just the integral we encountered in our discussion of the Yukawa potential, Eq. (4.126). Evaluating it in the same way, we find

$$D(\mathbf{x}) = \frac{H_0}{4\pi} \frac{1}{r} e^{-r/\xi}, \quad (8.15)$$

where

$$\xi = [2b(T - T_C)]^{-1/2} \quad (8.16)$$

is the *correlation length*, the range of correlated spin fluctuations. Notice that this length diverges as $T \rightarrow T_C$.

The main results of this analysis, Eqs. (8.5) and (8.16), involve unknown constants b, c that depend on physics at the atomic scale. On the other hand, the power-law dependence in these formulae on $(T - T_C)$ follows simply from the structure of the Landau equations and is independent of any details of the microscopic physics. In fact, our derivation of this dependence did not even use the fact that G describes a ferromagnet; we assumed only that G can be expanded in powers of an order parameter and that G respects the reflection symmetry $M \rightarrow -M$. These assumptions apply equally well to many other types of systems: binary alloys, superfluids, and even (though the reflection symmetry is less obvious here) the liquid-gas transition. Landau theory predicts that, near the critical point, these systems show a universal behavior in the dependence of M , ξ , and other thermodynamic quantities on $(T - T_C)$.

Critical Exponents

The preceding treatment of the Landau theory of phase transitions emphasizes its similarity to classical field theory. We set up an appropriate free energy and found the thermodynamically preferred configuration by solving a classical variational equation. This gives only an approximation to the full statistical problem, analogous to the approximation of replacing quantum by classical

dynamics in field theory. In Chapter 13, we will use methods of quantum field theory to account properly for the fluctuations about the preferred Landau thermodynamic state. These modifications turn out to be profound, and rather counterintuitive.

To describe the form of these modifications, let us write Eq. (8.15) more generally as

$$\langle s(\mathbf{x})s(0) \rangle = A \frac{1}{r^{1+\eta}} f(r/\xi), \quad (8.17)$$

where A is a constant and $f(y)$ is a function that satisfies $f(0) = 1$ and $f(y) \rightarrow 0$ as $y \rightarrow \infty$. Landau theory predicts that $\eta = 0$ and $f(y)$ is a simple exponential. This expression has a form strongly analogous to that of a Green's function in quantum field theory. The constant A can be absorbed into the field-strength renormalization of the field $s(\mathbf{x})$. The correlation length ξ is, in general, a complicated function of the atomic parameters, but in the continuum description we can simply trade these parameters for ξ . It is appropriate to consider ξ as a cutoff-independent, physical parameter, since it controls the large-distance behavior of a physical correlation. In fact, the analogy between Eq. (8.15) and the Yukawa potential suggests that we should identify ξ^{-1} with the physical mass in the associated quantum field theory. Then Eq. (8.17) gives a cutoff-independent, continuum representation of the statistical system.

If we were working in quantum field theory, we would derive corrections to Eq. (8.17) as a perturbation series in the parameter c multiplying the nonlinear term in (8.9). This would generalize the Landau result to

$$\langle s(\mathbf{x})s(0) \rangle = \frac{1}{r} F(r/\xi, c). \quad (8.18)$$

The perturbative corrections would depend on the properties of the continuum field theory. For example, $F(y, c)$ would depend on the number of components of the field $s(\mathbf{x})$, and its series expansion would differ depending on whether the magnetization formed along a preferred axis, in a preferred plane, or isotropically. For order parameters with many components, the expansion would also depend on higher discrete symmetries of the problem. However, we expect that systems described by the same Landau free energy (for example, a single-axis ferromagnet and a liquid-gas system) should have the same perturbation expansion when this expansion is written in terms of the physical mass and coupling. The complete universality of Landau theory then becomes a more limited concept, in which systems have the same large-distance correlations if their order parameters have the same symmetry. We might say that statistical systems divide into distinct *universality classes*, each with a characteristic large-scale behavior.

If this were the true behavior of systems near second-order phase transitions, it would already be a wonderful confirmation of the ideas required to formulate cutoff-independent quantum field theories. However, the true behavior of statistical systems is still another level more subtle. What one finds experimentally is a dependence of the form of Eq. (8.17), where the function

$f(y)$ is the same within each universality class. There is no need for an auxiliary parameter c . On the other hand, the exponent η takes a specific nonzero value in each universality class. Other power-law relations of Landau theory are also modified, in a specific manner for each universality class. For example, Eq. (8.5) is changed, for $T < T_C$, to

$$M \propto (T_C - T)^\beta, \quad (8.19)$$

where the exponent β takes a fixed value for all systems in a given universality class. For three-dimensional single-axis magnets and for fluids, $\beta = 0.313$. The powers in these nontrivial scaling relations are called *critical exponents*.

The modification from Eq. (8.18) to Eq. (8.17) does not imperil the idea that a condensed matter system, in the vicinity of a second-order phase transition, has a well-defined, cutoff-independent, continuum behavior. However, we would like to understand why Eq. (8.17) should be expected as the correct representation. The answer to this question will come from a thorough analysis of the ultraviolet divergences of the corresponding quantum field theory. In Chapter 12, when we finally conclude our explication of the ultraviolet divergences, we will find that we have in hand the tools not only to justify Eq. (8.17), but also to calculate the values of the critical exponents using Feynman diagrams. In this way, we will uncover a beautiful application of quantum field theory to the domain of atomic physics. The success of this application will guide us, in Part III, to even more powerful tools, which we will need in the relativistic domain of elementary particles.

Chapter 9

Functional Methods

Feynman once said that* “every theoretical physicist who is any good knows six or seven different theoretical representations for exactly the same physics.” Following his advice, we introduce in this chapter an alternative method of deriving the Feynman rules for an interacting quantum field theory: the method of *functional integration*.

Aside from Feynman’s general principle, we have several specific reasons for introducing this formalism. It will provide us with a relatively easy derivation of our expression for the photon propagator, completing the proof of the Feynman rules for QED given in Section 4.8. The functional method generalizes more readily to other interacting theories, such as scalar QED (Problem 9.1), and especially the non-Abelian gauge theories (Part III). Since it uses the Lagrangian, rather than the Hamiltonian, as its fundamental quantity, the functional formalism explicitly preserves all symmetries of a theory. Finally, the functional approach reveals the close analogy between quantum field theory and statistical mechanics. Exploiting this analogy, we will turn Feynman’s advice upside down and apply the same theoretical representation to two completely different areas of physics.

9.1 Path Integrals in Quantum Mechanics

We begin by applying the functional integral (or *path integral*) method to the simplest imaginable system: a nonrelativistic quantum-mechanical particle moving in one dimension. The Hamiltonian for this system is

$$H = \frac{p^2}{2m} + V(x).$$

Suppose that we wish to compute the amplitude for this particle to travel from one point (x_a) to another (x_b) in a given time (T). We will call this amplitude $U(x_a, x_b; T)$; it is the position representation of the Schrödinger time-evolution operator. In the canonical Hamiltonian formalism, U is given by

$$U(x_a, x_b; T) = \langle x_b | e^{-iHT/\hbar} | x_a \rangle. \quad (9.1)$$

**The Character of Physical Law* (MIT Press, 1965), p. 168.

(For the next few pages we will display all factors of \hbar explicitly.)

In the path-integral formalism, U is given by a very different-looking expression. We will first try to motivate that expression, then prove that it is equivalent to (9.1).

Recall that in quantum mechanics there is a *superposition principle*: When a process can take place in more than one way, its total amplitude is the coherent sum of the amplitudes for each way. A simple but nontrivial example is the famous double-slit experiment, shown in Fig. 9.1. The total amplitude for an electron to arrive at the detector is the sum of the amplitudes for the two paths shown. Since the paths differ in length, these two amplitudes generally differ, causing interference.

For a general system, we might therefore write the total amplitude for traveling from x_a to x_b as

$$U(x_a, x_b; T) = \sum_{\text{all paths}} e^{i \cdot (\text{phase})} = \int \mathcal{D}x(t) e^{i \cdot (\text{phase})}. \quad (9.2)$$

To be democratic, we have written the amplitude for each particular path as a pure phase, so that no path is inherently more important than any other. The symbol $\int \mathcal{D}x(t)$ is simply another way of writing “sum over all paths”; since there is one path for every function $x(t)$ that begins at x_a and ends at x_b , the sum is actually an integral over this continuous space of functions.

We can define this integral as part of a natural generalization of the calculus to spaces of functions. A function that maps functions to numbers is called a *functional*. The integrand in (9.2) is a functional, since it associates a complex amplitude with any function $x(t)$. The argument of a functional $F[x(t)]$ is conventionally written in square brackets rather than parentheses. Just as an ordinary function $y(x)$ can be integrated over a set of points x , a functional $F[x(t)]$ can be integrated over a set of functions $x(t)$; the measure of such a *functional integral* is conventionally written with a script capital \mathcal{D} , as in (9.2). A functional can also be differentiated with respect to its argument (a function), and this *functional derivative* is denoted by $\delta F / \delta x(t)$. We will develop more precise definitions of this new integral and derivative in the course of this section and the next.

What should we use for the “phase” in Eq. (9.2)? In the classical limit, we should find that only one path, the classical path, contributes to the total amplitude. We might therefore hope to evaluate the integral in (9.2) by the method of stationary phase, identifying the classical path $x_{\text{cl}}(t)$ by the stationary condition,

$$\frac{\delta}{\delta x(t)} \left(\text{phase}[x(t)] \right) \Big|_{x_{\text{cl}}} = 0.$$

But the classical path is the one that satisfies the principle of least action,

$$\frac{\delta}{\delta x(t)} \left(S[x(t)] \right) \Big|_{x_{\text{cl}}} = 0,$$

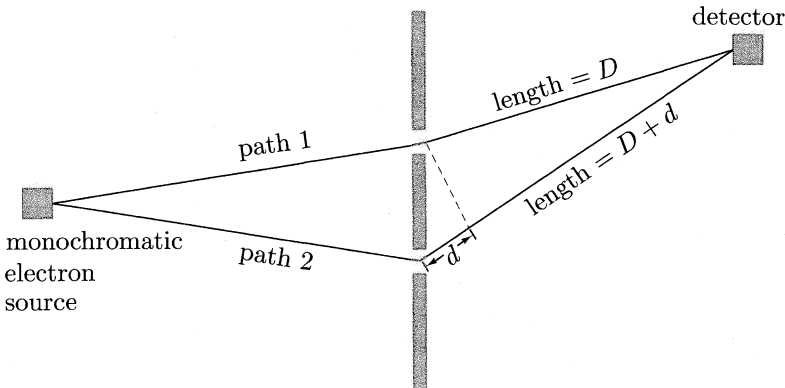


Figure 9.1. The double-slit experiment. Path 2 is longer than path 1 by an amount d , and therefore has a phase that is larger by $2\pi d/\lambda$, where $\lambda = 2\pi\hbar/p$ is the particle's de Broglie wavelength. Constructive interference occurs when $d = 0, \lambda, \dots$, while destructive interference occurs when $d = \lambda/2, 3\lambda/2, \dots$

where $S = \int L dt$ is the classical action. It is tempting, therefore, to identify the phase with S , up to a constant. Since the stationary-phase approximation should be valid in the classical limit—that is, when $S \gg \hbar$ —we will use S/\hbar for the phase. Our final formula for the propagation amplitude is thus

$$\langle x_b | e^{-iHT/\hbar} | x_a \rangle = U(x_a, x_b; T) = \int \mathcal{D}x(t) e^{iS[x(t)]/\hbar}. \quad (9.3)$$

We can easily verify that this formula gives the correct interference pattern in the double-slit experiment. The action for either path shown in Fig. 9.1 is just $(1/2)mv^2t$, the kinetic energy times the time. For path 1 the velocity is $v_1 = D/t$, so the phase is $mD^2/2\hbar t$. For path 2 we have $v_2 = (D+d)/t$, so the phase is $m(D+d)^2/2\hbar t$. We must assume that $d \ll D$, so that $v_1 \approx v_2$ (i.e., the electrons have a well-defined velocity). The excess phase for path 2 is then $mDd/\hbar t \approx pd/\hbar$, where p is the momentum. This is exactly what we would expect from the de Broglie relation $p = h/\lambda$, so we must be doing something right.

To evaluate the functional integral more generally, we must define the symbol $\int \mathcal{D}x(t)$ in the case where the number of paths $x(t)$ is more than two (and, in fact, continuously infinite). We will use a brute-force definition, by discretization. Break up the time interval from 0 to T into many small pieces of duration ϵ , as shown in Fig. 9.2. Approximate a path $x(t)$ as a sequence of straight lines, one in each time slice. The action for this discretized path is

$$S = \int_0^T dt \left(\frac{m}{2} \dot{x}^2 - V(x) \right) \longrightarrow \sum_k \left[\frac{m}{2} \frac{(x_{k+1}-x_k)^2}{\epsilon} - \epsilon V\left(\frac{x_{k+1}+x_k}{2}\right) \right].$$